FUNDAMENTALS IN NUCLEAR PHYSICS

Book · December 2014

CITATIONS
2

READS
56,523

1 author:

Khairi Abdullah
University of Duhok, College of Engineering, Duhok, Iraq
13 PUBLICATIONS **24** CITATIONS

SEE PROFILE

FUNDAMENTALS IN NUCLEAR PHYSICS

University of Duhok Publication
Khairi M-S. Abdullah

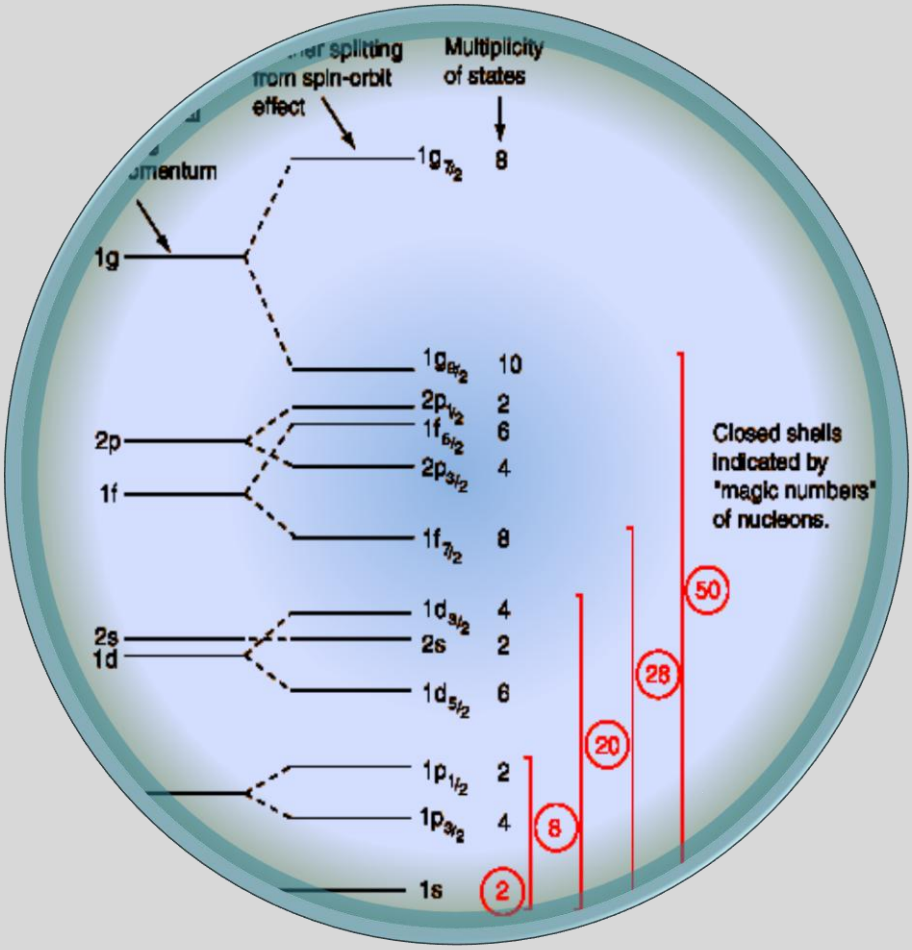

FUNDAMENTALS IN NUCLEAR PHYSICS

Khairi Mohammad Said Abdullah
Professor., Ph.D. in Nuclear Engineering,
Faculty of Engineering /University of Duhok

A textbook for
Nuclear Physics
College of Science and Education

Published by
University of Duhok/ under the authorization of
Directorate of Libraries in Duhok/ Kurdistan Region-Iraq
Card No. D-/2253/14 at 29/12/2014

بسم الله الرحمن الرحيم

أَوَلَمْ يَرَ الَّذِينَ كَفَرُوا أَنَّ السَّمَاوَاتِ وَالْأَرْضَ كَانَتَا رَتْقًا فَفَتَقْنَاهُمَا وَجَعَلْنَا مِنَ الْمَاءِ كُلَّ شَيْءٍ حَيٍّ أَفَلَا يُؤْمِنُونَ (٣٠)

سورة الانبياء

Do not the Unbelievers see that the heavens and the earth were "rateq" joined together (as one unit of creation), before We "fateq" clove (parted) them asunder? We made from water every living thing. Will they not then believe? (30) **AL-ANBIYA (THE PROPHETS)**

This version of holy Quran gives information about the beginning of the universe. The heavens and the earth contiguous with each other in the darkness do not see the severity of thing. Both had been combined together as one unit without any hole or distance between their constituents "rateq". God, then, by His light, clove this rateq and the separation between the heavens and the earth. The sky lifted into place, and passed the earth in place, and the separation by air between them.

Depending on nuclear and astronomical evidence, scientists suggest that the baryonic matter (everyday material) contributes only about 4% to the mass of the universe. The rest is composed of dark matter and energy.

In my opinion, the one dark matter or an extremely dense unique single constituent “Rateq” was the early phase of the universe in the hand of Exalted Allah, then disintegrated or spallated by His own power to form the early phase of the Big Bang “Fateq” with cosmological inflation.

Prof. Dr. Khairi M-S. Abdullah
April/2014

DEDICATED TO:

My parents whose loving memories still guide me through difficult times;
My wife Sharmeen, without her utmost love, support and encouragement in such a way that nothing can be seen;
My sons Diyar, Bilal, and Mustafa and my beloved daughter Shafak, who have taught me things about life I could never have learned myself

PREFACE

The thought of this text book originated from the author's research and academic experience in Iraqi Atomic Energy Commission (IAEC) and various universities in Iraq in departments of nuclear engineering and physics over several years. Furthermore, the previous experience and background of our students determined to a large extent the level of the included material.

As a lecturer and researcher of nuclear physics in the Department of Physics/University of Duhok, I noticed that the majority of undergraduates 'and to some extent graduates' have poor information in atomic physics and a lack of knowledge of the physical background of quantum mechanics. Chapter Five is devoted to relate the quantum mechanics concepts and their terminologies with the nuclear concepts. Integral parts of nuclear concepts and the interaction of radiation with matter are essential to have some knowledge of quantum mechanics to having full command of the language of nuclear physics.

Accordingly, this book is intended for junior as well as senior undergraduate courses, particularly for students who have had previous contact with quantum mechanics. This text can also be used in introductory graduate surveys of nuclear physics. The book is based on two semester course on nuclear physics (excluding particle physics) taught to undergraduate juniors.

I have not tried to be rigorous or present proofs of all statements in the text. Rather, I have taken the physical view that it is more important that students see an overview of the subject which for many 'possibly the majority' will be the only time they study nuclear and particle physics. Therefore, the first four chapters deal with nuclear properties and

radioactive decay. As mentioned a particular attention has been given to the discussion of the related nuclear concepts of quantum mechanics in Chapter Five. The rest of the chapters are devoted to the nuclear structure and interactions of radiation with matter.

In fact, more than just a slight contact is required in order to appreciate many of the subtleties I have infused into the book. I hope that this effort will be of benefit for our students.

Perfection is not attainable. It is an attribute of the Almighty God. Therefore, I apologize for any drawbacks in the text.

Finally I am grateful for the help of the University of Duhok for adopting this book for publication.

Prof. Dr. Khairi M-S. Abdullah
University of Duhok-Iraq
April- 2014

CONTENTS

CHAPTER 3

MODE OF RADIOACTIVE DECAY AND NUCLEAR REACTIONS

CHAPTER 4
RADIOACTIVE DECAY DYNAMIC

CHAPTER 5
QUANTUM MECHANICAL BEHAIVIOR OF NUCLEI

CHAPTER 6
NUCLEAR FORCES AND INTERACTIONS

CHAPTER 7
NUCLEAR MODELS

CHAPTER 8
INTERACTION OF CHARGED PARTICLES WITH MATTER
(DIRECT IONIZING RADIATION)

CHAPTER 9
INTERACTION OF GAMMA RAY WITH MATTER
(INDIRECT IONIZING RADIATION)

CHAPTER 10
NEUTRON PHYSICS AND INTERACTIONS
(INDIRECT IONIZING RADIATION)

CHAPTER 1

INTRODUCTION TO NUCLEAR PHYSICS

The atom is considered to be the basic building block of all matter. It is the smallest amount of matter that retains the properties of an element. Simple atomic theory tells us that it is composed of smaller particles (that no longer have the same properties as the overall element) and consists of two main components: a nucleus surrounded by an electron cloud. The situation seems similar in some respects to planets orbiting the sun. From the electrical point of view, the nucleus is said to be positively charged and the electrons negatively charged.

1.1. Historical View of Nuclear Physics

Early Greek philosophers speculated that the earth was made up of different combinations of basic substances, or elements which are earth, air, water, and fire. Modern science shows that the early Greeks held the correct concept that matter consists of a combination of basic elements, but they incorrectly identified the elements.

Later after the birth of Islam in the seventh century, the great Arab philosophers and scientists found, inspiried by the Holy Quran, answers to questions that Europe had hardly began to ask. Amongst many, Arab scholars believed that the world was round and the planets orbited the sun. They discovered and named many elements (atoms) and chemical compounds (molecules).

In 1661, the English chemist Robert Boyle published the modern criterion for an element. He defined an element to be a basic substance that could not be broken down into any simpler substance after it was isolated from a compound, but could be combined with other elements to form compounds.

The English chemist John Dalton was the first who proposed the modern proof for the atomic nature of matter in 1803. Dalton stated that each chemical element possessed a particular kind of atom and any quantity of the element was made up of identical atoms of this kind. What distinguishes one element from another element is the kind of atom of which it consists, and the basic physical difference between different kinds of atoms is their weight.

The decade from 1895 to 1905 may be termed the beginning of modern physics; the investigators applied the methods of *experimental science* to the problems of atom. From their studies, they obtained the evidences needed to raise the idea of atomism to the level of a full-fledged *scientific theory*. During this period, Roentgen discovered x-rays (1895), Becquerel discovered the phenomenon of natural radioactivity (1896), J. J. Thomson succeeded in demonstrating the existence of the electron, a fundamental unit of negative electricity with very small mass (1897) and the separation of the elements polonium and radium was done by Pierre and Marie Curie (1898). To these discoveries, we must add the bold hypothesis put forth by Planck to explain the distribution of energy in the spectrum of the radiation from a black body. Namely, that electromagnetic radiation, in its interaction with matter, is emitted or absorbed in whole units, called quanta of energy; each quantum has energy $E = hv$ where *v is the frequency of the radiation and h is the Planck constant*. Einstein (1905), in a treatment of the photoelectric effect, extended Planck's

hypothesis by showing that *electromagnetic radiation, in its interaction with matter, behaves as though it consists of particles, called photons*, each photon having an energy $E = hv$. N. Bohr (1913) used this concept in his very successful theory of the hydrogen atom. All these ideas led to one of the most important developments of twentieth-century physics, the *quantum theory*; this theory includes quantum mechanics and the quantum theory of radiation (1924-1928). Also during the same period (1905-1913) an equally important change in the foundation of physics resulted from the development of the *theory of relativity* by Einstein.

Concerning *nuclear physics*, the history can be divided into three periods. The first period started with the discovery of the radioactivity of the nucleus and the subsequence developments and ended in 1939 with the discovery of fission by Hahn and Strassman as a result of attempts to make transuranium elements of atomic number greater than 92 by bombardment of uranium with neutrons. The second period from 1940 to 1969, nuclear physics witnessed important developments in practical applications and theoretical explanations, such as nuclear spectroscopy, reactors and nuclear models. Finally, the emergence of a microscopic unifying theory in the 1960's allowed one to understand the structure and behavior of protons and neutrons in terms of the fundamental interactions of their constituent particles, quarks and gluons. That period also witnessed the identification of subtle non-classical mechanisms in nuclear structure.

To date, 105 different elements have been confirmed to exist, and researchers claim to have discovered three additional elements. Of the 105 confirmed elements, 90 exist in nature and 15 are man-made.

1.2. Subatomic Particles

For almost 100 years after Dalton established the atomic nature of atoms, it was considered impossible to divide the atom into even smaller parts. All of the results of chemical experiments during this time indicated that the atom was indivisible.

Eventually, experimentation into electricity and radioactivity indicated that particles of matter smaller than the atom did indeed exist. In 1906, J. J. Thompson won the Nobel Prize in physics for establishing the existence of electrons. *Electrons* are negatively-charged particles that have 1/1836.153 the mass of the hydrogen atom. Soon after the discovery of electrons, protons were discovered. *Protons* are relatively large particles that have almost the same mass as a hydrogen atom and a positive charge equal in magnitude (but opposite in sign) to that of the electron. Chadwick discovered the third subatomic particle (Neutron) in 1932. The *neutron* has almost the same mass as the proton, but it is electrically neutral.

1.3. Rutherford's Model of the Atom

The British physicist Ernest Rutherford proposed in 1911 a new theory of the scattering of α-particles (helium nuclei) by matter; based on a new atomic model and was successful in describing the experimental results. This theory abolished the suggestion made by Thomson in 1898, which was that "atoms are simply positively charged lump of matter with electrons embedded in them just like that raisins in a fruitcake" as shown in Fig. 1.1.

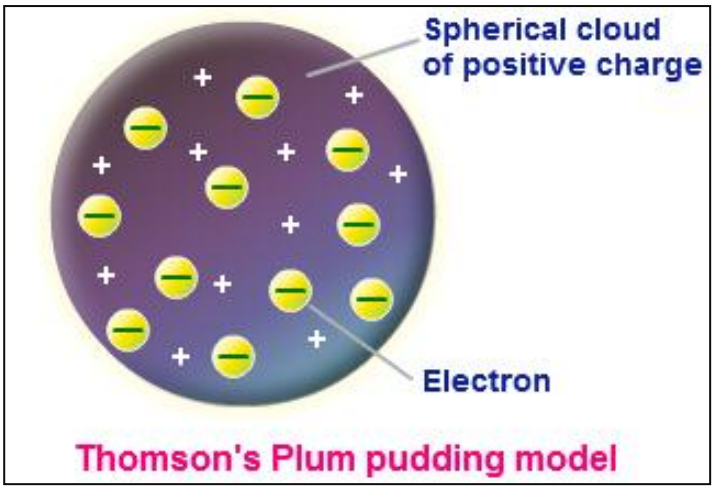

Figure 1.1. Thomson's model of atom.

Rutherford designed an experiment similar to that of Fig. 1.2 where α-particle emitted behind a screen with a small hole in it, so that a narrow beam of α-particles was produced. This beam was then directed at a thin gold foil. A zinc sulfide screen, which gives off a visible flash of light when struck by an alpha particle, was set on the side of the foil, replaced by a detector in Fig. 1.-2. What Rutherford actually found was that although most of the α-particles indeed were not deviated by much, a few were deflected in very large angles. Some were even deflected in the backward direction. He suggested that the deflection of an α-particle through a large angle could be caused by a single encounter with an atom rather than by multiple scattering. He supposed that there is an electric field near an atom which agreed well with this kind of experimental evidence.

Rutherford proposed a simple model of the atom, which could provide such a field. He assumed that the positive charge of the atom, instead of being distributed uniformly

throughout a region of the size of the atom, is concentrated in a minute center or nucleus, and that the negative charge is distributed over a sphere of radius comparable with the atomic radius; Fig. 1.3 shows the structure within the atom.

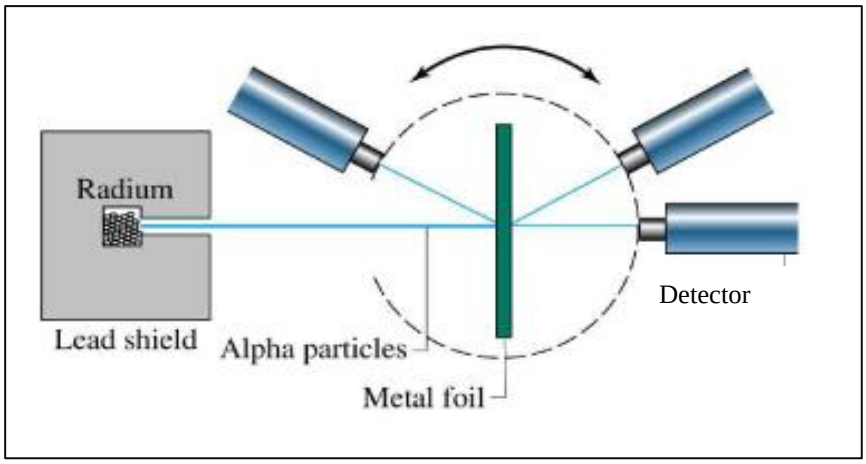

Figure 1.2. A novel apparatus for testing the angular dependence of α-particle scattering.

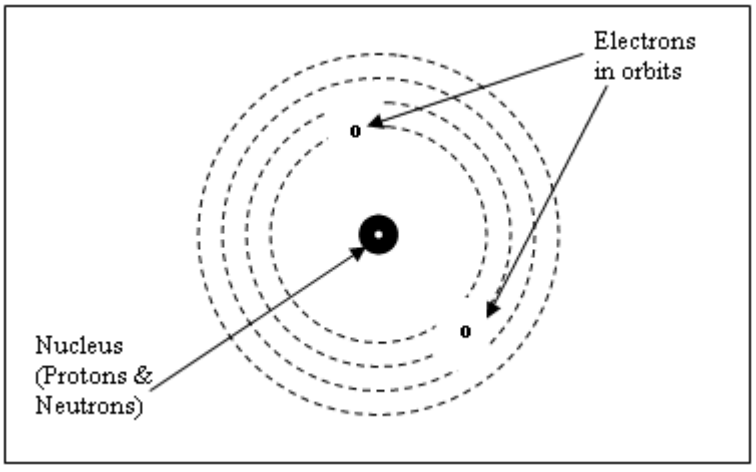

Figure 1.3. Rutherford's model of atom.

1.4. Bohr's Model of the Atom

In a series of epoch-making papers written between 1913 and 1915, the physicist Bohr developed a theory of the constitution of atoms, which accounted for many of the properties of atomic spectra and laid the foundations for later research on theoretical and experimental atomic physics. N. Bohr, coupling Rutherford's postulation with the quantum theory introduced by Max Planck, proposed the following postulates:

1- *The atom consists of a dense nucleus of protons surrounded by equal number of electrons traveling in discrete circular orbits (stationary states) at fixed distances from the nucleus, retaining their motion under the influence of the Coulomb force without emission of radiation*.

Since the Coulomb force between an orbiting electron and the stationary positive nucleus of charge *Ze* is equal to the centripetal force, we can find expressions for the total orbital energy *E* of the electron at an orbital radius *r*:

$$F = -k\frac{Ze^2}{r^2} = -\frac{m\upsilon^2}{r} \qquad 1.1$$

where the force *F* is equal to the Coulomb force and the centripetal force, respectively; $k = 1/4\pi\varepsilon_o = 8.99\times10^9\ N.m^2/C^2$ is a Coulomb force constant, *m* is the rest mass of the electron and υ is the electron speed.

It is a standard procedure in electrostatic to the Coulomb force Eq.1.1 to obtain the potential energy V of the electron:

$$V = -k\frac{Ze^2}{r} \qquad 1.2$$

The negative sign is present because the force is attractive. The kinetic energy T is $\frac{1}{2}m\upsilon^2$. Therefore the total energy E, being the sum of the potential and kinetic energies, is:

$$E = T + V = \frac{1}{2}m\upsilon^2 - k\frac{Ze^2}{r} = -k\frac{Ze^2}{2r} \qquad 1.3$$

2- *The different possible stationary states of a system consisting of an electron rotating about a positive nucleus are those for which the orbits are circles determined by the angular momentum L.*

$$L = m\upsilon r \quad = n\hbar \qquad 1.4$$

where n = 1, 2, 3… is a principle quantum number, and $\hbar = h/2\pi$ is Planck's constant, with h=6.63×10^{-34}J-s.

Eqs.1.3 and 1.4 can be solved for the radius of the n^{th} orbit r_n.

$$r_n = \frac{n^2\hbar^2}{kmZe^2} \qquad 1.5$$

The radius of the allowed orbits are proportional to n^2, and the radius of the smallest possible orbit (ground state) is obtained by setting n = 1, with the known values of the other quantities. For hydrogen Z = 1 the ground state radius called the *Bohr radius* is:

$$r_1 = \frac{\hbar^2}{kme^2} = 0.529\times10^{-10}m = 0.529\,\overset{o}{A} \qquad 1.6$$

The value of the radius from Eq.1.5 can be substituted into Eq.1.3 to get an expression for the energy that depends on known quantities.

$$E_n = -\frac{mk^2Z^2e^4}{2n^2\hbar^2} \qquad 1.7$$

The *ground state energy for hydrogen* obtained by using n = 1 and Z = 1 in this equation is E_1 = -13.58 eV. This energy is just the amount needed to ionize a hydrogen atom and is sometimes denoted by E_1 for ionization energy. Then the expression for the radius and energy of the n^{th} level is:

$$r_n = n^2 r_1, \quad and\ E_n = \frac{E_1}{n^2} \qquad 1.8$$

3- *Any emission or absorption of radiation will correspond to a transition between two stationary states*.

When an electron changes from one orbit n_i to another n_f, a photon is emitted whose energy is equal to the difference in energy between the two orbits:

$$h\upsilon = E_f - E_i = E_1\left(\frac{1}{n_f^2} - \frac{1}{n_i^2}\right) \qquad 1.9$$

where υ is the frequency of the emitted photon.

This equation for the frequency has exactly the same form as Balmer's formula, which was found to represent the lines of the Balmer's series of the hydrogen spectrum. Fig. 1.4 is Bohr's model of the hydrogen atom showing an electron as having just dropped from the third shell to the first shell with the emission of a photon that has energy $= h\nu$

(*Lyman series*). Hawever Bohr's theory was the first that successfully accounted for the discrete energy levels of this radiation as measured in the laboratory. Although Bohr's atomic model is designed specifically to explain the hydrogen atom, his theories apply generally to the structure of all atoms.

The properties of the three subatomic particles are listed in Table 1.1.

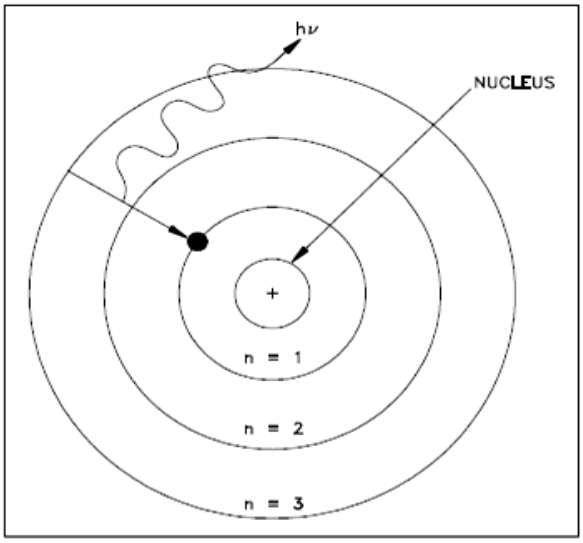

Figure 1.4. Bohr's model of the Hydrogen atom.

Table 1.1. Properties of subatomic particles.

Particle	Location	Charge	Mass
Electron	Shells around nucleus	-ve	0.0005486 u
Proton	Nucleus	+ve	1.007277 u
Neutron	Nucleus	none	1.008665 u

1.5. Measuring Units on the Atomic Scale

The size and mass of atoms are so small that the use of normal measuring units, while possible, is often inconvenient.

First, the conventional unit of mass, the kilogram, is rather large for use in describing characteristics of nuclei. For this reason, a special unit called the Atomic Mass Unit (amu or u) is often used. This unit is defined as $1/12^{th}$ of the mass of the stable most commonly occurring isotope of carbon, ^{12}C. In terms of grams, units of measure have been defined for mass and energy on the atomic scale to make measurements more convenient to express. One atomic mass unit is equal to1.66×10^{-27} *kg*.

Second, the unit for energy is the electron volt (eV); the electron volt is the amount of energy acquired by a single electron when it falls through a potential difference of one volt. Energy of one electron volt is equivalent to 1.602×10^{-19} joules.

Third, the unit of the size of the atom, comes from the radii of nuclei and atoms, is Fermi (fm), where $1fm=10^{-15}$ m $= 10^{-13}$ cm.

1.6. Equivalence of Mass and Energy

The great theory of 20^{th} century physics that is indispensable to the development of atomic and nuclear physics is the special theory of relativity proposed by Einstein in 1905. The first applications of the relativity theory depend on two closely related ideas. One idea is that of the variation of mass of a particle with its velocity; the second is that of the proportionality between mass and energy, so that the mass can be considered to be as another

form of energy. Thus, the law of conservation of energy is really the law of mass-energy. In normal every day interactions, the amount of mass that is transferred into other forms of energy (or vice versa) is such a tiny fraction of the total mass that it is beyond our sensory perceptions and measurement techniques. Thus, in a chemical reaction, for example, mass and energy truly seem to be separately conserved. In a nuclear reaction, however, the energy released is often about a million times greater than in a chemical reaction, and the change in mass can easily be measured. The mass and energy are related by what is certainly the best-known equation in physics:

$$E = mc^2 \qquad 1.10$$

In which E is the energy equivalent called *mass energy* of mass m, and c is the speed of light.

A real understanding of this relationship can come only from a careful study of the relativity theory that is beyond the scope of this textbook. However, the main relationships of the special theory of relativity will be discussed.

After the problem raised by the Michelson-Morley experiment of propagation of light, Einstein interpreted their negative results to mean that it is indeed impossible to detect any absolute velocity through the ether. He deduced the time as the fourth dimension and found the interdependence between the space and time coordinates. One of the most important concepts developed in the original formulation of the relativity theory was the mass of a particle, as measured by an observer, was a function of its *velocity* υ relative to the observer. The term *relativistic mass* m, was used for the mass of a particle moving with relativistic speed, that is, a speed comparable to the *speed of light c* (3×10^8 m s^{-1}). The

relativistic mass *m* was given in terms of mass m_0 of the particle at rest by the equation.

$$m = \frac{m_0}{\sqrt{1-\upsilon^2/c^2}} \qquad 1.11$$

The quantity m_0 is usually referred to as the *rest mass* of the particle. One of the consequences of this equation is that the relativistic mass approaches infinity as the velocity υ approaches the velocity of light c. Stated another way, no material particle can move with velocity greater than *c*.

The variation of mass with velocity leads to modifications of our ideas about energy. Because energy is the integral of force with respect to distance, *kinetic energy T* can be represented by the following expression:

$$T = \int_0^s F ds \qquad 1.12$$

where *F* is the component of the applied force in the direction of the displacement *ds*, and *s* is the distance over which the force acts.

Using the relativistic form of the second law of motion:

$$F = \frac{d(m\upsilon)}{dt} \qquad 1.13$$

Then the expression for kinetic equation (Eq.1.12) becomes:

$$T = \int_0^s \frac{d(m\upsilon)}{dt} ds = \int_0^{m\upsilon} \nu d(m\upsilon) \qquad 1.14$$

Now inserting Eq.1.11 for *m* we get:

$$T = \int_0^{\nu} \upsilon d\left(\frac{m_0 \upsilon}{\sqrt{1 - \upsilon^2 / c^2}} \right) \qquad 1.15$$

Integrating the last equation by parts, we get:

$$T = mc^2 - m_0 c^2 \qquad 1.16$$

This result states that the kinetic energy of a body is equal to the increase in its mass consequent upon its relative motion multiplied by the square of the speed of light. This equation may also be interpreted as meaning that the rest mass m_0 is associated with an amount of energy m_0c^2, which may be called the *rest energy* E_0 of the body. The *total energy E* of the body is then the sum of the kinetic energy and the rest energy, or:

$$\begin{aligned} E &= T + m_0 c^2 = T + E_0 \\ &= mc^2 = \frac{m_0 c^2}{\sqrt{1 - \upsilon^2 / c^2}} \end{aligned} \qquad 1.17$$

Hence, associated with a mass *m*, there is an amount of energy mc^2; conversely, to an energy *E*, there corresponds a mass given by:

$$m = \frac{E}{c^2} \qquad 1.18$$

The *momentum associated* with the transfer of energy is another important consequence of the proportionality between mass and energy. If a quantity of energy is

transferred with a velocity υ, we can write for the magnitude of the associated momentum P:

$$p = m\upsilon = \frac{E\upsilon}{c^2} \qquad 1.19$$

Eq.1.17 is a first-order relation for the total energy. In connection with Eq.1.19, a second-order relation can be found to express the total energy:

$$E^2 = c^2 p^2 + E_0^2 \qquad 1.20$$

For electromagnetic radiation or light quantum (photon), Eq.1.19 can be applied to the energy and momentum carried by the photon.

$$E = h\nu \qquad 1.21$$

$$p = \frac{E}{c^2}c = \frac{E}{c} = \frac{h\nu}{c} = \frac{h}{\lambda} \qquad 1.22$$

where h is, Planck's constant, υ and λ are the frequency and wavelength of the photon respectively.

In addition, its velocity is c. In Eq.1.22, the de Broglie wave wavelength is defined as $\lambda = h/p$.

Two limiting cases are worth mentioning.

1- Non-relativistic regime ($E_0 >> T$), then:

$$p = (2m_0T)^{1/2}, \qquad \lambda = \frac{h}{(2m_0T)^{1/2}} = \frac{h}{m_0\upsilon} \qquad 1.23$$

2- Extreme relativistic regime ($T >> E_0$), her energy is usually denoted as E rather than T, then:

$$p = \frac{E}{c}, \qquad \lambda = \frac{hc}{E} \tag{1.24}$$

Eq.1.24 also applies to photons and neutrinos, which have zero rest mass. The kinematical relations just discussed are general. In practice, we can safely apply the *non-relativistic expressions to neutrons, protons, and all nuclides*, because their rest mass energies are always much greater than any kinetic energies we will encounter. The same is not true for electrons, since we will be interested in electrons with energies in the MeV region. Thus, the two extreme regimes do not apply to electrons, and one should use Eq.1.20 for the energy-momentum relation.

The rest mass of the photon must be zero; otherwise the mass of a photon traveling with the velocity of light would be infinite, because the denominator of Eq.1.11 becomes zero for $\upsilon = c$. Although the rest mass of a photon is zero, the photon has a mass associated with its kinetic energy, according to Eq.1.18. This mass is $\frac{h\nu}{c^2}$, and corresponding to this mass is the momentum $\frac{h\nu}{c}$.

It is often convenient in nuclear physics to use the energy corresponding to one atomic mass unit (1 amu). This mass is 1.66×10^{-24} g, or 931.5 MeV. Then for any particle, its total energy is given by:

$$E\ (MeV) = m\ (u) \times 931.5 \tag{1.25}$$

1.7. Nuclide Classifications

The total number of protons in the nucleus of an atom is called the *atomic number* of the atom and is given the symbol Z. The number of electrons in an electrically neutral atom is the same as the number of protons in the nucleus. The number of neutrons in a nucleus is known as the neutron number and is given the symbol N. The *mass number* of the nucleus is the total number of nucleons, that is, total number of protons and neutrons in the nucleus. The mass number is given the symbol A and can be found by sum of $Z + N = A$.

Each of the chemical elements has a unique atomic number because the atoms of different elements contain a different number of protons. The atomic number of an atom identifies the particular element.

Each type of atom that contains a unique combination of protons and neutrons is called a *nuclide*. Not all combinations of numbers of protons and neutrons are possible, but about 2500 specific nuclides with unique combinations of neutrons and protons have been identified. Each nuclide is denoted by the chemical symbol of the element with the atomic number written as a subscript and the mass number written as a superscript, as shown in Fig. 1.5. Because each element has a unique name, chemical symbol, and atomic number, only one of the three is necessary to identify the element. For this reason, nuclides can also be identified by either the chemical name or the chemical symbol followed by the mass number (for example, U-235 or uranium-235). Another common format is to use the abbreviation of the chemical element with the mass number superscripted (for example, ^{235}U).

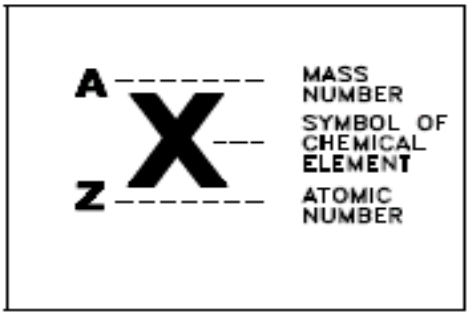

Figure 1.5. Nomenclature for identifying nuclides.

Example:

State the name of the element and the number of protons, electrons, and neutrons in the nuclides listed below:

$^{1}_{1}H$, $^{10}_{5}B$, $^{14}_{7}N$, $^{114}_{48}Cd$, $^{239}_{94}Pu$

Solution:

The name of the element can be found from the Periodic Table (refer to Chemistry Fundamentals Handbook) or the Chart of the Nuclides (to be discussed later). The number of protons and electrons is equal to Z. The number of neutrons is equal to A-Z.

Nuclide	*Element*	Protons	*Electrons*	*Neutrons*
$^{1}_{1}H$	*Hydrogen*	1	1	0
$^{10}_{5}B$	*Boron*	5	5	5
$^{14}_{7}N$	*Nitrogen*	7	7	7
$^{114}_{48}Cd$	*Cadmium*	48	48	66
$^{239}_{94}Pu$	*Plutonium*	94	94	145

1.7.1. Isotopes

Isotopes are nuclides that have the same atomic number and are therefore the same element, but differ in the number of neutrons. Most elements have a few stable isotopes and several unstable, radioactive isotopes. For example, oxygen has three stable isotopes that can be found in nature (oxygen-16, oxygen-17, and oxygen-18) and eight radioactive isotopes. Another example is hydrogen, which has two stable isotopes (hydrogen-1 and hydrogen-2) and a single radioactive isotope (hydrogen-3).

Different isotopes of the same element have essentially the same chemical properties. The isotopes of hydrogen are unique in that each of them is commonly referred to by a unique name instead of the common chemical element name. Hydrogen-1 is usually referred to as hydrogen. Hydrogen-2 is commonly called deuterium and symbolized ${}^{2}_{1}\mathrm{D}$. Hydrogen-3 is commonly called tritium and symbolized ${}^{3}_{1}\mathrm{T}$. It is convenient to use the symbols ${}^{2}_{1}\mathrm{H}$ and ${}^{3}_{1}\mathrm{H}$ for deuterium and tritium, respectively.

1.7.2. Isobars

Isobars are those nuclides that have the same mass number (A), but different numbers of protons and neutrons (Z & N). A special case is, when two isobars have proton and neutron numbers interchanged as in ${}^{A}_{Z}X_{A-Z}$ *and* ${}^{A}_{Z-1}Y_{A-Z+1}$, they are called *mirror nuclides, e.g.,* $\left({}^{15}_{8}O_{7} \text{ and } {}^{15}_{7}N_{8}\right)$.

1.7.3. Isotones

Isotones are those nuclides that have the same number of neutrons (N), but different numbers of protons and mass numbers (Z & A).

1.8. Nuclear Radii and Densities

It is difficult to define exactly the size of an atom because the electron cloud, formed by the electrons moving in their various orbitals, does not have a distinct outer edge. A reasonable measure of atomic size can be the average distance of the outermost electron from the nucleus. Except for a few of the lightest atoms, the average atomic radii are approximately the same for all atoms, about 2×10^{-8} cm. Like the atom, the nucleus does not have a sharp spherical outer boundary.

Like any other object, the size and the shape of an object is to examine the radiation scattered from it (taking its photograph). To see the object and its details, the wavelength of the radiation must be smaller than the dimensions of the object; otherwise, the effects of diffraction will partially or completely obscure the image. For nuclei with a diameter of about *10 fm*, we require $\lambda \leq 10\ fm$. corresponding to $p \geq 100\ MeV/c$. The experimental access to obtain information on nuclei radii comes from scattering particles (e^-, p, $\pi^{\pm}$,…) off the atomic nucleus with appropriate energy. Electron scattering off nuclei is, for example, one of the most appropriate methods to deduce nuclear radii and charge distribution. Experiments have shown that the nucleus is a shaped like a sphere with a radius that depends on the atomic mass number of the atom with the central nuclear charge and/or matter density is nearly the same for all nuclei. Nucleons do not seem to congregate near the center of the nucleus, but instead have a fairly constant distribution out to the surface. Thus, the number of nucleons per unit nuclear volume is roughly constant.

$$Nucleon\ density = \frac{A}{\frac{4}{3}\pi R^3} = Constant \qquad 1.26$$

where: R= mean radius of the nucleus

A = atomic mass number

Calling R_0 an elementary radius for a nucleon in the nucleus, a most naïve estimate is given for the nuclear volume $V=4/3\pi R^3$;

$$V = 4/3\pi R_0^3 A \qquad 1.27$$

or $$R = R_0 A^{1/3} \qquad 1.28$$

This relation describes the variation of the *nuclear radius*, with a value of $R_0 \approx 1.2\ fm$ when deducing a 'charge' distributing radius, and a value of $R_0 \approx 1.4\ fm$ for the full 'matter' distributing radius. The values of the nuclear radii for some light, intermediate, and heavy nuclides are shown in Table 1.2.

The table clearly shows that the radius of a typical atom (e.g. 2 x 10^{-8} cm) is more than 25,000 times larger than the radius of the largest nucleus.

Table 1.2 calculated values for nuclear radii.

Nuclide	Radius of nucleus
${}_{1}^{1}H$	$1.25\times10^{-13}cm$
${}_{5}^{10}B$	$2.69\times10^{-13}cm$
${}_{26}^{56}Fe$	$4.78\times10^{-13}cm$
${}_{72}^{178}Hf$	$7.01\times10^{-13}cm$
${}_{92}^{238}U$	$7.74\times10^{-13}cm$
${}_{98}^{252}Cf$	$7.89\times10^{-13}cm$

Experimental measurements as well as theoretical calculations based on quantum mechanics give the most detailed descriptions of the complete *nuclear charge and matter distribution*. A corresponding typical profile is a Fermi or Woods-Saxon shape, described by the expression:

$$\rho_{ch}(r) = \frac{\rho_0}{1 + e^{(r-R)/a}} \qquad 1.29$$

Here ρ_0 is the central density which has a value in the range 0.08-0.06 for medium to heavy nuclei and decreases slowly with increasing mass number. a = 0.524 fm describes the diffuseness of the nuclear surface.

Fig. 1.6 shows how diffuse the nuclear surface appears to be. The charge density, in unit efm^{-3} is roughly constant out to a certain point and then drops relatively slowly to zero. The distance, over which this drop occurs is nearly independent of the size of the nucleus, and is usually taken to be constant, the distance over which the charge density falls from 90% of its central value to 10% is defined as *skin thickness t*, its value is approximately 2.3 fm.

A useful quantity to determine the relationship between the nuclear radius and mass number, based on electron scattering result is the *mean square charge distribution radius*:

$$\left\langle r^2 \right\rangle = \int_0^\infty r^2 \rho_{ch}(r) dr \qquad 1.30$$

Then by solving the Schrödinger (or Dirac) equation using a Hamiltonian that includes the full electromagnetic interaction and using nuclear wavefunction or the so-called

Born approximation, the mean square charge radius for medium and heavy nuclei is given approximately by:

$$\left\langle r^2 \right\rangle = 0.94 A^{2/3}\ fm^2 \qquad 1.31$$

The nucleus is often approximated by a homogeneous charge sphere. The radius R of this sphere is then quoted as the nuclear radius. The relation of this to mean square radius is $R^2 = \frac{5}{3}\left\langle r^2 \right\rangle$, so that:

$$R_{ch} = 1.25\ A^{1/3}\ fm \qquad 1.32$$

On the other hand, to determine the *nuclear matter density*, instead of an electron, a strongly interacting particle (Hadron) has to be used as a projectile. At high energies, the nucleus behaves more like an absorbing sphere (elastic scattering is only a small part of interaction). In this case, the incident particle of momentum p will have an associated quantum mechanical wave of wavelength $\lambda = h/p$ (as will be seen in Chapter 5) and will suffer diffraction-like effects, as in optics, that is to say, we are dealing with the nuclear strong interaction (neglecting coulomb interaction).

Taking the presence of neutrons into account by multiplying $\rho_{ch}(r)$ by *A/Z*, we find an almost identical nuclear matter density in the nuclear interior for all nuclei, i.e. the decrease in ρ_0 with increasing A is compensated by the increase in A/Z with increasing A. The interior nuclear density, given by:

$$\rho_{mat} = nucleon\ density \times mass\ of\ nucleon$$
$$\rho_{mat} \approx 0.17\ nucleons/fm^3 \approx 2.845 \times 10^{17}\ kg/m^3, \qquad 1.33$$

is independent of *A*, and this density is approximately 10^{14} times normal matter density and expresses the highly packed density of nucleus.

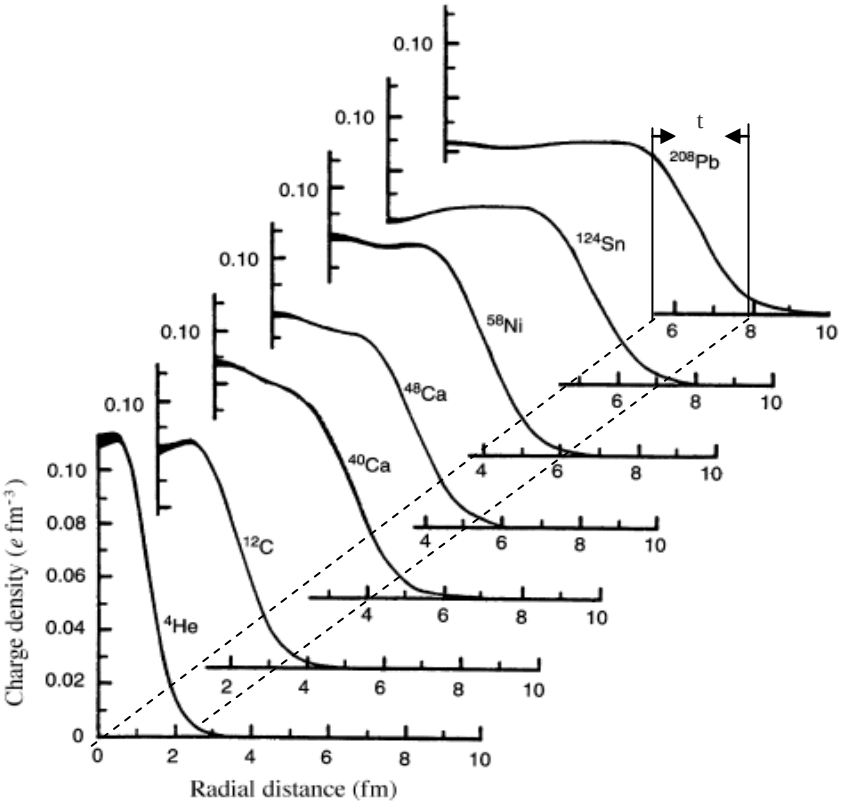

Figure 1.6. Radial charge distributions ρ_{ch} of various nuclei.

1.9. Forces in the Nucleus

In the Bohr's model of the atom, the nucleus consists of positively charged protons and electrically neutral neutrons. Since both protons and neutrons exist in the nucleus, they both referred to as nucleons. One problem that the Bohr's model of the atom faced was accounting for an attractive

force to overcome the repulsive force between protons inside the nucleus.

The two classical forces present in the nucleus are (1) electrostatic forces between charged particles and (2) gravitational forces between any two objects that have mass. It is possible to calculate the magnitude of the gravitational force and electrostatic force based upon principles from classical physics. However, to bind the nucleus together, there must be a strong attractive force of totally different kind, strong enough to overcome the repulsive force of the positively charged nuclear protons and to bind both protons and neutrons into this tiny volume.

1.9.1. Gravitational force

Newton stated that the *gravitational force* between two bodies is directly proportional to the masses of the two bodies and inversely proportional to the square of the distance between the bodies. This relationship is shown in the equation below:

$$F_g = \frac{G m_1 m_2}{r^2} \qquad 1.34$$

where:

F_g = gravitational force (Newton)
m_1 = mass of first body (kilogram)
m_2 = mass of second body (kilogram)
G = gravitational constant (6.67×10^{-11} N-m^2/kg^2)
r = distance between particles (meter)

The equation illustrates that the larger the masses of the objects are or the smaller the distance between the objects is,

the greater the gravitational force is. Therefore, even though the masses of nucleons are very small, the fact that the distance between nucleons is extremely short may make the gravitational force significant. It is necessary to calculate the value for the gravitational force and compare it to the value for other forces to determine the significance of the gravitational force in the nucleus. The gravitational force between two protons that are separated by a distance of 10^{-20} meters is about 10^{-24} Newtons.

1.9.2. Electrostatic force

Coulomb's Law can be used to calculate the force between two protons. The *electrostatic force* is directly proportional to the electrical charges of the two particles and inversely proportional to the square of the distance between the particles. Coulomb's Law is stated in terms of the following equation.

$$F_e = \frac{KQ_1Q_2}{r^2} \qquad 1.35$$

where:

F_e = electrostatic force (Newton)
$K = 1/4\pi\varepsilon_0$, electrostatic constant (9.0×10^9 N-m^2/C^2)
Q_1 = charge of first particle (coulomb)
Q_2 = charge of second particle (coulomb)
r = distance between particles (meter)

Using this equation, the electrostatic force between two protons that are separated by a distance of 10^{-20} meters is about 10^{12} Newtons. Comparing this result with the calculation of the gravitational force, (10^{-24} Newton) shows that the gravitational force is so small that one can neglect it.

1.9.3. Nuclear force

If only the electrostatic and gravitational forces existed in the nucleus, it would be impossible to have stable nuclei composed of protons and neutrons. The gravitational forces are much too small to hold the nucleons together compared to the electrostatic forces repelling the protons. Since stable atoms of neutrons and protons do exist in nature, there must be other attractive force acting within the nucleus; this force is called the nuclear force.

The *nuclear force* is a strong attractive force that is independent of charge. It acts only between pairs of neutrons, pairs of protons, or a neutron and a proton. The nuclear force has a very short range; it acts only over distances approximately equal to the diameter of the nucleus (10^{-15} m), even less. The attractive nuclear force between all nucleons drops off with distance much faster than the repulsive electrostatic force does between protons. As will be seen in the next section, the nuclear force can be divided into three families of interactions due to a strong force that binds quarks together to form neutrons and protons.

In stable atoms, the attractive and repulsive forces in the nucleus are balanced. If the forces do not balance, the atom cannot be stable, and the nucleus will emit radiation in an attempt to achieve a more stable configuration. Table 1.3 summarizes the behavior of each force.

Table 1.3 Forces acting in the nucleons.

Force	Interaction	Range
Gravitational	very weak attractive force between all nucleons	relatively long
Electrostatic	strong repulsive force between protons	relatively long
Nuclear force	strong attractive force between all nucleons	extremely short

1.10. Elementary Particles

It is hard to define elementary particle, but one can define it as 'that particle which has no internal constitution (construction) when bounded (not free)'.

As the scattering experiments technologies, as well as the quantum mechanics theory developed in early 1950s, very large numbers of unstable particles with very short lifetime have been discovered. This immerged in the mid 1960s in the form of QUARK model, by M.Gell-Mann. He postulated that new bounded particles were of three families of more fundamental physical particles called quarks. Each quark is characterized by its mass, electric charge and its spin.

Three nuclear interaction forces (Nuclear Force) can belong to three families of elementary particles. These different particles are responsible for the nuclear interaction phenomena. The three nuclear forces are.

1- Electromagnetic interaction force.

The most familiar elementary particle is the electron, which we know is bound in atom by the electromagnetic interaction, where the interaction force is transmitted discontinuously by the exchange of the PHOTONS; a particle of zero mass and zero charge. This interaction is described by a highly successful theory called Quantum Electrodynamics QED.

2- Strong nuclear interaction force.

It is responsible for binding the nucleus. It is a short-range force whose magnitude is independent of the type of nucleon, proton or neutron (charge independent). This force acts by the exchange of MESONS elementary particles.

The theory that describes the strong interactions, that is, the force that acts between quarks, is called Quantum Chromodynamics QCD, this force is repulsive at very short range as well as being attractive at greater nucleon-nucleon distances; this keeps the nucleons in the nucleus packed together but not mashed together.

3- Weak nuclear interaction force.

The weak force is a short-range force responsible for all kinds of decays (Beta, neutron decays …) by the exchange of BOSONS elementary particles.

1.10.1. Mesons

Are elementary particles that carry the nuclear force between nucleons, having a mass-energy of the order 200 MeV, and an integer spin momentum S=0. Free meson can be produced in nucleon-nucleon collisions and then decay

rapidly to lighter mesons or photons within a very short decay lifetime of order 10^{-20}– 10^{-8} s.

The families of mesons are.

1- π-mesons (PIONS) are the lightest member of spin momentum s = 0, mass about 270 times the mass of electron, and the rest mass energy $m_\pi c^2$ = 140 MeV. Pions exist in three forms, which are π^+ (of positive charge), π^- (of negative charge), and π^0 (neutral). The maximum range of mesons r_{max} can be computed by Heisenberg uncertainties, to be.

$$r_{\max} = \frac{\hbar}{m_\pi c} = \frac{\hbar c}{m_\pi c^2} \qquad 1.36$$

r_{max} = 197 MeV.fm/ 140 MeV = 1.4 fm

2- Bosons are massive mesons and accordingly are of shorter range, with integer spin momentum s = 1or 2. The common types of bosons which contribute to nuclear force are.

η meson	$m_\eta c^2$ = 549 MeV
B meson	$m_B c^2$ = 5278 MeV
ω meson	$m_\omega c^2$ = 782 MeV

Some other elementary particles, which are now considered to be a small member of physical entities, include quarks, (electron, neutrinos called Leptons), photon, and nucleons called Baryons, and more others.

Problems

1-1 What was the minimum distance to which the 7.69 MeV alpha particles could approach the center of the gold nuclei in Rutherford's experiments?

1-2 What is the largest quantum number of the atomic state of the Li^{+2} ion with an orbital radius less than 50 A^{o}?

1-3 Hydrogen atoms in states of high quantum number have been created in the laboratory and observed in space. They are called Rydberg atoms. a- Find the quantum number of the Bohr orbit in a hydrogen atom whose radius is 0.01 mm. b- What is the energy of a hydrogen atom in this state?

1-4 An electron collides with a hydrogen atom in its ground state to the excited state of n = 3. How much energy was given to the hydrogen atom in this inelastic collision (kinetic energy is not conserved)?

1-5 What is the orbital velocity of the electron in the excited state of the problem 1.4?

1-6 What is the wavelength and momentum of a photon of lowest energy in the Ballmer series of hydrogen?

1-7 Calculate the ratio of the mass of a particle to its rest mass when the particle moves with speeds that are the following fractions of the speed of light: 0.2, 0.5, 0.8, 0.9, 0.95, and 0.99.

1-8 Derive the following useful relationships concerning the relativistic properties of moving particles:

$a-\quad (Pc)^2 = (mc^2)^2 - (m_o c^2)^2 \qquad b-\quad P = \frac{1}{c}\sqrt{T^2 + 2m_o c^2 T}$

$c-\quad m_o = \frac{1}{c^2}\sqrt{E^2 - (Pc)^2} \qquad b-\quad T = \sqrt{(m_o c^2)^2 + (Pc)^2} - m_o c^2$

1-9 The speed of a proton is increased from 0.2c to 0.4c, by what factor does its kinetic energy increase? Now if the speed is doubled again to .8c, by what factor does the kinetic energy increase now?

1-10 Derive Eq.1.25.

1-11 A stationary body explodes into two fragments; each has mass 1.0 Kg that move apart at speeds of 0.6c relative to the original body. Find the mass of the original body.

1-12 Suppose two photons, each of energy 0.5 MeV, collide to form a particle, find the mass of that particle. If the velocity of the formed particle is 0.8c, what is its rest mass?

1-13 The greater the atomic number Z of an atom is, the larger its nucleus is and the closer its inner electrons are to the nucleus. Compare the radius of the $^{238}_{92}U$ nucleus with the radius of its innermost Bohr orbit.

1-14 Estimate the nuclear radius of the ground state of the following isotopes $^{111}_{51}Sb, ^{111}_{49}In$. What are their cross-sectional areas?

1-15 Using the $R \propto A^{1/3}$ observation, estimate the average mass density of a nucleus in (kg/m^3) and compare with the atomic density of hydrogen.

1-16 What is the charge density of the nucleus in a boron-10 and uranium-238 atoms? Compare your results with their material densities.

1-17 Determine the expected (possible) location of the following elementary particles: a- proton, b- η meson, c- m=0.05 u.

1-18 How much energy would a proton particle need in order to "just touch" the nuclear surface in a gold foil?

1-19 Find the expected elementary particle mass energy that may be responsible for the K-capture in the following isotopes; ${}_{1}^{1}H, {}_{64}^{152}Gd$.

CHAPTER 2

PERTINENT NUCLEAR PROPERTIES

2.1. Neutron - Proton Ratios

A nuclear species is characterized by its number of protons Z and number of neutrons N. There are thousands of combinations of N and Z that lead to nuclei that are sufficiently long-lived to be studied in the laboratory. The large number of possible combinations of neutrons and protons is to be compared with the only 100 or so elements characterized simply by Z.

Fig. 2.1 shows the distribution of the world nuclides plotted on the same axes as the *Chart of the Nuclides*. Most nuclei are unstable, i.e., radioactive. Generally, for each $A = N + Z$ there is only one or two combinations of (N, Z) sufficiently long-lived (or stable) to be naturally present on earth in significant quantities. These nuclei are the black squares in Fig. 2.1 that define the bottom of the *valley of stability*.

As the mass numbers become higher, the ratio of neutrons to protons in the nucleus becomes larger. For example, helium-4 (2 protons and 2 neutrons) and oxygen-16 (8 protons and 8 neutrons); this ratio is unity. While for indium-115 (49 protons and 66 neutrons), the ratio of neutrons to protons has increased to 1.35, and for uranium-238 (92 protons and 146 neutrons), the neutron to proton ratio is 1.59.

Generally speaking, when we examine the characteristics of stable nuclei, we find that for $A < 40$, the number of protons equals the number of neutrons (N = Z), as ^{40}Ca.

However, beyond A = 40, stable nuclei have $N \sim 1.7Z$, namely, neutrons far outnumber protons (see Fig. 2.1). This can be understood from the fact that, in larger nuclei, the charge density, and therefore the destabilizing effect of Coulomb repulsion, is smaller when there is a neutron excess.

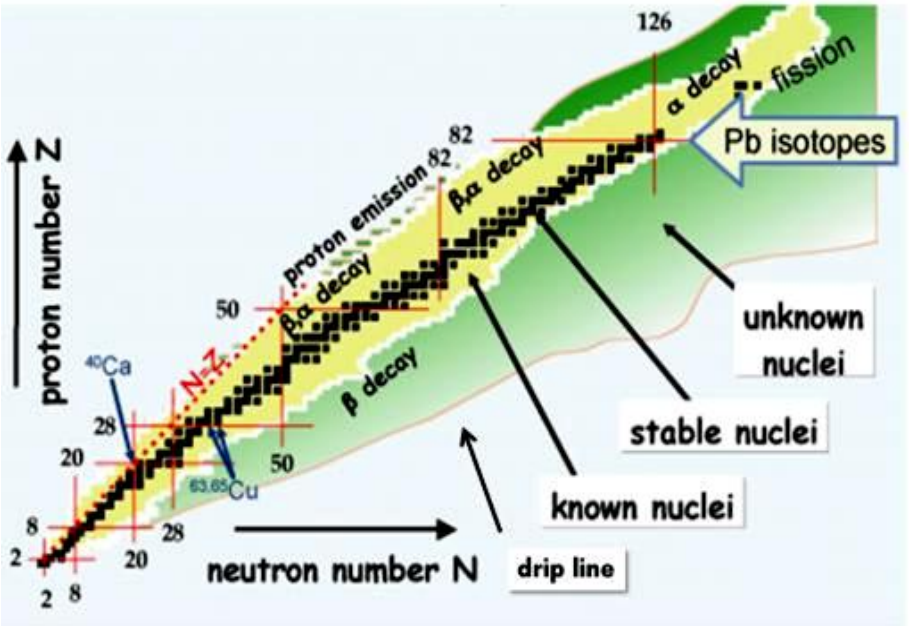

Figure 2.1. Neutron - Proton Plot of the world Nuclides.

Furthermore, a survey of the stable nuclei (see Table 2.1) reveals that even-even nuclei are the ones most abundant in nature. This again lends support to the strong-pairing hypothesis, namely that pairing of nucleons leads to nuclear stability.

In Fig. 2.1, the black squares are long-lived nuclei present on earth. Unbound combinations of (N, Z) lie outside the lines marked 'last proton/neutron unbound' which are predicted to be unbound. Most other nuclei are β-decay or α-decay to stable nuclei.

Table 2.1. Number of stable nuclei in nature.

N	Z	Number of stable nuclei
Even	Even	156
Even	Odd	48
Odd	Even	50
Odd	Odd	5

If a heavy nucleus were to split into two fragments, each fragment would form a nucleus that would have approximately the same neutron-to-proton ratio as the heavy nucleus. This high neutron-to-proton ratio places the fragments below and to the right of the stability curve displayed by Fig. 2.1. The instability caused by this excess of neutrons is generally rectified by successive beta emissions, each of which converts a neutron to a proton and moves the nucleus toward a more stable neutron-to-proton ratio.

2.2. Chart of the Nuclides

A tabulated chart called the *Chart of the Nuclides*, *National Nuclear Data Center,* http://www.nndc.bnl.gov/chart/, lists the world stable and unstable nuclides in addition to pertinent information about each one. Fig. 2.2 shows a small portion of a typical chart. This chart plots a box for each individual nuclide, with the number of protons (Z) on the vertical axis and the number of neutrons (N =A - Z) on the horizontal axis.

The completely white squares indicate stable isotopes. Those in gray (colored in the original chart) squares are *artificially radioactive*, meaning that they are produced by artificial techniques and do not occur naturally. By consulting a complete chart, other types of isotopes can be found, such as naturally occurring radioactive types (but none are found in the region of the chart that is illustrated in Fig. 2.2).

Located in the box on the far left of each horizontal row is general information about the element. The box contains the chemical symbol of the element in addition to the average atomic weight of the naturally occurring substance and the average thermal neutron absorption cross section. The known isotopes (elements with the same atomic number Z but different mass number A) of each element are listed to the right.

The chart of nuclides is very useful in determining the different radioactive decays, and allows visualizing entire decay chains in the effective fashion. The different radioactive decays can easily be connected with movement in the chart, e.g. *alpha-decay* corresponds to two-left, two-down, *beta*(-ve) *decay* corresponds to one-left, one–up, and *beta*(+ve) *decay* corresponds to one-right, one–down, as shown in Fig. 2.3.

2.2.1. Information for stable nuclides

For the stable isotopes, in addition to the symbol and the atomic mass number, the number percentage of each isotope in the naturally occurring element (the abundance) is listed in the chart of nuclides, as well as the thermal neutron activation cross section and the mass in *atomic mass units* (u) may be available.

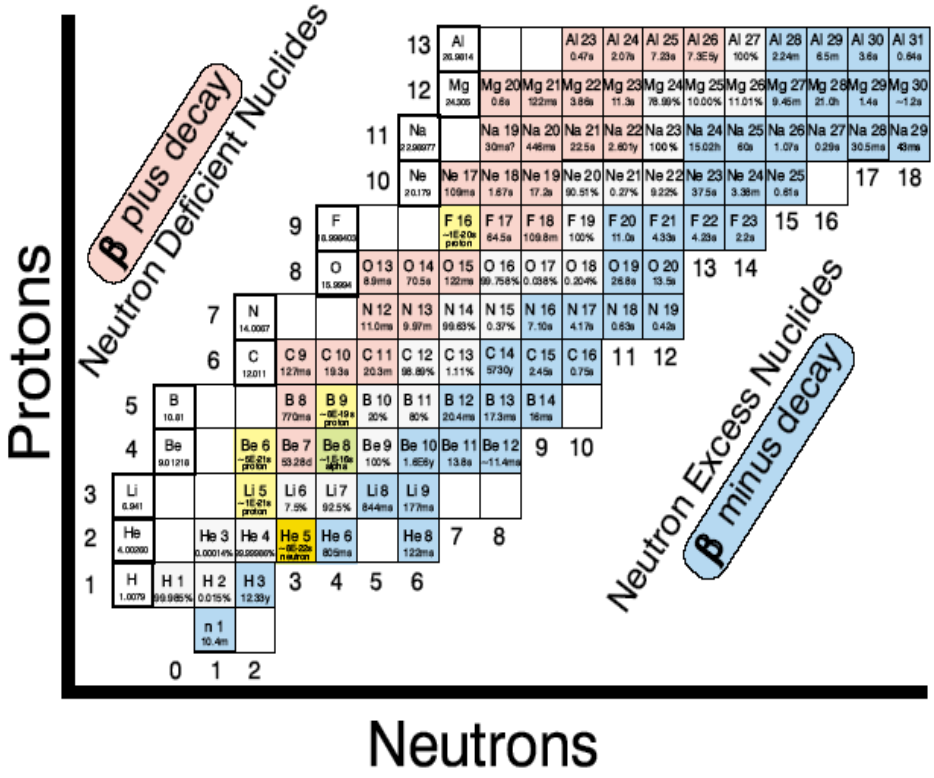

Figure 2.2. Chart of the nuclide for atomic numbers 1 to 13.

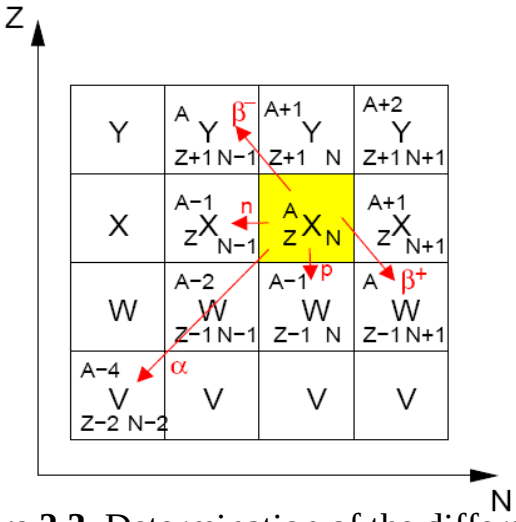

Figure 2.3. Determination of the different radioactive decays.

2.2.2. Information for unstable nuclides

For unstable isotopes the additional information includes the half-life, the mode of decay (for example, β, α), the total disintegration energy in MeV (million electron volts), and the mass in u when available.

2.3. Natural Abundance of Isotopes

The relative abundance of an isotope in nature compared to other isotopes of the same element is relatively constant. The chart of the nuclides presents the relative abundance of the naturally occurring isotopes of an element in units of atom percent. Atom percent is the percentage of the atoms of an element that are of a particular isotope. Atom percent is abbreviated as a/p.

For example, if a cup of water contains 8.23×10^{24} atoms of oxygen, and the isotopic abundance of oxygen-18 is 0.20%, there are 1.65×10^{22} atoms of oxygen-18 in the cup.

The atomic weight for an element is defined as the average atomic mass of the isotopes of the element. The atomic weight for an element can be calculated by summing the products of the isotopic abundance of the isotope with the atomic mass of the isotope.

$$Atomic\ weight = \sum_{\text{Isotopes}} a/p * atomic\ mass\ of\ isotope \qquad 2.1$$

Example:

Calculate the atomic weight for the element lithium. Lithium-6 has an atom percent abundance of 7.5% and an atomic mass of 6.015122 u. Lithium-7 has an atomic abundance of 92.5% and an atomic mass of 7.016003 u.

Solution:

Atomic weight (Lithium) = (0.075)(6.015122 u)+(0.925)(7.016003 u)
= 6.9409 u

The other common measurement of isotopic abundance is weight percent (w/o). Weight percent is the percentage weight of an element that is a particular isotope. For example, if a sample of material contained 100 kg of uranium that was 28 w/o uranium-235, 28 kg of ^{235}U was present in the sample.

The atomic percentage of isotopes can be changed artificially in processes called *enrichment processes* because they selectively increase the proportion of a particular isotope. The enrichment process typically starts with feed material that has the proportion of isotopes that occur naturally.

Natural uranium mined from the earth contains the isotopes ^{238}U, ^{235}U and ^{234}U. The majority (99.2745%) of all the atoms in natural uranium are ^{238}U. Most of the remaining atoms (0.72%) are ^{235}U, and slight traces (0.0055%) are ^{234}U. Although all isotopes of uranium have similar chemical properties, each of the isotopes has significantly different nuclear properties. The isotope ^{235}U is usually the desired material for use in reactors.

A vast amount of equipments and energy are expended in processes that separate the isotopes of uranium. The details of these processes are beyond the scope of this book. The process results in two types of uranium, the natural uranium ore is 0.72 a/o ^{235}U. The desired outcome of the enrichment process is to produce enriched uranium. *Enriched uranium* is defined as uranium in which the isotope ^{235}U has a concentration greater than its natural value. The enrichment process will also result in the byproduct of depleted uranium. *Depleted uranium,,* is defined as uranium in which

the isotope ^{235}U has a concentration less than its natural value. Although depleted uranium is referred to as a by-product of the enrichment process, it does have uses in the nuclear field and in commercial and defense industries.

2.4. Mass Defect and Binding Energy

The separate laws of conservation of mass and conservation of energy are not applied strictly to the nuclear level. It is possible to convert between mass and energy. Instead of two separate conservation laws, a single conservation law states that the sum of mass and energy is conserved. Mass does not magically appear and disappear at random. A decrease in mass will be accompanied by a corresponding increase in energy and vice versa.

Before going on the discussion of mass defect and binding energy, it is convenient to introduce a conversion factor derived by the mass-energy relationship from Einstein's Theory of Relativity.

Einstein's famous equation relating mass and energy is $E = mc^2$ (Eq.1.1) where c is the velocity of light (c = 2.998 x 10^8 m/sec). The energy equivalent of 1 u can be determined by inserting this quantity of mass into Einstein's equation and applying conversion factors.

$$
\begin{aligned}
E &= mc^2 \\
&= 1\text{u}\{1.6606\times10^{-27}\text{kg/1u}\}\ \{2.998\times10^{8}\text{m/sec}\}^2 \\
&\qquad (1\text{N/1kg.m/sec}^2)(1\text{J/1N.m}) \\
&= 1.4924\times10^{-10}\ \text{J}\{1\ \text{MeV}/1.6022\times10^{-13}\ \text{J}\} \\
&= 931.5\ \text{MeV}
\end{aligned}
$$

2.4.1. Mass defect

Careful measurements have shown that the mass of a particular atom or isotope is always slightly less than the number of nucleons (sum of the individual neutrons and protons) of which the atom consists. The difference between the atomic mass of the atom and the total number of nucleons (A) in the nucleus is called the *mass defect or mass excess* (Δm). The mass defect can be expressed in terms of atomic mass units and/or in terms of energy as:

$$\Delta m = M(Z,N) - A \text{ u} \qquad 2.2a$$

$$\Delta m = \{M(Z,N) - A\}931.5\ MeV \qquad 2.2b$$

where: Δm = mass defect (u or MeV)
$M(Z, N)$ = mass of nuclide ${}^{A}_{Z}X$ (u)
A = mass number

In calculating the mass defect, it is important to use the full accuracy of mass measurements because the difference in mass is small compared to the mass of the atom. Rounding off the masses of atoms and particles to three or four significant digits prior to the calculation will result in a calculated mass defect of zero.

Example:

Calculate the mass defect for lithium-7. The mass of ^{7}Li is 7.016003 u.

Solution:

Apply Eq. 2.2a	Applying Eq. 2.2b
Δm = 7.016003 -7	Δm = (7.016003 -7)931.5
= 0.016003 u	= 14.9067945 MeV

2.4.2. Binding energy

Binding energy is defined as the amount of energy that must be supplied to a nucleus to completely separate its nuclear particles (nucleons). It can also be understood as the amount of energy that would be released if the nucleus was formed from the separate particles.

Since 1 u is equivalent to 931.5 MeV of energy, the binding energy can be calculated by the mass difference between the nucleus and the sum of those of the free nucleons, including the mass of electrons associated with protons.

$$BE(Z,A) = \{Zm_p + Zm_e + (A-Z)m_n - M(Z,N)\}c^2 \quad 2.3a$$

or

$$BE(Z,A) = \{Zm_H + Nm_n - M(Z,N)\}931.5\ MeV \quad 2.3b$$

m_p = mass of proton (1.0072764 u)
m_n = mass of neutron (1.008665 u)
m_e = mass of electron (0.000548597 u)
$m_H = m_p + m_e$ = mass of hydrogen atom = (1.007825 u)

Appendix II tabulates, in addition to some other usefull informations, the atomic weight of all elements and the mass defect in MeV of all important isotopes. These values can be used to find the atomic mass of each isotope.

Example:

Calculate the mass defect and binding energy for uranium-235. One uranium-235 atom has a mass of 235.043924 u.

Solution:

Step 1: Calculate the mass defect using Equation (2.2*)*

$\Delta m = \{M(Z,N) - A\} 931.5\ MeV$

$= (235.043924 - 235)931.5 = 40.9152$ MeV

Step 2: Use the mass defect and Equation (2.3) to calculate the binding energy.

$BE = \{Zm_H + Nm_n - M(Z,N)\}931.5\ MeV$

$= \{[92(1.007826\ u) + (235-92)1.008665\ u]$

$- 235.043924\}931.5$

$BE = 1.91517\ u \times 931.5\ MeV/u = 1784$ MeV

2.4.3. Separation energy

The useful and interesting property of the binding energy is the neutron and proton separation energies. The neutron separation energy S_n *is the amount of energy required to remove a neutron from a nucleus,* ${}^{A}_{Z}X$ (sometimes called the binding energy of the last neutron). This is equal to the difference in binding energies between ${}^{A}_{Z}X$ and ${}^{A-1}_{Z}X$.

$$S_n = BE\,({}^{A}_{Z}X) - BE\,({}^{A-1}_{Z}X) \qquad 2.4$$

$$S_n = \{M\,({}^{A-1}_{Z}X) - M\,({}^{A}_{Z}X) + m_n\}\,c^2 \qquad 2.5$$

Similarly one can define proton separation energy S_p *as the energy needed to remove a proton from a nucleus* ${}^{A}_{Z}X$ (also called the binding energy of the last proton) which convert to another nuclide, ${}^{A-1}_{Z-1}Y$ and can be calculated as follows.

$$S_p = BE\,({}^{A}_{Z}X) - BE\,({}^{A-1}_{Z-1}Y) \qquad 2.6$$

$$S_p = \{M\,({}^{A-1}_{Z-1}Y) - M\,({}^{A}_{Z}X) + m\,({}^{1}H)\}\,c^2 \qquad 2.7$$

The Hydrogen mass appears in this equation instead of proton mass, since the atomic mass is m $(^1H) = m_p + m_e$.
The neutron and proton separation energies are analogous to the ionization energies in atomic physics, in terms of the binding of the outermost valance nucleons. Just like the atomic ionization energies, the separation energies show evidence for nuclear shell structure that is similar to atomic shell structure.

2.4.4. Binding energy per nucleon

As with many other nuclear properties that will be discussed in the coming sections, we gain valuable clues to nuclear structure from a systematic study of nuclear binding energy. As the number of particles in a nucleus increases, the total binding energy also increases. The rate of increase, however, is not uniform. This lack of uniformity results in a variation in the amount of binding energy associated with each nucleon within the nucleus. In other wards since the binding energy increases more or less linearly with atomic mass number A, it is convenient to show the variation of the average binding energy per nucleon, BE/A as function of A. Fig. 2.4 shows the average BE/A as plotted versus atomic mass number A.

Fig. 2.4 illustrates that as the atomic mass number increases, the binding energy per nucleon increases almost linearly for light elements (except for $^4_2He, ^8_4Be, ^{12}_6C, ^{16}_8O$), then rapidly for A < 60 reaches a maximum value of 8.79 MeV at A = 56 (close to iron) and decreases to about 7.6 MeV for A = 238. The average BE/A of most nuclei is, to within 10%, about 8 MeV.

The general shape of the BE/A curve can be explained using the general properties of nuclear forces. Very short-

range attractive nuclear forces that exist between nucleons hold the nucleus together. On the other hand, long-range repulsive electrostatic (coulomb) forces that exist between all the protons in the nucleus are forcing the nucleus apart. So the nuclear forces are very short range of the order of the diameter of one nucleon, or they saturate to pairs of nucleons (two protons and two neutrons) to form α-cluster. This is clear in light stable nuclei for A < 20 where the sharp rise appear to be off the curve. Those specific light stable nuclei are ${}_{2}^{4}He, {}_{4}^{8}Be, {}_{6}^{12}C, {}_{8}^{16}O$. This is due to the fact of higher BE/A of ${}_{2}^{4}He$ particle (or α-cluster) bounded in the nucleus and the other (A = 4n nuclei for n=1, 2 ...) stable nuclei for A < 20 compared to their neighbors. In other words, the 4n nuclei for n=1, 2, .. trend to make α-particles.

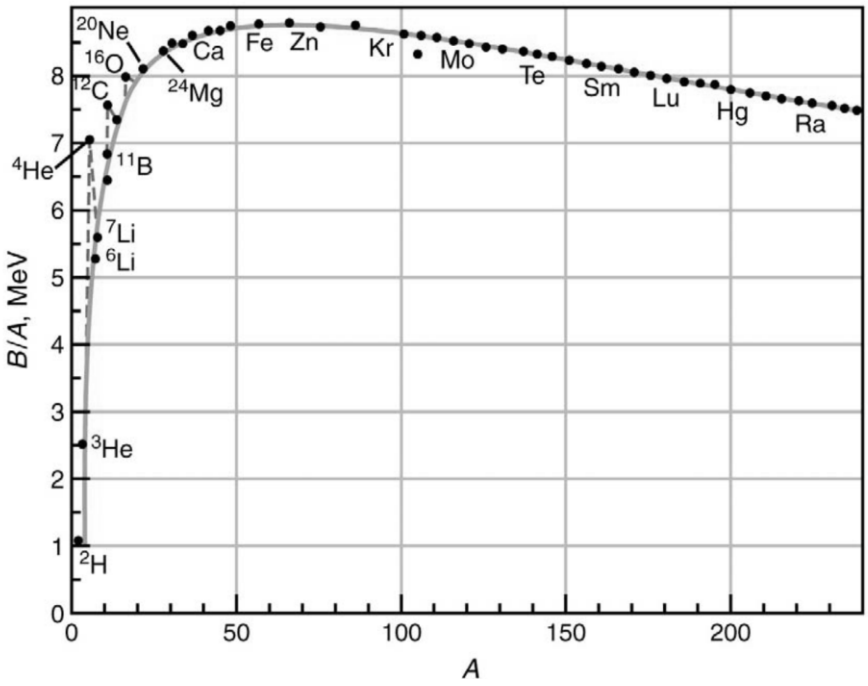

Figure 2.4. Binding Energy per Nucleon vs. Mass Number.

As the atomic number and the atomic mass number increase, the repulsive electrostatic forces within the nucleus increase due to the greater number of protons in the heavy elements. To overcome this increased repulsion, the proportion of neutrons in the nucleus must increase to maintain stability. This increase in the neutron-to-proton ratio only partially compensates for the growing proton-proton repulsive force in the heavier, naturally occurring elements. Because the repulsive forces are increasing, less energy must be supplied, on the average to remove a nucleon from the nucleus. The BE/A has decreased.

The BE/A of a nucleus is an indication of its degree of stability. Generally, the more stable nuclides have higher BE/A than the less stable ones. The increase in the BE/A as the atomic mass number decreases from 260 to 60 is the primary reason for the energy liberation in the fission process. In addition, the increase in the BE/A as the atomic mass number increases from 1 to 60 is the reason for the energy liberation in the fusion process, which is the opposite reaction of fission.

The heaviest nuclei require only a small distortion from a spherical shape (small energy addition) for the relatively large coulomb forces forcing the two halves of the nucleus apart to overcome the attractive nuclear forces holding the two halves together. Consequently, the heaviest nuclei are easily fissionable compared to lighter nuclei.

2.5. Mass Spectroscopy

Binding energies may be calculated if masses are measured accurately. One way of doing this is by using the techniques of mass spectroscopy. The principle of the method is shown in Fig. 2.5.

All mass spectroscopes begin with **ion source** region, which produces a beam of ionized atoms or molecules. Often a vapor of the material under study is bombarded with electrons to produce ions; in other cases, the ions can be formed as a result of a spark discharge between electrodes coated with the material. Ions emerging from the source have broad range of velocities, as might be expected for a thermal distribution, and many different masses might be included.

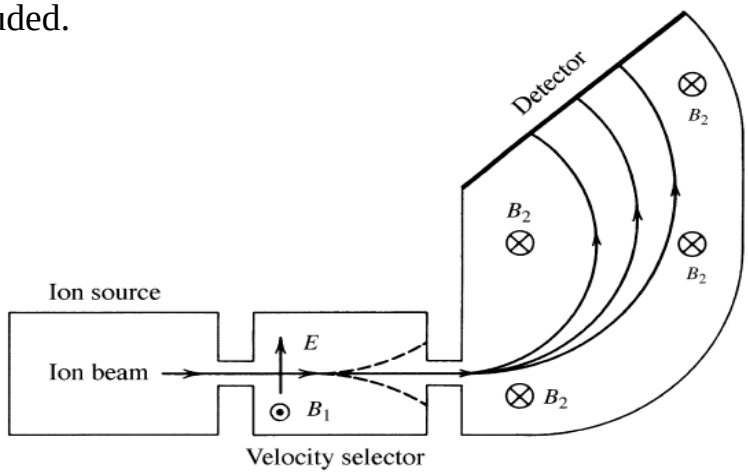

Figure 2.5. Schematic diagram of a mass spectrometer.

A source of ions of charge q, containing various isotopes passes through a second region called **velocity selector** where there are uniform electric (E) and magnetic (B_1) fields at right angles. The electric field will exert a force

$$F_E = qE \qquad 2.8$$

in one direction and the magnetic field will exert a force

$$F_B = q\upsilon B_1 \qquad 2.9$$

in the opposite direction, where υ is the speed of the ions. By balancing these forces, ions of a specific speed $\upsilon = E/B_1$

can be selected and allowed to pass through a collimating slit. Ions with other velocities (shown as dashed lines) are deflected. The beam is then allowed to continue through a third region **momentum selector** where a second uniform magnetic field B_2 will be exerted on the beam, then the beam will be bent into a circular path of radius r, given by:

$$m\upsilon = qB_2r \qquad 2.10$$

and since q, B_2 and v are fixed, particles with a fixed ratio q/m will bend in a path with a unique radius. Hence, isotopes may be separated and focused onto a detector (e.g. a photographic plate) with a proportional radii r.

$$\frac{q}{m} = \frac{E}{B_1B_2r} \qquad 2.11$$

In the common case where $B_1 = B_2 = B$.

$$\frac{q}{m} = \frac{E}{B^2r} \qquad 2.12a$$

or $$m = \frac{qB^2r}{E} \qquad 2.12b$$

In practice, to achieve high accuracy, the device is used to measure mass differences rather than absolute values of mass. We could calibrate for one particular mass, and then determine all masses by relative measurements. The fixed point on the atomic mass scale is ^{12}C, which is taken to be exactly 12.000000 u.

To determine the mass of another atom, such as ^{1}H, it would need to make considerable changes in E, $B_1$and B_2,

and it is perhaps questionable whether the calibration would be valid to one part in 10^6 over such a range. It would be preferable to measure the smaller difference between two nearly equal masses.

For example, let as set the apparatus for mass 128 and measure the difference between the molecular masses of C_9H_{20} (nonane) and $C_{10}H_8$ (naphthalene). This difference is measured to be Δm = 0.09390032 ± 0.00000012 u. Neglecting corrections for the difference in the molecular binding energies of the two molecules, which is of the order of 10^{-9} u, the mass difference can be calculated as follows:

$$\Delta m = M(C_9H_{20}) - M(C_{10}H_8) = 12M(^1H) - M(^{12}C)$$

Thus $$m(^1H) = 1/12\,[\,M(^{12}C) + \Delta m\,]$$
$$= 1.00000000 + 1/12\ \Delta m$$
$$= 1.00782503 \pm 0.00000001 \text{ u}$$

Then set the apparatus for mass 28 and determine the difference between C_2H_4 and N_2:

$$\Delta m = M(C_2H_4) - M(N_2) = 2M(^{12}C) + 4m(^1H) - 2M(^{14}N)$$
$$= 0.025152196 \pm 0.00000003 \text{ u}$$

Then the mass of ^{14}N can be found:

$$M(^{14}N) = M(^{12}C) + 2m(^1H) - \tfrac{1}{2}\Delta m$$
$$= 14.00307396 \pm 0.00000002 \text{ u}$$

This system of measuring small differences between close-lying masses is known as the mass doublet method.

In addition, the conventional mass spectroscopy cannot be used to find the masses of very short lived nuclei and in

these cases, the masses are determined from kinematical analysis of nuclear reactions.

2.6. Energy Levels of Atoms

The electrons that circle the nucleus move in fairly well defined orbits. Some of these electrons are more tightly bound in the atom than others. For example, only 7.38 eV is required to remove the outermost electron from a lead atom, while 88,000 eV is required to remove the innermost electron. The process of removing an electron from an atom is called ionization, and the energy required to remove the electron is called the ionization energy.

In a neutral atom (number of electrons = Z), it is possible for the electrons to be in a variety of different orbits, each with a different energy level. The state of lowest energy is the one in which the atom is normally found and is called the ground state. When the atom possesses more energy than its ground state energy, it is said to be in an excited state.

An atom cannot stay in the excited state for an indefinite period of time. An excited atom will either eventually transfer to a lower-energy excited state or directly to its ground state. This is performed by emitting a discrete bundle of electromagnetic energy called an x-ray. The energy of the x-ray will be equal to the difference between the energy levels of the atom and will typically range from several eV to 100,000 eV in magnitude.

2.7. Energy Levels of the Nucleus

The nucleons in the nucleus of an atom, like the electrons that circle the nucleus, exist in shells that correspond to energy states. The difference between them is that in

contrast to electrons, the nucleons have no center to orbit arroud it, as will be clarified in Chapter-7. The energy shells of the nucleons in the nucleus are less defined and less understood than those of the electrons of the atom. There is a state of lowest energy (the ground state) and discrete possible excited states for a nucleus. Where the discrete energy states for the electrons of an atom are measured in eV or keV, the energy levels of the nucleus are considerably greater and typically measured in MeV.

A nucleus that is in the excited state will not remain at that energy level for an indefinite period. Like the electrons in an excited atom, the nucleons in an excited nucleus will make a transition towards their lowest energy configuration, and in doing so, emit a discrete bundle of electromagnetic radiation called a gamma ray (γ-ray). The only differences between x-rays and γ-rays are their energy levels and whether they are emitted from the electron shell or from the nucleus.

The ground state and the excited states of a nucleus can be depicted in a nuclear energy-level diagram. The nuclear energy-level diagram consists of a stack of horizontal bars, one bar for each of the excited states of the nucleus. The vertical distance between the bar representing an excited state and the bar representing the ground state is proportional to the energy level of the excited state with respect to the ground state. This difference in energy between the ground state and the excited state is called the *excitation energy* of the excited state. The ground state of a nuclide has zero excitation energy. The bars for the excited states are labeled with their respective energy levels. Fig. 2. 6 is the energy level diagram for Nickel-60.

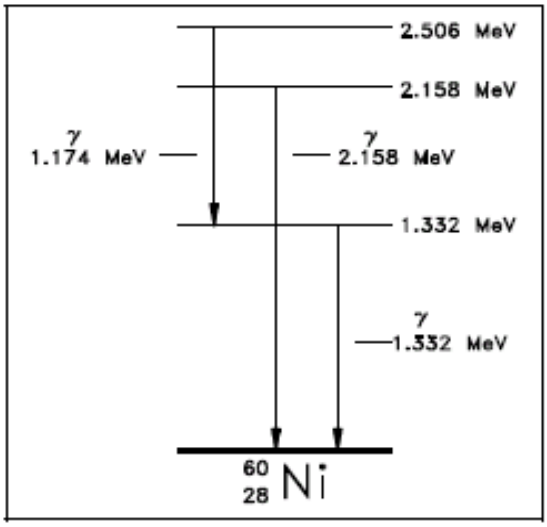

Figure 2.6. The energy level diagram for nickel-60.

2.8. Angular Moments in the Nucleus

Recall in classical mechanics, the angular momentum ***L*** of a particle moving with a linear momentum **p** at a location **r** around a reference point is:

$$\boldsymbol{L} = \boldsymbol{r} \times \boldsymbol{p} \qquad 2.13$$

While in quantum mechanics, as will be discussed in Chapter-5, in solution of Schrödinger equation in space we must evaluate the angular components of the wave function directly. The fundamental idea of the dual wave and particle nature of matter are expressed mathematically by means of a wave equation first derived by Schrödinger to describe the atomic and nuclear structures, degenerate energy states and other problems in terms of quantum numbers.

2.8.1. Orbital angular momentum

Since protons and neutrons move in an average field and so cause orbital angular momentum to build up, as will be seen in details in Chapter-5, the *expectation value of the angular momentum* of a nucleon is evaluated, and for simplicity by calculating the magnitude of the average value of $<L^2>$, instead of $<L>$.

Since the nucleus is an isolated system (no external torque acting on a system), then its angular momentum is conserved, and represented by *orbital quantum number* ℓ with a value:

$$<L^2> = \hbar^2 \ell(\ell + 1) \qquad 2.14$$

or

$$|L| = \hbar\sqrt{\ell(\ell+1} \qquad 2.15$$

with orbital quantum number restricted to the values $\ell = 0, 1, 2, 3$.

In addition, $< L^2 >=< L_x^2 + L_y^2 + L_z^2 >$ is a function of position, as shown in Fig. 2.7.

Analogy to the atomic physics, the nuclear physics use the same spectroscopic notation as shown below:

ℓ value	0	1	2	3	4	5	6
symbol	s	p	d	f	g	h	i

It is the very act of measuring one component of L that makes the others indeterminate; we usually choose the z-component to be determined to get:

$$<L_z> = \hbar m_\ell \qquad 2.16$$

Where m_ℓ = 0, ±1, ±2…, ± ℓ. is the *magnetic quantum number*. Notice that:

$$|< L_z >| < |\mathrm{L}| = \hbar\sqrt{\ell(\ell+1)} \qquad 2.17$$

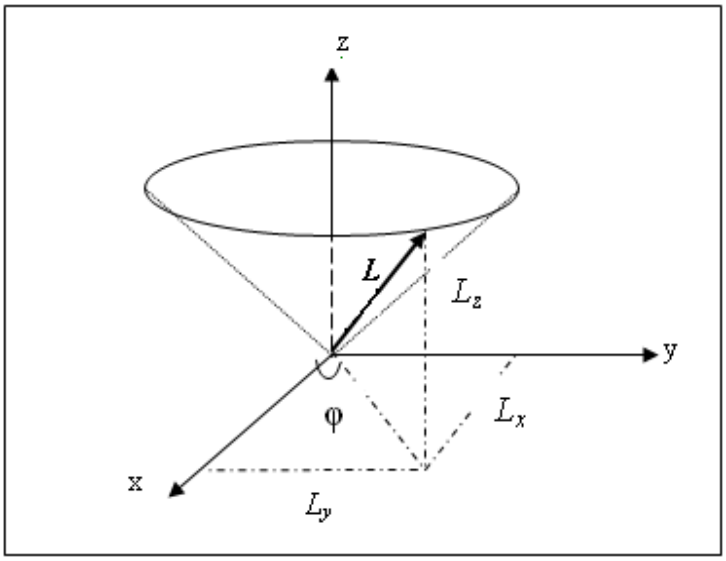

Figure 2.7. The vector ***L*** rotates about the z-axis, so that L_z stays constant, but L_x and L_y are variable.

2.8.2. Intrinsic angular momentum

As in the electronic state in atom, it is required to introduce a new quantum number called intrinsic quantum number or simply *spin* denoted by (s) with a value s = ½ for the nucleon. The spin can be treated as an angular momentum. Thus:

$$<s^2> \; = \; \hbar^2 s\,(s+1) \;\text{ or }\; |\mathrm{s}| = \hbar\sqrt{s(s+1}} \qquad 2.18$$

$$<s_z> \; = \; \hbar m_s \qquad 2.19$$

where $m_s = \pm ½$ is the *spin quantum number*.

It is often useful to imagine the spin as a vector **s** with possible z components of value:

$$<s_z> = \pm ½\hbar \qquad 2.20$$

2.8.3. Total angular quantum momentum

The bounded nucleons inside the nucleus, like electrons of the atom, move in a central potential with orbital angular momentum ***L*** and spin **s** will have a total angular momentum.

$$\boldsymbol{j = L + s} \qquad 2.21$$

The total angular momentum ***j*** has the same behavior of ***L*** and **s,** so that:

$$<j^2> = \hbar^2 j\,(j + 1) \text{ or } |j| = \hbar\sqrt{j(j+1}} \qquad 2.22$$

where j is the total angular momentum quantum number, then it can be written in term of the vector sum of the orbital angular momentum and spin momentum as shown in Fig. 2.8, with:

$$<j_z> = <\ell_z + s_z> = \hbar m_j \qquad 2.23$$

where $m_j = -j, -j+1, -j+2 \ldots, j-2, j-1, j$ $(m_j \neq 0)$

$$= m_\ell + m_s = m_\ell \pm ½ \qquad 2.24$$

is the *total angular quantum number*.

Since m_ℓ is always integer, m_j must be half-integer:

$m_j = \pm 1/2, \pm 3/2, \pm 5/2, \ldots\ldots$, then j also is a half integer.

Unlike electrons of the atom where electrons move in well-defined orbits with definite ***L*** and ***j,*** it is not clear that ***L*** and ***j*** of nucleons inside the nucleus have the same picture, will be described in nuclear shell model (Chapter-7).

Fig. 2.8 showes the relationship between the three angular momentua, (Left) the coupling giving j = ***L*** + ½. The vector ***L*** and ***s*** have definite lengths, as does ***j***. the coupling ***L*** and ***s*** vectors rotate about the direction of ***j***; in this coupling, the z components L_z and s_z thus do not have definite values. The vector ***j*** rotates about the z direction so that j_z has definite value. (Right) The similar case of j = L - ½. In interpreting both figures, keep in mind that all such representations of vectors governed by the rules of quantum mechanics are at best symbolic and at worst misleading.

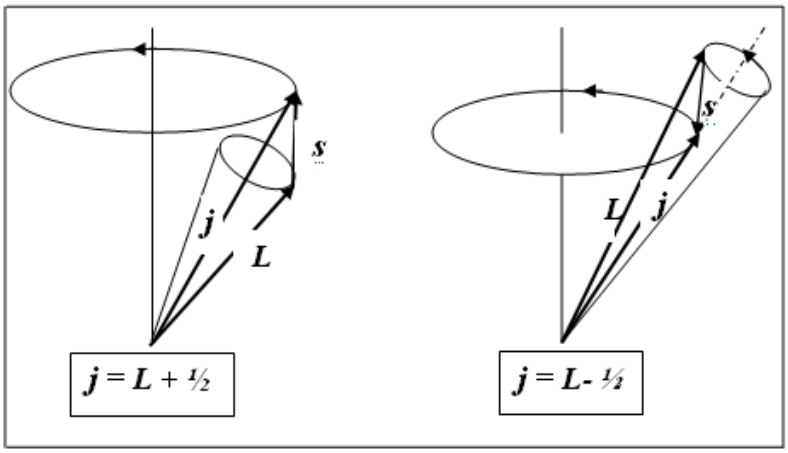

Figure 2.8. The coupling of orbital angular momentum ***L*** to spin angular momentum ***s*** giving total angular momentum ***j***.

2.8.4. Nuclear angular momentum

The original indication that nuclei have spin came from atomic spectroscopy. Many lines in atomic spectra, when examined with very high resolving power spectroscopes, are found to consist of several lines very close together. Such lines are said to exhibit *hyperfine structure*. Two sources of such structure, one due to the present of isotopes, the other has been found in spectral lines of nucleus of single isotope such as bismuth ^{209}Bi, the explanation of the last hyperfine structure spectral lines, is suggested by Pauli. Just like nucleons inside the nucleus, *the nucleus of the atom also spins about an axis and possesses a nuclear angular momentum.*

In the application of quantum mechanics to the nucleus, we label every nucleon (proton or neutron) with the corresponding quantum numbers ℓ, s, and j. The total angular momentum of a nucleus having (A) nucleons would then be the *vector sum of the total angular momentums of all nucleons* $\boldsymbol{j}$ and it is often called the *intrinsic angular momentum* or *nuclear spin* and is represented by the symbol ***I.*** It can be represented by:

$$\mathbf{I} = \sum_i \mathbf{j}_i \qquad 2.25$$

The nuclear spin $\boldsymbol{I}$ has the same properties of the quantum mechanical angular momentum vectors:

$$\langle I^2 \rangle = \hbar^2 I\,(I+1) \text{ and } I_z = m_I \hbar \qquad 2.26$$

where ($m_I = -I, -I+1..., I-1, +I$)

For many applications involving angular momentum, the nucleus behaves as if it is a single entity with an intrinsic angular momentum of (***I***). Moreover, we observe that the nucleus is a single spinning particle. For this reason, the nuclear spin (***I***) and the corresponding *spin quantum number* (*I*) are used to describe nuclear states, which can take on integral or half-integral values. The rules we must follows are:

even-A nuclei	I = integer
even Z – even N	$I = 0$
odd Z – odd N	I = integer
odd-A nuclei	I = odd half integer
even Z – odd N	I = odd half integer
odd Z – even N	I = odd half integer

The explanation of that is based on the assumption that the spin angular momentum ***I*** is a vector sum of the spin and the orbital angular moments of the particles within the nucleus and that these spins are aligned with their axes either parallel or anti-parallel.

2.9. Nuclear Magnetic Moments

We know that both, the protons (having an elementary positive charge e) and neutrons (have no charge) are moving inside the nucleus. Consequently, there are charge, mass and current densities. As a result, magnetic dipole and electric quadrupole moment produced.

Associated with the nuclear spin is a magnetic moment **μ**, which can take on any value because it *is not quantized*. This will provide additional information on the nature of

nuclear forces and help in selecting an appropriate nuclear model.

A method known as the *magnetic resonance method* was developed, and experiment carried out depending essentially on resonance between the precision frequency of the nuclear magnet about a constant magnetic field direction and the frequency of an impressed high-frequency magnetic field.

Just like for electrons of the atom, the nuclear magnetic moment of the orbital motion of a proton is expressed in terms of a *nuclear magneton* μ_N.

$$\mu_N = e\hbar/2m_p \qquad 2.27$$

where, m_p is the mass of the proton.

For the intrinsic spin of the nucleus, introduce a nuclear *g factor,* called *gyromagnatic ratio g,* to relate the magnetic moment $\boldsymbol{\mu}$ of a nucleus to its spin angular momentum $\boldsymbol{I}$. *The nuclear g factor is defined as the ratio of the nuclear magnetic moment, expressed in terms of nuclear magneton, to the spin angular momentum, expressed in units of* $\hbar$:

$$g = \boldsymbol{\mu}/\boldsymbol{I}\,\mu_N \qquad 2.28$$

hence

$$\boldsymbol{\mu}/g = \boldsymbol{I}\,\mu_N = \boldsymbol{I}\,e\hbar/2m_p \qquad 2.29$$

where $\mu_N = \mu_B/1840$

$= 0.505\times10^{-23}$ ergs/gauss

$= 3.15245\times10^{-14}$ MeV/T

Here, μ_B *is the Bohr magneton* $= 5.78838\times10^{-11}$ MeV/T.

When a nucleus of magnetic moment $\boldsymbol{\mu}$ is in a constant magnetic field $\boldsymbol{B}$, it will presses about the direction of $\boldsymbol{B}$ with a frequency f given by Larmor's theorem.

$$f = \boldsymbol{\mu B/I\hbar} \qquad 2.30$$

The magnetic moment $\boldsymbol{\mu}$ of a nucleus can thus be found by measuring Larmor frequency f.

Of very great importance in nuclear physics are the magnetic moments of the proton μ_p, neutron μ_n, and deuteron μ_d, their measured values are:

$$\mu_p = 2.792847 \ \mu_N$$
$$\mu_n = -1.913043 \ \mu_N$$
$$\mu_d = 0.857438 \ \mu_N$$

It is worthwhile to mention the fact that, since the nuclear magnetic moments are only of the order of magnitude of the nuclear magneton (<< Bohr magneton) is, therefore, another strong argument against the existence of electrons inside the nucleus.

2.10. Nuclear Electric Quadrupole Moment

Any distribution of electric charges and currents produces electric and magnetic fields that vary with distance in a characteristic fashion, the electric moment of a nucleus reflect the charge distribution (or shape) of the nucleus. It is customary to assign to the charge and current distribution an electromagnetic multi-pole moment:

The $1/r^2$ electric field arises from the spherical net charge, assign as zeros or monopole moment.

The $1/r^3$ electric field arises from the first or dipole moment.

The $1/r^4$ electric field arises from the second (quadrupole moment), and so on.

We consider a classical calculation of the energy that is due to electric quadruple moment. Suppose the nuclear charge has a cylindrical symmetry about an axis along the nuclear spin I, Fig. 2.9. The coulomb energy at the point S_1 is:

$$V(r,\theta) = \int d^3r \frac{\rho(r)}{d} \qquad 2.31$$

where $\rho(r)$ is the charge density, and $d = |\boldsymbol{r_1} - \boldsymbol{r}|$. We will expand this integral in a power series in $1/r_1$ by noting the expansion of $1/d$ in a Legendre polynomial series:

$$\frac{1}{d} = \frac{1}{r_1}\sum_{n=0}^{\infty}\left(\frac{r}{r_1}\right)^n P_n(\cos\theta) \qquad 2.32$$

where $P_0(x) = 1$, $P_1(x) = x$, $P_2(x) = (3x^2 - 1)/2$ …

Then Eq.2.31 can be written as:

$$V(r_1,\theta_1) = \frac{1}{r_1}\sum_{n=0}^{\infty}\frac{a_n}{r_1^n} \qquad 2.33$$

with:

$$\begin{aligned} a_0 &= \int \rho(r) d^3r = Ze \\ a_1 &= \int z\rho(r) d^3r = electric \quad dipole \\ a_2 &= \int \frac{1}{2}(3z^2 - r^2)\rho(r) d^3r = \frac{1}{2}eQ \end{aligned} \qquad 2.34$$

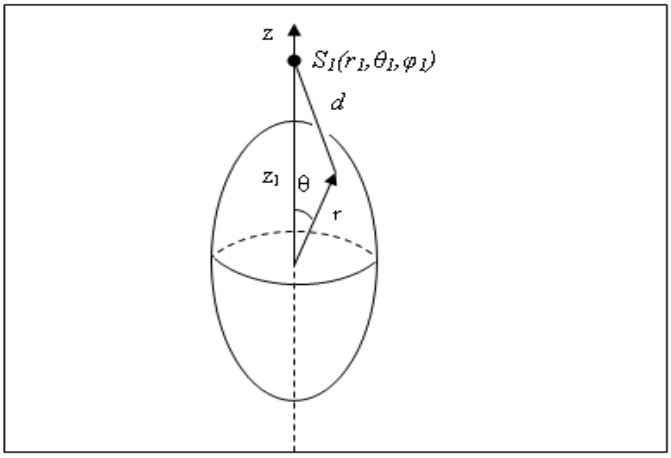

Figure 2.9. Geometry for calculating the Coulomb potential energy at the field point S_1 due to a charge distribution $\rho(r)$ on the spheroidal surface. The sketch is for r_1 located along the z – axis.

The coefficients in the expansion for the energy, Eq. 2.33, are recognized to be the total charge, the dipole (here it is equal to zero), the quadrupole, etc. In Eq.2.34, Q is defined to be the quadrupole moment (in unit of 10^{-24} cm^2, or barns). Notice that if the charge distribution were spherically symmetric, $\langle x^2\rangle = \langle y^2\rangle = \langle z^2\rangle = \langle r^2\rangle/3$, $Q = 0$.

We see also, $Q > 0$, if $3\langle z^2\rangle > \langle r^2\rangle$ and $Q < 0$, if $3\langle z^2\rangle < \langle r^2\rangle$. The corresponding shape of the nucleus in these two cases would be prolate or oblate spheroid, respectively. While for $Q = 0$, the shape of the nucleus remains sphere (see Fig. 2.10).

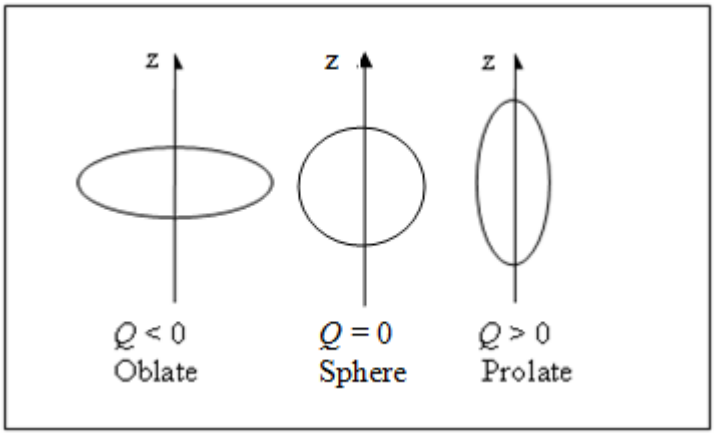

Figure 2.10. The spheroidal shapes of nuclei as indicated by the value of the electric quadrupole moment *Q*.

For many nuclei, *the quadrupole moment can be estimated from the valance nucleon that orbit near the nucleus surface*, then we can estimate $|eQ| \leq e\, R_0^2 A^{2/3}$, as shown in Table 2.2.

Table 2.2. Some values of the spin and quadrupole moments.

Nucleus	I	Q [10^{-24} cm^2]
n	1/2	0
p	1/2	0
^{2}H	1	0.00274
^{4}He	0	0
^{6}Li	1	-0.002
^{233}U	5/2	3.4
^{235}U	7/2	4
^{239}Pu	5/2	4.9

In quantum mechanics, electric quadrupole moment is determined with respect to the *probability density* $|\Psi|^2$.

$$eQ = e\int \Psi^*(3z^2 - r^2)\ \Psi\, dv \qquad 2.35$$

2.11. Nuclear Parity

In addition to their magnetic and electric properties, nuclei have certain properties which are not obviously physical in nature. Among them is the *parity*. To a good approximation, the wave function of a nucleus may be expressed as the product of a function of the space coordinates and a function depending only on the spin orientation. The motion of a nucleus is said to have *even parity* if the spatial part of its wave function is unchanged when the space coordinates (x, y, z) are replaced by (-x, -y, -z), or ($\mathbf{r} \rightarrow \mathbf{-r}$) i.e., reflection of the nucleus. While when reflection changes the sign of the spatial part of the wave function, the motion of the nucleus is said to have *odd parity*.

For example:

If $\Psi(\mathbf{r}) = +\Psi(\mathbf{-r})$ is even parity wave function
If $\Psi(\mathbf{r}) = -\Psi(\mathbf{-r})$ is odd parity wave function
$\Psi(x) = \cos(kx)$ is even parity wave function
$\Psi(x) = \sin(kx)$ is odd parity wave function
$V(x) = \frac{1}{2}\, kx^2$ is even parity wave potential
$V(x) = \frac{1}{2}kx$ is odd parity wave potential

In relation to the value of the orbital angular momentum L, as will be discussed in Chapter 5, the parity of the energy state donated is by π. The parity of a state is determined by

the orbital angular momentum quantum number ℓ as, $\pi = (-1)^{\ell}$.

A quantum state of a nucleus is defined by the parity, its energy and its total angular momentum of the constituent nucleons *j* written conventionally as:

$$j^{\pi} \equiv j^{(-1)^{\ell}} \qquad 2.36$$

For example, the nucleus of mass number A with the last proton in a state with $\ell = 2$, its parity is even, while the neutron in the last state with $\ell = 3$ has odd parity. The parity of the nucleus is therefore odd.

The electric moment and magnetic moment are also determined by the parity:

$$\pi = \begin{cases} (-1)^{L} & \text{Electric moment.} \\ (-1)^{L+1} & \text{Magnetic moment.} \end{cases} \qquad 2.37$$

where:

L = 0 means monopole
L = 1 means dipole
L = 2 means quadrupole
L = 3 means octupole etc

With the following restrictions, all odd parity multipole momentums must vanish, while only E2 (electric quadrupole) & M1 (magnetic Dipole) remain.

Problems

2-1 What happens to the atomic number and mass number of a nucleus when it a- emits an alpha particle, b- emits a positron, c- emits an electron, d- captures an electron?

2-2 Which nucleus would you expect to be more stable, ${}^{7}_{3}Li$ *or* ${}^{8}_{3}Li$; ${}^{13}_{6}C$ *or* ${}^{15}_{6}C$? Then what type of decay the unstable isotope may undergoe?

2-3 Gallium occurs with two natural isotopes, ^{69}Ga (60.2% abundant) and ^{71}Ga (39.8%), having atomic weights 68.93 u and 70.92 u. What is the atomic weight of the element?

2-4 The atomic weight of lithium is 6.941 u. It has two natural isotopes, ^{6}Li and ^{7}Li, with atomic weights of 6.015 u and 7.016 u. What is the relative abundance of the two isotopes?

2-5 Calculate the total binding energy of the alpha particle He^{++}, compare with the binding energy of the ^{4}He nuclide.

2-6 Calculate the mass defect and binding energy per nucleon for the nuclide ^{40}K.

2-7 The binding energy per nucleon of ${}^{24}_{12}Mg$ is 8.26 MeV. Find its mass defect and its atomic mass.

2-8 (a) Find the energy needed to remove a neutron from the nucleus of the calcium isotope ${}^{42}_{20}Ca$.

(b) Find the energy needed to remove a proton from this nucleus.

(c) Why are these energies different?

2-9 For the following two nuclei ${}^{65}_{29}Cu, {}^{65}_{30}Zn$, determine which one must decay to the other and what is the type of decay?

2-10 A nuclear scientist attempts to perform experiments on the ${}^{56}_{26}Fe$ stable nuclide. Determine the energy (in MeV) required to:
(a) Remove a single neutron,
(b) Remove a single proton,
(c) Completely dismantle the nucleus into its individual components,
(d) Fission it symmetrically into two identical lighter nuclides ${}^{28}_{13}Al$. [The exact masses of the ${}^{56}_{26}Fe$ and ${}^{28}_{13}Al$ atoms are 55.934942 u and 27. 981910 u, respectively.]

2-11 Show that the potential energy of two protons 1.7 fm (the maximum range of nuclear force) apart is of the correct order of magnitude to account for the difference in binding energy between ^{3}H and ^{3}He. How does this result bear upon the question of the dependence of nuclear forces on electron charge?

2-12 The neutron in free space decays into a proton and electron. What must be the minimum energy contributed by a neutron to a nucleus in order that the neutron does not decay inside the nucleus? How does this figure compare with the observed BE/A in stable nuclei?

2-13 Calculate the binding energy of the last neutron in ^{4}He and the last proton in ^{16}O. How do these compare with BE/A

for these nuclei? What does this tell you about the stability of ^{4}He relative to ^{3}He, and of ^{16}O relative to ^{15}N?

2-14 Figure 2.4 shows a plot of the average binding energy per nucleon BE/A vs. the mass number A. In the fission of a nucleus of mass number A_o (mass M_o) into two nuclei A_1 and A_2 (masses M_1 and M_2), the energy released is:

$$Q = M_o c^2 - M_1 c^2 - M_2 c^2$$

Express Q in terms of (BE/A) and A. Estimate Q for symmetric fission of a nucleus with $A_o = 240$.

2-15 The ionization energy E_I of the first three elements are:

Z	Element	E_I
1	H	13.6 eV
2	He	24.6 eV
3	Li	5.4 eV

(a) Explain qualitatively the change in E_I from H to He, Li.

(b) What is the second ionization energy of He that is the energy required to remove the second electron after the first one is removed?

2-16 Find the total quantum numbers (m_j) for *p* and *d* orbital angular momentum.

2-17 Determine the nuclear g value for the ground state of ^{1}H, ^{2}H, and free neutron. What will be the value for first excited state of ^{1}H nucleus?

2-18 Give the expected spin and parity assignments for the ground states of the nucleus having the following nucleons and orbital angular momenta.

(a) A proton in $\ell=0$; (b) two protons in $\ell=1$; (c) 2 protons and 3 neutrons in $\ell=2$; (d) 3 neutrons and 3 protons in $\ell=3$.

CHAPTER 3

MODE OF RADIOACTIVE DECAY AND NUCLEAR REACTIONS

Most atoms found in nature are stable and do not emit particles or energy that change form over time. Some atoms, however, do not have stable nuclei. These atoms emit radiation in order to achieve a more stable configuration.

3.1. Radioactive Decay Mechanisms

As mass numbers become larger, the ratio of neutrons to protons in the nucleus becomes larger for the stable nuclei. Non-stable nuclei may have an excess or deficiency of neutrons and undergo a transformation process known as beta (β) decay. Non-stable nuclei can also undergo a variety of other processes such as alpha (α) or neutron (n) decay …etc; see Fig. 2.1. As a result of these decay processes, the final nucleus is in a more stable or more tightly bound configuration.

3.1.1. Natural radioactivity

In 1896, the French physicist Becquerel discovered that crystals of a uranium salt emitted rays that were similar to x-rays in that they were highly penetrating, could affect a photographic plate, and induced electrical conductivity in gases. Becquerel's discovery followed in 1898 by the identification of two other radioactive elements, polonium and radium, by Pierre and Marie Curie.

Heavy elements, such as uranium or thorium, and their unstable decay chain elements emit radiation in their naturally occurring state. Uranium and thorium, present since their creation at the beginning of geological time, have an extremely slow rate of decay. All naturally occurring nuclides with atomic numbers greater than 82 are radioactive.

Whenever a nucleus can attain a more stable (i.e., more tightly bound) configuration by emitting radiation, a spontaneous disintegration process known as radioactive decay or nuclear decay may occur. In practice, this "radiation" may be electromagnetic radiation, particles, or both.

Detailed studies of radioactive decay and nuclear reaction processes have led to the formulation of useful conservation principles.

3.1.2. Conservation principles

The investigation of the fundamental constituents of matter and their interactions comes from the experimental and theoretical analysis of nuclear reactions. These reactions include decays of the unstable particles, natural or produced in nuclear reactions, and scattering experiments with or without production of particles.

The laws allow the identification of particles and various fundamental *conservation laws* govern nuclear reactions, i.e., the determination of their masses, spins, energies, moments etc.

The four principles of most interest in this module are discussed below.

1- *Conservation of electric charge* implies that charges neither created nor destroyed. Single positive and

negative charges however, may neutralize each other. It is also possible for a neutral particle to produce one charge of each sign.

2- *Conservation of mass number* does not allow a net change in the number of nucleons. However, the conversion of a proton to a neutron and vice versa is allowed.

3- *Conservation of mass and energy* implies that the total of the kinetic energy and the energy equivalent of the mass in a system must be conserved in all decays and reactions. Mass can be converted to energy and energy can be converted to mass, but the sum of mass and energy must be constant.

4- *Conservation of momentum* is responsible for the distribution of the available kinetic energy among product nuclei, particles, and/or radiation. The total momentum is the same before and after the reaction even though it may be distributed differently among entirely different nuclides and/or particles.

The most important laws are energy-momentum conservation and electric charge conservation. In nuclear physics, other laws play an important role such as angular momentum conservation, lepton number, baryon number and isospin conservation (which will be discussed in the subsequent chapters).

3.2. Nuclear Reactions

In order to understand the analysis and mechanism of the nuclear radioactivity, it is essential to study the nuclear reactions. The quantitative aspects we will stress on are those of the mass and energy balance. The nuclear reactions may be caused by any kind of incident particle, and may

result in the emission of any kind of particle (proton, neutron, deuteron, α-particle, or even nucleus), and/or γ-ray.

The Bohr's theory of the compound nucleus assumed (1936) that, a nuclear reaction takes place in two steps; first, the incident particle is absorbed by the initial, or target, nucleus to form a compound nucleus, second, the compound nucleus disintegrates by ejecting a particle (proton, neutron, α-particle, etc.) or a γ-ray, leaving the final, or product nucleus. He assumed also that the mode of disintegration of the compound nucleus is independent of the way in which the later is formed, and depends only on the properties of the compound nucleus itself, such as its energy and angular momentum.

The natural or artificial radioactive decay indeed can be considered as a nuclear reaction process with no incident particles, since s*ome atoms do not have stable nuclei.* Non-stable nuclei may have an excess or deficiency of neutrons and undergo a transformation process similar to that of the compound nucleus.

The great number of nuclear reactions and radioactive decays provide a wealth of experimental data for the field of nuclear spectroscopy and for the theory of nuclear structure.

The analysis of nuclear reactions is similar to that used for chemical reactions except that the relativistic relation between mass and energy must be taken into account.

Consider a nuclear reaction represented by the reaction:

$$a + X \rightarrow Y + b \qquad 3.1$$

Here *X* is the target nucleus, *a* is the bombarding particle, *Y* is the product nucleus and *b* is the product particle.

As for all practical cases, it will be assumed that the target nucleus X is initially at rest, so that it has no kinetic

energy. Since the total energy of a particle or atom is the sum of the rest energy and the kinetic energy, the conservation of mass and energy yield:

$$(T_a + m_a c^2) + M_X c^2 = (T_Y + M_Y c^2) + (T_b + m_b c^2) \qquad 3.2$$

where m_a, M_X, M_Y, and m_b represent the masses of the incident particle, target nucleus, product nucleus, and product particle, respectively, T_a, T_Y, and T_b represent the kinetic energies of the incident particle, product nucleus, and product particle, respectively.

The above equation can be rearranged as:

$$(T_Y + T_b) - T_a = (M_X + m_a - M_Y - m_b)c^2 \qquad 3.3$$

Now introduce the quantity Q, which represents the difference between the kinetic energy of the products of the reaction and that of the incident particle, hence Eq.3.3, can be written in term of the so-called *Q-value* as:

$$Q = (T_Y + T_b) - T_a = (M_X + m_a - M_Y - m_b)c^2 \qquad 3.4$$

The Q-value can then be determined either from the energy difference or from the mass difference in Eq.3.4.

Examining Eq.3.4 shows that if the value of Q is positive, the kinetic energy of the products is greater than that of the reactants or the masses of the reactants are greater than that of the products; the reaction is then said to be *exothermic or exoergic*. Then in this case, the total mass of the reactants is greater than that of the products, which means that the nuclear mass or binding energy is released as kinetic

energy of the final products. While, if the *Q*-value is negative ($M_{reactants} < M_{products}$ *or* $T_{products} < R_{reactants}$), the reaction is *endothermic or endoergic*, and the initial kinetic energy is converted into nuclear mass or binding energy.

Eq.3.4 is valid in any frame of reference in which we choose to work, let us apply them to the laboratory reference frame. The term T_Y in Eq.3.4, represent the recoil (kinetic) energy of the product nucleus. It is usually small and hard to measure, but it can be eliminated by taking into account the conservation of momentum. Consider that the momentum vector is directed along the x-axis before the collision, and the out-coming particle b and nuclei Y are observed at an angle θ and φ, respectively. Fig. 3.1 shows the basic geometry in the reaction plane. Conservation of linear momentum along and perpendicular to the beam direction (x-axis) gives:

$$p_a = p_b \cos\theta + p_Y \cos\varphi \qquad 3.5a$$

and

$$0 = p_b \sin\theta - p_Y \sin\varphi \qquad 3.5b$$

where $p_a = m_a \upsilon_a$, $p_y = M_Y V_Y$, $p_b = m_b \upsilon_b$, *and* υ_a, V_Y, υ_b are the velocities of the incident particle, the recoil nucleus, and the ejected particle, respectively, and θ, φ are the angle of the direction of the ejected particle, and the direction of the recoil nucleus with x-axis.

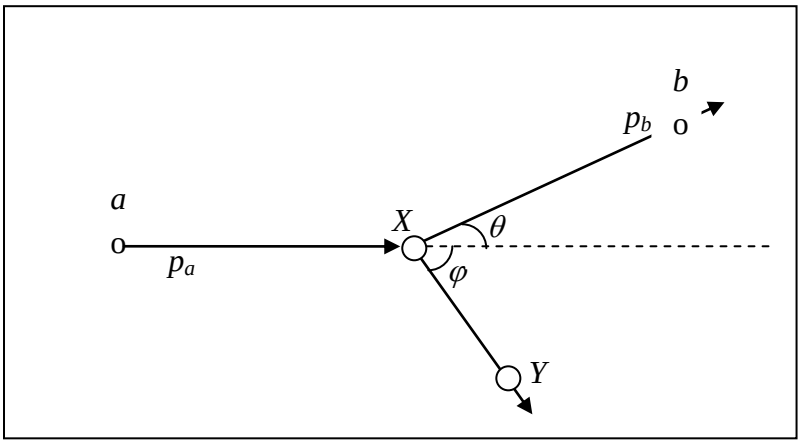

Figure 3.1. Basic geometry for the nuclear reaction in laboratory reference frame.

Regarding Q as a known quantity and T_a (and therefore p_a) as a parameter we control, Eqs.3.4 and 3.5a, b represent three equations in unknowns (φ, θ, T_b, and T_a) which have no unique solution. If we do not observe the nucleus Y, (as is usually case), we can eliminate T_Y and φ, then we can determine the *Q-value* of the reaction. If we know m_a, m_b, and M_x, and we observe the angle of out-coming particle θ, we have a way of determining the mass of Y. Solving the last three equations for *Q-value*, we obtain:

$$Q = T_b\left(1+\frac{m_b}{M_Y}\right) - T_a\left(1-\frac{m_a}{M_Y}\right) - \frac{2}{M_Y}\left(T_a T_b m_a m_b\right)^{1/2}\cos\theta \qquad 3.6$$

This procedure is not strictly valid, for M_Y also appears on the right side of the equation, but is usually of sufficient accuracy to replace the masses with the integer mass

numbers *A*, especially if we measure ejected particle at angle $\theta = 90^o$ where the last term of Eq.3.6 vanishes.

In an endothermic reaction, the energy $-Q$ is needed to excite the compound nucleus sufficiently so that it will break up. This energy must be supplied in the form of kinetic energy of the incident particle. But not all of that kinetic energy is available for excitation because some is used to impart momentum to the compound nucleus; this momentum is then distributed among the products of the reaction. Consequently, for $-Q$ to be available for excitation of the compound nucleus, we must supply some energy in addition to $-Q$. The minimum amount of energy needed for an endothermic reaction is called the *threshold energy* T_{th} and can be calculated easily. Since the threshold condition always occurs for $\theta = 0^o$(in this case $\varphi = 0^o$ too), the products *Y* and *b* move in a common direction but still as separate nuclei, or we may deal with the compound nucleus, as follows:

If we let, M_C and V_C denote the mass and velocity of the compound nucleus, conservation of momentum requires:

$$m_a \upsilon_a = M_C V_C \qquad or \qquad V_C = \frac{m_a}{M_C}\upsilon_a \qquad 3.7$$

The part of the kinetic energy of the incident particle needed for excitation of the compound nucleus is:

$$-Q = \frac{1}{2}m_a\upsilon_a^2 - \frac{1}{2}M_C V_C^2 = \frac{1}{2}m_a\upsilon_a^2\left(1 - \frac{m_a}{M_C}\right) \qquad 3.8$$

But, $M_C = M_X + m_a$, and

$$-Q = \frac{1}{2} m_a \upsilon_a^2 \left(\frac{M_X}{M_X + m_a} \right) \qquad 3.9$$

Then the threshold energy is then:

$$T_{th} = \frac{1}{2} m_a \upsilon_a^2 = (-Q)\left(1 + \frac{m_a}{M_X} \right) \qquad 3.10$$

The threshold energy can be determined experimentally and the result is used to find the value of *Q*. If *Q > 0* (exothermic reaction), there is no threshold condition and the reaction will occur even for very small energy.

Finally, if the reaction reaches the excited state of *Y*, the *Q-value* equation should include the mass energy of the excited state:

$$\begin{aligned} Q_{ex} &= (M_X + m_a - M_Y^* - m_b)c^2 \\ &= Q_0 - E_{ex} \end{aligned} \qquad 3.11$$

where Q_0 is the *Q-value* corresponding to the ground state of *Y*, while Q_{ex} and E_{ex} are the excitation Q-value and energy above the ground state respectively, then the mass energy relation is:

$$M_Y^* c^2 = M_Y c^2 + E_{ex} \qquad 3.12$$

3.3. Types of Radioactivity

A nucleus in an excited state is unstable because it can always undergo a transition (decay) to a lower-energy state of the *same or different nucleus*.

A nucleus which undergoes a transition spontaneously, that is, without being supplied with additional energy as in bombardment, is said to be radioactive. It is found experimentally that naturally occurring radioactive nuclides emit one or more of the three types of radiations, α- particles, β- particles, and γ-rays.

3.3.1. Alpha decay (α)

Alpha decay is the emission of alpha particles (helium nuclei) which may be represented as either ${}_2^4He$ *or* ${}_2^4\alpha$. When an unstable (parent) nucleus disintegrates to a daughter through ejection an alpha particle, the atomic number is reduced by 2 and the mass number decreased by 4, and the transition is:

$$ {}_Z^A X \rightarrow {}_{Z-2}^{A-4} Y + {}_2^4 He \qquad 3.13 $$

If we assume that the parent nucleus is initially at rest, which is a common case, the conservation of energy requires:

$$ M_p c^2 = M_d c^2 + T_d + M_\alpha c^2 + T_\alpha \qquad 3.14 $$

where M_p, M_d *and* M_α are the masses of the parent, daughter and α particle respectively. Similarly, T_d *and* T_α represent the kinetic energies of the daughter and of the α-particle.

Eq.3.2 can be written as:

$$ T_d + T_\alpha = (M_p - M_d - M_\alpha)\, c^2 = \Delta \mathrm{M c}^2 = \mathrm{Q} \qquad 3.15 $$

Here, we use atomic masses instead of nuclear masses since the masses of electrons cancel. We define the

disintegration energy *Q-value* as the difference in the rest masses of the initial and final states and obviously equal the sum of the kinetic energies of the final state particles.
Applying the law of conservation of momentum:

$$P_i = P_f \qquad 3.16$$

where P_i *and* P_f are the initial and final momentum of reactants.

Now, since the parent nucleus, in α-decay, decays from the rest, then the daughter nucleus and the α-particle must necessarily move in opposite directions to conserve momentum. For non-relativistic particles, the momentum and kinetic energies can be written as:

$$M_d\, \upsilon_d = M_\alpha\, \upsilon_\alpha \text{ or } \upsilon_d = M_\alpha\, \upsilon_\alpha / M_d \qquad 3.17$$

$$T_\alpha = \tfrac{1}{2}\, M_\alpha\, \upsilon^2_\alpha, \text{ and } T_d = \tfrac{1}{2}\, M_d\, \upsilon^2_d = (M_\alpha / M_d) T_\alpha \qquad 3.18$$

In almost all α-decay cases, the mass of the daughter nucleus is much greater than that of the α-particle. Then $\upsilon_d << \upsilon_\alpha$, and consequently the kinetic energy of the daughter nucleus is far smaller than that of the α particle. υ_d can be eliminated by Eq. 3.17, then the expressions for T_α in terms of the *Q-value*, using Eq. 3.15 and 3.18, is:

$$T_\alpha = \frac{M_d}{M_\alpha + M_d} Q = \frac{1}{1 + \dfrac{M_\alpha}{M_d}} Q \qquad 3.19$$

The kinetic energy of the emitted α particle cannot be negative, that is, $T_\alpha \geq 0$. Consequently, for α-decay to occur, we must have an exothermic process.

$$\Delta M \geq 0, \qquad Q \geq 0 \tag{3.20}$$

As α-decay mainly occurs in heavy nuclei, most of the energy is carried off by the α-particle. The kinetic energy of the daughter nucleus is then obtained from Eqs. 3.15 and 3.19.

$$T_d = Q - T_\alpha = \frac{M_\alpha}{M_\alpha + M_d} Q = \frac{M_\alpha}{M_d} T_\alpha \tag{3.21}$$

If we approximate the atomic masses of the nuclei by their mass numbers, the masses ratio can be approximated $M_\alpha/M_d \approx 4/(A-4)$. We can then rewrite Eq.3.21 as:

$$\begin{aligned} T_\alpha &\approx \frac{A-4}{A} Q \\ T_d &\approx \frac{4}{A} Q \end{aligned} \tag{3.22}$$

It is clear from Eq.3.19 that the kinetic energy of the α-particle in the decay is unique. Careful measurements, however, have revealed a fine splitting in the energies of α-particles emitted from radioactive material, corresponding to possibly different *Q-values*. The most energetic α-particles are observed to be produced alone. Less energetic α-particles are always accompanied by the emission of gamma photons, i.e. the parent nucleus can transform to an excited state of the daughter nucleus, in which the *Q-value* will be lower by a value of the gamma energies. An example is uranium-234, which decays by the ejection of an alpha particle accompanied by the emission of a 0.068 MeV gamma.

$$^{234}_{92}U \rightarrow {}^{230}_{90}Th + {}^{4}_{2}\alpha + \gamma + T$$

The combined kinetic energy of the daughter nucleus (Thorium-230) and the α-particle is designated as kinetic energy. The sum of the *KE* and the gamma energy is equal to the difference in mass between the original nucleus (Uranium-234) and the final particles (equivalent to the binding energy released, since $\Delta mc^2 = BE$ *or Q-value*). The alpha particle will carry off as much as 98% of the kinetic energy and, in most cases, can be considered to carry off all the kinetic energy.

3.3.2. Beta decay (β)

The theory of *beta decay* was developed by Fermi (1934) in analogy with the quantum theory of electromagnetic decay. Our concern is not the elements of this theory; rather we will be content to mention just one aspect of the theory, that concerning the statistical factor describing the momentum and energy distributions of the emitted β particles.

Beta decay is considered to be a weak interaction since the interaction potential is ~ 10^{-6} that of nuclear interactions, which are generally regarded as strong. β-decay is the emission of electrons of nuclear rather than orbital origin. These particles are electrons that have been expelled by excited nuclei and may have a charge of either sign e^-, e^+. β -decay is the most common type of radioactive decay, all nuclides not lying in the valley of stability are unstable against this transition.These electrons are emitted with a continuous spectrum of energies, as shown in Fig. 3.2.

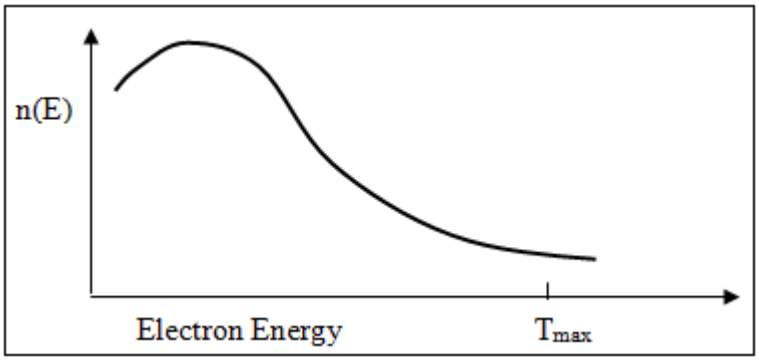

Figure 3.2. The observed differential distribution in the number of emitted electrons as a function of their energy.

If both energy and momentum are to be conserved, a third type of particle, the neutrino (υ) must be involved. The neutrino is associated with the positive electron emission, and its antiparticle, the antineutrino ($\bar{\upsilon}$) is emitted with a negative electron. These uncharged particles have only the weakest interaction with matter, no charge, neglecting its small mass (no mass as proposed by Pauli), and travel at the speed of light. For all practical purposes, they pass through all materials with so few interactions that the energy they possess cannot be recovered. The neutrinos and antineutrinos are included here only because they carry a portion of the kinetic energy that would otherwise belong to the beta particle, and therefore, must be considered for energy and momentum to be conserved. Also, linear and angular momenta are now conserved. They are normally ignored since they are not significant in the context of nuclear reactor applications.

3.3.2.1. β^- decay:

A nucleus with an over abundance of neutrons (with value of *N/Z* greater than that for stable nuclei, as shown in the chart of nuclides Fig. 2.2 and Fig. 3.5) can transform to a more stable nucleus as one excess neutron converts to a proton inside the nucleus and emit a negative electron associated with antineutrino. This kind of process is known as e^- or β^- decay and the transformation can be denoted by:

$$ {}^{A}_{Z}X \rightarrow {}^{A}_{Z+1}Y + e^- + \bar{\upsilon} \qquad 3.23 $$

If the parent nucleus decays from rest, the conservation of energy for electron emission will yield:

$$ M_p c^2 = T_d + M_d c^2 + T_e + m_e c^2 + T_{\bar{\upsilon}} + m_{\bar{\upsilon}} c^2 $$

or

$$ T_d + T_e + T_{\bar{\upsilon}} = \{M_p - M_d - m_e - m_{\bar{\upsilon}}\} c^2 $$

$$ = \Delta M c^2 = Q \qquad 3.24 $$

where M_p, M_d, m_e and $m_{\bar{\upsilon}}$, are respectively, the masses of the parent nucleus, the daughter nucleus, the electron and the antineutrino.

Similarly, T_d, T_e and $T_{\bar{\upsilon}}$ represent the kinetic energies of the decay daughter nucleus, the electron and antineutrino, respectively. We see from Eq. 3.24 that electron emission can take place only if the disintegration energy *Q* is positive, that is, when the mass of the parent nucleus is greater than the sum of the masses of the decay products. In fact, neglecting small differences in atomic binding energies, we conclude that electron emission will take place if:

$$Q = \{M(A, Z) - M(A, Z + l) - m_{\bar{\upsilon}}\} c^2$$

$$\approx \{M(A,Z) - M\{A,Z+1)\} c^2 \geq 0 \qquad 3.25$$

Eq. 3.25 represents the atomic masses, including the mass of atomic electrons, with neglecting the small mass of the neutrino. Furthermore, because the daughter nucleus is much heavier than either the electron or the antineutrino, the small recoil energy of the daughter can be ignored, and for any β^- decay we can write:

$$T_e + T_{\bar{\upsilon}} \approx Q \qquad 3.26$$

Eq.3.26 shows clearly that, with a $\bar{\upsilon}$ in the final state, the energy of the electron is no longer unique. In fact, any continuous value $0 \leq T_e \leq Q$ is kinematically allowed and the maximum electron energy, corresponding to $T_{\bar{\upsilon}} = 0$, is given by the endpoint value of Eq. 3.26.

$$(T_e)_{max} = Q \qquad 3.27$$

Pauli's postulate therefore accommodates the continuous energy spectrum in β^- decay, and simultaneously restores all the accepted conservation laws.

3.3.2.2. β^+ decay:

Positively charged electrons (beta-plus) are known as positrons β^+ (electron antiparticle). Except for sign, both β^+ *and* β^- are nearly identical. The positron, represented as e^+, or β^+, is ejected from the nucleus (with value of *N/Z* less than that for stable nuclei, Fig. 2.2 and 3.5), the atomic

number of the nucleus decreased by one and the mass number remains unchanged. A proton converts to a neutron by emission of β^+ and neutrino υ. The process represented as:

$$ {}^{A}_{Z}X \rightarrow {}^{A}_{Z-1}Y + e^{+} + \upsilon \qquad 3.28 $$

Similar to the β^- decay, the disintegration energy for positron emission is given by:

$$ Q = (M_p - M_d - m_{e+} - m_{\upsilon})\, c^2 $$

$$ = (M(A,Z) - M(A,Z\text{-}l) - 2m_e - m_{\upsilon})\, c^2 $$

$$ \approx (M(A,Z) - M(A,Z\text{-}l) - 2m_e)\, c^2 \qquad 3.29 $$

Where, again, all the $M\ (A, Z)$ in the last line of Eq. 3.29 refer to full atomic weights, and Q must be positive for the decay to occur.

3.3.2.3. *Electron capture* (*K-capture*)

Nuclei having an excess of protons may capture an electron from one of the inner orbits, which immediately combines with a proton in the nucleus to form a neutron. This process is called *electron capture* (EC). The electron is normally captured from the innermost orbit (the K-shell), and, consequently, this process is sometimes called K-capture. This process can be represented as:

$$ {}^{A}_{Z}X + e^{-} \rightarrow {}^{A}_{Z-1}Y + \upsilon \qquad 3.30 $$

A neutrino is formed at the same time that the neutron is formed and energy carried off by it serves to conserve momentum. Any energy that is available due to the atomic mass of the product being appreciably less than that of the parent will appear as gamma radiation. In addition, there will always be characteristic x-rays given off when an electron from one of the higher energy shells moves in to fill the vacancy in the K-shell. Electron capture is shown graphically in Fig. 3.3.

Electron capture and positron emission result in the radioactive production of the same daughter product, and they exist as competing processes. For positron emission β^+ to occur, however, the mass of the daughter product must be less than the mass of the parent by an amount equal to at least twice the mass of an electron Eq.3.29. This mass difference between the parent and daughter is necessary to account for two items present in the parent but not in the daughter. One item is the positron ejected from the nucleus of the parent. The other item is that the daughter product has only one less orbital electron than the parent does. If this requirement is not met, orbital electron capture takes place exclusively.

Similarly, electron capture process can take place only if:

$$Q = (M_p + m_e - M_d - m_\upsilon)\, c^2$$

$$= \{M(A, Z) - M(A, Z\text{-}1) - m_\upsilon\}\, c^2$$

$$\approx \{M(A,Z) - M(A,Z\text{-}1)\}\, c^2 \geq 0 \qquad 3.31$$

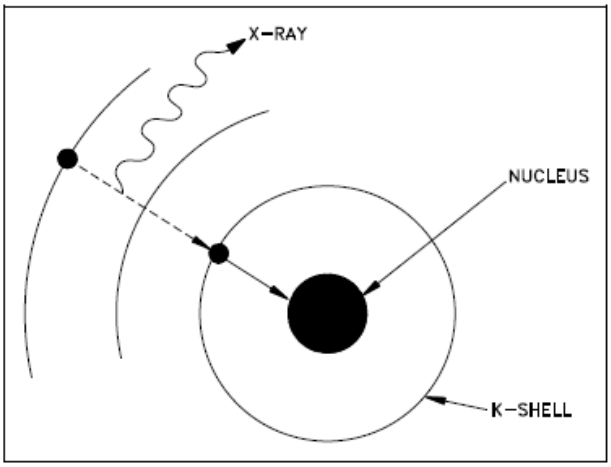

Figure 3.3. Orbital Electron Capture.

3.3.2.4. Selection rules for beta decay

For each nuclear level, there is an assignment of spin and parity. This information is essential for determining whether a transition of a particular transition between initial and final states is allowed according to certain selection rules of quantum mechanics. Also if a transition is allowed, what mode of decay is most likely?

Consider a beta transition between two nuclear states of well defined angular momentum with the emission of, say, a positron and neutrino or an electron and an antineutrino. In this transition, the total angular momentum and the parity of the angular momentum states must be conserved; see Ch. 2. Then the angular momentum and parity are generally expressed in beta decay P → D + β +υ as:

$$\boldsymbol{j}_P = \boldsymbol{j}_D + \boldsymbol{L}_\beta + \boldsymbol{S}_\beta \,,\ L = 0, 1, 2 \ldots and\ S = 0\ and\ 1 \qquad 3.32$$

$$\pi_P = \pi_D (-1)^{L_\beta} \qquad 3.33$$

Here, $\mathbf{L}_\beta$ and $\mathbf{S}_\beta = \mathbf{s}_\beta + \mathbf{s}_\upsilon$ are the orbital angular momentum and *the intrinsic spin of* the outgoing leptons (*electron-antineutrino or positron neutrino system*). The transitions with $L_\beta = 0$ are known as allowed transitions; the parity change is $\Delta\pi_\beta = (-1)^{L_\beta} = 1$ or -1 corresponds to no parity change or parity change respectively, and so allowed transitions must have the same parity in initial and final states $\pi_P = \pi_D$. Transitions with $L_\beta \neq 0$ are known as forbidden (although they can occur).

The magnitude S_β can take on values of 0 and 1 which would correspond to the *antiparallel and parallel* coupling of the *electron and neutrino spins*, respectively. Thus, for the allowed transitions ($\mathbf{j}_P - \mathbf{j}_D = \mathbf{L} + \mathbf{S}_\beta = \mathbf{L} + \mathbf{s}_\beta + \mathbf{s}_\upsilon$), since the leptons have spin half, there are two cases to be considered; $S_\beta = 0$ or $S_\beta = 1$. The $S_\beta = 0$ transitions are known as *Fermi* (F) transitions for Low A, where the electron and antineutrino have "antiparallel" spins and $j_P - j_D = 0$. While the $S_\beta = 1$ transitions are known as *Gamow-Teller* (GT) transitions for High A, where the electron and antineutrino have ``parallel" spins and $j_P - j_D = 0$ or 1. The spin changes since neutron number tends to be larger than protons. Even though we have sources produce a mixture of these two orientations. This is because the decay constant is governed by the square of a transition matrix element M, which can be written as a series of contributions, one for each L_β.

$$\lambda_\beta \propto |M|^2 = |M\,(L_\beta = 0)|^2 + |M\,(L_\beta = 1)|^2 + |M\,(L_\beta = 2)|^2 + \ldots \quad 3.34$$

Transitions with $L_\beta = 0, 1, 2$ …are called allowed, first-forbidden, second-forbidden…etc. The magnitude of the matrix element squared decreases from one order to the next higher one by at least a factor of 10^2. For this reason, we are

interested only in the lowest order transition that is the most likely transition among all the allowed transitions.

To illustrate how the selection rules are determined, we consider the transition:

$$^{6}_{2}He(0^{+}) \rightarrow {}^{6}_{3}Li(1^{+}) + \beta^{-} + \upsilon$$

To determine the combination of L_β and s_β for the first transition that is allowed, we begin by noting that parity conservation requires L_β to be even. Then, we see that $L_\beta = 0$ plus $S_\beta = 1$ would satisfy both Eqs. 3.32 and 3.33. Thus, the most likely transition is the transition designated as allowed, G-T. Following the same line of argument, one can arrive at the following assignments:

$^{14}_{8}O(0^{+}) \rightarrow {}^{14}_{7}N(0^{+}) + \beta^{+} + \bar{\upsilon}$ allowed, F
$^{1}_{0}n(½^{+}) \rightarrow {}^{1}_{1}H(½^{+}) + \beta^{-} + \upsilon$ allowed, GT and F
$^{38}_{17}Cl(2^{-}) \rightarrow {}^{38}_{18}Ar(2^{+}) + \beta^{+} + \bar{\upsilon}$ first-forbidden, GT & F
$^{10}_{4}Be(3^{+}) \rightarrow {}^{10}_{5}B(0^{+}) + \beta^{-} + \upsilon$ second-forbidden, GT

The following table lists the $\Delta j = j_P - j_D$ and $\Delta\pi$ values for the first few values of *L*:

Forbiddances	**Δ*J***	**Δπ**
Super allowed	$0^{+} \rightarrow 0^{+}$	no
Allowed	0, 1	no
First forbidden	0, 1, 2	yes
Second forbidden	1, 2, 3	no
Third forbidden	2, 3, 4	yes

3.3.2.5. Parity violation

The presence of neutrino in β -decay leads to a certain type of non-conservation of parity. C.S. Wu, in 1957, devised and carried some experiments to test the possibility of parity violation in beta decay. The basic idea of C.S. Wu's experiment is to build two sets of experimental arrangement for ^{60}Co which are mirror images of each other. She aligned them in a magnetic field, so that all their spin vectors lined up and then let them decay, measuring the direction of the outgoing electron. She found that electrons were emitted preferentially in the direction of the spin vector, i.e., a clear violation of parity conservation.

It is known that *neutrinos have intrinsic spin antiparallel* to their velocity, whereas the spin orientation of the *antineutrino is parallel to their velocity* (keeping in mind that υ and $\bar{\upsilon}$ are different particles).

To demonstrate parity violation or non-conserving property of neutrino, consider the *mirror word experiment* where a neutrino is moving toward the mirror from the left, Fig. 3.4. Applying the inversion symmetry operation ($x \rightarrow -x$), the velocity reverses direction, while the angular momentum (spin) does not. Thus, on the other side of the mirror, we have an image of a particle moving from the right, but its spin is now parallel to the velocity so it has to be an antineutrino instead of a neutrino.

This means that the property of υ and $\bar{\upsilon}$, namely definite spin direction relative to the velocity, is not compatible with parity conservation (symmetry under inversion).

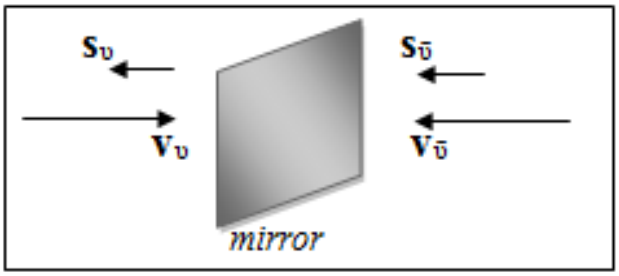

Figure 3.4. Mirror reflection demonstrating of parity non-conserving property of neutrino.

3.3.3. Gamma emission (γ)

Gamma radiation is a high-energy electromagnetic radiation that originates in the nucleus. It is emitted in the form of photons, discrete bundles of energy that have both waved and particle properties. Often a daughter nuclide is left in an excited state after a radioactive parent nucleus undergoes a transformation by alpha decay, beta decay or electron capture. If the excited nucleus does not break apart or emit another particle, it can de-excite to the lower energy state or ground state by emitting a high-energy photon or γ ray. These transformations take place within the same nucleus ${}^{A}_{Z}X$ in contrast to the β decay or α-decay processes. They merely represent a re-ordering of the nucleons within the nucleus with lowering of mass from the excited ($M_0^* c^2$) to the lowest ($M_0 c^2$) value.

This type of radiation does not have to occur as radioactive decay only, but may accompany random types of nuclear transmutations, including nuclear reactions, or even changes of elementary particles. In this general sense, we usually talk about nuclear radiation.

3.3.3.1. γ-decay

The total energy balance follows from conservation of energy is:

$$M_0^* c^2 = M_0 c^2 + E_\gamma + T_R$$
$$or \quad E_i = E_f + h\nu + T_R \qquad 3.35$$

where (E_γ) is the energy of the emitted photon, (E_i, E_f) is the initial and final energy state, respectively and (T_R) is the kinetic energy of the recoiling nucleus.

Linear momentum conservation, Eq.3.16, leads to:

$$\vec{p}_\gamma + \vec{p}_0 = 0 \qquad 3.36$$

The recoil energy is very small compared to the γ energy, so non-relativistic expression can be used, derived from Eq.1.20 to find the recoil energy:

$$T_R = \frac{p_0^2}{2M_0} = \frac{p_0^2 c^2}{2M_0 c^2} \approx \frac{p_\gamma^2 c^2}{2M_0 c^2} = \frac{E_\gamma^2}{2M_0 c^2} = \frac{(h\nu)^2}{2M_0 c^2} \qquad 3.37$$

From Eq. 3.35 the γ energy can be written as:

$$h\nu = E_i - E_f - T_R \qquad 3.38$$

The study of the emission and absorption of nuclear γ-rays forms an essential part of the development of nuclear spectroscopy. Consider, for example, a system initially in a state of energy E_i making a transition to a state with energy E_f through the absorption or emission of a photon of frequency ν. In such processes, we can define what is known

as resonant or recoilless transitions, for which Eq.3.38 can be rewritten as:

$$h\nu = \pm(E_i - E_f - T_R) \qquad 3.39$$

where "+" corresponds to emission and "–" to absorption. Thus, in principle, measuring υ determines the energy level spacing.

The characteristic spacing of nuclear energy levels is of the order of 50 keV, and typical energies of nuclear γ-rays can therefore range from fraction to several MeV. Because this kind of de-excitation is electromagnetic, we expect lifetimes for such processes to be typically in the range 10^{-15} to 10^{-10} sec (because of the short lifetime, with few exceptions only nuclei in the ground state are present on Earth, but they can be produced in collisions with high energetic particles).

For 1 MeV photon energy and a nucleus of mass number *A* about 100, the recoil energy is only about 5 eV. Even though this energy is very small, see Fig. 3.5, the recoil nucleus shifts the γ radiation out of resonance condition since the natural energy line-width Γ of the radiation is even smaller.

Simply, every unstable energy level has a "natural" width Γ and a lifetime τ, which can be related through the uncertainty principle:

$$\Gamma \approx \hbar/\tau \approx (6.6\times10^{-22}\text{MeV.sec}) / (\tau \text{ sec})$$
$$\approx \text{Uncertainty in } (E_i - E_f) \qquad 3.40$$

Since nuclear states are typically separated by energies in the MeV range, the width is small compared to state separations if the lifetime is greater than 10^{-22} sec. This is

generally the case for states decaying through the weak or electromagnetic interactions. Eq. 3.40 shows that the exact value, of an energy level, is uncertain, and cannot be denied in any given transition to better than ~Γ. Consequently, if the kinetic energy of the recoil is such that $T_R << \Gamma$, essentially $E_\gamma = -(E_i - E_f)$, and resonant absorption can take place. On the other hand, if $T_R >> \Gamma$, it is impossible to excite the system to a higher level through resonant absorption within the bounds provided by the uncertainty relation.

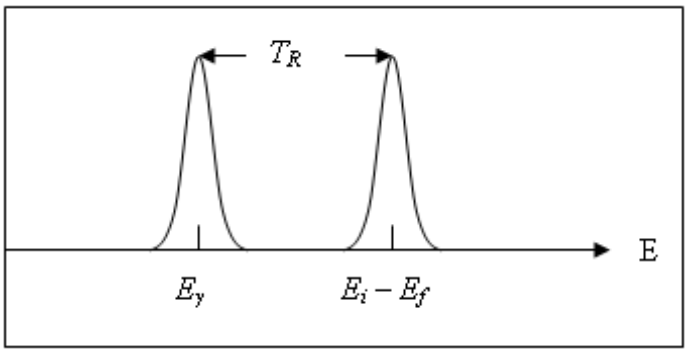

Figure 3.5. Illustration of the fact that in γ-decay process, the initial excited nucleus is at rest and receives a certain recoil energy T_R, so that $E_\gamma < E_i - E_f$.

For example, a typical nuclear spacing have $h\nu > 1$ MeV $= 10^6$ eV. If we consider again a nucleus with $A = 50$, we still have The characteristic spacing $E_f = Mc^2 \approx 5 \times 10^{10}$ eV, now with the higher photon energy, the nuclear recoil energy is given by Eq.3.37:

$$T_R = \frac{(h\nu)^2}{2Mc^2} \approx \frac{(10^6 ev)^2}{2 \times 5 \times 10^{10} eV} = 10 \quad eV$$

If we assume a typical lifetime of about 10^{-12} sec for a nuclear level, then:

$$\Gamma \approx \frac{\hbar}{\tau} \approx \frac{6.6\times10^{-16} eV.\text{sec}}{10^{-12}\,\text{sec}} = 6.6\times10^{-4} eV$$

It is clear, therefore, that for such nuclear transitions $T_R >> \Gamma$ and resonant absorption cannot occur.

3.3.3.2. Decay Constants

Nuclear excited states have half-lives for γ-emission ranging from 10^{-16} sec to > 100 years. A rough estimate of λ_γ can be made using semi-classical ideas. From Maxwell's equations one finds that an accelerated point charge *e* radiates electromagnetic radiation at a rate given by the Lamor formula:

$$\frac{dE}{dt} = \frac{2}{3}\frac{e^2 a^2}{c^3} \qquad 3.41$$

where a is the acceleration of the charge. Suppose the radiating charge has a motion like the simple oscillator:

$$x(t) = x_o \cos\omega t \qquad 3.42$$

where we take $x_0^2 + y_0^2 + z_0^2 = R^2$, R being the radius of the nucleus. From Eq. 3.42 we have:

$$a(t) = R\omega^2 \cos\omega t \qquad 3.43$$

To get an average rate of energy radiation, we average (20.22) over a large number of oscillation cycles:

$$\left(\frac{dE}{dt}\right)_{avg} = \frac{2}{3}\frac{R^2\omega^4e^2}{c^3}(cos\ \omega t)_{avg} \approx \frac{R^2\omega^4e^2}{3c^3} \qquad 3.44$$

Now we assume that each photon is emitted during a time interval τ (having the physical significance of a mean lifetime). Then:

$$\left(\frac{dE}{dt}\right)_{avg} = \frac{\hbar\omega}{\tau} \qquad 3.45$$

Equating this with Eq. 4.43 gives:

$$\lambda_\gamma \approx \frac{e^2R^2E_\gamma^3}{3\hbar^4c^3} \qquad 3.46$$

If we apply this result to a process in atomic physics, namely the de-excitation of an atom by electromagnetic emission, we would take R ~ 10^{-8} cm and E_γ ~ 1 eV, in which case Eq. 3.46 gives:

λ_γ ~10^6 sec^{-1}, or $t_{1/2}$~ 7 x 10^{-7} sec

On the other hand, if we apply Eq.3.46 to nuclear decay, where typically R ~ 5 x 10^{-13} cm, and E_γ ~ 1 Mev, we would obtain:

λ_γ~ 10^{15} sec^{-1}, or $t_{1/2}$ ~ 3 x 10^{-16} sec

These results only indicate typical orders of magnitude. What Eq.3.46 does not explain is the wide range of values of the half-lives that have been observed.

3.3.3.3. Selection Rules for γ-decay

In quantum limits, as will be discussed in Ch. 5, each photon carries a definite angular momentum. The multipole operator of order L includes the factor $Y_{\ell m_\ell}(\theta, \varphi)$, which is associated with an angular momentum L. For this reason, it is concluded that a multipole of order L transfers at an angular momentum of $\ell\hbar$ per photon.

We can write down the conservation of angular momentum and parity for γ-decay in a form similar to Eqs. 3.32 and 3.33:

$$\boldsymbol{I}_i = \boldsymbol{I}_f + \boldsymbol{L}_\gamma \qquad 3.47$$

Notice that the orbital and spin angular momenta are incorporated in L_γ, playing the role of the total angular momentum. Since the photon has spin $\hbar$, the possible values of L_γ are 1 (corresponding to the case of zero orbital angular momentum), 2, 3 …For the conservation of parity, we know the parity of the photon depends on the value of L_γ. Similar to Eq.2.37, we encounter two possibilities because in photon emission, which is the process of electromagnetic multipole radiation, *one can have either electric or magnetic multipole radiation*,

$$\pi_\gamma = (-1)^{L\gamma} \quad \text{electric multipole}$$

$$(-1)^{L\gamma+1} \quad \text{magnetic multipole} \qquad 3.48$$

Thus we can set up the following table:

Radiation	Designation	L_γ	π_γ
electric dipole	E1	1	-1
magnetic dipole	M1	1	+1
electric quadrupole	E2	2	+1
magnetic quadrupole	M2	2	-1
electric octupole	E3	3	-1
etc.			

For more simplification of getting the allowed γ-transitions, we may rewrite the above two equations for angular momentum and parity selection rules as:

$$|I_i - I_f| \leq L_\gamma \leq I_i + I_f \qquad (\text{no } L_\gamma = 0) \qquad 3.49$$

$$\Delta \pi_\gamma = \text{no:} \quad (\text{even electric, odd magnetic})$$
$$\Delta \pi_\gamma = \text{yes:} \quad (\text{odd electric, even magnetic}) \qquad 3.50$$

The exception to the angular momentum selection rule occurs when $I_i = I_f$ because there are no monopole ($L_\gamma = 0$) transition in which a single photon is emitted.

Similar to the case of β-decay, the decay constant can be expressed as a sum of contributions from each electric and magnetic multipole:

$$\lambda_\gamma = \lambda_\gamma (E1) + \lambda_\gamma (M1) + \lambda_\gamma (E2) + ... \qquad 3.51$$

provided that each contribution is allowed by the selection rules. Again we are only interested in the lowest order allowed transition, and if both E and M transitions are allowed, E will dominate. Take, for example, a transition

between an initial state with spin and parity of 2^+ and a final state of 0^+. This transition requires the photon parity to be positive, which means that for an electric multipole radiation L_γ would have to be even, and for a magnetic radiation it has to be odd. In view of the initial and final spins, we see that angular momentum conservation Eq. 3.49 requires L_γ to be 2. Thus, the most likely mode of γ-decay for this transition is E2. A few other examples are:

$$1^+ \rightarrow 0^+ \quad M1$$
$$\left(\frac{1}{2}\right)^- \rightarrow \left(\frac{1}{2}\right)^+ \quad E1$$
$$\left(\frac{9}{2}\right)^+ \rightarrow \left(\frac{1}{2}\right)^- \quad M4$$
$$0^+ \rightarrow 0^+ \quad \text{no } \gamma - \text{decay allowed}$$

3.3.4. Internal conversion

The usual method for an excited nucleus to go from the excited state to the ground state is by an emission of gamma radiation. However, internal conversion (IC) is another electromagnetic process which can occur in the nucleus and competes with gamma emission.

Alternative to gamma emission, an excited nucleus may interact electromagnetically with an electron in one of the lower atomic orbital. In this case, an excited nucleus is transformed to a lower energy state by ejecting an orbital electron from the cloud surrounding the nucleus. This orbital electron ejection is known as internal conversion and gives rise to an energetic electron. Most internal conversion electrons come from the K atomic shell, as these two electrons have the highest probability of being coupled to nuclear fields. However, the state in the L, M, and N shells

are also able to couple to nuclear fields and cause IC electrons from these shells.

Internal conversion electrons are different from beta radiation electrons because they do not involve the conversion of a nucleon and are not accompanied by a neutrino. The lack of neutrino also gives internal conversion electrons discrete energy values. The conversion electron is ejected from the atom with kinetic energy equal to the gamma energy minus the binding energy of the orbital electron (ignoring nuclear recoil)

$$T_e = E_i - E_f - E_B \qquad 3.52$$

where $E_i - E_f$ is the energy of de-excitation, and E_B is the binding energy of the atomic electron.

If we denote the decay constant for internal conversion by λ_e, the total decay constant for de-excitation is:

$$\lambda = \lambda_\gamma + \lambda_e \qquad 3.53$$

An orbital electron then drops to a lower energy state to fill the vacancy, and this is accompanied by the emission of characteristic x-rays.

Internal conversion is favored when the energy gap between nuclear levels is small, and is also the primary mode of de-excitation for $0^+ \rightarrow 0^+$ (i.e. E0) transitions. These occur where an excited nucleus has zero spin, and is thus unable to rid itself of energy by gamma emission. Internal conversion is also the predominant mode of de-excitation whenever the initial and final spin states are the same (but with other different quantum numbers).

The tendency towards IC can be expressed by the internal conversion coefficient (α), which is empirically

determined by the ratio of the rate of conversion electrons (e) to the rate of gamma-ray emission (γ):

$$\alpha = \frac{e}{\gamma} \qquad 3.54$$

For example, in the decay of an excited state of the nucleus of ^{125}I, 7% of the decays emit energy as a gamma ray, while 93% release energy as conversion electrons. Therefore, this excited state of ^{125}I has an internal conversion coefficient of α =13.6. Internal conversion coefficients are observed to increase for increasing atomic number (Z) and decreasing gamma-ray energy.

3.3.5. Isomers and isomeric transition

Isomeric transition commonly occurs immediately after particle emission; however, the nucleus may remain in an excited state for a measurable period of time before dropping to the ground state at its own characteristic rate. A nucleus that remains in such an excited state is known as a nuclear *isomer* because it differs in energy and behavior from other nuclei with the same atomic number and mass number. The decay of an excited nuclear isomer to a lower energy level is called an *isomeric transition*. It is also possible for the excited isomer to decay by some alternate means, for example, by beta emission. Isomeric states are generally specified by placing an *m* after A. An example of gamma emission accompanying particle emission is illustrated by the decay of nitrogen-16 below.

$$^{16}_{7}N \rightarrow {}^{16m}_{8}O + {}^{0}_{-1}\beta + {}^{0}_{0}\overline{\upsilon}$$

$$^{16m}_{8}O \rightarrow {}^{16}_{8}O + {}^{0}_{0}\gamma$$

3.4. Decay Chains

When an unstable nucleus decays, the resulting daughter nucleus is not necessarily stable. The nucleus resulting from the decay of a parent is often itself unstable, and will undergo an additional decay. This is especially common among the larger nuclides.

It is possible to trace the steps of an unstable atom as it goes through multiple decays trying to achieve stability. The list of the original unstable nuclides, the nuclides that are involved as intermediate steps in the decay, and the final stable nuclide is known as the *decay chain*. One common method for stating the decay chain is to state each of the nuclides involved in the standard ${}^{A}_{Z}X$ format. Arrows are used between nuclides to indicate where decays occur, with the type of decay indicated above the arrow and the half-life below the arrow. The half-life for decay will be discussed in Chapter-4.

Example:

Write the decay chains for rubidium ^{91}Rb and actinium ^{215}At. Continue the chains until a stable nuclide or a nuclide with a half-life greater than 1 x 10^6 years is reached.

Solution:

$$ {}^{91}_{37}Rb \xrightarrow[58\text{sec}]{\beta^-} {}^{91}_{38}Sr \xrightarrow[9.5hr]{\beta^-} {}^{91}_{39}Y \xrightarrow[58.5d]{\beta^-} {}^{91}_{40}Zr $$

$$ {}^{215}_{85}At \xrightarrow[0.1\text{min}]{\alpha} {}^{211}_{83}Bi \xrightarrow[2.14\text{min}]{\alpha} {}^{207}_{81}Ti \xrightarrow[4.77\text{min}]{\beta^-} {}^{207}_{82}Pb $$

3.5. Radioactive Series (Primordial Radionuclides)

Radioactive sires refer to any of four independent sets of unstable heavy atomic nuclei that decay through a sequence of alpha and beta decays until a stable nucleus is achieved; the members of a given series having mass numbers that differ by jumps of 4.

Three of the sets, the *thorium series, uranium series, and actinium series*, called natural or classical series, are headed by naturally occurring species of heavy unstable nuclei that have half-lives comparable to the age of the elements as shown in table 3.1. The fourth neptunium-237 (the *4n+1*series) exists only with man-made isotopes, but probably existed early in the life of the earth.

The three main series decay schemes produce radon (but primary radon source, the longest half-life, is the uranium series). The series beginning with ^{238}U and ending with lead-206 is known as the $4n+2$ series because all the mass numbers in the series are 2 greater than an integral multiple of 4 (e.g., $238=4\times59+2$, $206=4\times51+2$). In the thorium series ^{232}Th, the mass number of each member can be expressed in the form $4n$, while in the actinium series ^{235}U, $4n+3$. These series sometimes called by these forms. Table 3.1 shows the three natural series with the half-life and the mode of decay of each member.

Because the rates of disintegration of the members of a radioactive decay series are constant, the age of rocks and other materials can be determined by measuring the relative abundances of the different members of the series. All of the decay series end in a stable isotope of lead, so that a rock containing mostly lead as compared to heavier elements would be very old.

Table 3.1. The major characteristics of the radionuclides that comprise the natural decay series for ^{232}Th, ^{235}U, ^{238}U.

Natural ^{232}Th decay series			**Natural ^{235}U decay series**			**Natural ^{238}U decay series**		
nuclide	**decay mode**	**half-life (*a*=year)**	**nuclide**	**decay mode**	**half-life (*a*=year)**	**nuclide**	**decay mode**	**half-life (*a*=year)**
^{232}Th	α	1.405×10^{10}a	^{235}U	α	$7.04\cdot10^{8}$ a	^{238}U	α	$4.468\cdot10^{9}$ a
^{228}Ra	β^-	5.75 a	^{231}Th	β^-	25.52 h	^{234}Th	β^-	24.10 d
^{228}Ac	β^-	6.25 h	^{231}Pa	α	32760 a	^{234m}Pa	β^- 99.84% 0.16%IT	1.16 min
^{228}Th	α	1.9116 a	^{227}Ac	β^- 98.62% α 1.38%	21.772 a	^{234}Pa	β^-	6.70 h
^{224}Ra	α	3.6319 d	^{227}Th	α	18.68 d	^{234}U	α	245500 a
^{220}Rn	**α**	**55.6 s**	^{223}Fr	β^- 99.994% α 0.006%	22.00 min	^{230}Th	α	75380 a
^{216}Po	α	0.145 s	^{223}Ra	α	11.43 d	^{226}Ra	α	1602 a
^{212}Pb	β^-	10.64 h	^{219}At	α 97.00% β^- 3.00%	56 s	**^{222}Rn**	**α**	**3.8235 d**
^{212}Bi	β^- 64.06% α 35.94%	60.55 min	**^{219}Rn**	**α**	**3.96 s**	^{218}Po	α 99.98% β^- 0.02%	3.10 min
^{212}Po	α	299 ns	^{215}Bi	β^-	7.6 min	^{218}At	α 99.90% β^- 0.10%	1.5 s
^{208}Tl	β^-	3.053 min	^{215}Po	α 99.99977% β^- 0.00023%	1.781 ms	^{218}Rn	α	35 ms
^{208}Pb	stable	.	^{215}At	α	0.1 ms	^{214}Pb	β^-	26.8 min
			^{211}Pb	β^-	36.1 min	^{214}Bi	β^- 99.98% α 0.02%	19.9 min
			^{211}Bi	α 99.724% β^- 0.276%	2.14 min	^{214}Po	α	0.1643 ms
			^{211}Po	α	516 ms	^{210}Tl	β^-	1.30 min
			^{207}Tl	β^-	4.77 min	^{210}Pb	β^-	22.3 a
			^{207}Pb	.	stable	^{210}Bi	β^- 99.99987% α 0.00013%	5.013 d
						^{210}Po	α	138.376 d
						^{206}Tl	β^-	4.199 min
						^{206}Pb	-	stable

3.6. Predicting Type of Decay

Radioactive nuclides tend to decay in a way that results in a daughter nuclide that lies closer to the line of stability. Due to this, it is possible to predict the type of decay that a nuclide will undergo based on its location relative to the line of stability on the Chart of the Nuclides.

Fig. 3.6 illustrates the type of decay nuclides in different regions of the chart will typically undergo. Nuclides that are below and to the right of the line of stability will usually undergo β^- decay. Nuclides that are above and to the left of the line of stability will usually undergo either β^+ decay or electron capture. Most nuclides that will undergo α decay are found in the upper right hand region of the chart. These are general rules that have many exceptions, especially in the region of heavy nuclides.

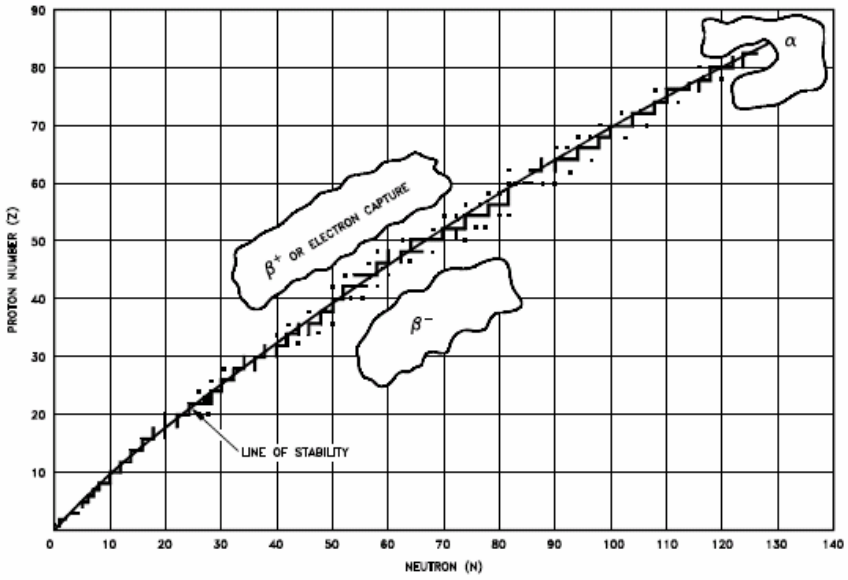

Figure 3.6. Types of radioactive decay relative to the line of stability.

3.7. Decay Schemes

Decay schemes are widely used to give a visual representation of radioactive decay. A scheme for relatively straightforward decay is shown in Fig. 3.7 below:

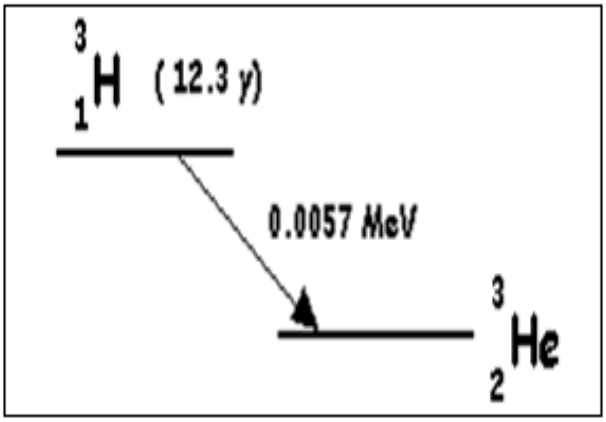

Figure 3.7. Decay scheme of ^{3}H to the ground state of ^{3}He.

This scheme is for ^{3}H, which decays to ^{3}He with a half-life of 12.3 years through the emission of a beta-minus particle with an energy of 0.0057 MeV.

A scheme for a more complicated decay is that of ^{137}Cs, Fig. 3.8. This isotope can decay through two beta-minus processes. In one, which occurs in 5% of disintegrations a beta-minus particle is emitted with energy of 1.17 MeV to produce ^{137}Ba. In the second which occurs more frequently (in the remaining 95% of disintegrations), a beta-minus particle of energy 0.51 MeV is emitted to produce $^{137}Ba^{*}$; in other words a barium-137 nucleus in a meta-stable state or excited state. The $^{137}Ba^{*}$ then decays via isomeric transition with the emission of a gamma ray of energy 0.662 MeV.

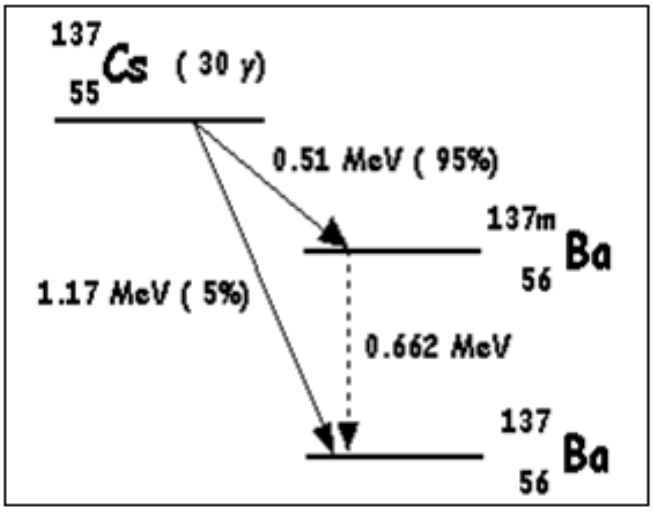

Figure 3.8. Decay of ^{137}Cs showing the fraction of β^- decays to the ground state and to the excited state of ^{137}Ba, which in turn decays by γ-emission.

The general method used for decay schemes is illustrated in Fig. 3.9. The energy is plotted on the vertical axis and atomic number on the horizontal axis - although these axes are rarely displayed in actual schemes. The isotope from which the scheme originates is displayed at the top **X** in the case above. This isotope is referred to as the parent. The parent looses energy when it decays and hence the products of the decay referred to as daughter**s** are plotted at a lower energy level.

The figure illustrates the situation for common forms of radioactive decay. Alpha decay is illustrated on the left where the mass number is reduced by 4 and the atomic number is reduced by 2 to produce daughter **Y**. To its right, the scheme for beta-plus decay is shown to produce daughter **B**. The situation for beta-minus decay followed by gamma

decay is shown on the right side of the diagram where a daughter **C** in the excited energy state is produced to decay to its ground state by emitting a gamma ray.

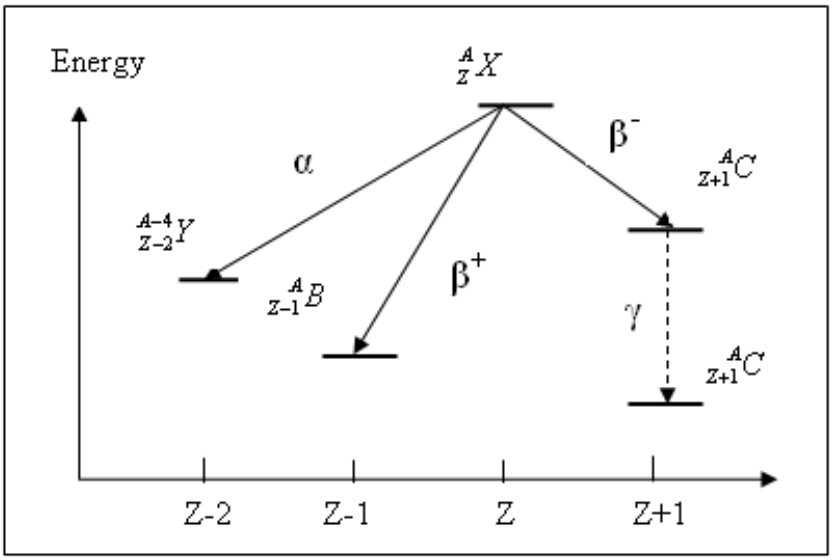

Figure 3.9. Schematic diagram describing all types of decay.

Problems

3-1 The following are atomic masses in units of u.

Electron	0.000549	$^{152}_{62}Sm$	151.919756
Neutron	1.008665	$^{152}_{63}Eu$	151.921749
^{1}H	1.007825	$^{152}_{64}Gd$	151.919794

a- What is the recoil nucleus and Q-value of the reaction ^{152}Eu (n, p)?

b- What types of weak-interaction decay can occur for ^{152}Eu?

c- What is the maximum energy of the particles emitted in each of the processes given in (b)?

3-2 Find the minimum energy in the laboratory system that a neutron must have in order to initiate the reaction:

$$^{1}_{0}n + ^{16}_{8}O + 2.22MeV \rightarrow ^{13}_{6}C + ^{4}_{2}He$$

3-3 Find the minimum energy in the laboratory system that a proton must have in order to initiate the reaction:

$$^{1}_{1}p + ^{2}_{1}H + 2.22MeV \rightarrow ^{1}_{1}H + ^{1}_{1}p + ^{1}_{0}n$$

3-4 Find the minimum kinetic energy in the laboratory system that a proton must have to initiate the reaction:
M($^{14}_{7}N$) = 14.0031 u, M($^{15}_{8}O$) = 14.9905 u.

$$^{1}_{1}p + ^{14}_{7}N \rightarrow ^{15}_{8}O + ^{1}_{0}n$$

3-5 What minimum energy would an alpha particle need in order to react with a ^{238}U nucleus?

3-6 How much energy is released when a ^{6}Li atom absorbs a thermal neutron in the reaction ^{6}Li (n, α) ^{3}H?

3-7 In the nuclear reaction ^{27}Al (d, p) ^{28}A1, deuterons are used with a kinetic energy of 2.10 MeV. In this experiment (measuring in the laboratory system), the outgoing protons are detected at right angles with respect to the direction of the incoming deuterons. If protons are detected with energy E_P corresponding to ^{28}Al in its ground state and with energy E_p^* corresponding to ^{28}A1* remaining in its excited state at 1.014 MeV, show that $|E_p - E_p^*| \neq 1.014$ MeV. Explain this difference.

3-8 Calculate the Q values for the following α-decays between ground-state levels of the nuclei:
(a) ^{208}Po → ^{204}Pb + α, and (b) ^{230}Th → ^{226}Ra + α
What are the kinetic energies of the α-particles and of the nuclei in the final state if the decays proceed from rest?

3-9 Show that it is essentially possible for $^{80}_{35}Br$ to undergo beta decay by electron emission, positron emission and electron capture and find the energy released in each case.

3-10
(a) Calculate the energy released in the beta decay of ^{32}P.
(b) If a beta particle has 650 keV, how much energy does the antineutrino have?

3-11 The A = 40 isotopes of calcium (Z = 20), potassium (Z= 19) and argon (Z = 18) have respective binding energies 332.65MeV, 332.11MeV and 335.44MeV. What β decays are allowed between these nuclei? Specify the available energy Q in the final state. What peculiarity appears?

3-12
(a) Calculate the *Q* value for K orbital-electron capture by the $^{37}_{18}Ar$ nucleus, neglecting the electron binding energy.
(b) Repeat (a), including the binding energy, 3.20 keV, of the K-shell electron in argon.
(c) What becomes of the energy released as a result of this reaction?

3-13 We give the atomic binding energy in the following elements: $^{163}_{67}Ho$=1329.604 MeV and $^{163}_{66}Dy$=1330.389 MeV. Which decay processes can occur in this particular case?
Knowing that: $(m_n - m_H)c^2$ =0.782 MeV.

3-14 Show that ^{55}Fe, which decays by electron capture, cannot decay by positron emission.

3-15 The isotope ^{126}I can decay by EC, β^-, and β^+ transitions.
(a) Calculate the *Q* values for the three modes of decay to the ground states of the daughter nuclei.
(b) Draw the decay scheme.
(c) What kinds of radiation can one expect from a ^{126}I source?

3-16 Discuss the recoil energy for α, β and γ-decay.
Calculate and compare the order of magnitude in each case for a nucleus with mass number A = 40, Z = 20 and an equal Q-value ($Q_\alpha = Q_{\beta^-} = Q_\gamma$ = 5 MeV). In which decay process can one neglect this recoil energy and still have a satisfactory energy balance.

3-17 When an excited nucleus emits a gamma-ray photon, some of the excitation energy goes into the kinetic energy of the recoil of the nucleus. Fig. 2.6 shows energy levels for nickel-60. Calculate the recoil energy for each energy level and comment on its effect on the energy of the γ-photon emitted if the lifetime of the excited state is 10^{-14} sec.

3-18 The radionuclide ^{41}Ar decays by β^- emission to an excited level of ^{41}K that is 1.293 MeV above the ground state. What is the maximum kinetic energy of the β^- emitted particle?

3-19 The radioisotope ^{64}Cu decays by three different mechanisms: β^- decay (39.0%), electron capture (EC) (43.1%) and β^+ decay (17.4 %). The Q value for the β^- decay is 578.7 keV. The Q value for β^+ the decay is 653.1 keV. In addition, there is a gamma emission (0.5% probability) at 1.345 MeV. Sketch the energy level diagram for the decay scheme.

3-20 For the following γ transitions, give all permitted multipoles and indicate which multipole might be the most intense in the emitted radiation.

(a) $9/2^- \rightarrow 5/2^-$ (d) $4^+ \rightarrow 2^+$

(b) $1/2^- \rightarrow 7/2^-$ (e) $3^+ \rightarrow 3^+$

(c) $1^- \rightarrow 2^+$ (f) $11/2^- \rightarrow 3/2^+$

3-21 A nucleus has the following sequence of states beginning with the ground state: $3/2^+$, $7/2^+$, $5/2^+$, $1/2^-$, and $3/2^-$. Draw a level scheme showing the intense γ transitions likely to be emitted and indicate their multipole assignment.

CHAPTER 4

RADIOACTIVE DECAY DYNAMIC

The rate at which a sample of radioactive material decays is not constant. As individual atoms of the material decay, there are fewer of those types of atoms remaining. Since the rate of decay is directly proportional to the number of atoms, the rate of decay will decrease as the number of atoms decreases.

4.1. Radioactive Decay Rates

Radioactivity is the property of certain nuclides of spontaneously emitting particles or electromagnetic waves, or is the process in which an unstable atomic nucleus loses energy by emitting radiation in the form of particles or gamma radiation. This decay, or loss of energy, results in an atom of one type, called the parent nuclide transforming to an atom of a different type, called the daughter nuclide. This is a random process on the atomic level, in that it is impossible to predict when a particular atom will decay. However, the average behavior of a very large sample can be predicted accurately by using statistical methods. These studies have revealed that there is a certain probability that, in a given time interval, a certain fraction of the nuclei within a sample of a particular nuclide will decay. This probability per unit time that an atom of a nuclide will decay is known as the *radioactive decay constant*, λ. The units for the decay constant are inverse time.

4.2. Units of Radioactivity

The *activity* (*A*) of a sample of any radioactive nuclide is the rate of decay of the nuclei of that sample. For a sample containing billions of atoms, this rate of decay is usually measured in the number of disintegrations that occur per second. If *N* is the number of nuclei present in the sample at a certain time, the change in number of those nuclei with time, rate of decay, is the activity *A*, and can be given by:

$$A = -\frac{dN}{dt} \qquad 4.1$$

The minus sign is used to make *A* a positive quantity since *dN/dt* is, of course, intrinsically negative.

In addition, the activity is the product of the decay constant and the number of atoms present in the sample. The relationship between the activity *A*, number of atoms *N*, and decay constant λ is given by:

$$A = \lambda N \qquad 4.2$$

Since λ is a constant, the activity and the number of atoms are always proportional.

Two common units to measure the activity of a substance are the Curie (Ci) and Becquerel (Bq). A *curie* is a unit of measure of the rate of radioactive decay equal to 3.7×10^{10} disintegrations per second. This is approximately equivalent to the number of disintegrations that one gram of radium ^{226}Ra will undergo in one second. A *Becquerel,* as the metric system, is a more fundamental unit of measure of radioactivity than Curie. The conversion between Curie and Becquerel is shown below.

1 Bq = 1 dis/sec

1 Curie = 3.7×10^{10} Bq

Note that the activity tells us only the number of disintegrations per second; it says nothing about the kind if radiations emitted their energies, or the effect of radiation on a biological system, since different radiations may give different effects. In the next section, some alternative units for measuring radiation that take into account their relative biological effects will be discussed.

4.3. Radioactive Decay Law

From the previous two basic relationships, Eq.4.1 and Eq. 4.2, it is possible to use calculus to derive an expression that can be used to calculate how the number of atoms present will change over time.

$$- dN = N\lambda\, dt$$

or

$$-\frac{dN}{N} = \lambda dt \qquad 4.3$$

This equation describes the situation for any short time interval, *dt.* To find out what happens for all periods of time, we simply add up what happens in each short time interval. In other words, we integrate the above equation. Expressing this more formally, we can say that for the period of time from $t = 0$ to any later time t, the number of radioactive nuclei will decrease from N_0 to N_t, so that:

$$N_t = N_0 \exp(-\lambda t) \qquad 4.4$$

This final expression is known as the *Radioactive Decay Law*. It tells us that the number of radioactive nuclei N_0 at time $t = 0$ will decrease in an exponential fashion to N_t with time with the rate of decrease being controlled by the decay probability per unit time, decay constant λ.

The decay constant is characteristic of individual radionuclide, i.e., has a different values for each. Some, like uranium-238, have a small value and the material, therefore, decays quite slowly over a long period of time. Other nuclei such as technetium-99m ($^{99}Tc^{*}$) are metastable, have a relatively large decay constant and decay far more quickly. The radioactive decay law is shown in graphical form in Fig. 4.1 for three typical radionuclides of different decay constants.

The graph plots the number of radioactive nuclei at any time, N_t against time, t. The influence of the decay constant can be seen clearly.

Since the activity A and the number of atoms N are always proportional, they may be used interchangeably to describe any given radionuclide population. Therefore, the following is true:

$$A_t = A_0 \exp(-\lambda t) \qquad 4.5$$

where:

A_t = activity present at time t
A_0 = activity initially present

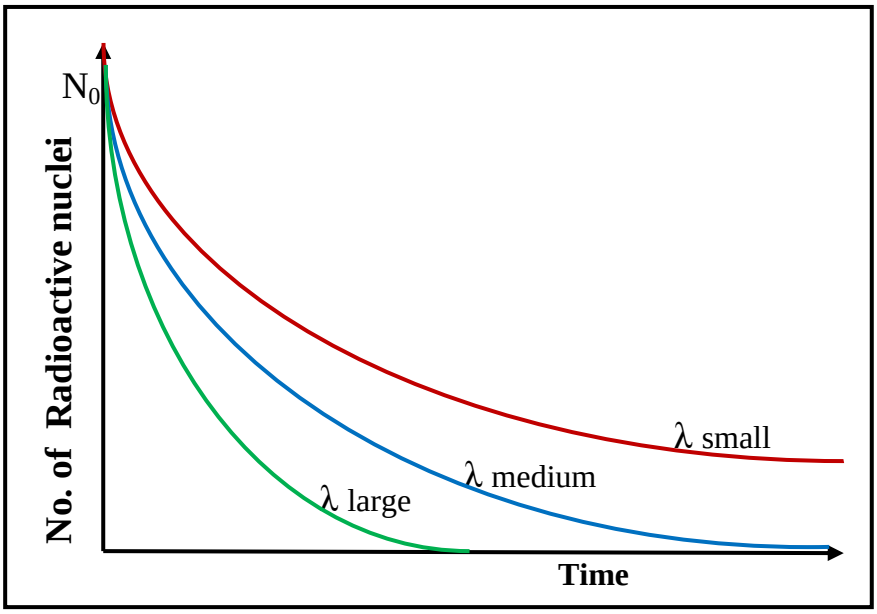

Figure 4.1. The influence of the decay constant.

4.4. Radioactive Half-Life

One of the most useful terms for estimating how quickly a nuclide will decay is the radioactive half-life. The *radioactive half-life* is defined as the amount of time required for the activity to decrease to one-half of its original value. A relationship between the half-life and decay constant can be developed from Eq.4.5. The half-life can be calculated by solving Eq.4.5 for the time, t, when the current activity, *A*, equals one-half the initial activity $A = ½A_0$. First, solve Eq.4.5 for *t*:

$$t = -\frac{Ln(A_t / A_0)}{\lambda} \qquad 4.6$$

Now if A is equal to one-half of A_0, A/A_0 is equal to one-half. Substituting this ratio in the above equation yields an expression for $t_{½}$:

$$t_{1/2} = -\frac{Ln(1/2)}{\lambda} = \frac{\ln(2)}{\lambda} = \frac{0.693}{\lambda} \qquad 4.7$$

The basic features of decay of a radionuclide sample are shown by the normalized graph in Fig. 4.2.

Note that the half-life does not express how long a material will remain radioactive but simply the length of time for its radioactivity to reduce by half. Assuming an initial number of atoms N_o, the population, and consequently, the activity may be noted to decrease by one-half of this value in a time of one half-life. Additional decreases occur so that whenever one half-life elapses; the number of atoms drops to one-half of what its value was at the beginning of that time interval. After five half-lives have elapsed, only 1/32, or 3.1%, of the original number of atoms remains. After seven half-lives, only 1/128, or 0.78%, of the atoms remains. The number of atoms existing after 5 half-lives can usually be assumed to be negligible.

Another useful term is the *mean lifetime* of the nuclei, which is given by the total time of existence of all nuclei divided by the number of nuclei present initially. Since the decay process is a statistical one, any single atom may have a life from *zero* to ∞. Hence, the mean lifetime τ is given:

$$\tau = \frac{1}{N_0}\int_0^\infty N_0 \lambda t e^{-\lambda t} dt = \lambda \int_0^\infty t e^{-\lambda t} dt = \frac{1}{\lambda} \qquad 4.8$$

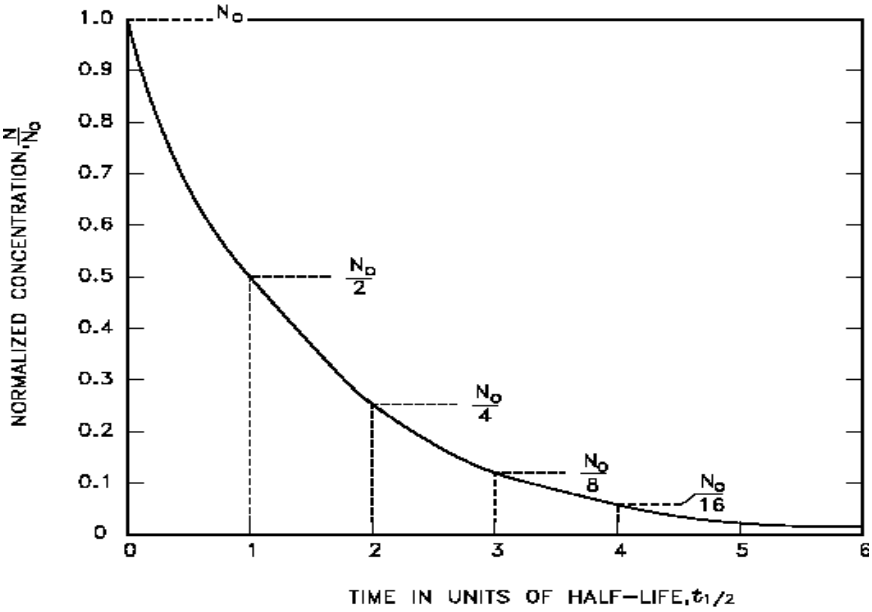

Figure 4.2. Radioactive decay as a function of time in units of half-life.

It is also possible to consider the radioactive decay law from another perspective by plotting the logarithm of N against time. In other words from our analysis above by plotting the expression:

$$Ln(N/N_0) = -\lambda t \quad \text{in the form} \quad Ln(N) = -\lambda t + Ln(N_0) \qquad 4.9$$

Notice that this expression is simply an equation of the form $y = mx + c$ where $m = -\lambda$ and $c = ln(N_0)$. As a result, it is the equation of a straight line of slope $-\lambda$ as shown in Fig. 4.3. Such a plot is sometimes useful when we wish to consider a situation without the complication of the direct exponential behavior.

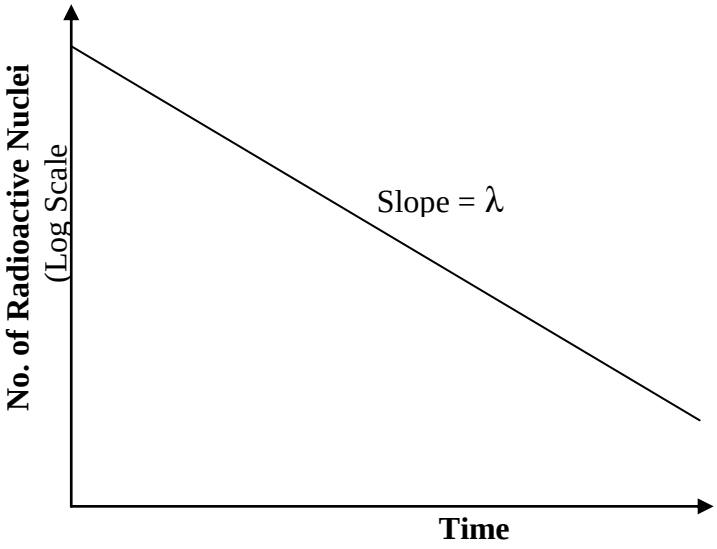

Figure 4.3. Semi-log plots of radioactive Decay.

Example:

A sample of material contains 1 gram of radium-226, half-life of 1620 years.

Calculate:

(a) The number of ^{226}Ra atoms initially present
(b) The activity of the ^{226}Ra in curies
(c) The number of ^{226}Ra atoms that will remain in 12 years
(d) The time it will take for the activity to reach 0.01 curies

Solution:

Avogadro's number: $N_{Av} = 6.023 \times 10^{23}$atoms/g.mol

(a) The number of atoms of ^{226}Ra can be determined as below:

$$N_o = \frac{N_{Av} m}{A} = \frac{\left(6.023 \times 10^{23} atom / g.mol\right)\left(1g\right)}{226} = 2.7 \times 10^{21} atoms$$

(b) First, use Equation (4.6) to calculate the decay constant:

$$\lambda = \frac{0.693}{t_{1/2}} = \frac{0.693}{1620} = 4.28 \times 10^{-4} \text{ year}^{-1}$$

$$\lambda = 1.36 \times 10^{-11}\ s^{-1}$$

Note that the length of a year used in converting from 'per year' to 'per second' above is 365.25 days to account for leap years. In addition, the reason for converting to units of 'per second' is that the unit of radioactivity is expressed as the number of nuclei decaying per second. Then, using this value for the decay constant in Eq.4.2 we determine the activity:

$$A_0 = \lambda N_0 = (1.36 \times 10^{-11}\ \text{s}^{-1})(\ 2.7\times10^{21}\ \text{atoms})$$
$$A_0 = 3.7 \times 10^{10}\ \text{dis/s} = 1\ \text{Ci}$$

So the radioactivity of our 1 g sample of ^{226}Ra is approximately 1 Ci.

This is not a surprising answer since the definition of the **Curie** was originally conceived as the radioactivity of 1 g of ^{226}Ra!

(c) The number of Radium atoms that will remain in 12 years can be calculated from Eq.4.4 using unit of yr^{-1} for decay constant:

$$N_t = 2.7\times10^{21} \exp(-4.28 \times 10^{-4}\ \text{yr}^{-1} \times 12\ \text{yr})$$
$$= 2.69 \times 10^{21}\ \text{atoms}$$

(d) The time that it will take for the activity to reach 0.01 Ci can be determined from Eq.4.6:

$$t = -\frac{Ln(A_t / A_0)}{\lambda} = \frac{-Ln\left\{\frac{0.01\ \ Ci}{1\ \ Ci}\right\}}{(4.28\times10^{-4}\ yr^{-1}\ )} = 10760 \text{ yr}$$

If a substance contains more than one radioactive nuclide, the total activity is the sum of the individual activities of each nuclide:

$$A_{total} = \sum_{i=1}^{n} A_i \qquad i=1, 2, 3 \ldots n \qquad 4.10$$

Example

Calculate the activity a sample of material that contained the following three isotopes:

1- $1x10^6$ atoms of ^{59}Fe of $t_{1/2}$ = 44.51 days (λ=1.80 x $10^{-7}s^{-1}$)

2- $1x10^6$ atoms of ^{54}Mn of $t_{1/2}$ = 312.2 days (λ=2.57x10^{-8} s^{-1})

3- $1x10^6$ atoms of ^{60}Co of $t_{1/2}$ = 1925 days (λ=4.17x10^{-9} s^{-1}).

Solution

The initial activity of each of the nuclides would be the product of the number of atoms and the decay constant using Eq.4.2.

For ^{59}Fe $A_1 = N_1 \lambda_1 = (1\times10^6\ atoms)(1.80\times10^{-7}\ s^{-1})$=0.180 *Bq*

$= 0.18/3.7 \times 10^{10} = 0.049\times10^{-10}$ Ci

For ^{54}Mn $A_2 = N_2 \lambda_2 = (1\times10^6\ atoms)(2.57\times10^{-8}\ s^{-1})$=0.0257 *Bq*

$= 0.0257/3.7 \times 10^{10} = 0.0069\times10^{-10}$ Ci

For ^{60}Co $A_3 = N_3 \lambda_3 = (1\times10^6\ atoms)(4.17\times10^{-9}\ s^{-1})$=0.00417 *Bq*

$= 0.00417/3.7 \times 10^{10} = 0.00113\times10^{-10}$ Ci

$A_{total} = A_1+A_2+A_3 = 0.180+0.0257+0.00417 = 0.20987$ *Bq*

Plotting the manner in which the activities of each of the three nuclides decay over time demonstrates that, initially, the activity of the shortest-lived nuclide (^{59}Fe) dominates the

total activity, and then ^{54}Mn dominates. After almost all of the iron and manganese have decayed away, the only contributor to activity will be the ^{60}Co. A plot of this combined decay is shown in Fig. 4.4.

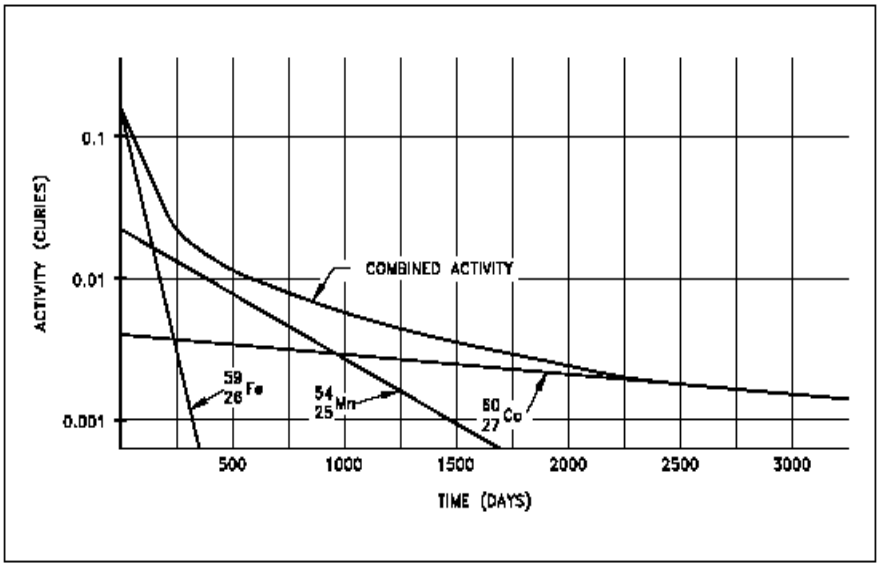

Figure 4.4. Combined Decay of ^{56}Fe, ^{54}Mn, and ^{60}Co.

4.5. Specific Activity

The specific activity of a radioactive source is defined as the activity per unit mass of the radioactive sample:

$$S.A. = \frac{Activity}{mass} = \frac{\lambda N}{m} = \frac{\lambda N_{Av}}{M} Bq/g \qquad 4.11$$

where $m=NM/N_{Av}$ is the mass of the sample in g, N_{Av} is the Avogadro's number = 6.023×10^{23} nuclei/g and M is the molecular weight, can be replaced by the mass number A for

the pure radioactive isotope. In practice, using the atomic mass number A in place of M usually gives sufficient accuracy, then in terms of half life and mass number Eq.4.11 gives:

$$S.A. = \frac{6.023\times10^{23}\lambda}{A} = \frac{4.17\times10^{23}}{At_{1/2}} Bq/g \qquad 4.12$$

If $t_{1/2}$ is in seconds, this formula gives the specific activity in $Bq.g^{-1}$.

The fact that ^{226}Ra has unit specific activity in terms of $Ci\ g^{-1}$, as been shown in the first example, can be used in place of Eq. 4.12 to find SA for other radionuclides. Compared with ^{226}Ra, a nuclide of shorter half-life and smaller atomic mass number A will have, in direct proportion, a higher specific activity than ^{226}Ra. The specific activity of a nuclide of half-life (*expressed in years*) $t_{1/2}$ (y) and atomic mass number A is therefore given by:

$$S.A. = \frac{1620\,years}{t_{1/2}\,years} \times \frac{226}{A} Ci/g \qquad 4.13$$

4.6. Production of Radioactive Isotopes

A production of radioactive isotopes has a wide range of applications, in medicine, industries, agriculture…, if stable (non-radioactive) nuclei are bombarded with alpha, beta, neutron, etc., the particles are frequently captured in the nuclei and new isotopes result. Most of the isotopes formed in this manner have excess energy and are thus radioactive. This is a frequent phenomenon in nuclear reactor cores or an

accelerator, called *activation analysis,* where structural materials are subject to high levels of radiation.

Suppose that a sample of stable nuclei is bombarded using a projectile that can induce transmutations at a given rate of R atoms/sec for a time interval $(0, T)$ and so forms radioactive isotope that decay again with a decay constant λ. The law, describing the change of the number of elements dN_t/dt, during radioactive production, $t < T$, is a balance between the production rate R and the decay activity $-\lambda N_t$, or:

$$\frac{dN_t}{dt} = R - \lambda N \qquad 4.14$$

This equation (for constant formation rate R) can be rewritten as:

$$\frac{d(R-\lambda N)}{R-\lambda N} = -\lambda dt \qquad 4.15$$

Integrating this differential equation, with the time at which the irradiation starts, N_0 (at t = 0) = 0 atoms, one obtains:

$$N_t = \frac{R}{\lambda}\left(1 - e^{-\lambda t}\right), \quad t \le T \qquad 4.16$$

Equation 4.16 can be used to calculate the values of the amount of the isotope present at different times of activation. As the time increases, the exponential term approaches zero, and the number of atoms will approach R/λ or the activity $A_t = \lambda N_t$ will approach R (i.e. saturation). The corresponding results for the activity A_t and $dN_t/dt = e^{-\lambda t}$ is given in Fig. 4.5.

Here, it becomes clear that activity λN_t and the quantity dN_t/dt are completely different: the activity grows to an almost constant value, approaching saturation near $A_t \approx R$ whereas dN_t/dt approaches the value of zero.

After irradiation during $t = 3t_{1/2}$, $4t_{1/2}$ the number of radioactive elements formed is 0.875 and 0.938, respectively of the maximal number (when $\mathbf{t} \rightarrow \infty$). Therefore, in practice, irradiations time T should not last longer than *3* to *4* half-life periods.

For $t > T$, the governing equation is Eq. 4.14 without the source term. The solution is:

$$N(t) = \frac{R}{\lambda}\left(1 - e^{-\lambda T}\right)e^{-\lambda(t-T)}, \quad t > T \qquad 4.17$$

Fig. 4.5 also shows the activity *A(t)*, after production, undergoes an exponential decay.

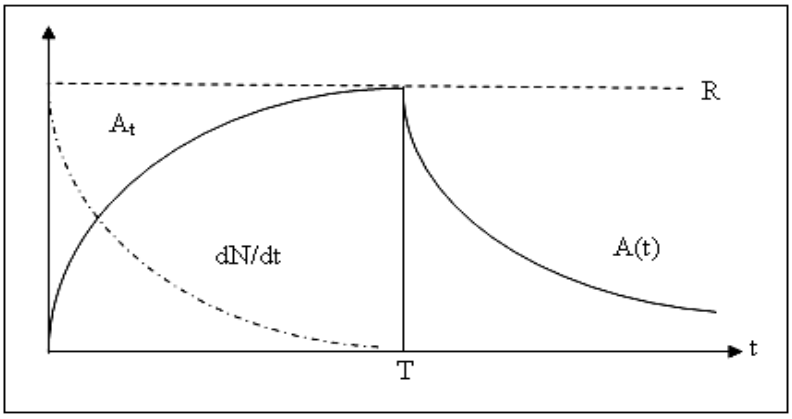

Figure 4.5. Time variation of the activity of a radioisotope produced at a constant rate R for a time interval of T after which the system is left to decay.

4.7. Successive Radioactive Transformations

In the more applied situations, the naturally radioactive nuclides form three series. The *thorium* ^{232}Th series, *uranium* ^{238}U series, and *actinium* ^{235}U series, these series are headed by naturally occurring species of heavy unstable nuclei that have half-lives comparable to the age of the elements; Table 3.1 shows the major characteristics of these series. In the study of radioactive series, it is important to know the number of atoms of each member of the series as a function of time. The answer to a problem of this kind can be obtained by solving a system of differential equations. Consider the case of a three-member chain:

$$N_1 \xrightarrow{\lambda_1} N_2 \xrightarrow{\lambda_2} N_3\ stable$$

where, λ_1 and λ_2 are the decay constants of the parent (*N1*) and the daughter (*N2*), respectively.

The governing equations are:

$$\begin{aligned} \frac{dN_1(t)}{dt} &= -\lambda_1 N_1(t) && a \\ \frac{dN_2(t)}{dt} &= \lambda_1 N_1(t) - \lambda_2 N_2(t) && b \\ \frac{dN_3(t)}{dt} &= \lambda_2 N_2(t) && c \end{aligned} \qquad 4.18$$

The details of the solution of this system of equations depend on the initial condition, the general case is when the three nuclides have N_{10}, N_{20}, N_{30} number of atoms at time

($t = 0$). The number of atoms N_1, Eq.4.18a, can be written down immediately:

$$N_1(t) = N_{10}e^{-\lambda_1 t} \qquad 4.19$$

This expression for $N_1(t)$ is inserted into Eq.4.18b, then multiplied by the integrating factor $e^{\lambda_2 t}$ and taking its integration to get:

$$N_2(t)e^{\lambda_2 t} = N_{10}\frac{\lambda_1}{\lambda_2 - \lambda_1}e^{(\lambda_2 - \lambda_1)t} + C$$

where C is a constant of integration, which is obtained by inserting the initial value of number of atoms at $t = 0$, N_{20}, and inserting into the above equation to get:

$$N_2(t) = N_{10}\frac{\lambda_1}{\lambda_2 - \lambda_1}(e^{-\lambda_1 t} - e^{-\lambda_2 t}) + N_{20}e^{-\lambda_2 t} \qquad 4.20$$

The number of atoms of the third specie is found by inserting this expression for $N_2(t)$ into Eq.4.18c and integrating it with respect to time, gives:

$$N_3(t) = \left(N_{10}\frac{\lambda_1}{\lambda_2 - \lambda_1} - N_{20}\right)e^{\lambda_2 t} - N_{10}\frac{\lambda_2}{\lambda_2 - \lambda_1}e^{-\lambda_1 t} + D \qquad 4.21$$

where D is an integration constant, determined by the condition $N_3(t) = N_{30}$ at t = 0.
This condition gives:
$D = N_{30} + N_{20} + N_{10}$. and when inserted into Eq.4.21, the result is:

$$N_3(t) = N_{30} + N_{20}(1-e^{-\lambda_2 t}) + N_{10}\left(1+\frac{\lambda_1}{\lambda_2-\lambda_1}e^{-\lambda_2 t} - \frac{\lambda_2}{\lambda_2-\lambda_1}e^{-\lambda_1 t}\right) \quad 4.22$$

The special case of this system is that in which only radioactive atoms of the first specie N_{10} are present initially, most often in production of radioisotopes. In this case, the constants N_{20} and N_{30} are both equal to zero, and the solution for $N_2(t)$ and $N_3(t)$ reduce to:

$$N_2(t) = N_{10}\frac{\lambda_1}{\lambda_2-\lambda_1}(e^{-\lambda_1 t} - e^{-\lambda_2 t}) \quad 4.23$$

$$N_3(t) = N_{10}\frac{\lambda_1\lambda_2}{\lambda_2-\lambda_1}\left(\frac{1-e^{-\lambda_1 t}}{\lambda_1} - \frac{1-e^{-\lambda_2 t}}{\lambda_2}\right) \quad 4.24$$

One should notice from Eq.4.18 that the sum of these three differential equations is zero. This means that $N_1(t) + N_2(t) + N_3(t)$ = constant for any time t. We also know from our initial conditions that this constant must be N_{10}. One can use this information to find $N_3(t)$ given $N_1(t)$ and $N_2(t)$, or use this as a check that the last solutions are indeed correct.

The amount of the successive radioactive daughters, N_2 in Eq.4.23 is zero at time t=0 and at t=∞ while N_3 in Eq.4.24 is zero at time t=0 and N_{10} at t=∞. As the chain decay starts, the amount of these daughters increases with time in a fashion that at some intermediate time, their amounts and hence their activities will pass through a maximum value. The time of maximum activity of daughters (t_{max}) can be calculated simply by equating the differentiation of Eqs.4.23 and 4.24 to zero, i.e. $dN_i/dt=0$, where i=2, 3….

4.8. Radioactive Equilibrium

Radioactive equilibrium exists when a radioactive nuclide is decaying at the same rate at which it is being produced. Since the production rate and decay rate are equal, the number of atoms present remains constant over time. Mathematically, it is the condition that the derivative of a function with respect to time is equal to zero. When applied to the set of Eq.4.18 we get:

$$\lambda_1 N_1 = \lambda_2 N_2 = \lambda_3 N_3 = \ldots \qquad 4.25$$

Eqs.4.19, 4.23, 4.24 are known as the Bateman equations. One can use them to analyze situations when the decay constants λ_1 and λ_2 take on different relative values. We consider three such scenarios, the case where the parent is short-lived, $\lambda_1 >> \lambda_2$, the opposite case where the parent is long-lived, $\lambda_1 < \lambda_2$ *and,* $\lambda_1 << \lambda_2$.

4.8.1. Series decay with short-lived parent

In this case, one expects the parent to decay quickly and the daughter to build up quickly. The daughter then decays more slowly which means that the granddaughter will build up slowly, eventually approaching the initial number of the parent. Fig. 4.6 shows schematically the behavior of the three isotopes. The initial values of $N_2(t)$ and $N_3(t)$ can be readily deduced from an examination of Eq.4.23 and 4.24. For a time $t >> 1/\lambda_1$, one can neglect the first exponential in Eq.4.23, $e^{-\lambda_1 t} \rightarrow 0$:

$$N_2(t) = N_{10} \frac{\lambda_1}{\lambda_1 - \lambda_2} e^{-\lambda_2 t} \qquad 4.26$$

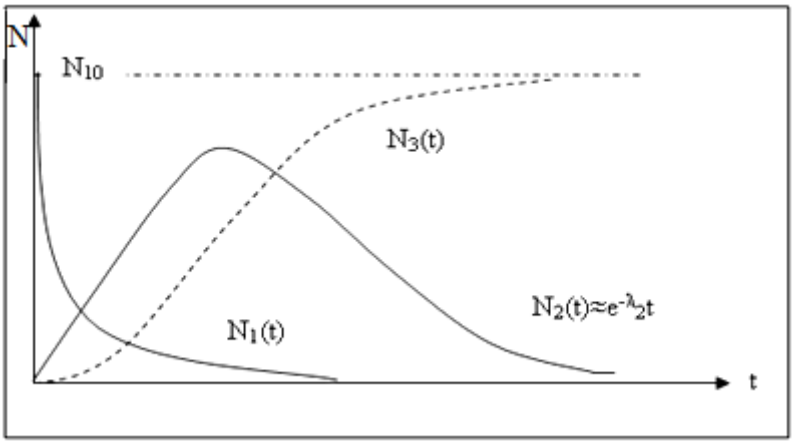

Figure 4.6. Schematic diagram of time variation of the three-member decay chain for the case $\lambda_1 >> \lambda_2$.

4.8.2. Series decay with long-lived parent

When $\lambda_1 < \lambda_2$, we expect the parent to decay slowly so the daughter and granddaughter will build up slowly. Since the daughter decays quickly, the long-time behavior of the daughter follows that of the parent. Fig. 4.7 shows the general behavior. In this case, for a time $t >> 1/\lambda_2$, one can neglect the second exponential in Eq.4.23 ($e^{-\lambda_2 t} \rightarrow 0$); this situation is known as *transient equilibrium*, to get:

$$N_2(t) = N_{10} \frac{\lambda_1}{\lambda_2 - \lambda_1} e^{-\lambda_1 t} \qquad 4.27$$

Accordingly, the activity relationship will be:

$$\frac{A_2}{A_1} = \frac{\lambda_2}{\lambda_2 - \lambda_1} \qquad 4.28$$

The second interesting case is the *secular equilibrium*, i.e., of a very long-lived parent, $\lambda_1 << \lambda_2$. The parent decays at an essentially constant rate, for all practical times $e^{-\lambda_1 t} \approx 1$ and Eq.4.23 reduced to:

$$N_2(t) = N_{10} \frac{\lambda_1}{\lambda_2}(1 - e^{-\lambda_2 t}) \qquad 4.29$$

Fig. 4.8 shows the general behavior of variation number of atoms of the three nuclides, and an example, clarifying the activities, of the case $t_{1/2}(1)$ = 8 h and $t_{1/2}(2)$ = 0.8 h is given in Fig. 4.9.

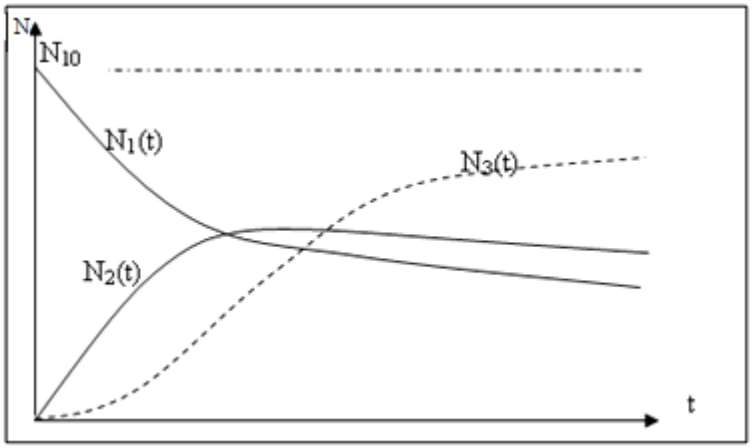

Figure 4.7. Schematic diagram of time variation of the three-member decay chain for the case $\lambda_1 < \lambda_2$.

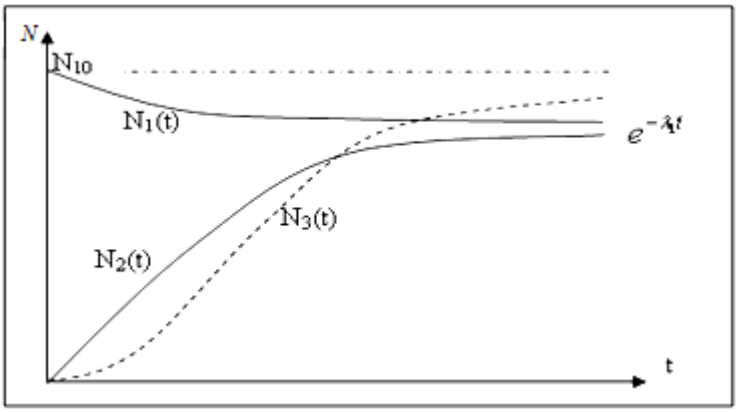

Figure 4.8. Time variation of the three-member decay chain, case $\lambda_1 << \lambda_2$.

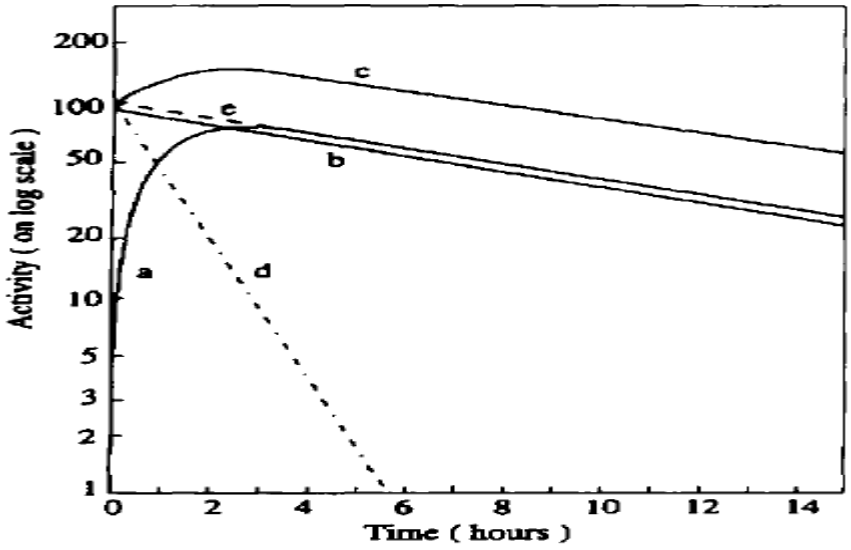

Figure 4.9. *Transient* equilibrium *(a)* Daughter activity growing in a freshly purified parent, *(b)*Activity of parent ($t_{1/2}$ *=8* h), *(c)*Total activity of an initially pure parent fraction, *(d)*Decay of freshly isolated daughter fractions ($t_{1/2}$ *=0.8* h), and *(e)*Total daughter activity in parent-plus-daughter fractions.

The last interesting case is the situation where $\lambda_1 \approx 0$, or $\lambda_1 <<< \lambda_2$, then $N_2(t) = N_{10}$ and consequently the activities:

$$A_2(t) = A_{10} \text{ or } A_2(t)/A_{10} = 1 \qquad 4.30$$

{i.e. $A_1(t)=A_{10}$ almost constant} since from Eq.4.29 at a time $t >> t_{1/2}$*(daughter)*, $e^{-\lambda_2 t} \approx 0$, and we approach again *secular equilibrium*. In this case, we reach equilibrium, as shown in Fig. 4.10. While at a short-time $t \gtrsim t_{1/2}$*(daughter)*, the parent behaves as a constant productive of the daughter.

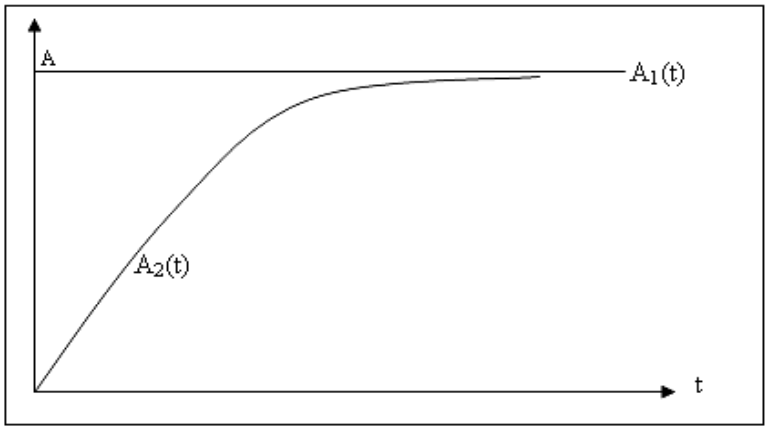

Figure 4.10. Activity curve for the secular equilibrium as $\lambda_1 \approx 0$.

4.9. Units of Measuring Radiation

To understand the effect of radiation on the environment and living tissues, The knowledge of the units of measuring radiation, which are exposure and dose, must be taken into account.

The most important interactions of radiation with matter are with electrons of atoms that cause the atoms to separate

into ions, this ionization may be direct (by interaction of α or β particles) or indirect by γ ray.

4.9.1. Exposure and exposure rate

The unit of exposure depends on the concept of γ ray exposure, and it is a quantity, which is roughly analogous to the strength of an electric field created by a point charge, defined only for sources of X-ray or γ ray.

The basic unit of exposure is defined in terms of the charge *dQ* due to the ionization created by the secondary electrons (electrons and positrons) formed within a volume element of air of mass *dm*, when these secondary electrons are completely stopped in air. The exposure value *X* is then given by:

$$X = \frac{dQ}{dm} \qquad 4.31$$

The SI unit is the coulomb per kilogram (C/kg). The historical unit has been the roentgen (*R*), *defined as the exposure which results in the generation of one electrostatic unit of charge of either sign per 0.001293 g (1 cm^3 at standard temperature and pressure STP) of air*. Thus:

$$1R = \frac{1esu}{0.001293g} = \frac{3.33\times10^{-10}C}{1.293\times10^{-6}kg} = 2.58\times10^{-4}C/kg \qquad 4.32$$

Then the number of ion pairs produced by one roentgen per kg is given by:

$$\frac{total \quad charge}{electron \quad carge} = \frac{2.58\times10^{-4}C/kg}{1.602\times10^{-19}C} = 1.61\times10^{15}\text{ion pair / kg,}$$

and because the average energy required to produce an ion pair in air is about 34 eV or 5.45×10^{-18} J, then the absorbed energy in air is equivalent to exposure of one roentgen:

$$1R = (\text{ ion pairs})\times(\text{energy/ion pair})$$

$$= 1.61\times10^{15}\times5.45\times10^{-18}=0.0088 \text{ J/kg} \qquad 4.33$$

Similarly, the absorbed energy in living tissue exposed to 1R = 0.0096 J/kg.

The γ ray exposure is often of interest in gamma ray dosimetry. Therefore, it is convenient to calculate the exposure rate at a known distance from a point radioisotope source. Assuming that the yield per disintegration of x- and γ-rays is accurately known for the radioisotope of interest, the exposure rate $(\dot{X})$, *exposure per unit activity of the source at a known distance* can be simply expressed under the following conditions (R/h):

1- The source is sufficiently small so that spherical geometry holds (i.e. the photon flux diminishes as $1/d^2$, where d is the distance to the source (cm).
2- No attenuation of the rays takes place in the air or other material between the source and measuring point. Only photons passing directly from the source to the measuring point contribute to the exposure, and any gamma rays scattered in surrounding materials may be neglected.

$$\dot{X} = \Gamma_{\delta} \frac{A}{d^2} \qquad 4.34$$

where A is the activity of the source (*mCi*) and $\Gamma_{\delta,}(R.h^{-1}.cm^2.mCi^{-1})$ is the exposure rate constant for the specific radioisotope of interest, *defined as the exposure rate in R/h at 1 cm from a 1 mCi point source*. The subscript δ implies that all X- and γ-rays energies must be above an energy δ.

An empirical formula, which may be used to calculate Γ_δ, is:

$$\Gamma_\delta = 6 \times f_\gamma \times E \quad \textit{at 1 foot} \qquad 4.35$$

Here E is the energy of the emitted photons in MeV and f_γ is the fraction of decays resulting in photons with energy of E. It should be noted that this formula and the gamma constants are for exposure rates from gammas and x-rays only. Any dose calculations would also have to include the contribution from any particulate radiation that may be emitted. Table 4.1 lists the values of Γ_δ for particular radioisotopes.

Table 4.1. Exposure rate constant for some common radioisotope gamma ray sources.

Nuclide	Γ_δ
Antimony-124	9.8
Cesium-137	3.3
Cobalt-57	0.9
Cobalt-60	13.2
Iodine-125	0.7
Iodine-131	2.2
Manganese-54	4.7
Radium-226	8.25
Sodium-22	12.0
Sodium-24	18.4
Zinc-65	2.7

4.9.2. Absorbed dose

Energy is deposited in the absorber when radiation interacts with it. It is usually quite a small amount of energy but energy nonetheless. The quantity that is measured is called the *Absorbed Dose* and it is of relevance to all types of radiation, such as X- or gamma-rays, alpha- or beta-particles, etc….

If two different materials are subjected to the same particles or γ ray exposure, they will in general absorb different amounts of energy. Because many important physical phenomena and chemical reactions would be expected to change as the energy absorbed per unit mass of the material chages. Then the absorbed dose *D* is defined as "*the energy absorbed from any type of radiation (particles or photons) per unit mass of the absorber*". The historical unit of absorbed dose has been the "*rad*", defined as 100 ergs/g or 0.01 J/kg. Because the exposure to one roentgen will cause absorption of energy equal 0.0088 J/kg in air (Eq.4.31) and 0.0096 J/kg in living tissue, then the dose of:

$$1R \equiv 0.0088/0.01 = 0.88 \text{ rad in air} \qquad 4.36a$$

And

$$1R \equiv 0.0096/0.01 = 0.96 \text{ rad in living tissue} \qquad 4.36b$$

The rad unit now is replaced by its SI equivalent, the gray (symbol *Gy*) defined as 1 J/kg. The two units are therefore related:

$$1 \text{ Gy} = 100 \text{ rad} \qquad 4.37$$

4.9.3. Dose equivalent and dose effective

It has been found that the effects of absorption of equal amount of energy per unit mass (absorbed dose) deposited in the form of heavy charged, uncharged particles, electrons or photons on living organism does not guarantee the same biological effect. For example, the absorption dose of 0.01 Gy from neutrons create biological damages equivalent to the damage created by a dose of 0.1 Gy from γ ray.

Concepts of *dose equivalent* and *dose effective* have therefore been introduced to more adequately quantify the probable biological effect, living matter - human tissue for example, of a given radiation exposure. These quantities include the dose equivalent, *H*, and the dose effective, *E*.

The *dose equivalent* is based on estimates of the ionization capability of the different types of radiation which are called *Radiation Weighting Factors* (W_R), previously called *quality factor* (Q) such that:

$$H = W_R D \qquad 4.38$$

The Radiation Weighting Factors (W_R) is used to compare the biological damage producing potential of various types of radiation, given equal absorbed dose. The effectiveness of radiation in producing damage is related to the energy loss of the radiation per unit path length. The term used to express this is *Linear Energy Transfer (LET)*. Generally, the greater the LET in tissue, the more effective the radiation is in producing damage. The radiation weighting factors (W_R) for radiations frequently encountered are shown Table 4.2:

Table 4.2. The quality factors for different radiation types.

Radiation Type and Energy Range	Radiation Weighting Factor, W_R
X- and γ-rays, all energies	1
Electrons, positrons and muons, all energies	1
Neutrons:	
< 10 keV	5
10 keV to 100 keV	10
> 100 keV to 2 MeV	20
> 2 MeV to 20 MeV	10
> 20 MeV	5
Protons,(other than recoil protons) and energy > 2 MeV,	2-5
A particles, fission fragments, heavy nuclei	20

The *dose effective* includes W_R as well as estimates of the sensitivity of different living tissues called *Tissue Weighting Factors* (W_T), such that:

$$ED = \Sigma\, W_T\, H = \Sigma\, \mathrm{W_T\, W_R\, H} \qquad 4.39$$

where the summation, Σ, is over all the tissue types involved. The tissue weighting factors (W_T) for different living tissues are tabulated in Table 4.3:

Table 4.3. The tissue weighting factors (W_T) for different living tissues.

Tissue	**Tissue Weighting Factor W_T**
Gonads	0.20
Red bone marrow	0.12
Colon	0.12
Lung	0.12
Stomach	0.12
Bladder	0.05
Breast	0.05
Liver	0.05
Thyroid, Bone surfaces	0.01
Remainder	0.05

The *rem* is a historical unit of both the dose equivalent and the dose effective. While the SI unit for both is the Sievert (Sv), with the following relation:

$$1\ Sv = 100\ rem. \qquad 4.40$$

The units used for H and ED depend on the corresponding units of absorbed dose D in Eq. 4.38. If D expressed in *rad*, H will be in *rem*, while if D is in *Gy*, H is in *Sv*. Table 4.4 shows the relationships between all radiation measurements.

Dose equivalent determinations for internally deposited radioactive materials also take into account other factors

such as the non-uniform distribution of some radionuclides (for example, I-125 in the thyroid).

Table 4.4. The dosimetric quantities and relationships.

Quantity	**Definition**	**New units**	**Old Units**
Exposure	Charge per unit mass of air $1R = 2.58 \times 10^{-4}$ C/kg	---	Roentgen (R)
Absorbed dose to tissue T from radiation of type R $D_{T,R}$	Energy of radiation R absorbed per unit mass of tissue T 1 rad = 100 ergs/g 1 Gy = 1 joule/kg 1 Gy = 100 rads	gray (Gy)	Radiation absorbed dose (rad)
Dose Equivalent to tissue T H_T	Sum of contributions of dose to T from different radiation types, each multiplied by the radiation weighting factor (w_R) $H_T = \Sigma_R w_R D_{T,R}$	Sievert (Sv)	Roentgen equivalent man (rem)
Dose Effective ED	Sum of equivalent doses to organs and tissues exposed, each multiplied by the appropriate tissue weighting factor (w_T) $ED = \Sigma_T w_T H_T$	Sievert (Sv)	rem

Guidelines for radiation exposure limits to persons are quoted in units of dose equivalent in order to place exposures to different types and energies of radiation on a common basis. The dosimetric quantities and the relationships between units are concluded in Table 4.4.

Problems

4-1. How many atoms of ^{32}P ($t_{1/2}$=14.3 d) are there in a 5 mCi source?

4-2. How many grams are there in a 1.16 MBq source of
(a) ^{24}Na? $t_{1/2}$ = 14.95 h
(b) ^{238}U? $t_{1/2} = 4.5\times10^{9}$ y

4-3. The activity of a radioisotope is found to decrease by 30% in 1 wk. What are the values of its
(a) Decay constant
(b) Half-life
(c) Mean life?

4-4. What percentage of the original activity of a radionuclide remains after
(a) 5 half-lives
(b) 10 half-lives?

4-5. The activity A of a sample of an unknown radionuclide is measured at hourly intervals. The results, in MBq are 80.5, 36.2, 16.3, 7.3, and 3.3. Find the half-life of the radionuclide in the following way. First, show that, in general $\ln(A/A_o)=-\lambda t$, second, plot $\ln(A/A_o)$ verses t and find λ from the resulting curve, then calculate $t_{1/2}$ from λ.

4-6. The isotope ^{132}I decays by β^- emission into stable ^{132}Xe with a half-life of 2.3 h.
(a) How long it will take for 7/8 of the original ^{132}I atoms to decay?
(b) How long it will take for a sample of ^{132}I to lose 95% of its activity?

4-7. Compute the specific activity of the following isotopes:
(a) ^{238}U, $t_{1/2} = 4.47\times10^{9}$ yr
(b) ^{90}Sr, $t_{1/2} = 28.5$ yr
(c) ^{3}H, $t_{1/2} = 12.3$ yr

4-8. ^{59}Fe has a half-life of 45.53 d.
(a) What is the mean life of a ^{59}Fe atom?
(b) Calculate the specific activity of ^{59}Fe.
(c) How many atoms are there in a 10-mCi source of ^{59}Fe?

4-9. The half-life of ^{210}Po is 138 days. What mass of ^{210}Po is needed for a 10 mCi source?

4-10. At time $t = 0$ a sample consists of 2 Ci of ^{90}Sr and 8 Ci of ^{90}Y.
(a) What will be the activity of the sample after 90 h?
(b) At what time will the ^{90}Y activity be equal to 3 Ci?

4-11. A sample contains 1 mCi of ^{191}Os at time $t = 0$. The isotope decays by β^- emission into metastable ^{191m}Ir, which then decays by γ emission into ^{191}Ir. The decay and half-lives can be represented by writing:

$$^{191}_{76}Os \xrightarrow[15.4days]{\beta^-} {}^{191m}_{77}Ir \xrightarrow[4.94sec]{\gamma} {}^{191}_{77}Ir$$

(a) How many grams of ^{191}Os are present at $t = 0$?
(b) How many millicuries of ^{191m}Ir are present at $t = 25$ day?
(c) How many atoms of ^{191m}Ir decay between $t = 100$ sec and $t = 102$ sec?
(d) How many atoms of ^{191m}Ir decay between $t = 30$ day and $t = 40$ day?

4-12. Under the transient condition ($\lambda_1 < \lambda_2$), illustrated in Fig. 4.7, the total activity also reaches a maximum at a time earlier than that of the maximum daughter activity.
(a) Find the time at which the daughter activity is largest (by differentiation of Eq.4.23).
(b) Prove that the total activity is largest at the earlier time, $t = \frac{1}{\lambda_2 - \lambda_1} \ln \frac{\lambda_2^2}{2\lambda_1\lambda_2 - \lambda_1^2}$, for maximum $A_1 + A_2$.
(c) Similar to Fig. 4.7, draw the activities A_1, A_2 and A_1+A_2 as a function of time.

4-13. Repeat problem 4-12 for the second case of equilibrium (*secular equilibirium*) ($\lambda_1 << \lambda_2$).
4-14. A rock sample contains 1.0 mg of ^{206}Po and 4.0 mg of ^{238}U whose half-life is 4.47×10^9 years. How long ago was the rock formed?

4-15. The relative radiocarbon activity in a piece of charcoal from the remains of ancient campfire is 0.18 that of a contemporary specimen. How long ago did the fire occur?

4-16. A 6.2 mg sample of ^{90}Sr is in secular equilibrium with its daughter ^{90}Y.
(a) How many Bq of ^{90}Sr are present?
(b) How many Bq of ^{90}Y are present?
(c) What is the mass of ^{90}Y?
(d) What will the activity of the ^{90}Y be after 100 yr?

4-17. In a measurement of a mineral sample, it is found that the three nuclides ^{214}Bi, ^{214}Po and ^{210}Pb, belong to the ^{238}U decay series, in a radioactive equilibrium. Write down the decay Scheme of each isotope. If the sample contains 1.0 g

of ^{210}Pb, what are the masses of ^{238}U, ^{214}Bi and ^{214}Po in the sample? Refer to Table 3.1.

4-18. (a) Estimate the specific gamma-ray constant for ^{137}Cs.
(b) Estimate the exposure rate at a distance of 1.7 m from a 100-mCi point source of ^{137}Cs.

4-19. Repeat problem 4-18 for ^{22}Na of two gamma energies, 1.274 MeV with fraction of decay 100% and 0.511 MeV with 180% fraction of decay.

4-20.
(a) What is the average absorbed dose in a 40-cm^3 region of a body organ (density = 0.93 g cm^{-3}) that absorbs 3×10^5 MeV of energy from a radiation field?
(b) If the energy is deposited by electron and neutron of energy 50 keV, what is the dose equivalent according to Table 4.2?
(c) Express the answers to (a) and (b) in rads and rems as well as Gy and Sv.

4-21. A portion of the body receives 0.15 mGy from radiation with a quality factor Q = 6 and 0.22 mGy from radiation with Q = 10.
(a) What is the total dose?
(b) What is the total dose equivalent?

4-22. A beam of X rays produces 4 esu of charge per second in 0.08 g of air. What is the exposure rate in
(a) mR.s^{-1}?
(b) SI units?

4-23. If all of the ion pairs are collected in the previous problem (4-22), what will be the current?

4-24. Calculate the effective dose to an individual who has received the following exposures:

5 mGy alpha to the lung
10 mGy thermal neutron, to the skin
5 mGy gamma, whole body
100 mGy beta to the thyroid.

CHAPTER 5

QUANTUM MECHANICAL BEHAIVIOR OF NUCLEI

The concepts and terminologies in quantum mechanics are such integral parts of nuclear concepts and the interaction of radiation with matter that some knowledge of quantum mechanics is essential to having full command of the language of nuclear physics.

5.1. Introduction

Nucleons in a nucleus do not behave like classical particles (colliding like billiard balls); instead, the wave behavior of the nucleon determines the properties of the nucleus. Therefore, we need quantum mechanics, which is a mathematical technique that enables us to calculate the wave behavior of a material particle.

The quantum behavior of light and the photoelectric effect that had been analyzed, showed that the light or electromagnetic waves should also be considered as if its energy were delivered not smoothly and continuously as wave but instead in concentrated bundles or *quantum* effect (particle of light).

The analogy between matter and light (wave) was made in 1924 by de Broglie; he postulated that associated with a particle moving with momentum p is a wave of wavelength $\lambda = h/p$ (Eq.1.22). Experimental confirmation soon followed through the diffraction of electrons (particles) like waves with de Broglie wavelength. The de Broglie theory was successful in those instances, but it is incomplete and

unsatisfying in describing the particle by classical physics, since the classical particle has a definite position in space and unique momentum p.

The solution of this problem comes from quantum physics, the size of a quantum particle varies with the experiment performed. Thus, an electron or particle may have a certain size in one experiment and a very different size in another. Only through this coupling of the observing system and the observed object can we define observation in quantum physics. The particle then is localized within some region of space of dimension Δx. It is likely to be found in that region and unlikely to be found elsewhere. We improve our knowledge of Δx at the expense of our knowledge of momentum p_x, the very act of confining the particle to Δx destroys the precision of our knowledge of p_x.

It is not our goal to take up the study of quantum mechanics as a topic by itself. On the other hand, we have no reasons to avoid using quantum mechanics whenever it is the proper way to understand nuclear concepts and radiation interactions.

In the following sections, the concepts and terminologies in quantum mechanics (Schrödinger equation) will be given, since they are such integral parts of nuclear concepts, nuclear structure and the interaction of radiation with matter that some knowledge of quantum mechanics is *essential* to having full command of the language of nuclear physics.

5.2. Uncertainty Principles

The uncertainty principle is one of the most significant laws of physics, discovered by Werner Heisenberg in 1927 (*We cannot know the future because we cannot know the present*). Accordingly, if we try to make a simultaneous

determination of x and p_x, our result will show that each is uncertain by respective amounts Δx and Δp_x, which are related by the *Heisenberg uncertainty relationship*.

$$\Delta x \, \Delta p_x \geq \hbar/2 \qquad 5.1$$

where $\hbar = h/2\pi = 1.0545\times10^{34}$ j.sec

This equation states that if we arrange matters so that Δx is small (corresponding to a narrow wave group), Δp will be large. If we reduce Δp in some way, a broad wave group is inevitable and Δx will be large.

The same arguments hold for other form of the uncertainty principle, the other measurements concern energy and time. We might wish to measure the energy emitted during the time interval Δt in an atomic or nuclear process. Since energy $E = h\nu = hc/\lambda$ where ν is the frequency (Eq.1.11), and $\Delta\nu \geq 1/\Delta t$ also $\Delta E = h\Delta\nu$ then:

$$\Delta E \, \Delta t \geq \hbar/2 \qquad 5.2$$

If a system live for a time Δt, we cannot determine its energy except to within uncertainty ΔE.

A third uncertainty relationship involves the angular momentum L_z, and the azimuthally angle φ, Fig. 5.1.

$$\Delta L_z \, \Delta\varphi \geq \hbar/2 \qquad 5.3$$

That is, if we have L_z exactly, we know nothing at all about φ.

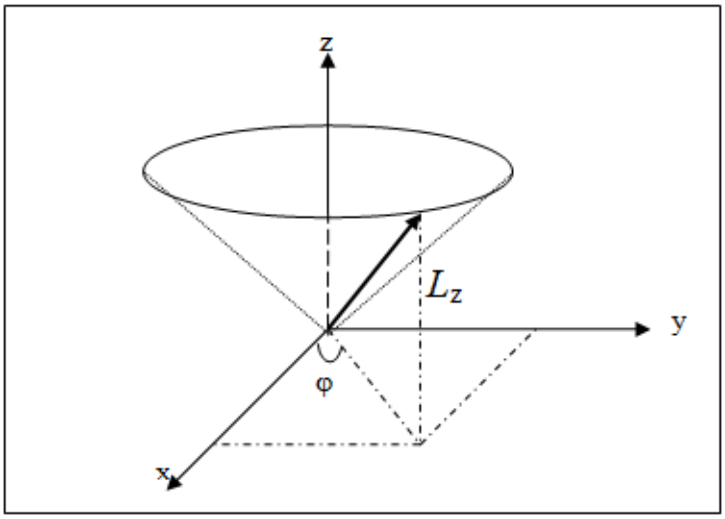

Figure 5.1. Bounded particle uncertainty relationships.

5.3. de Broglie Wave Descriptions

It is instructive to begin with the classical wave equation that incorporates the concept of de Broglie waves and to review some basic properties of waves and the concept of wave-particle duality.

The wave nature of a moving particle leads to some remarkable consequences when the particle is restricted to a certain region of space instead of being able to move freely, as the electron bounded to the atom or a nucleon in the nucleus, and when it interacts with the nucleus or other particle.

In classical mechanics, the wave equation for a one-dimensional periodic disturbance $\xi(x, t)$ is:

$$\frac{\partial^2 \xi(x,t)}{\partial t^2} = c^2 \frac{\partial^2 \xi(x,t)}{\partial x^2} \qquad 5.4$$

Solutions of the above equation may be of many kinds, reflecting the variety of waves that can occur, such as a single traveling pulse, a standing wave, a group (train) of waves or of superposed waves, etc…, the general solution is of the form:

$$\xi(x,t) = \xi_0 e^{i(kx-\omega t)} \qquad 5.5$$

where ω= 2πν is the angular frequency, υ the linear frequency, and *k* is the *wavenumber* related to the wavelength λ by $k = 2\pi / \lambda$. If Eq.5.5 is to be a solution of Eq.5.4, k and ω must satisfy the relation:

$$\omega = ck \qquad 5.6$$

Therefore, our solution has the form of a traveling wave with phase velocity equal to *c*, which we will denote it by υ_{ph}. In general, *the relation between frequency and wavenumber is called the dispersion relation*. We will see that different kinds of particles can be represented as waves, which are characterized by different *dispersion relations*.

The solution Eq.5.5 is called a plane wave. In three dimensions, a plane wave is of the form $e^{i\boldsymbol{k}.\boldsymbol{r}}$. It is a wave in space that can be visualized as a series of planes perpendicular to the wavevector $\boldsymbol{k}$ at any spatial point on a given plane, the phase of the wave is the same. That is to say, the perpendicular planes are planes of constant phase. When we include the time variation $e^{(-i\omega t)}$, then $e^{[i(\boldsymbol{k}.\boldsymbol{r}-\omega t)]}$ becomes a *traveling plane wave*, meaning that the planes of constant phase are now moving in the direction along $\boldsymbol{k}$ at a speed of ω / k , which is the phase velocity of the wave υ_{ph}.

The wave equation Eq.5.4 also admits solutions of the form:

$$\xi(x,t) = a_o \sin kx \cos \omega t \qquad 5.7$$

These are standing wave solutions. One can tell a standing wave from a traveling wave by the behavior of the nodes, the spatial positions where the wave function is zero. For a standing wave, the nodes do not move, or change with time, whereas for a traveling wave Eq.5.5, the nodes are:

$$x_n = (n\pi + \omega t)/k \qquad 5.8$$

Clearly the nodes are positions moving in the $(+x)$ direction with the velocity $dx/dt = \omega/k$.

The choice between traveling and standing wave solutions as we will see depends on the physical solution of interest (which kind of problem one is solving). For the calculation of energy levels of a nucleus, the bound state problem, we will be concerned with standing wave solutions Eq.5.7. In contrast, for the discussion of scattering problem, it will be more appropriate to consider traveling wave solutions Eq.5.5.

Our interest in the properties of waves lies in the fact that the quantum mechanical description of a nucleus is based on the wave representation of the nucleus. It was first postulated by de Broglie (1924) that one can associate a particle of momentum p and total energy E with a group of waves (wave packet) which are characterized by a wavelength λ and a frequency ν , with the relation, given in Chapter One:

$$\lambda = h/p = h/\gamma m v, \text{ where } \gamma = (1 - v^2/c^2)^{-1/2} \qquad 5.9$$

$$\nu = E/h = \gamma m c^2/h \qquad 5.10$$

Here, υ is the particle velocity. Moreover, the motion of the particle is governed by the propagation of the wave packet. This statement is the essence of particle-wave duality, a concept that we adopt throughout our study of nuclear physics. It is important to distinguish between a single wave and a group of waves. This distinction is seen most simply by considering a group of two waves of slightly different wavelengths and frequencies. Suppose we take as the wave packet:

$$\Psi(x,t) = \Psi 1(x,t) + \Psi 2(x,t) \qquad 5.11$$

with

$$\Psi 1(x,t) = \sin(kx - \omega t) \qquad 5.12$$

$$\Psi 2(x,t) = \sin[(k + dk)x - (\omega + d\omega)t] \qquad 5.13$$

Using the identity:
$\sin A + \sin B = 2\cos[(A - B)/2]\sin[(A + B)/2]$, we can rewrite Ψ(x,t) as:

$$\Psi(x,t) = 2\cos[(dkx - d\omega t)/2]\sin\{[(2k + dk)x - (2\omega + d\omega)]t/2\}$$

$$\approx 2\cos[(dkx - d\omega t)/2]\sin(kx - \omega t) \qquad 5.14$$

In this approximation, terms of higher order in *dk/k* or *dω/ω* are dropped. Eq.5.14 shows two oscillations, one is the wave packet oscillating in space with a period of *2π/k*, while its amplitude oscillates with a period of *2π/dk* (Fig. 5.2). Notice that the latter oscillation has its own propagation velocity, *dω/dk*. This velocity is in fact the speed with which the associated particle is moving. Thus, we identify

$$v_g = d\omega/dk \qquad 5.15$$

as the *group velocity*. The group velocity should not be confused with the propagation velocity of the wave packet, called the phase *velocity* (v_{ph}), given by:

$$v_{ph} = \nu\lambda = E / p = c\,[1 + (m_o c / p)^2]^{1/2} \qquad 5.16$$

Here, m_o is the rest mass of the particle and c the speed of light. We see the wave packet moves with a velocity greater than c, whereas the associated particle speed is necessarily less than c. This means that the *phase velocity is greater than or equal to the group velocity*.

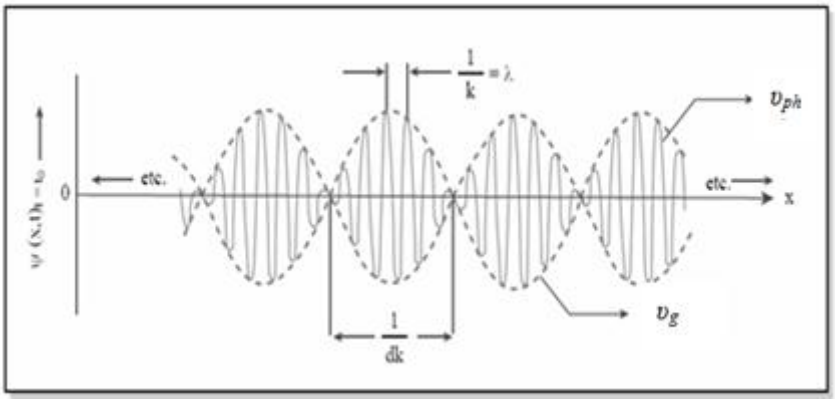

Figure 5.2. Spatial variation of a sum of two waves of slightly different frequencies and wave-numbers showing the wave packet moves with velocity v_{ph} that is distinct from the propagation (group) velocity v_g of the amplitude.

In the coming chapters, we will deal with three kinds of particles whose wave representations are of interest. These are:

1. Nucleons or nuclides, which can be treated as non-relativistic particles.
2. Electrons and positrons that usually should be treated as relativistic particles since their energies tend to be comparable or greater than the rest-mass energy.
3. Photons, which are fully relativistic, since they have zero rest mass energy.

For a non-relativistic particle of mass m moving with momentum p, the associated wavevector $\boldsymbol{k}$ and its kinetic energy is:

$$\boldsymbol{p} = \hbar\boldsymbol{k} \qquad 5.17a$$

and

$$T = p^2/2m = \hbar^2k^2/2m \qquad 5.17b$$

This is the "particle view". The corresponding "wave view" would have the momentum magnitude $p = h/\lambda$, with $\lambda = 2\pi/k$, and energy (usually denoted as E rather than T) as $h\nu = \hbar\omega$. The wavevector, or its magnitude, the wavenumber k, is a useful variable for the discussion of particle scattering since in a beam of such particles, the only energies are kinetic, and both momentum and energy can be specified by giving $\boldsymbol{k}$.

For electromagnetic waves, the associated particle (the photon), has momentum $\boldsymbol{p}$, which is also given by $\hbar\boldsymbol{k}$, but its energy is:

$$E = c\hbar k = cp \qquad 5.18$$

Comparing these two cases, we see that the *dispersion relation* ω and *group velocity* v_g (Eq.5.15) are:

$$\omega = \hbar k^2/2m, \quad v_g = \hbar k/m = p/m \qquad 5.19$$

for a non-relativistic particle, and

$$\omega = ck, \qquad v_g = c \tag{5.20}$$

for a photon.

This is consistent with our intuitive notion about particle speed and the universal speed of a photon in Chapter One.

For the calculation of energy levels of a nucleus, the bound state problem, such system is like a standing wave in a string stretched between the box's walls, the wave variable (wave function Ψ for the moving particle) must be zero at the walls, i.e., $\Psi(0) = 0$ and $\Psi(a) = 0$ for a box of width a.

The possible de Broglie wavelengths of the particle trapped in the box of width (a) is determined by the largest wavelength (steady state of Eq.5.8) of $\lambda = 2a$ and the next $\lambda = a$ then $\lambda = 2a/3$ … for $n = 1, 2, 3\ldots$ respectively. So that the general form as shown in Fig. 5.3, is:

$$\lambda = 2a/n \qquad n = 1, 2, 3\ldots \tag{5.21}$$

Accordingly, the momentum of the particle p and its kinetic energy T will be limited, as Eq.5.9 and Eq5.17 and so, because the particle has no potential energy in this model, the only energies the particle can have are:

$$E_n = \frac{h^2}{2m\lambda^2} = \frac{h^2 n^2}{8ma^2} = \frac{\hbar^2 \pi^2}{2ma^2} n^2 \qquad n = 1,2,3,..... \tag{5.22}$$

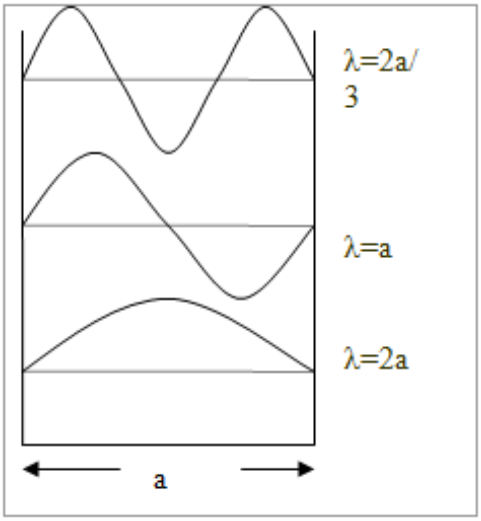

Figure 5.3. de Broglie wave and principle quantum number (*n*).

Each permitted energy is called *Energy Level*, and the integer (*n*) that specifies energy levels E_n is called its *quantum number*.

We can draw three general conclusions from the above equation:

1. A bounded particle cannot have an arbitrary energy as a free particle can. These discreet energies depend on the mass of the particle and on the detailed forces acting on the particle to bond it (trapped).
2. A bounded particle cannot have zero energy, since $\lambda = h/m\upsilon$, a speed $\upsilon = 0$, means an infinite λ, but there is no way to reconcile an infinite wavelength with trapped particle.
3. Because Plank's constant is so small, $h = 6.63\times10^{-34}$ j.sec, then quantization of energy is conspicuous only when the mass (*m*) and the width (*a*) are also small.

It is convenient to mention that this quantum number (n) is precisely the same formula of the principle quantum number determined by the solution of the Schrödinger equation applied to a potential well, as we will see in the next section, where the quantization of the bounded nucleon in the nucleus is therefore described by the principle quantum number (n).

Example:

An electron trapped in a box, 0.10 *nm* across (order of magnitude of atomic dimensions). Find the permitted energies.

Solution

$$m_e = 9.1\times10^{-31}\ kg \text{ and } a = 0.1\ nm = 1.0\times10^{-10}\ m$$

From Eq.5.5, the permitted energies are:

$$E_n = \frac{n^2\,(6.63\times10\text{-}34\ j.s)^2}{8\times(9.1\times10^{-31}\ kg)(1.0\times10^{-10}\ m)} = 6.0\times10^{-18}n^2\ j$$

$$= 38\ n^2\ eV$$

Then

$$E_{min} = E_1 = 38\ eV \qquad \text{for } n=1$$
$$E_2 = 152\ eV \qquad \text{for } n=2$$
$$E_3 = 342\ eV \qquad \text{for } n=3$$

5.4. Schrödinger Wave Equation

Schrödinger developed an equation describing the motion of a particle and its associated de Broglie wave, which has become the foundation of wave mechanics or quantum mechanics. As a result, it provides a quantitative description of matter in the atomic and nuclear scale. In other words, the mathematical aspects of nonrelativistic quantum mechanics are determined by solution to the Schrödinger equation. The ways to get the development of such equation is beyond the scope of this book, rather its applications to the quantized parameters are involved in nuclear structure.

The wave function $\Psi(\boldsymbol{r},t)$, a mathematical description of the wave packet, is to be treated as a space-time dependent quantity. We can write the Schrödinger equation in its time dependent form for a particle in a potential field V(**r**) as:

$$ih\frac{\partial\Psi(\boldsymbol{r},t)}{\partial t} = \left[-\frac{h^2}{m}\nabla^2 + V(\boldsymbol{r})\right]\Psi(\boldsymbol{r},t) \qquad 5.23$$

The two terms in the brackets can be thought of as an operator *H*, called the *Hamiltonian* of the system. *H* is a mathematical operator whose physical meaning is the total energy. Thus, it consists of the kinetic part $E = p^2/2m$ and the potential part $V(\boldsymbol{r})$. The appearance of the Laplace operator ∇^2 is to be expected, since the particle momentum $\boldsymbol{p}$ (vector quantity) is an operator in configuration space, with $\boldsymbol{p} = -i\hbar\vec{\nabla}$. The momentum operator is, therefore, a first-order differential operator in configuration space. By defining the *Hamiltonian H* as the operator:

$$H = -\frac{\hbar^2}{2m}\nabla^2 + V(\boldsymbol{r}) \qquad 5.24$$

We can express the time-dependent Schrödinger equation in operator notation:

$$i\hbar \frac{\partial \Psi(\boldsymbol{r},t)}{\partial t} = H\Psi(\boldsymbol{r},t) \qquad 5.25$$

It should be noticed thatEq.5.23 is valid only for a non-relativistic particle (the particle speed is much less than the speed of light); whereas Eq.5.25 is more general if *H* is left unspecified. This means that one can use a relativistic expression for *H*, and then Eq.5.25 would lead to an equation first derived by Dirac. The Dirac equation is what one should consider if the particle was an electron.

Compared to the classical wave equation, Eq.5.4, which relates the second spatial derivative of the wave function to the second-order time derivative, the time-dependent Schrödinger wave equation, Eq. 5.23 or 5.25, is seen to relate the spatial derivative of the wave function to the first-order time derivative. This is a significant distinction. Among the implications is the fact that the classical wave is real and measurable (for example, an elastic string or an electromagnetic wave), whereas the Schrödinger wave function is complex and therefore not measurable.

An important property of Schrödinger equation is that it is linear in the wave function $\Psi(\boldsymbol{r},t)$. To ascribe physical meaning to the wave function, one needs to consider the particle density or probability density defined as $\Psi^*(\boldsymbol{r},t)\Psi(\boldsymbol{r},t)$, where $\Psi^*(\boldsymbol{r},t)$ is the complex conjugate of the wave function, from which the probability to find the particle(the wave packet) between $\mathbf{r}_1$ and $\mathbf{r}_2$ is the integral of all infinitesimal probabilities:

$$P = \int_{\boldsymbol{r}_1}^{\boldsymbol{r}_2} \Psi^* \Psi d\boldsymbol{r} \qquad 5.26$$

Almost all our discussions are concerned with the time-independent form of the Schrödinger equation. This is obtained by solving Eq.5.25 for time (the energy operator $E = i\hbar\frac{\partial}{\partial t}$) and considering a periodic solution of the form:

$$\Psi(\boldsymbol{r}, t) = \psi(\boldsymbol{r})e^{-i\omega t} = \psi(\boldsymbol{r})e^{-\frac{iEt}{\hbar}} \qquad 5.27$$

where, E is the total energy. Inserting this solution into Eq.5.25 gives the time-independent Schrödinger equation:

$$H\psi(\boldsymbol{r}) = E\psi(\boldsymbol{r}) \qquad 5.28$$

We see that Eq.5.28 has the form of an eigenvalue problem with H being a linear operator, E the eigenvalue, and $\psi(\boldsymbol{r})$ the eigenfunction.

In spite of the fact that a full treatment of the Schrödinger equation would require at least three dimensions, we shall, for better understanding, start with one-dimensional problems. In addition, we shall assume that our system is time-independent, Eq.5.28 can be written:

$$-\frac{\hbar^2}{2m}\frac{d^2\psi(x)}{dx^2} + V(x)\psi(x) = E\psi(x) \qquad 5.29$$

or

$$\frac{d^2\psi(x)}{dx^2} = -k^2\psi(x) \quad \text{where} \quad k^2 = \frac{2m}{\hbar^2}[E - V(x)] \qquad 5.30$$

The physical meaning of the above equation is essentially the statement of energy conservation, the total energy E is the sum of kinetic and potential energies. Since Eq.5.29 holds at every point in space, the fact that the potential

energy *V(x)* varies in space means that the kinetic energy of the particle will also vary in space.

In general, k^2 is a function of x because of the potential energy *V(x)*, but for piecewise constant potential functions such as a rectangular well or barrier, we can write a separate equation for each region where *V(x)* is constant and thereby treat k as a constant in Eq.5.30.

A general solution to Eq. 5.30 is then:

$$\left.\begin{aligned} &\psi(x) = Ae^{ikx} + Be^{-ikx} \\ &\text{or equivalently} \\ &\psi(x) = A'\sin kx + B'\cos kx \end{aligned}\right\} \qquad 5.31$$

where A, A′ and B, B′ are constants to be determined by appropriate boundary conditions.

Eq. 5.28 is a second order differential equation (boundary value problem). The method of solving this equation is very much dependent on the specific form of the potential energy *V(x)*. The wave function must have the following conditions and properties for the solution to be physically meaningful:

1. $\psi(x)$ is continuous across any boundary, say at $x = a$:

$$\lim_{\varepsilon\to 0}\left[\psi(a+\varepsilon) - \psi(a-\varepsilon)\right] = 0 \qquad 5.32$$

2. $d\psi/dx$ is continuous across any boundary, at $x = a$:

$$\lim_{\varepsilon\to 0}\left[\left(\frac{d\psi}{dx}\right)_{x=a+\varepsilon} - \left(\frac{d\psi}{dx}\right)_{x=a-\varepsilon}\right] = 0 \qquad 5.33$$

3. From the probability density Eq.5.26, the probability to find the particle between the limits x_1 and x_2 is the integral of all infinitesimal probabilities:

$$P = \int_{x_1}^{x_2} \psi^* \psi dx \qquad 5.34$$

The total probability to find the particle from $x_1 = -\infty$ to $x_2 = \infty$, must be 1, which is known as the normalization condition.

4. Prediction of the averaging value of any measurement quantity, if f is the operator associated with some observable quantity $f(x)$, the *average value* of the function $f(x)$ is:

$$\langle f \rangle = \int \psi^* f \psi dx \qquad 5.35$$

5. From our knowledge of *particle density* (number of particles per unit volume, or the probability of the finding the particle in an element of volume d^3r about r Eq.5.26), the Particle current density $j(r)$ associated with $\psi(r)$ is continuous everywhere. Then the net current of this quantity gives the number of particles per unit area per second passing any point x:

$$j = -i\frac{\hbar}{2m}\left(\psi^* \frac{d\psi}{dx} - \psi \frac{d\psi^*}{dx}\right) \qquad 5.36$$

In the following section, we will illustrate the application of a simple one-dimensional problem. The next one extends the bound state calculation to three-dimensional systems to determine the bound state energy levels of the nucleus and corresponding wave functions.

5.5. One Dimension Problems

5.5.1. Free particle

This is a simplest one region problem, representing a source of particles such as an accelerator located at $x = -\infty$, emitting particles at a rate I particle per second. The particle is free to move in a $+x$ direction with a momentum $+\hbar k$ without being acted on by any force. Then $V(x) = 0$ everywhere and no boundary conditions, accordingly Eq.5.30 is reduced to:

$$\frac{d^2\psi(x)}{dx^2} = -k^2\psi(x) \qquad where \qquad k^2 = \frac{2mE}{\hbar^2} \qquad 5.37$$

The solution to this equation is given by Eq.5.31, since the wave traveling in $+x$, then the constant $B \equiv 0$ to get; $\psi(x) = Ae^{ikx}$, where A is the amplitude of the incident particle.

To find the constant A, we use Eq.5.36 for the particle current density to get:

$$j = \frac{\hbar k}{m}|A|^2 \qquad 5.38$$

which must be equal to I. thus we can get $A = \sqrt{\frac{mI}{\hbar k}}$.

5.5.2. Particle interaction

This is a multiregional problem, describe the interaction of free particle and nuclei with each other to scatter, if $E > V_0$ or initiate nuclear reactions, if $E < V_0$. In each case (experiment), a beam of free particles (electrons, nucleons….) traverses a target containing nuclei. A certain fraction of the beam particles will interact with the target nuclei, either scattering into a new direction or reacting in a way that particles are created or destroyed.

In the following subsections, we will first deal with semi finite-range target potential, which is called step potential, with finite-range target potential which is called barrier potential.

5.5.2.1. Step potential

As a simple example (two regions) of quantum-mechanical scattering problem, let us consider a particle of momentum $+\hbar k_1$ from a source at $x = -\infty$ incident on the stationary wall (step) of finite height V_0 at $x = 0$, as shown in Fig. 5.4.

The potential energy of the particle for each region is given by:

$$\begin{aligned} V(x) &= 0 \qquad -\infty < x < 0, \text{ region 1} \\ V(x) &= V_0 \qquad 0 < x < \infty, \text{ region 2} \end{aligned} \tag{5.39}$$

In region 1, the Schrödinger equation is the same as Eq.5.37 with a wave number $k_1 = (2mE/\hbar^2)^{1/2}$ and the solution is as Eq.5.31:

$$\psi_1(x) = Ae^{ik_1 x} + Be^{-ik_1 x} \qquad 5.40$$

while in region 2, the Schrödinger equation is identical to Eq.5.30, with a wave number $k_2 = \sqrt{\frac{2m}{\hbar^2}(E - V_0)}$, and the solution is:

$$\psi_2(x) = Ce^{ik_2 x} + De^{-ik_2 x} \qquad 5.41$$

where *A, B, C* and *D* represent the amplitude of each wave term.

In order to proceed, we depend on the physical analysis of each term of the two solutions. As the particle incident on the step in *+ve x* direction of region 1(Fg. 5.4), then the *A* term of Eq.5.40 represents the *incident-traveling wave* of momentum $+\hbar k_1$, while the *B* term is the *reflected-traveling wave* of momentum $-\hbar k_1$. Also for region 2, the *C* term of Eq.5.41 represents the *transmitted-traveling wave* of momentum $+\hbar k_2$ and the *D* term cannot represent any part of solution because there is nothing to return the wave toward the origin in region 2, therefore the constant *D* must be setting to zero (*D = 0*).

Applying the continuity conditions across *x = 0*, Eq.5.32 and Eq.5.33 we get:

$$A + B = C \qquad 5.42a$$

and

$$k_1 (A - B) = k_2 C \qquad 5.42b$$

then solving Eq.5.42a and Eq.5.42b, we get:

$$B = A\frac{1-k_2/k_1}{1+k_2/k_1}$$
$$C = A\frac{2}{1+k_2/k_1} \qquad 5.43$$

In order to have a complete solution, we depend on the physical interpretation of the mathematical formalism. The exact form of the interpretation depends crucially on the relative values of E and V_0.

***First case*:** If $E > V_0$:

We are talking about a particle which, in classical theory, would have possessed enough energy to climb the wall and continue along the +ve x-axis. In this case, k_2 is a real number; the incident, reflected, and transmitted waves are ll simply propagating with no attenuation. The only thing unusual about all this is that quantum mechanics does not tell us whether a given projectile will be reflected or not. Classically, a particle with $E > V_0$ would proceed-slowed down but not reflected. While in the quantum description, there will always be a reflected wave from the interface ($x = 0$), since $B \neq 0$ (except for the trivial case in which $k_1 = k_2$ that arises only when $V_0 = 0$). We cannot predict for certain that the particle will be reflected, but we can calculate the probability that it will be reflected. In a similar interpretation, we can calculate the probability of the transmission of the particle through the interface.

Let us define the *reflection coefficient R* as the current in the reflected wave divided by the incident current:

$$R = \frac{j_{reflected}}{j_{incident}} \qquad 5.44$$

From the application of Eq.5.36 to the wave function in region 1, we obtain the net current:

$$j_1 = \frac{\hbar k_1}{m}\left[|A|^2 - |B|^2\right] = j_{incident} - j_{reflected} \qquad 5.45$$

The net current is the difference between the current goings to the right ($j_{incident}$) and that going to the left ($j_{reflected}$). The quantities $|A|^2$ *and* $|B|^2$ are particle densities with the dimension of number of particles per unit volume.

$$R = \frac{|B|^2}{|A|^2} = \left(\frac{1 - k_2/k_1}{1 + k_2/k_1}\right)^2 \qquad 5.46$$

In addition, the *transmission coefficient T* is defined as the fraction of the incident current that is transmitted past the boundary:

$$T = \frac{j_{transmitted}}{j_{incident}} \qquad 5.47$$

Applying Eq.5.36 for the transmitted to region 2, $j_{transmitted} = \frac{\hbar k_2}{m}|C|^2$ and incident current from Eq.5.45 to have:

$$T = \frac{k_2}{k_1}\frac{|C|^2}{|A|^2} = \frac{4k_2/k_1}{(1+k_2/k_1)^2} \qquad 5.48$$

Notice that for the case in which k_2 is real, $R + T = 1$, indicating that an incident particle must undergo either reflection or transmission. The resulting solution is illustrated in Fig. 5.4.

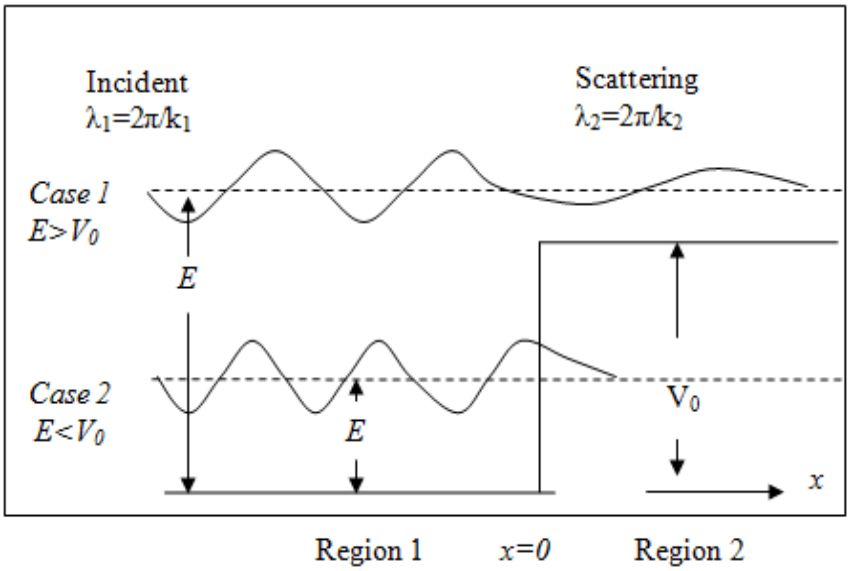

Figure 5.4. Schematic behavior of the wave function of incident particle on a step potential.

***Second case*:** if $E < V_0$.

The case $E < V_0$ is an example of quantum-mechanical attenuation problem. The incident particle would be reflected from the step according to classical physics, which is completely different from that according to quantum mechanical treatment. In quantum mechanics, there would

be some transmission wave into region 2 because $C \neq 0$ for all finite values of k_2 in Eq.5.43. In region 2 we realize that $E < V_0$ implies that k_2 is imaginary, what this means is, there is no wave-like solution in this region. So it must be written in the form $k_2 = iK_2$, here $\kappa_2 = \sqrt{\frac{2m}{\hbar^2}(V_0 - E)}$ is a real wave number and with the fact ($i.i$ = -1), the solution becomes:

$$\psi_2(x) = Ce^{-\kappa_2 x} + De^{\kappa_2 x} \qquad 5.49$$

Again, the D term should be eliminated and the transmitted wave is the C term but it is no longer traveling, propagating, or oscillating wave, it is now purely attenuating as is illustrated with the first case in Fiq.5.4.

5.5.2.2. Barrier potential

The barrier potential is a more realistic (three regions) problem in nuclear physics, where we look for positive-energy solutions as in scattering problem. Again, the exact form of the physical interpretation depends crucially on the relative values of E and V_0.

***First case*:** If $E > V_0$.

We consider a one-dimensional system where a particle of mass m and energy E is projecting from a source at -∞ and incident upon a potential barrier with width a and height V_0 ($E > V_0$), as shown in Fig. 5.5.

The potential is simplified as:

$$\begin{aligned} &V(x) = 0 && -\infty < x < 0, \text{ region 1} \\ &V(x) = V_0 && 0 \le x \le a, \text{ region 2} \\ &V(x) = 0 && a < x < \infty, \text{ region 3} \end{aligned} \qquad 5.50$$

In the three regions, the solutions are:

$$\begin{aligned} \psi_1(x) &= Ae^{ik_1x} + Be^{-ik_1x} \\ \psi_2(x) &= Ce^{ik_2x} + De^{-ik_2x} \\ \psi_3(x) &= Fe^{ik_3x} + Ge^{-ik_3x} \end{aligned} \qquad 5.51$$

where $k_1 = \quad k_3 = \sqrt{\frac{2m}{\hbar^2}E}$ and $\quad k_2 = \sqrt{\frac{2m}{\hbar^2}(E - V_0)}$ Are real wave numbers.

In a similar way to the step potential case, we proceed to apply the boundary conditions 1 and 2 at $x = 0$ and $x = a$, to find the constants. Set the constant $G=0$ since there is nothing in region 3 that can reflect the particle to travel to the left, and organize these information into a useful form, namely the transmission and reflection coefficients.

Using the wave functions in region 1 to get the net current, given by Eq.5.45 and in region 3 to obtain:

$$j_3 = \frac{\hbar k_3}{m}|F|^2 \qquad 5.52$$

With this interpretation we define:

$$R = \frac{|B|^2}{|A|^2} \quad \textit{and} \quad T = \frac{|F|^2}{|A|^2} \qquad 5.53$$

Since particles cannot be absorbed or created in region 2 and there is no reflection in region 3, the net current in region 1 must be equal to the net current in region 3, or $j_1 = j_3$. It then follows that the condition T + R = 1 is always satisfied. For the purpose of calculating the transmission coefficient, we need to keep A and F to get after multiple steps of algebra:

$$T = \frac{1}{1 + \frac{V_0^2}{4E(E - V_0)} \sin^2 k_2 a} \qquad 5.54$$

***Second case*:** if $E < V_0$.

For this case, the ψ_1 and ψ_2 solutions are as above, but in region 2, the kinetic energy E - V_0 is negative. So the wave number k_2 is imaginary in a propagating wave (or we can say the wave function is monotonically decaying rather than oscillatory). This means that there is no wave-like solution in this region. The solution then is similar to that of region 2 of the second case of step potential Eq.5.49.

Now, following the same procedure of the first case, we arive at the solution for the transmission coefficient:

$$T = \frac{1}{1 + \frac{V_0^2}{4E(V_0 - E)} \sinh^2 \kappa_2 a} \qquad 5.55$$

The transmission coefficient is sometimes called the penetration factor and denoted as *P*. Using the leading expression of sinh(x) = $(e^x - e^{-x})/2$ for small and large

arguments, one can readily obtain simpler (approximated) expression for *T* or *P* in the limit of thin and thick barriers:

$$P \approx 1 - \frac{V_0}{4E(V_0 - E)}(\kappa a)^2 = 1 - \frac{(V_0 a)^2 2m}{4E\hbar^2}, \qquad \kappa a << 1$$
$$P \approx \frac{16E}{V_0}\left(1 - \frac{E}{V_0}\right)e^{-2\kappa a}, \qquad \kappa a >> 1 \qquad 5.56$$

Thus the transmission coefficient decreases monotonically with increasing V_0 or a, relatively slowly for thin barrier and more rapidly for thick barrier.

For example, which limit is more appropriate for our interest? Consider a 5 *MeV* proton incident upon a barrier of height 10 *MeV* and width 10 *fm* (10^{-12} cm). This gives $\kappa \sim 5 \times 10^{12}$ cm^{-1}, or $\kappa a \sim 5$. Then using the second equation of Eq.5.56 we find:

$$P \sim 16 \times \frac{1}{2} \times \frac{1}{2} \times e^{-10} \sim 2 \times 10^{-4}$$

As a further simplification, one sometimes even ignores the prefatory in Eq.5.56 and takes:

$$P \approx e^{2\kappa a} = e^{\frac{2a}{\hbar}\sqrt{2m(V_0 - E)}} \qquad 5.57$$

This phenomenon of barrier penetration or quantum mechanical tunneling has important applications in nuclear physics, especially in the theory of α-decay. Fig. 5.5 shows a schematic of the wave function in each region for both cases of the barrier potential.

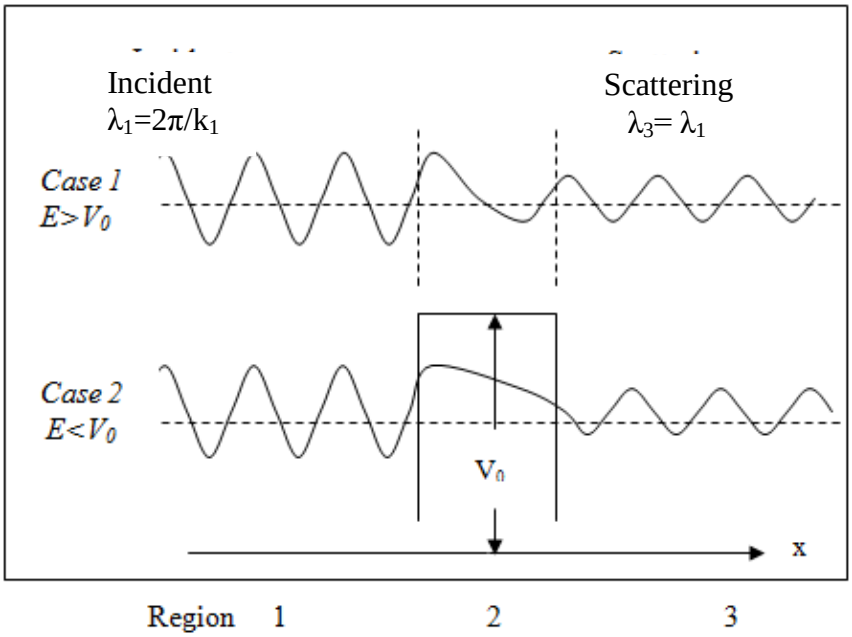

Figure 5.5 Schematic behavior of the wave function of incident particle on a barrier potential.

5.5.3. Bound state

This is a problem of a particle in a potential well, which is the simplest problem in quantum mechanics describing the binding of the nucleons in the nucleus. The problem is treated by dividing the system (nucleus) into two regions, the *interior* where the particle feels a *constant negative potential* and the *exterior* where the particle is a free particle (zero potential). The solutions to the Schrödinger equation have to be different in these two regions to reflect the binding of the particle; the wave function is oscillatory in the interior region and exponentially decaying (non-oscillatory) in the exterior region. Matching these two solutions at the boundary where the potential goes from a finite value (interior) to zero (exterior) gives a condition on

the wavenumber (or wavelength), which turns out to be the condition of *quantization*. The meaning of quantization is that solutions exist only if the wavenumbers take on certain discrete values, which then translate into discrete energy levels for the particle. For a given potential well of certain depth and width, only a discrete set of wave functions can exist in the potential well. These wave functions are the eigenfunctions of the Hamiltonian (energy) operator, with corresponding energy levels as the eigenvalues. Finding the wavefunctions and the spectrum of eigenvalues is what we mean by solving the Schrödinger wave equation for the particle in a potential well. Changing the shape of the potential means a different set of eigenfunctions and the eigenvalues. The procedure to find them, however, is the same.

We will use Eq.5.29 to investigate the bound-states of a particle in a square well potential of *depth* V_0 (i.e. the potential $V(x) = -V_0$, is constant) and width a.

For a square well potential, $V(x)$ has the following form:

$$\begin{aligned} V(x) &= -V_0 \qquad && -a/2 \le x \le a/2 \\ &= 0 \qquad && \textit{elswhere} \end{aligned} \tag{5.58}$$

Fig. 5.6 shows the interior region and the left and right exterior regions as one region. The Schrödinger equation for interior and the two exterior regions can be put into the standard form of second-order differential equation:

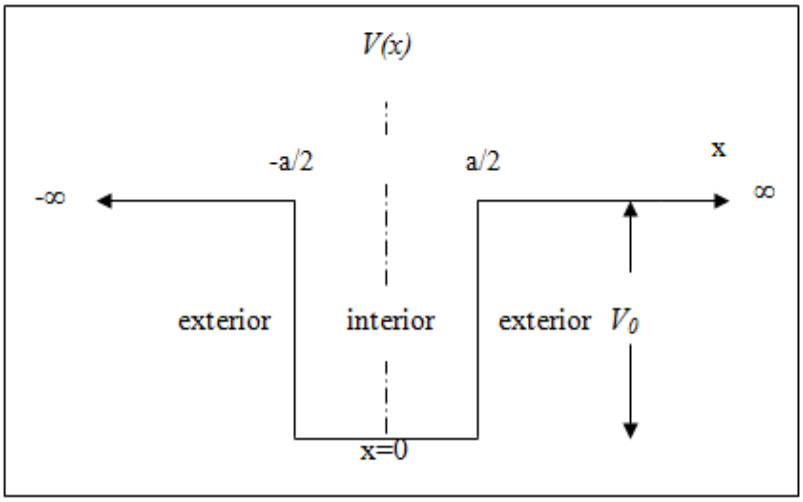

Figure 5.6 The square well potential centered at the origin of width *a*.

$$\frac{d^2\psi_{in}(x)}{dx^2} + k^2\psi_{in}(x) = 0 \qquad |x| \le a/2 \qquad 5.59$$

$$\frac{d^2\psi_{ex}(x)}{dx^2} - \kappa^2\psi_{ex}(x) = 0 \qquad |x| \ge a/2 \qquad 5.60$$

where $k = \sqrt{\frac{2m}{\hbar^2}(E + V_0)}$ is the wavenumber of the wave inside the well that is always positive, so that k is real and $\kappa = \sqrt{-\frac{2m}{\hbar^2}E}$ is the wavenumber of exterior wave; it is also real.

In other words, the wavenumber we introduce is always real, whereas the sign of the second term in the wave equation can be plus, as seen in Eq.5.59, or minus, as in Eq.5.60. For k^2 to be positive, we understand that the solution where $-E > V_0$ will be excluded from our

considerations. Accordingly, the general solutions of the above equations are:

$$\begin{aligned} \psi_{ex}(x) &= Ae^{\kappa x} + Be^{-\kappa x} && x < -a/2 \\ \psi_{in}(x) &= C\sin kx + D\cos kx && -a/2 \le x \le a/2 \\ \psi_{ex}(x) &= Fe^{\kappa x} + Ge^{-\kappa x} && x > a/2 \end{aligned} \qquad 5.61$$

To keep the wave function finite in the left external region (when $x \rightarrow -\infty$), we must have $B = 0$, and to keep it finite in the right external region (for $x \rightarrow +\infty$), we must have $F=0$. This is justified on physical ground, for bound state the particle should mostly be localized inside the potential well. This means that away from the well the wave function should decay rather than grow.

Now to obtain solutions of physical interest, we keep in mind that the solutions should have certain symmetry properties. In this case they should have definite parity, or inversion symmetry (see section 5.7). This means that when $x \rightarrow -x$, $\psi(x)$ must be either invariant or it must change sign. The reason for this requirement is that the Hamiltonian H is symmetric under inversion (the potential is symmetric given our choice of the coordinate system (see Fiq.5.5)). Thus, we take for our solutions:

$$\begin{aligned} \psi_{ex}(x) &= Ae^{\kappa x} && x < -a/2 \\ \psi_{in}(x) &= C\sin kx \quad or \quad D\cos kx && |x| \le a/2 \\ \psi_{ex}(x) &= Ge^{-\kappa x} && x > a/2 \end{aligned} \qquad 5.62$$

The choice of a solution with odd-parity *sin kx* or even-parity *cos kx* is arbitrary because both solutions would be

equally acceptable. While a linear combination of the two solutions, such as the sum, $C\sin kx + D\cos kx$ would not be acceptable because the sum of odd and even parity solutions violates the requirement that all solutions must have definite parity.

Now, applying the continuity conditions at $x=-a/2$ and at $x=a/2$, and the normalization condition, we find the following relationships for even-parity solutions and odd-parity solutions, respectively:

$$k_{in}\tan\frac{k_{in}a}{2}=\kappa_{ex} \qquad 5.63a$$

or

$$k_{in}\cot\frac{k_{in}a}{2}=-\kappa_{ex} \qquad 5.63b$$

Eq.5.63a and b are the most important results of this calculation; they are sometimes called a dispersion relation. They are relations of determining the allowed values of eigenvalue E. These are then the discrete (*quantized*) energy levels that the particle can have in the particular potential well given, a square well of width a and depth V_0.

Since both solutions are equally acceptable, one has two distinct sets of energy levels given by Eq.5.63 a and b. These transcendental equations cannot be solved directly. They can be solved numerically or graphically. The graphical solutions are easiest by rewriting Eq.5.63 in the following *dimensionless* form:

$$\alpha\tan\alpha=\eta \qquad even-parity \qquad 5.64a$$

or

$$\alpha\cot\alpha=-\eta \qquad odd-parity \qquad 5.64b$$

where $\alpha = k_{in}a/2$, $\eta = \kappa_{ex}a/2$, then we notice that

$$\alpha^2 + \eta^2 = \frac{2ma^2|V_0|}{4\hbar^2} = R \qquad 5.65$$

is a constant for fixed values of *Vo* and *a*. In Fig. 5.7, we plot the left- and right-hand sides of Eq.5.64a and b, and obtain from their intersections the allowed energy levels. The figure shows that there could be no odd-parity solutions if *R* is not large enough (the potential is not deep enough or not wide enough), while there is at least one even-parity solution no matter what values are the well depth and width.

The graphical method thus reveals the following features. It exist as a minimum value of *R* below which no odd-parity solutions are allowed. On the other hand, there is always at least one even-parity solution. *The first even-parity energy level occurs at* $\alpha < \pi/2$, whereas *the first odd-parity level occurs at* $\pi/2 < \alpha < \pi$. Thus, the even- and odd-parity levels alternate in magnitudes, with the lowest level being even in parity. We should also note that the solutions depend on the potential function parameters only through the variable *R*, or the combination of V_0a^2, so that the effect of any change in well depth can be compensated by a change in the square of the well width.

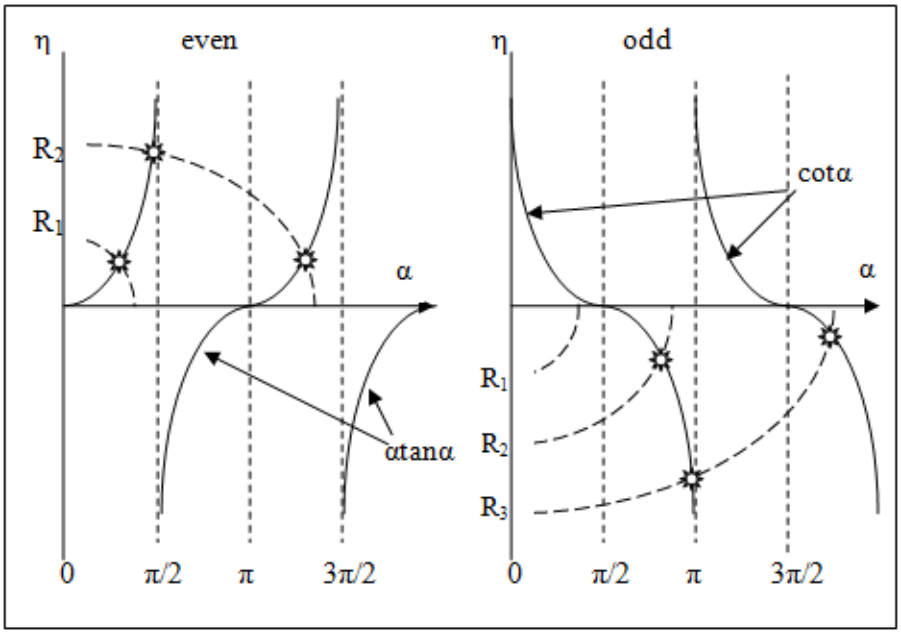

Figure 5.7 Graphical solutions of Eq.5.64a and b.

We now summarize our results for the allowed energy levels of a particle in a square well potential and the corresponding wave functions.

The discrete values of the bound-state energies (the allowed energy levels) E, k or κ can be obtained from Eq.5.63 and Eq.5.65:

$$E = -|V_0| + \frac{\hbar^2 k^2}{2m} - \frac{\hbar^2 \kappa^2}{2m} \qquad 5.66$$

Fig. 5.8 shows a sketch of the three lowest-level solutions, the ground state with even-parity, the first excited state with odd-parity and the second excited state with even-parity. Notice that the number of excited states that one can have depends on the value of V_0 because our solution is

valid only for *negative E*. This means that for a potential of a given depth, the particle can be bound only in a finite number of states.

At this point it can be noted that we anticipate that for a particle in a potential well in three dimensions (next section), the cosine solution to the wave function has to be discarded because of the condition of regularity (wave function must be finite) at the origin. This means that there will be a minimum value of R or V_0a^2 below which no bound states can exist. This is a feature of problems in three dimensions, which does not apply to problems in one dimension.

Now, to obtain results that are more explicit, it is worthwhile to consider an approximation to the boundary condition at the interface. Instead of the continuity of ψ and its derivative at the interface, one might assume that the penetration of the wave function into the external region can be neglected (i.e. $\psi_{ex} = 0$) and therefore require that ψ_{in} vanishes at $x = \pm a/2$; this case is called *infinite well potential*.

Applying this condition to Eq.5.62 gives $ka = n\pi$, where n is any integer or equivalently:

$$E_n = -|V_0| + \frac{n^2\pi^2\hbar^2}{2ma} \qquad n = 1, 2, 3\ldots \qquad 5.67$$

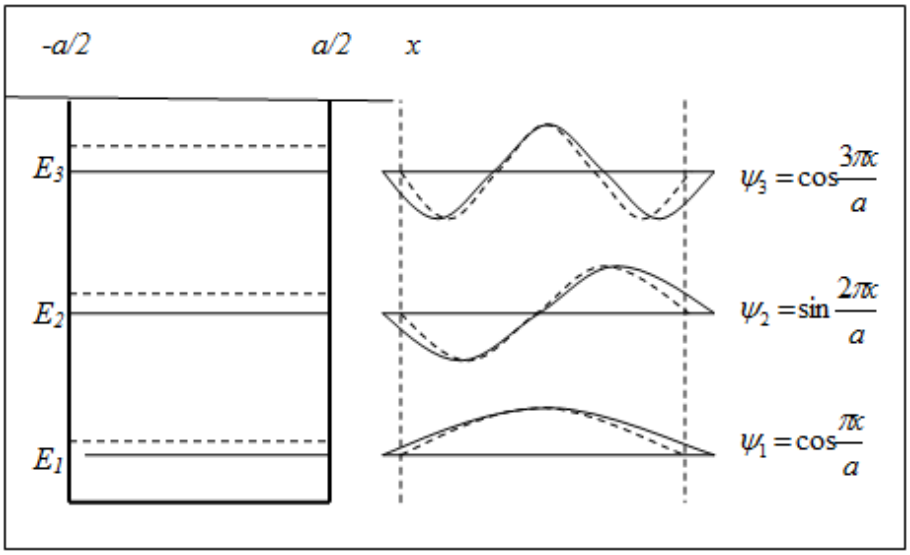

Figure 5.8 Ground state and the first two excited state solutions. Approximate solutions (*infinite potential well*) are indicated by the dashed lines.

This shows explicitly how the energy eigenvalue E_n varies with the level index n, which is the quantum number for the one-dimensional problem under consideration. The corresponding wave functions under this approximation are:

$$\psi_n(x) = D_n \cos\left(\frac{n\pi x}{a}\right) \qquad n = 1,3.....$$
$$\psi_n(x) = C_n \sin\left(\frac{n\pi x}{a}\right) \qquad n = 2,4..... \qquad 5.68$$

This is equivalent to the result obtained by de-Broglie. The first solutions in this approximate calculation are also shown in Fig. 5.8 by the dashed lines. We see that requiring the wave function to vanish at the interface has the effect of confining the particle in a potential well of width a, with

infinitely steep walls (the infinite well potential or limit of $V_0 \rightarrow \infty$). It is, therefore, to be expected that the problem becomes independent of V_0 and there is no limit on the number of excited states. Clearly, the approximate solutions become the more useful the greater is the well depth and the error is always an overestimate of the energy levels as a result of squeezing of the wave function (physically; this makes the wave have a shorter period or a larger wavenumber).

5.6. Bound State in Three Dimensions

5.6.1. Spherical well potential

We will now extend the bound-state calculation, the particle restricted to a certain region of space, to three-dimensional systems. The problem we want to solve is essentially the same as before, except that we wish to determine the bound-state energy levels and corresponding wave functions for a particle in a three-dimensional *spherical well potential*. Although this is a three-dimensional potential, we can take advantage of its symmetry in angular space and reduce the calculation to an equation still involving only one variable, the radial distance between the particle position and the origin. In other words, the spherical potential is still a function of one variable:

$$\begin{aligned} V(r) &= -V_0 \qquad r < r_o \\ &= 0 \qquad \textit{otherwise} \end{aligned} \tag{5.69}$$

Here, r is the radial position of the particle relative to the origin. Any potential that is a function only of r, the

magnitude of the position **r** and not the position vector itself, is called a *central-force potential*. As we will see, this form of the potential makes the solution of the Schrödinger wave equation particularly simple. For a system where the potential or interaction energy has no angular dependence, one can reformulate the problem by factorizing the wave function into a component that involves only the radial coordinate and another component that involves only the angular coordinates. The wave equation is then reduced to a system of uncoupled one-dimensional equations, each describing a radial component of the wave function. As to the justification for using a central-force potential for our discussion, this will depend on which properties of the nucleus we wish to study.

We, again, begin with the time-independent wave equation, so that Eq.5.23 is reduced to:

$$\left[-\frac{\hbar^2}{2m}\nabla^2 + V(r)\right]\psi(\mathrm{r}) = \mathrm{E}\,\psi(\mathrm{r}) \qquad 5.70$$

Since the potential function has spherical symmetry, it is natural for us to carry out the analysis in the spherical coordinate system rather than the Cartesian system. A position vector ***r*** is then specified by the radial coordinate *r* and two angular coordinates, θ and φ, the polar and azimuthally angles, respectively, see Fig. 5.9. Therefore, another new feature that will be important in our subsequent investigations of nuclear structure arises. Accordingly, we search for separable solutions of the form:

$$\psi(r\theta\varphi) = R(r)\Theta(\theta)\Phi(\varphi) = R(r)Y_{\ell m_\ell}(\theta,\varphi) \qquad 5.71$$

where $Y_{\ell m_\ell}(\theta,\varphi) = \Theta(\theta)\Phi(\varphi)$ is the spherical harmonic function, as will be seen later. In this coordinate system, the Laplace operator ∇^2 can be written in the following form:

$$\nabla^2 = D_r^2 + \frac{1}{r^2}\left[\frac{-L^2}{\hbar^2}\right] \qquad 5.72$$

where D_r^2 is an operator involving only the radial coordinate:

$$D_r^2 = \frac{1}{r^2}\frac{\partial}{\partial r}\left[r^2\frac{\partial}{\partial r}\right] \qquad 5.73$$

and the *operator* L^2 involves only the angular coordinates:

$$-\frac{L^2}{\hbar^2} = \frac{1}{\sin\theta}\frac{\partial}{\partial\theta}\left[\sin\theta\frac{\partial}{\partial\theta}\right] + \frac{1}{\sin^2\theta}\frac{\partial^2}{\partial\varphi^2} \qquad 5.74$$

In terms of these operators, the wave equation Eq.5.70 becomes:

$$\left[-\frac{\hbar^2}{2m}D_r^2 + \frac{L^2}{2mr^2} + V(r)\right]\psi(r,\theta,\varphi) = E\psi(r,\theta,\varphi) \qquad 5.75$$

For any potential *V(r)*, the angular variation of ψ is always determined by the operator $L^2/2mr^2$. Therefore, one can study the operator L^2 separately and then use its properties to simplify the solution of Eq.5.74. This needs to be done only once, since the angular variation is independent of whatever form one takes for *V(r)*. It turns out that L^2 is very well known (it is the square of ***L*** *or* ***L.L***

which is the angular momentum operator); it is the operator that describes the angular motion of a free particle in three-dimensional space.

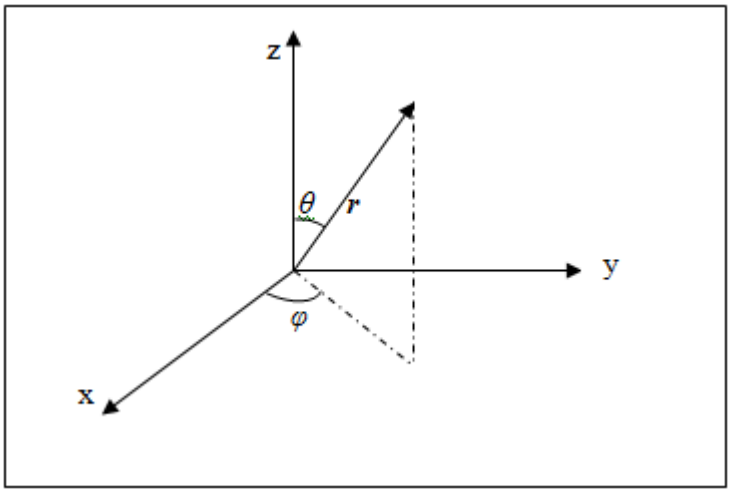

Figure 5.9 A position vector ***r*** in the spherical coordinate system.

5.6.2. Orbital angular momentum

With a little manipulation, we get the differential equation for Φ(φ) from Eq.5.74 is:

$$\frac{d^2\Phi}{d\Phi^2} + m_\ell^2\Phi = 0 \qquad \textit{with} \quad \textit{solution} \quad \Phi_{m_\ell}(\varphi) = e^{im_\ell\varphi} \qquad 5.76$$

where m_ℓ^2 is the separation constant, that will be called the *magnetic quantum number* and $m_\ell = 0, \pm1, \pm2, \pm3\ldots$.

While the differential equation for $\Theta(\theta)$ is:

$$\frac{1}{\sin\theta}\frac{d}{d\theta}\left(\sin\theta\frac{d\Theta}{d\theta}\right)+\left[\ell(\ell+1)-\frac{m_\ell^2}{\sin^2\theta}\right]\Theta=0 \qquad 5.77$$

with a solution:

$$\Theta_{\ell m_\ell}(\theta)=\left[\frac{2\ell+1(\ell-|m_\ell|)!}{4\pi(\ell+|m_\ell|)!}\right]^{1/2}P_\ell^{m_\ell}(\theta) \qquad 5.78$$

where ℓ = *0, 1, 2, 3 ...* is the *orbital angular quantum number*. The solution $\Theta_{\ell m_\ell}(\theta)$ can be expressed as a polynomial of degree ℓ in $\sin\theta$ or $\cos\theta$. Together, and normalized, $\Phi_{m_\ell}(\varphi)$ and $\Theta_{\ell m_\ell}(\theta)$ give the *spherical harmonics* $Y_{\ell m_\ell}(\theta,\varphi)$. It can be shown from Eq.5.74 and 5.78 that the eigenfunction of L^2 are the spherical harmonics functions, $Y_{\ell m_\ell}(\theta,\varphi)$:

$$L^2Y_{\ell m_\ell}(\theta,\varphi)=\hbar^2\ell(\ell+1)Y_{\ell m_\ell}(\theta,\varphi) \qquad 5.79$$

where

$$Y_{\ell m_\ell}(\theta,\varphi)=\left[\frac{2\ell+1(\ell-|m_\ell|)!}{4\pi(\ell+|m_\ell|)!}\right]^{1/2}P_{\ell m_\ell}(\cos\theta)e^{im_\ell\varphi} \qquad 5.80$$

and

$$P_{\ell m_\ell}(\mu)=\frac{(1-\mu^2)^{m_\ell/2}}{2^\ell\,\ell!}\frac{d^{\ell+m_\ell}}{d\mu^{\ell+m_\ell}}(\mu^2-1)^\ell \qquad 5.81$$

With $\mu=\cos\theta$, the function $P_{\ell m_\ell}(\mu)$ is the associated Legendre polynomials, which are in turn expressible in terms of Legendre polynomials $P_\ell(\mu)$:

$$P_{\ell m_\ell}(\mu) = (1-\mu)^{|m_\ell|/2} \frac{d^{|m_\ell|}}{d\mu^{|m_\ell|}} P_\ell(\mu) \qquad 5.82$$

with the well-known first four Legendre polynomials $P_\ell(\mu)$:

$$P_0(\mu) = 1, \quad P_1(\mu) = \mu, \quad P_2(\mu) = \frac{3\mu^2 - 1}{2}, \quad P_3(\mu) = \frac{5\mu^3 - 3\mu}{2}$$

and the first four spherical harmonic functions $Y_{\ell m_\ell}(\theta, \varphi)$:

$$Y_{0,0} = \sqrt{\frac{1}{4\pi}}, \quad Y_{1,-1} = \sqrt{\frac{3}{8\pi}} e^{-i\varphi} \sin\theta, \quad Y_{1,0} = \sqrt{\frac{3}{4\pi}} \cos\theta, \quad Y_{1,1} = \sqrt{\frac{3}{8\pi}} e^{i\varphi} \sin\theta$$

Special functions like $Y_{\ell m_\ell}$ and $P_{\ell m_\ell}$ are quite extensively discussed in standard texts and reference books on mathematical functions. For our purposes, it is sufficient to regard them as well known and tabulated quantities like sines and cosines, and whenever the need arises, we will invoke their special properties as given in the mathematical handbooks.

It is clear from Eq.5.79 that $Y_{\ell m_\ell}(\theta, \varphi)$ is an *eigenfunction* of L^2 with corresponding *eigenvalue* $\ell(\ell+1)\hbar^2$. Since the angular momentum of the particle, like its energy, is *quantized*, the index ℓ can take on only positive integral values or zero, $\ell = 0, 1, 2, 3 \ldots$ and the index m_ℓ can have integral values from $-\ell$ to ℓ ($m_\ell = 0, \pm 1, \pm 2 \ldots \pm \ell$). Then for a given ℓ, there can be $2\ell + 1$ values of m_ℓ, in other words, $m_\ell = -\ell, -\ell+1, -\ell+2 \ldots, -1, 0, 1 \ldots, \ell-2, \ell-1, \ell$.

In quantum mechanics, we evaluate the expectation value of the angular momentum of a nucleon, for simplicity by

calculating the magnitude of the average value of $<L^2>$, instead of $<L>$:

$$<L^2> = \int \psi^* L^2 \psi dx \qquad 5.83$$

where ψ, ψ^* are the Schrödinger wave function and its conjugate, respectively.
In addition, $< L^2 >=< L_x^2 + L_y^2 + L_z^2 >$ is a function of position, as shown in Fig. 5.10:

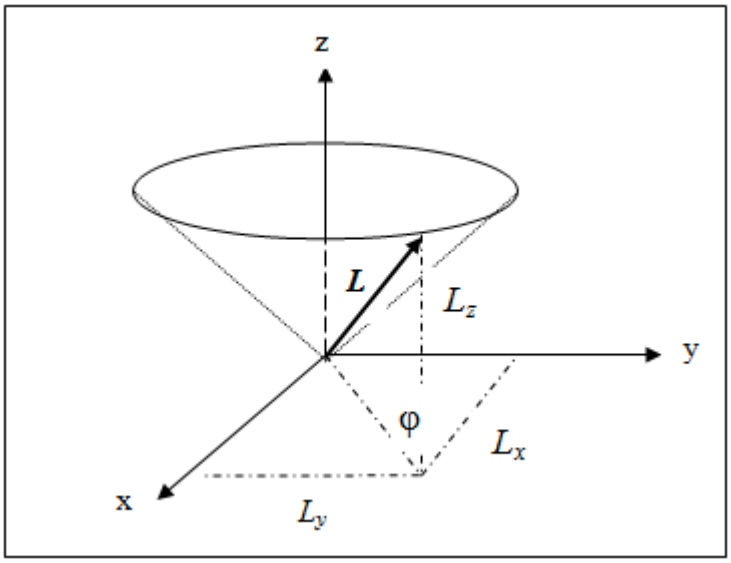

Figure 5.10 The vector ***L*** rotates rapidly about the z-axis, so that L_z stays constant, but L_x and L_y are variable.

For an isolated nucleus, the angular momentum is conserved and represented by the *orbital angular quantum number* (ℓ) and the *magnetic quantum number* m_ℓ with values of:

$$<L^2> = \hbar^2 \ell\,(\ell + 1), \qquad m_\ell = 0, \pm 1, \pm 2\ldots, \pm \ell. \qquad 5.84$$

In addition, the directed orbital angular momentum (the magnitude of L) is:

$$|\mathrm{L}| = \hbar\sqrt{\ell(\ell+1)} \qquad with \quad \ell = 0,1,2,3... \tag{5.85}$$

The angular momentum quantum number (ℓ) has the same function in all three-dimensional problems involving central potentials, where $V = V(r)$. The significance of m_ℓ can be seen from the property of L_z, the projection of the orbital angular momentum vector $\boldsymbol{L}$ along a certain direction in space (in the absence of any external field, this choice is up to the observer). Following convention, we will choose this direction to be along the *z-axis* of our coordinate system, in which case the operator L_z has the representation, $L_z = -i\hbar\dfrac{\partial}{\partial\varphi}$, and its eigenfunctions are also $Y_{\ell m_\ell}(\theta,\varphi)$, with eigenvalues $m_\ell\hbar$. For z component of L to be determined, we have:

$$<\mathrm{L_z}> = \hbar\mathrm{m}_\ell \tag{5.86}$$

Notice from Fig. 5.10 that, $<\mathrm{L_z}> < |\mathrm{L}| = \hbar\sqrt{\ell(\ell+1)}$, the *z component* of the vector is always less than its length.

Now, it is clear that since the angular space is two-dimensional θ,φ (corresponding to two degree of freedom), it is to be expected that *two quantum numbers* will emerge from our analysis, those are the indices ℓ and m. For the same reason, we should expect *three quantum numbers* in our description of three-dimensional systems, i.e., adding another quantum number for radial coordinate. We should regard the particle (nucleon) as existing in various states,

which are specified by a unique set of quantum numbers, each one is associated with a certain orbital angular momentum that has a definite magnitude and orientation with respect to our chosen direction along the z-axis. The particular angular momentum state is described by the function $Y_{\ell m_\ell}(\theta,\varphi)$ with ℓ known as the *orbital angular momentum quantum number*, and m_ℓ the *magnetic quantum number*.

Finally, we can specify the magnitude and one Cartesian component (usually called the z-component) of $\boldsymbol{L}$ by specifying ℓ and m_ℓ, an example of an orbital angular momentum with ℓ=2 is shown in Fig. 5.11, which gives $2\ell+1=5$ projections along z-axis with a magnitude $|\mathrm{L}| = \sqrt{6}\hbar$. In this case, the x and y-components are undetermined, in that they cannot be observed simultaneously with the observation of L^2 and L_z.

5.6.3. Radial wave equation

Returning to the wave equation Eq.5.75, we are looking for a solution as an expansion of the wave function in spherical harmonics series:

$$\psi(r\theta\varphi) = \sum_{\ell,m_\ell} R_\ell(r) Y_{\ell m_\ell}(\theta,\varphi) \qquad 5.87$$

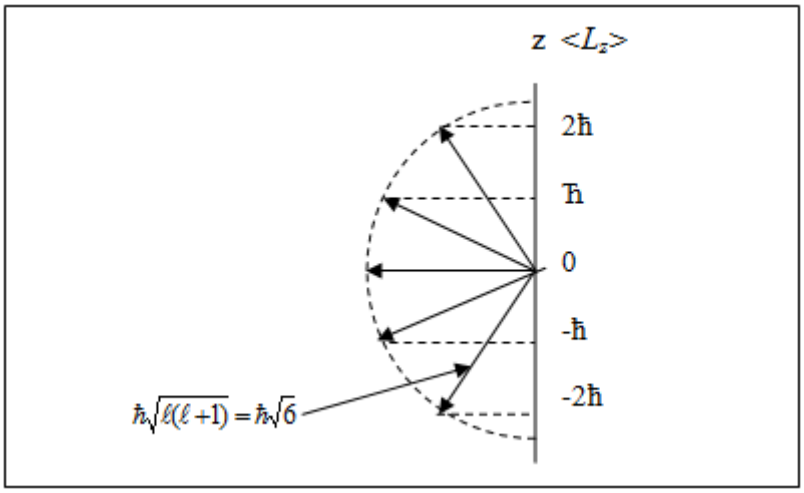

Figure 5.11 The projection of an orbital quantum number along z-axis.

We can eliminate the angular part of the problem by multiplying the wave equation by the complex conjugate of a spherical harmonic and integrating over all solid angles (recall an element of solid angle is $sin\theta d\theta d\varphi$), since the property of orthogonality gives:

$$\int_0^{\pi} \sin\theta d\theta \int_0^{2\pi} d\varphi Y^*_{\ell m_\ell}(\theta,\varphi) Y_{\ell' m'_\ell}(\theta,\varphi) = \delta_{\ell\ell'}\delta_{mm'} \qquad 5.88$$

where $\delta_{\ell\ell'}$ denotes the Kronecker delta function:

$$\delta_{\ell\ell'} = 1 \quad if \ \ell = \ell'$$
$$\delta_{\ell\ell'} = 0 \quad if \ \ell \neq \ell'$$

and because of Eq.5.75, the L^2 operator in Eq.5.79 can be replaced by the factor $\ell(\ell+1)\hbar^2$, obtaining the following *r*-dependent equation:

$$\left[-\frac{\hbar^2}{2m}D_r^2+\frac{\ell(\ell+1)\hbar^2}{2mr^2}+V(r)\right]R_\ell(r)=ER_\ell(r) \qquad 5.89$$

This is an equation in one variable, the radial coordinate *r*, although we are treating a three-dimensional problem. We can make this equation look like a one-dimensional problem by transforming the dependent variable R_ℓ. Define the radial function:

$$u_r(r)=rR_\ell(r) \qquad 5.90$$

Inserting this into Eq.5.89, we get:

$$-\frac{\hbar^2}{2m}\frac{d^2u_\ell(r)}{dr^2}\left[\frac{\ell(\ell+1)\hbar^2}{2mr^2}+V(r)\right]u_\ell(r)=Eu_\ell(r) \qquad 5.91$$

We will call Eq.5.91 *the radial wave equation*. It is the basic starting point of three-dimensional problems involving a particle interacting with a central potential field.

We observe that Eq. 5.91 is actually a system of uncoupled equations, one for each fixed value of the orbital angular momentum quantum number ℓ. With reference to the wave equation in one dimension, the extra term involving $\ell\ (\ell+1)$ in Eq.5.91 represents the contribution to the potential field due to the centrifugal motion of the particle. *The $1/r^2$ dependence makes the effect particularly important near the origin; in other words, centrifugal*

motion gives rise to a barrier that tends to keep the particle away from the origin. This effect is of course absent in the case of $\ell = 0$, a state of zero orbital angular momentum, as one would expect. The first few ℓ states are usually the only ones of interest in our discussion (because they tend to have the lowest energies). Therefore, the solution of the radial wave equation Eq.5.91 depends on the form of the central potential *V(r)* applied, as we will see in the next chapter.

The wave function that describes the state of orbital angular momentum ℓ is often called the ℓ^{th} partial wave:

$$\psi_\ell(r,\theta,\varphi) = R_\ell(r)Y_{\ell m_\ell}(\theta,\varphi) \qquad 5.92$$

Notice that in the case of s-wave the wave function is spherically symmetric since $Y_{0,0}$ is independent of θ and φ.

5.6.4. Square well potential

Thus far, we have confined our discussions of the wave equation to its solution in spherical coordinates. There are situations where it will be more appropriate to work in another coordinate system. As a simple example of a bound-state problem, we can consider the system of a free particle confined in a cubical box of dimension *a* along each side, $0< x, y, z <a$. In this case, it is clearly more convenient to write the wave equation Eq.5.70 in Cartesian coordinates:

$$-\frac{\hbar^2}{2m}\left[\frac{\partial^2}{\partial x^2}+\frac{\partial^2}{\partial y^2}+\frac{\partial^2}{\partial z^2}\right]\psi(xyz) = E\psi(xyz) \qquad 5.93$$

The potential energy inside this region is zero, $V_{(0<x,\,y,\,z<a)}=0$. Outside it is infinite (*infinite square well*). The boundary

conditions are ψ = 0 whenever x, y, or z is 0 or *a*. Since both the equation and the boundary conditions are separable in the three coordinates, the solution is of the product form:

$$\begin{aligned}\psi(x,y,z) &= \psi_{n_x}(x)\psi_{n_y}(y)\psi_{n_z}(z) \\ &= (2/a)^{3/2}\sin(n_x\pi x/a)\sin(n_y\pi y/a)\sin(n_x\pi z/a)\end{aligned} \qquad 5.94$$

where n_x =*1, 2, 3*... n_y =*1, 2, 3*... n_z =*1, 2, 3*... and the energy becomes a sum of three contributions:

$$\begin{aligned}E_{n_x,n_y,n_z} &= E_{n_x} + E_{n_y} + E_{n_z} \\ &= \frac{(\hbar\pi)^2}{2ma^2}[n_x^2 + n_y^2 + n_z^2]\end{aligned} \qquad 5.95$$

To provide the interpretation of this result, we notice that there are three quantum numbers (n_x, n_y, n_z), which are necessary to describe each energy state. *This fact is the general property of three-dimensional systems* and none of the quantum numbers may be zero. The lowest energy, the ground state, occurs when $n_x = n_y = n_z = 1$. While each state of the system is described by a unique set of quantum numbers, there can be more than one state at particular energy levels. Whenever this happens, the energy level is said to be *degenerate*.

For example, there are three possibilities for the first excited state:

n_z =*2*	$n_x = n_y$ =*1* or defined as (112)
n_y =*2*	$n_x = n_z$ =*1* or defined as (121)
n_x =*2*	$n_y = n_z$ =*1* or defined as (211)

Though they are three different states, they are all at the same energy, so the level at $6(\hbar\pi)^2/2ma^2$ is triply degenerate. The concept of degeneracy is useful in our coming discussion of the nuclear shell model, in the next chapter, where one has to determine how many nucleons can be put into a certain energy level. Fig. 5.12 shows the energy level diagram for a particle in a cubical box. Another way to display the information is through a table, such as Table 5.1.

The energy unit is seen to be $\Delta E = \frac{(\hbar\pi)^2}{2ma^2}$.

For example, we can use this expression to estimate the magnitude of the energy levels for electrons in an atom, for which $m = 9.1\times10^{-28}$ g and $a \sim 3\times10^{-8}$ cm, and for nucleons in a nucleus, for which $m = 1.6\times10^{-24}$ g and $a \sim 5\times10^{-13}$ cm. The energies come out to be ~30 eV and 6 MeV, respectively; values which are typical in atomic and nuclear physics. Notice that if an electron were in a nucleus, it would have energies of the order 10^4 MeV!

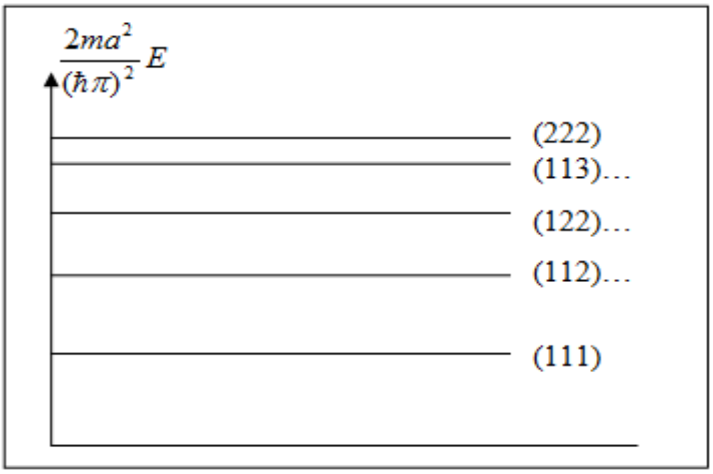

Figure 5.12 Bound states of a particle in a cubical box of width a.

Table 5.1. The first few energy levels of a particle in a cubical box.

n_x	n_y	n_z	$\frac{2ma^2}{(\hbar\pi)^2}E$	degeneracy
1	1	1	3	1
1	1	2	6	3
1	2	1		
2	1	1		
1	2	2	9	3
1	1	3	11	3
2	2	2	12	1

5.7. Parity

As mentioned in section 2.11, parity is the effect of a reflection of the coordinates, through the origin: $\boldsymbol{r} \rightarrow \boldsymbol{-r}$, on the observable properties of the system, such as a potential and wave function of a nucleus. If a system is left unchanged by the parity operation, the system is *symmetric*, *even parity or positive parity*, then we expect that none of the observable properties should change as a result of the reflection. While if the sign of the system changed, it is *asymmetric with odd parity or negative parity*. As a result of measuring the observable quantities, which depend on $|\psi|^2$, we have the following reasonable assertion:

If $V(\boldsymbol{r}) = V(\boldsymbol{-r})$ then $|\Psi(\boldsymbol{r})|^2 = |\Psi(\boldsymbol{-r})|^2$, or $\Psi(\boldsymbol{r}) = \pm\Psi(\boldsymbol{-r})$

That is:

If $\Psi(\mathbf{r}) = +\Psi(-\mathbf{r})$ then symmetric, even or positive parity
If $\Psi(\mathbf{r}) = -\Psi(-\mathbf{r})$ then asymmetric, odd or negative parity.

and its reverse is also true:

$$\text{if } |\Psi(\mathbf{r})|^2 \neq |\Psi(-\mathbf{r})|^2 \quad \text{then} \quad V(\mathbf{r}) \neq V(-\mathbf{r})$$

That is the system is not invariant with respect to parity.

In Cartesian coordinates change of sign by (x, y, z) to (-x, -y, -z) and in Spherical coordinates change of sign by (r, θ, φ) to (r, $\pi - \theta$, $\varphi + \pi$).

For physical systems, which are not subjected to an external vector field, we expect that these systems will remain the same under an inversion operation, or the Hamiltonian is invariant under inversion. If $\psi(\boldsymbol{r})$ is a solution to the wave equation, applying the inversion operation we get:

$$H\Psi(-\boldsymbol{r}) = E\Psi(-\boldsymbol{r}) \qquad 5.96$$

which shows that $\psi\ (-\boldsymbol{r})$ is also a solution. A general solution is, therefore, obtained by adding or subtracting the two solutions.

$$H[\Psi(\boldsymbol{r}) \pm \Psi(-\boldsymbol{r})] = E[\Psi(\boldsymbol{r}) \pm \Psi(-\boldsymbol{r})] \qquad 5.97$$

Since the function $\psi_+(\boldsymbol{r}) = \psi(\boldsymbol{r}) + \psi(-\boldsymbol{r})$ is manifestly invariant under inversion, it is said to have positive parity, or its parity, *denoted by the symbol* π *,* is +1. Similarly, $\psi_-(\boldsymbol{r}) = \psi(\boldsymbol{r}) - \psi(-\boldsymbol{r})$ changes sign under inversion, *so it has negative parity, or* π = -1. The significance of Eq.5.97 is that

a physical solution of our quantum mechanical description should have definite parity; which is the condition we have previously imposed on our solutions in solving the wave equation (see section 5.5.3). Notice that there are functions, which do not have definite parity, for example, Csinkx + Dcoskx. This is the reason that we take either the sine function or the cosine function for the interior solution in section 5.5.3. In general, one can accept a solution as a linear combination of individual solutions, all having the same parity. A linear combination of solutions with different parities has no definite parity and is, therefore, unacceptable.

In spherical coordinates, the effect of the transformation on the spherical harmonic function $Y_{m_\ell}^{\ell}(\theta,\varphi) \sim e^{im_\ell\varphi}P_\ell^{m_\ell}(\theta)$ is:

$$\begin{aligned} e^{im_\ell\varphi} &\rightarrow e^{im_\ell\varphi}e^{im_\ell\pi} = (-1)^{m_\ell}e^{im_\ell\varphi} \\ P_\ell^{m_\ell}(\theta) &\rightarrow (-1)^{\ell-m_\ell}P_\ell^{m_\ell}(\theta) \end{aligned} \qquad 5.98$$

So the parity of $Y_{\ell m_\ell}(\theta,\varphi)$ is $(-1)^{\ell}$. In other words, the parity of a state is even with a definite orbital angular momentum is even, and odd if ℓ is odd. All eigenfunctions of the Hamiltonian with a spherically symmetric potential are therefore, either even or odd in parity.

Problems

5-1. An electron's position is known to an accuracy of about 10^{-8} cm.

a- How accurately can its velocity be known?

b- Find the uncertainty in the position 1.0 sec later.

5-2. A typical atomic nucleus is about 5.0×10^{-15}m in radius. Use the uncertainty principle to place a lower limit on the energy an electron must have if it is to be part of a nucleus.

5-3. The range of the potential between two hydrogen atoms is approximately ˚A. For a gas in thermal equilibrium, obtain a numerical estimate of the kinetic energy below which the atom-atom scattering is essentially s-wave when $ka \leq 1$.

5-4. a- In Bohr's original theory of the hydrogen atom (circular orbits), what postulate led to the choice of the allowed energy levels?

b- Later de Broglie pointed out a most interesting relationship between the Bohr postulate and the de Broglie wavelength of the electron. State and derive this relationship.

5-5. Derive Eq. 5.16 from the relativistic equation for the total energy E of a particle of mass m and momentum p (Eq.1.20).

5-6. Prove that the phase velocity υ_{ph} is always greater than or equal to the particle velocity υ, while it is equal to the group velocity υ_g.

5-7. An electron has a de Broglie wavelength of 2.0×10^{-12} m. Find its kinetic energy and the phase and group velocities of its de Broglie waves. What will be the wavelength of a proton of the same velocity ($\upsilon = \upsilon_g$) of the electron?

5-8. Prove that the Schrödinger equation Eq. 5.29 is linear. In other words, show that if ψ_i and ψ_j both are solutions, $(A\psi_i + B\psi_i)$ is also a solution.

5-9. For a free particle described in section 5.5.1, show that the kinetic energy T of the particle is exactly $\hbar^2k^2/2m$ by calculating $\langle T\rangle$ and $\langle T^2\rangle - \langle T\rangle^2$.

5-10. For a plane wave incident on a step potential (Fig 5.4), calculate the reflection coefficient R for the case in which $E < V_o$.

5-11. What ratio E/V_o is necessary for scattering from one-dimensional step potential so that the transmission probability will be 50 percent?

5-12. A stream of electrons, each having an energy E = 4 eV is directed toward a potential barrier of height V_o = 5 eV. The width of the barrier is 2×10^{-7} cm.

a- Calculate the percentage transmission of this beam through this barrier.
b- How is this affected if the barrier is doubled in width?

5-13. Assume that an alpha particle has en energy of 10 MeV and approaches a potential barrier of height 30 MeV. Determine the width of the barrier if the transmission coefficient is 0.002.

5-14. Derive Eq.5.56 for the penetration factor.

5-15. Derive the condition for perfect transmission through a rectangular potential barrier.

5-16. Obtain the amplitude for the wave reflected from a rectangular potential barrier and show directly that probability is conserved in the collision process.

5-17. For a particle (mass m, quantum number n) in an infinite square well of width a:

a- What is the probability of finding the particle within a distance ϵ of the left-hand edge?
b- Find the limit as $n \rightarrow \infty$.
c- For finite n, find the limit as $\epsilon/a << 1$.

5-18. Show that $\langle x^2 \rangle = a^2/3 - a^2/(2n^2\pi^2)$ for the particle in an infinite square well with limits $(0, a)$.

5-19. An object in one dimension is described by a wave function:

$$\psi = x\sqrt{3} \qquad 0 < x < 1$$
$$\psi = 0 \qquad elswhere$$

a- What is the probability of finding the object within the interval (0, 0.5)?
b- What is the average position of the object?

5-20. Find and draw the angle between the angular momentum vector **L** and the z-axis for all possible orientations when $\ell = 3$.

5-21. Show that for a spherical potential V(r) such that $V(r\rightarrow\infty) = 0$, the radial solution of Eq.5.91 for a bound state has the asymptotic solution: $u(r \rightarrow \infty) \sim e^{-\kappa r}$ where κ is given by $\frac{1}{2}\hbar^2\kappa^2/m_o = |E|$. Also show that Eq.5.91 is satisfied for $r\rightarrow 0$ by a solution: $R(r\rightarrow 0) \sim r^{\ell}$.

5-22. To some approximation, a medium weight nucleus can be regarded as a flat-bottomed potential with rigid walls. To simplify this picture still further, model a nucleus as a cubical box of length equal to the nuclear diameter. Consider a nucleus of iron-56 which has 28 protons and 28 neutrons. Estimate the kinetic energy of the highest energy nucleon. Assume a nuclear diameter of 10^{-12} cm (this is a full derivation of Eqs.5.94 and 5.95 from Eq.5.93).

5-23. A particle of mass m is just barely bound by a one-dimensional potential well of width L. Find the value of the depth V_o.

5-24. Suppose you are given the result for the transmission coefficient T for the barrier penetration problem, one-dimensional barrier of height Vo extending from x=0 to x=L,

$$T = \left[1 + \frac{V_o^2}{4E(V_o - E)} sinh^2 KL\right]^{-1}$$

where $K^2 = 2m(V_o - E)/\hbar^2$ is positive ($E < V_o$).

a- From the expression given, deduce T for the case $E > V_o$ without solving the wave equation again.

b- Deduce T for the case of a square well potential from the result for a square barrier.

5-25. Compare the ground state energy of a particle in a cubical box of width *a,* with that of the particle in a one dimensional infinite well of width *a*.

5-26. Explain the expected change of the wave function If one interchanges the spatial coordinates of two protons in:

a- A state of total spins 0.
b- A state of total spins 1.

CHAPTER 6

NUCLEAR FORCES AND INTERACTIONS

There is a dominant short-range part of the nucleon-nucleon interaction potential, which is central and provides the overall shell-model potential. A part, whose range is much smaller than the nuclear radius, tends to make the nucleus spherical and to pair up with nucleons. A second part, whose range is of the order of the nuclear radius, tends to distort the nucleus. There is a spin-orbit interaction and spin-spin interaction. The force is charge independent (Coulomb interaction excluded). The force saturates.

6.1. Introductory Remarks

One of the aims of nuclear physics is to calculate the energies and quantum numbers of nuclear bound states. In atomic physics, one can do this starting from first principles. In fact, Coulomb's law (or more generally the equations of electromagnetism) determines the interactions between electrons and nuclei. Spin corrections and relativistic effects can be calculated perturbatively to a very good accuracy because of the smallness of the fine structure constant $\alpha = e^2/(4\pi\varepsilon_0\hbar c) \approx 1/137$. Together with the Pauli exclusion principle which leads to the shell structure of electron orbitals, these facts imply that one can calculate numerically spectra of complex atoms despite the difficulties of the many-body problem.

Unfortunately, none of these holds in nuclear physics. Forces between nucleons are neither simple nor fully understood. One of the reasons for this is that the interactions between nucleons are “residuals” of the fundamental interactions between quarks inside the nucleons. In that sense, nuclear interactions are similar to Van der Waals forces between atoms or molecules, which are also residual or “screened” Coulomb interactions. For these reasons, forces between nucleons are described by semi-phenomenological forms, e.g., the potential proposed by Yukawa in 1939, which are only partly deduced from fundamental principles.

The subject of nucleon–nucleon potentials is very complex and we will give only a qualitative discussion. Our basic guidelines are the following facts:

1- Protons and neutrons are spin 1/2 *fermions* and, therefore, obey the Pauli Exclusion Principle which states, *in a closed system no two identical particles can be in the same energy state*. More details will be clarified in the following sections.

2- Nuclear forces are *attractive* and *strong*, since binding energies are roughly a 10^6 times the corresponding atomic energies. They are, however, *short range forces* (a few fm). The combination of strength and short range makes 2 nucleon systems only marginally bound but creates a rich spectrum of many-nucleon states.

3- Nuclear forces are "*charge independent*". They are blind to the electric charge of nucleons. If one were to “turn off” Coulomb interactions, the nuclear proton–proton potential would be the same as the neutron–neutron potential. A simple example is given by the binding energies of isobars, such as tritium and helium-3: $BE\ (^3\mathrm{H}) = 8.492\mathrm{MeV} > BE\ (^3\mathrm{He}) = 7.728\mathrm{MeV}$. If the

difference $\Delta BE = 0.764$MeV is attributed to the Coulomb interaction between the two protons in ^{3}He, $\Delta BE = e^2 < 1/r_{12} > /4\pi\varepsilon_0$, one obtains a very reasonable value for the mean radius of the system: $R \approx 2$ fm (this can be calculated or measured by other means). We shall come back to this question in a more quantitative way when we discuss *isospin*, section 6.4.

4- Nuclear forces *saturate*. As we will see in the next section, this results in the volumes and binding energies of nuclei being *additive* and, in first approximation, proportional to the mass number *A*. This is a remarkable fact since it is reminiscent of a *classical* property and not normally present in quantum systems. It appears as if each nucleon interacts with a given fixed number of neighbors, whatever the nucleus is.

Reversing the order of inference, physicists could have derived the form of Coulomb's law from the spectrum of bound states of the hydrogen atom. This is not possible in nuclear physics because there is only one two-nucleon bound state, *the deuteron*. In the next subsection, we will find that there is much to be learned from this fact but it will not be sufficient to derive the nucleon–nucleon potential in all its details. To do this, we will need to attack the more difficult problem *of nucleon–nucleon scattering*.

6.2. The Deuteron

There is only one $A = 2$ nucleus, the deuteron, and it has no excited states. It is the simplest bound state of nucleons and, therefore, gives an ideal system for studying the nuclear force and nucleon-nucleon interaction. Its binding energy is a very precisely measured quantity and can be determined in three different ways. First by mass spectroscopy, we have

(BE_d = 2.22463 ± 0.00004 MeV), then by directly bringing a proton and neutron together to form ^{2}H and measuring the energy of gamma ray photon emitted, we have:

$$^1\text{H} + \text{n} \rightarrow \ \ ^2\text{H} + \gamma \qquad 6.1$$

The deduced binding energy is equal to the observed energy of the photon less a small recoil correction (BE_d = 2.224589 ± 0.000002 MeV). Finally by using the reverse reaction called photo-dissociation, in which a γ-ray photon breaks apart a deuteron (2.224 ± 0.002 MeV), all are in excellent agreement with each other.

Note that *B*E is quite small compared to typical nuclear binding energies of 8 MeV per nucleon.

6.2.1. Nuclear force is spin dependent

The deuteron quantum numbers ($J^\pi = 1^+$) and total angular momentum (spin) is:

$$\boldsymbol{I} = \boldsymbol{s}_n + \boldsymbol{s}_p + \boldsymbol{\ell} \qquad 6.2$$

The measured spin of the deuteron is I = 1. Since the neutron and proton spins can be either parallel (for a total of 1) or antiparallel (for total of 0), there are four possibilities to couple s_n, s_p, ℓ to get total I =1:

a- s_n and s_p parallel with $\ell = 0$
b- s_n and s_p antiparallel with $\ell = 1$
c- s_n and s_p parallel with $\ell = 1$
d- s_n and s_p parallel with $\ell = 2$

The other important property of deuteron is the magnetic dipole moment $\mu_d = 0.857\ \mu_N$, (μ_N is the nuclear magneton). We also note (in section 2.9) that, to a good approximation, $\mu_d = \mu_p + \mu_n$. This suggests that the magnetic moment comes only from the spins of the constituents, implying that the nucleons are in a state of vanishing orbital angular momentum, $\ell = 0$. In fact, this turns out only to be a good first approximation since the deuteron is *slightly deformed*, possessing a small quadrupole moment. This requires that the wave function has a small admixture of $\ell = 2$.

Both $\ell = 0$ and $\ell = 2$ (case a and b)are consistent with the parity of the deuteron since for two-nucleon states, the parity is $(-1)^{\ell}$, in the context of the above discussion, one can assume the discrepancy to arise from a small mixture of d state (ℓ=2) in the deuteron wavefunction:

$$\Psi = a_s\Psi\ (\ell=0) + a_d\Psi\ (\ell=2) \qquad 6.3$$

and consequently its magnetic moment can be calculated as:

$$\mu = a_s^2\,\mu(\ell = 0) + a_d^2\,\mu(\ell = 2) \qquad 6.4$$

where

$\mu\ (\ell=0) = 0.879804\ \mu_N$ (calculated), and

$\mu\ (\ell=2) = (1/4)\ (3 - g_{sp} - g_{sn})\ \mu_N = 0.3100982\ \mu_N$

with $g_{sp} = 2\mu_p = 5.585691$, $g_{sn} = 2\mu_n = -3.826084$, the observed value is consistent with $a_s^2 = 0.96$, and $a_d^2 = 0.04$; that is, the deuteron is 96% ℓ=0 and only 4% ℓ=2. Then, the assumption of the pure ℓ=0 state, which we made in

calculating the well depth, is thus pretty good but not quite exact.

Since the deuteron has spin-1 and is (mostly) in an $\ell = 0$ state, the spins of the nucleons must be aligned, i.e., the total spin, $\boldsymbol{s}_{\text{tot}} = \boldsymbol{s}_{\text{n}} + \boldsymbol{s}_{\text{p}}$, must take on the quantum number $s = 1$. The other possibility is $s = 0$. Since the deuteron is the only bound state, we can state that:

n p (s = 1) bound n p (s = 0) unbound

Then we conclude that *the neutron–proton potential is spin-dependent*.

What about the neutron–neutron and proton–proton potentials and the fact that there are no bound states for these two systems (no nucleus exist of only two neutrons or only two protons)? If the strong interactions do not distinguish between neutrons and protons, the non-existence of an $s = 0$ neutron–proton state is consistent with the non-existence of the analogous pp and nn states:

n n (s = 0) unbound p p (s = 0) unbound,

i.e., all nucleon–nucleon $s = 0$, $\ell = 0$ states are unbound *which is incorrect*. The non-existence of pp and nn $s = 1$, $\ell = 0$ states is explained by the Pauli principle. This principle requires that the total wave-function of pairs of identical fermions be antisymmetric. Loosely speaking, this is equivalent to saying that when two identical fermions are at the same place ($\ell = 0$), their spins must be anti-parallel. *Thus, the $s = 1$, $\ell = 0$ proton–proton and neutron–neutron states are forbidden*.

We make the important conclusion that the existence of a (*np*) bound state and the non-existence of *nn* and *pp* bound

states is consistent with the strong force not distinguishing between neutrons and protons *but only if the force is spin-dependent*.

The existence of an $s = 1$ state and non-existence of $s = 0$ states would *naively suggest* that the nucleon–nucleon force is attractive for $s = 1$ and repulsive for $s = 0$. This is incorrect. *In fact, the nucleon–nucleon force is attractive in both cases. For s = 1 it is sufficiently attractive to produce a bound state while for s = 0, it is not quite attractive enough.*

We can understand how this comes about by considering the 3-dimensional spherical well potential shown in Fig. 6.1:

$$\begin{aligned} V(r) &= -V_0 \quad r < R \\ V(r) &= 0 \qquad r > R \end{aligned} \tag{6.5}$$

while it is hardly a realistic representation of the nucleon–nucleon potential, its finite range, R, and its depth V_0 can be chosen to correspond more or less to the range and depth of the real potential. In fact, since for the moment we only want to reproduce the deuteron binding energy and radius, we have just enough parameters to do the job.

Let us model the nuclear force as a three dimensional spherical well with radius R. The bound states are found by solving the Schrödinger eigenvalue equation Eq.5.23 for the spherically symmetric s state:

$$-\frac{\hbar^2}{2m}\left(\frac{d^2R(r)}{dr^2}+\frac{2}{r}\frac{dR(r)}{dr}\right)+V(r)R(r)=ER(r) \tag{6.6}$$

Here, $V(r)$ is the potential and m is the reduced mass of proton and neutron:

$$m = \frac{m_p m_n}{m_p + m_n}, \qquad or \qquad m \approx \frac{1}{2} m_p \approx \frac{1}{2} m_n \tag{6.7}$$

This arises from working in the relative coordinate only.

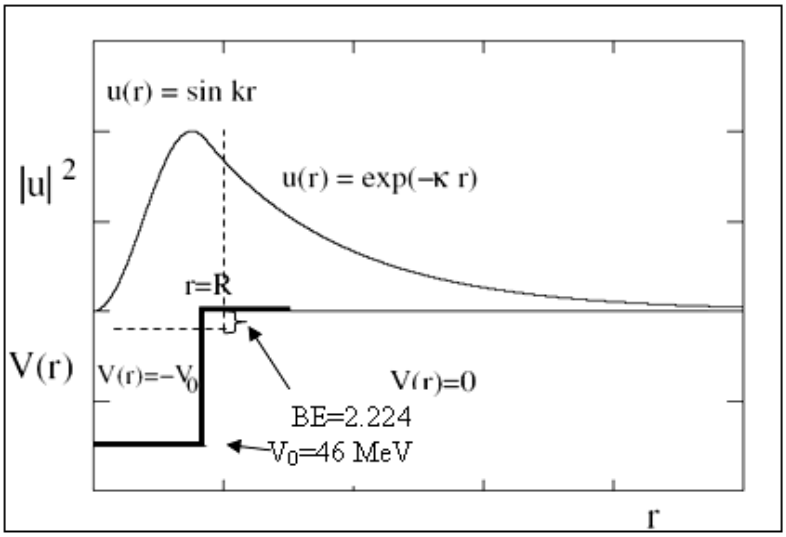

Figure 6.1. A spherical well potential and the wave-function $\Psi(r)$ or $R(r) = u(r)/r$. The depth and width of the well are chosen to reproduce the binding energy and radius of the deuteron.

It is easier to work with $u(r) = rR(r)$, which satisfies the condition:

$$-\frac{\hbar^2}{2m}\frac{d^2u(r)}{dr^2} + V(r)u(r) = Eu(r) \tag{6.8}$$

As well as $u(0) = 0$. The equation in the interior well

$$-\frac{\hbar^2}{2m}\frac{d^2u(r)}{dr^2} - V_0 u(r) = Eu(r) \qquad u(0) = 0 \qquad 6.9$$

has the solutions for $E < 0$ oscillate for $r < R$.

$$u(r) = A\sin kr, \qquad k(E) = \sqrt{\frac{2m}{\hbar^2}(V_0 + E)} \qquad r < R \qquad 6.10$$

and outside the well, we find the standard damped exponential:

$$u(r) = B\exp(-\kappa r), \qquad \kappa(E) = \sqrt{\frac{2m}{\hbar^2}(-E)} \qquad r > R \qquad 6.11$$

Requiring continuity at $r = R$ of $u(r)$ and $u'(r)$, we find the condition that determines the allowed values of E and radius R of the deuteron:

$$-\cot kR = \frac{\kappa}{k} = \sqrt{\frac{-E}{V_0 + E}} \qquad 6.12a$$

or

$$k\cot kR = -\kappa \qquad 6.12b$$

We note that for $r \rightarrow 0$, the function on the left of Eq. 6.12b, $k\cot kr$, is positive and remains so until $kr = \pi/2$; see Fig. 5.7. Since the quantity on the right is negative, the requirement for at least one bound state is that there exists an energy $E << 0$ such that:

$$kR > \frac{\pi}{2} \qquad 6.13$$

i.e., we can fit at least 1/4 of a wave inside the well. Since it is known from experiment of neutron–proton scattering that the deuteron has only one bound state at energy -2.224573 ± 0.000002 MeV, then *k(E) < k(E=0)* and *kR>π/*2 Substituting *k(E=0)* in Eq.6.13, we see that:

$$\sqrt{\frac{2mV_0R^2}{\hbar^2}} > \frac{\pi}{2} \quad i.e \quad V_0R^2 > \frac{\pi^2\hbar^2c^2}{8mc^2} = 109 \ \ MeVfm^2 \qquad 6.14$$

The existence of a single s = 1 state and the non-existence of s = 0 states can be understood by supposing that the effective values of V_0R^2 are respectively slightly greater than or slightly less than 109MeV fm^2 respectively. The deuteron binding energy is correctly predicted if:

$$V_0R^2\ (s = 1) = 139.6\ \text{MeVfm}^2 \qquad 6.15$$

This can be verified by substituting it into Eq.6.12a along with the energy E = BE_d =−2.224573 MeV.

Data from neutron-proton scattering shows that there is no bound state for s = 0 since V_0R^2 (s = 0) ≈ 93.5 *MeV fm*^{2} is slightly less than *109 MeV fm*^{2}. Including scattering data, we can determine both V_0 and R:

$$V_0(\text{s} = 1) = 46.7\text{MeV} \qquad R = 1.73\ \text{fm} \qquad 6.16$$

The wavefunction is shown in Fig. 6.1. The fact that BE_d is small causes the wavefunction to extend far beyond the

effective range R of the potential and explains the anomalously large value of the deuteron radius (2.73 fm).

The scattering data allow one to estimate the values of V_0 and R for $s = 0$. One finds for the proton–neutron system:

$$V_0(\mathrm{s} = 0) = 12.5 \text{ MeV} \quad R = 2.79 \text{ fm} \qquad 6.17$$

This potential is quite different from the $s = 1$ potential.

In summary, the strong interactions have a strength and range that places them precisely at the boundary between the interactions that have no bound states (e.g., the weak interactions) and those that have many bound states (e.g., the electromagnetic interactions).

6.2.2. Yukawa potential and its generalizations

It is necessary to consider more realistic potentials than the simple potential Eq.6.5 to completely describe the results of nucleon–nucleon scattering and to understand the saturation phenomenon on nuclear binding.

The theoretical explanation of the saturation of nuclear forces is subtle. The physical ingredients are the short range attractive potential ($r \approx 1$ fm), a hard core repulsive force at smaller distances ($r < 0.5$ fm), and the Pauli principle. Being the result of these three distinct features, there is no simple explanation for saturation. It is simple to verify that the Pauli principle alone cannot suffice and that any power law force does not lead to saturation.

Many properties of nuclear forces can be explained quantitatively by the potential proposed by Yukawa in 1939:

$$V(r) = g\frac{\hbar c}{r}\exp(\frac{-r}{r_0}) \qquad 6.18$$

The factor $\hbar c$ is present, so that the coupling *constant g* is dimensionless. As shown in Chapter-One, forces between particles are due to the quantum exchange of *virtual particles*. The range r_0 of a force is the Compton wavelength $\hbar/mc$ of the exchanged particle of mass *m*. Yukawa noticed that the range of nuclear forces $r_0 \approx 1.4$ fm, corresponds to the exchange of a particle of mass about 140 MeV. *This is how he predicted the existence of the π meson. The discovery of that particle in cosmic rays was a decisive step forward in the understanding of nuclear forces.*

When applied to a two-nucleon system, the potential Eq.5.18 is reduced by a factor of $(m_\pi/2m_p)^2 \approx 10^{-2}$ because of spin-parity considerations. A dimensionless coupling constant of $g \approx 14.5$ explains the contribution of the π meson to the nucleon–nucleon force. It is necessary to add other exchanged particles to generate a realistic potential. In fact, the general form of nucleon–nucleon strong interactions can be written as a linear superposition of Yukawa potentials:

$$V(r) = \sum_i g_i \frac{\hbar c}{r}\exp(-\mu_i r) \qquad 6.19$$

where the sum is over a discrete or continuous set of exchanged particles with masses given by $\mu_i = m_i c/\hbar$.

6.3. Nuclear force is Tensor dependent

However, we need some more elements to explain saturation and prevent a nuclear "pile-up" where all nucleons collapse to an object of the size of the order of the range of the strong interactions.

First, one must add a strong *repulsive* shorter range potential, called a "*hard core*" interaction. This potential is of the form Eq.6.18 with a negative coupling constant g and a range $r_0 \approx 0.3$ fm. The physical origin of the repulsive core is not entirely understood but it certainly includes the effect of the Pauli principle that discourages placing the constituent quarks of nucleons near each other.

Second, spin effects and relativistic effects must be taken into account.

One writes the potential as the sum of central potentials with spin-dependent coefficients:

$$V(r) = V_C(r) + \Omega_T V_T(r) + \Omega_{SO} V_{SO}(r) + \Omega_{SO2} V_{SO2}(r) \qquad 6.20$$

where V_C is a pure central potential and the other terms are spin dependent. The most important is the *tensor potential* V_T "spin-position interactions" with:

$$\Omega_T = [3(\boldsymbol{s_1} \cdot \boldsymbol{r}/r)\,(\boldsymbol{s_2} \cdot \boldsymbol{r}/r) - \boldsymbol{s_1} \cdot \boldsymbol{s_2}] \qquad 6.21$$

here $\boldsymbol{s_1}$ and $\boldsymbol{s_2}$ are the Pauli spin matrices for the two nucleon spins. This term has the important effect of inducing a correlation between the position and spin of the two nucleons. Fig. 6.2 shows for the $s = 1$ state, the tenser potaintial makes the configuration on the right ($\boldsymbol{s} \cdot \boldsymbol{r} = 0$) have a different potential energy than the two configurations on the left ($\boldsymbol{s} \cdot \boldsymbol{r} \neq 0$). This results in the permanent

quadrupole moment of the deuteron. It is also the dominant force in binding the deuteron. However, it averages to zero for multi-nucleon systems where it plays a minor role.

The last two terms in Eq.6.20 are the *spin-orbit interactions*:

$$\hbar\Omega_{SO} = (\boldsymbol{s_1} + \boldsymbol{s_2}) \cdot \boldsymbol{L} \qquad 6.22$$

$$\hbar 2\Omega_{SO2} = (\boldsymbol{s_1} \cdot \boldsymbol{L})\,(\boldsymbol{s_2} \cdot \boldsymbol{L}) + (\boldsymbol{s_2} \cdot \boldsymbol{L})\,(\boldsymbol{s_1} \cdot \boldsymbol{L}) \qquad 6.23$$

where $\boldsymbol{L}$ is the orbital angular momentum operator for the nucleon pair. Fig. 6.3 shows the most important contributions to the nucleon–nucleon potential in the $s = 0$ state (left) and the $s = 1$ state (right) (the so-called Paris potential). The two central potentials V_C depend only on the relative separations. The tensor potential V_T of the form Eq.6.21 is responsible for the deuteron binding and for its quadrupole moment while the spin-orbit potential is V_{SO}.

For spin-anti-aligned nucleons ($s = 0$), only the central potential contributes.

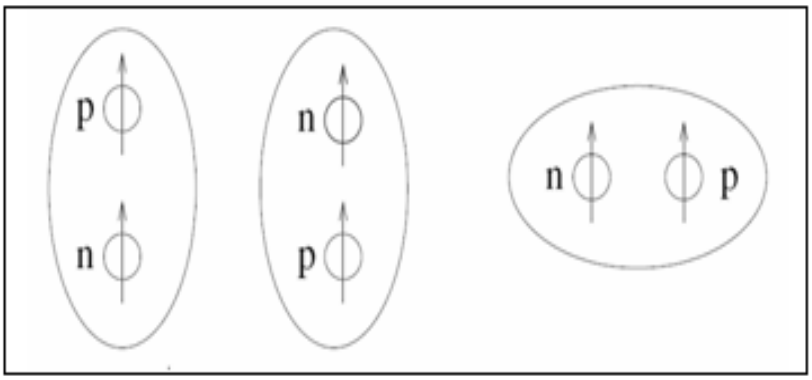

Figure 6.2. The permanent quadrupole moment of the deuteron due to the tensor potential for the $s = 1$ state.

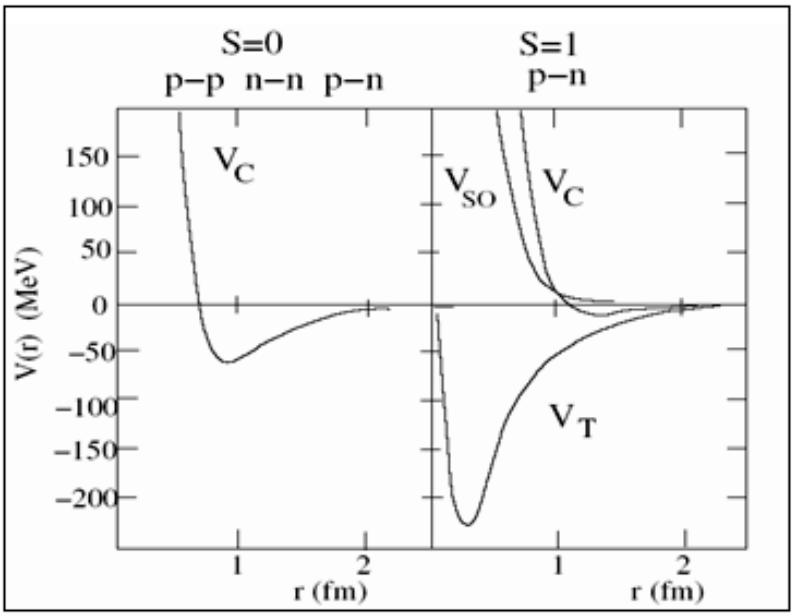

Figure 6.3. The most important contributions to the nucleon–nucleon potentials in the $s = 0$ state (left) and the $s = 1$ state (right).

6.4. Isospin Space and Charge Independence

Finally, we note that to correctly take into account the charge independence of nuclear forces the formalism of isospin must be used. Charge independence is more subtle than just saying that protons and neutrons can be replaced by one another in nuclear forces. It is formalized by using the concept of "isotopic spin" or, simply, *isospin T*, which was introduced by Heisenberg in 1932.

6.4.1. One-nucleon states

The interactions of a nucleon with its other surrounding nucleons in most cases do not depend on whether the

nucleon has spin components m_s = +1/2 or -1/2 relative to an arbitrary chosen z-axis. That is, there is no need to distinguish in the formalism of nuclear physics between a *spin-up* nucleon and a *spin-down* nucleon. *The multiplicity of spin orientations (two-state system for a single nucleon) may enter into the equations, but the actual value of the projection does not appear*, except when a magnetic field is applied. The formalism for nuclear interactions may depend on the multiplicity of nucleon state (two) but it is independent of whether the nucleons are protons or neutrons.

The projections of the spin vector of the nucleon (*isospin* ***T***) are measured with respect to an arbitrary axis T_3, called the "3-axis" in a coordinate system whose axes are labeled 1, 2, 3, in order to distinguish it from the laboratory z-axis of the x, y, z, coordinate system. We therefore introduced an abstract three-dimensional Euclidean-like space called "isospin space." The proton and the neutron can be considered as two different states $T_3 = \pm 1/2$ of a *single* physical object of *isospin* $T = 1/2$, the nucleon. The spin formalism in isospin space is the same as that for normal spin in the Euclidean space. The isospin obeys the usual rules for angular momentum vectors, thus, we use an isospin vector **T** of length:

$$< T >= \sqrt{T(T+1)}\hbar \qquad 6.24$$

with 3-axis projections $T_3 = \hbar m_t$.

6.4.2. Two-nucleon system

The isospin states of a two-nucleon system are constructed in the same manner as the states of two spin-1/2 particles. The total isospin T of the system corresponds to symmetric isospin *triplet* state $T = 1$ or antisymmetric isospin *singlet* state $T = 0$.

The generalized Pauli principle states that two identical fermions must be in an antisymmetric state. If the proton and the neutron were truly identical particles up to the projection of their isospin along the axis T_3, a state of several nucleons should be completely antisymmetric under the exchange of all variables, including isospin variables. If we forget about electromagnetic interactions and assume exact invariance under rotations in isospin space, the Pauli principle is generalized by stating that *an A-nucleon system is completely antisymmetric under the exchange of space, spin and isospin variables*. This assumption does not rest on as firm foundation as the normal Pauli principle and is only an approximation. However, we can expect that it is a good approximation up to electromagnetic effects.

The generalized Pauli principle restricts the number of allowed quantum states for a system of nucleons. A series of simple but important consequences follow from these considerations.

1- The Hamiltonian of two (or more) nucleons is invariant under rotations in isospin space so we can expect that the energies of all states in a given multiplet are equal (neglecting electromagnetic effects). In the two-nucleon system, rather than three independent Hamiltonians (i.e., one for p−p, one for p−n and one for n−n), there are only two, one Hamiltonian for the three $T = 1$ states and an independent Hamiltonian for the $T = 0$ state.

2- The antisymmetric isospin $T = 0$ state is the state of the deuteron, the only nucleon–nucleon bound state. Indeed *the deuteron has a symmetric spatial wavefunction*; *it is mainly an s-wave*, from Eqs-5.80 and 5.92:

$$\psi(r,\theta,\varphi) = \frac{u_\ell(r)}{r}\left[\frac{2\ell+1(\ell-|m_\ell|)!}{4\pi(\ell+|m_\ell|)!}\right]^{1/2} P_{\ell m_\ell}(\cos\theta)e^{im_\ell\varphi} \quad 6.25$$

which is even (odd) if ℓ is even (odd). Thus, Ψ to be anti-symmetric, one can have two possibilities:

ℓ even, S = 0 (space symmetric, spin anti-symmetric)
ℓ odd, S = 1 (space anti-symmetric, spin symmetric)

These are called T = 1 states, available to the n-p, n-n, p-p systems.
By contrast, states which are symmetric (T = 0) are:

ℓ even, S = 1
ℓ odd, S = 0

These are available only to the n-p system for which there is no Pauli Exclusion Principle.

The ground state of the deuteron is, therefore, a *T = 0 state, i.e. ℓ = 0, s = 1, and a total angular momentum J = 1*.

3- The lowest T = 1 state is ℓ = 0, s = 0, as mentioned above, is known to be unbound. The interaction is only slightly weaker than in the $T = 0$ state, there exists what is called technically a "virtual state," nearly bound.

4- We see with this example that charge independence is more subtle than a simple invariance with respect to interchange of neutrons and protons. Otherwise, we would be sure to observe a neutron–neutron bound state (possibly unstable under β decay) in addition to the deuteron. We should, therefore, expect that the lowest T = 1 state in n-n and p-p to be also unbound, i.e., there is no stable di-neutron or di-proton.

Isospin states of a system of A nucleons are constructed in the same way as total spin states of A spin-1/2 particles. If a nucleus has isospin T, we expect to observe $2T+1$ isobar which has similar physical properties. This is the case for the isobars ^{11}B and ^{11}C which form an isospin 1/2 doublet.

For a nucleus (Z, N), the isospin follows coupling rules identical with the rules of ordinary angular momentum vectors. The 3-axis component of the total isospin vector T is the sum of the 3-axis components of the individual nucleons and thus for any nucleus T_3 expressed in units of ħ:

$$T = \frac{1}{2}|N - Z| \qquad 6.26$$

Inserting the value of T into the above equation, we expect to observe at least $2T+1 = |N-Z|+1$ isobars of different charges, but with similar nuclear properties.

In actual physics, the operator T plays a special rule, since the electric charge of a system of A nucleons is related to the total isospin T by:

$$Q = T + A/2 \qquad 6.27$$

Problems

6-1. A neutron and a proton can undergo radioactive capture at rest: $p + n \rightarrow d + \gamma$. Find the energy of the photon emitted in this capture. Is the recoil of the deuteron important?

6-2. Calculate the minimum photon energy necessary to dissociate the deuteron, i.e., $\gamma + d \rightarrow p + n$. Take the deuteron binding energy to be 2.224589 MeV and use a nonrelativistic approach.

6-3. A deuteron of mass M and binding energy B ($B << Mc^2$) is disintegrated into a neutron and a proton by a gamma ray of energy E_γ. Find, to lowest order in B/Mc^2, the minimum value of $(E_\gamma - B)$ for which the reaction can occur.

6-4. The deuteron is a bound state of a proton and a neutron of total angular momentum J = 1. It is known to be principally an S($\ell = 0$) state with a small admixture of a D($\ell = 2$) state.

a- Explain why a P state cannot contribute.

b- Explain why a G state cannot contribute.

6-5. The deuteron ^2H has $J = 1^-$ and a magnetic moment ($\mu = 0.857\mu_N$) which is approximately the sum of proton and neutron magnetic moments.

a- From these facts, what can one infer concerning the orbital motion and spin alignment of the neutron and proton in the deuteron?

b- How might one interpret the lack of exact equality of μ and $\mu_n+\mu_p$?

c- How can the neutron have a nonzero magnetic moment?

6-6. What fraction of the time do the neutron and proton in the deuteron spend beyond the range of their nuclear force?

6-7. Prove that the di-neutron cannot exist.

6-8. According to a simple-minded picture, the neutron and proton in a deuteron interact through a square well potential of width $a = 1.9\times10^{-15}$ m and depth $V_0 = 40$ MeV in an $\ell = 0$ state. Start with Eq.6.8.

a- Calculate the probability that the proton moves within the range of the neutron. Use the approximation that $m_n = m_p = m$, $ka = \pi/2$, where $k = \sqrt{\frac{m(V_o-\varepsilon)}{\hbar^2}}$ and ε is the binding energy of the deuteron.

b- Find the mean-square radius of the deuteron.

6-9. From Eq.6.12, plot V_o against R for R in the range of 1.0 to 3.0 fm. Discuss the sensitivity of V_o to R.

6-10. Show that Eq.6.12 can be written in the transcendental form $x = -\tan bx$,

Where $x = \sqrt{-(V_o + E)/E}$.

a- Evaluate the parameter b for R=2fm, by using the reduced mass.

b- Solve the transcendental equation in two ways: graphically and iteratively using programmable calculator or suitable computer software.

6-11. The only bound two-nucleon configuration that occurs in nature is the deuteron with total angular momentum J = 1 and binding energy ~2.22 MeV.

a- From the above information alone, show that the n − p force must be spin dependent.
b- Write down the possible angular momentum states for the deuteron in an LS coupling scheme. What general liner combinations of these states are possible? Explain.
c- Which of the states in (b) are ruled out by the existence of the quadrupole moment of the deuteron? Explain. Which states, in addition, are ruled out if the deuteron has pure isospin T = 0?

6-12. Consider a nonrelativistic two-nucleon system. Assume the interaction is charge independent and conserves parity.

a- By using the above assumptions and the Pauli principle, show that S^2, the square of the two-nucleon spin, is a good quantum number.
b- What is the isotopic spin of the deuteron? Justify your answer.

6-13. Both nuclei ${}^{14}_{7}N$ *and* ${}^{12}_{6}C$ have isospin T = 0 for the ground state. The lowest T = 1 state has an excitation energy of 2.3 MeV in the case of ${}^{14}_{7}N$ and about 15.0 MeV in the case of ${}^{12}_{6}C$. Why is there such a marked difference? Indicate also the basis on which a value of T is ascribed to such nuclear states. (Consider other members of the T = 1 triplets and explain their relationship in terms of systematic nuclear properties, such as the excited states with T = 1 of ${}^{12}_{6}C$ form an

isospin triplet which consists of ${}^{12}_{5}B, {}^{12}_{6}C\ and {}^{12}_{7}N$. ${}^{12}_{5}B\ and\ {}^{12}_{7}N$ have $|T_3| = 1$, so they are the ground states of the triplet. Likewise, ${}^{14}_{6}C\ and\ {}^{14}_{8}O$ are the ground states of the isospin triplet of the T = 1 excited states of ${}^{14}_{7}N$.)

CHAPTER 7

NUCLEAR MODELS

Different model approaches try to accentuate various aspects of nuclear structure in a simple and schematic way. No single model, as yet, is detailed enough to encompass all aspects of the nucleus.

7.1. Introduction

In order to understand the processes of atomic electrons, we began the development by considering the Coulomb force between pairs of charged particles and proceeded to consideration of the energy levels which are associated with electrons in an atom. Great progress in this study has been possible because the mathematical form of coulomb's law is simple and well known and because the spectroscopy of atoms is rich with energy levels.

The situation in nuclear physics is quite different. The mathematical form of the nuclear force is not yet known and we know that a simple form (such as a potential function dependent only on the separation of two nucleons) is not a possible solution to the problem.

On the basis of the available experiments and information, it is understandable that we cannot discuss the nuclear force in detail. Yet, there are some qualitative observations that can be made. The nuclear force has short range, probably no greater than nuclear dimensions, of the order of 10^{-13} or 10^{-14} cm. This specifically nuclear force must be strongly attractive in order to overcome the electrostatic repulsion between protons, but it may also be

repulsive to some extent to prevent the collapse of the nucleus. Another attribute the nuclear force possesses is charge independence: that the nuclear force between two protons is the same as that between two neutrons.

In the absence of detailed information about the nuclear force, theoretical descriptions of nuclei have been centered on models for nuclear structure which are admittedly inadequate but which represent to some extent the observed phenomena.

Among the models currently in use in nuclear physics are the Fermi-gas model, the liquid-droop model, the shell model, the collective model, the cluster model, the optical model, the direct reaction model, and recently the standard model. In this chapter, we will discuss the first four models but highlight on the shell model.

7.2. Fermi-Gas Model

Fermi gas model is sometimes called the statistical model or the uniform Particle model. It was proposed by E. Wigner (1937). It assumes that as a result of the very strong interactions between nucleons, the motions of individual nucleons cannot be considered in detail, but must be treated statistically, i.e., obeying Fermi-Dirac statistics. The mathematical treatment of nuclei in this model resembles the discussion of free electron gas in a solid state physics, where electrons move quasi-freely in a background of positively charged ions.

7.2.1. Fermi momentum and energy

The theoretical concept of a Fermi-gas can be applied to systems of weakly interacting fermions. Then, nucleons are

considered as moving quasi-freely within the nuclear volume, the binding potential is generated by all nucleons, those neutrons and protons are distinguishable fermions and are therefore situated in two separate potential wells.

As a very simple approximation, these nuclear potential wells are considered as rectangular. Each state is filled with two nucleons of the same type with different spin orientations, obeying Pauli Exclusion Principle. The two potentials, though, have slightly different shapes, mainly because of the Coulomb part: The well for protons is less deep because of the Coulomb potential by the amount E_c and externally; the l/r dependence of the Coulomb potential extends the range and the last bound nucleons have equal energy; and the zero coincides, as shown in Fig. 7.1.

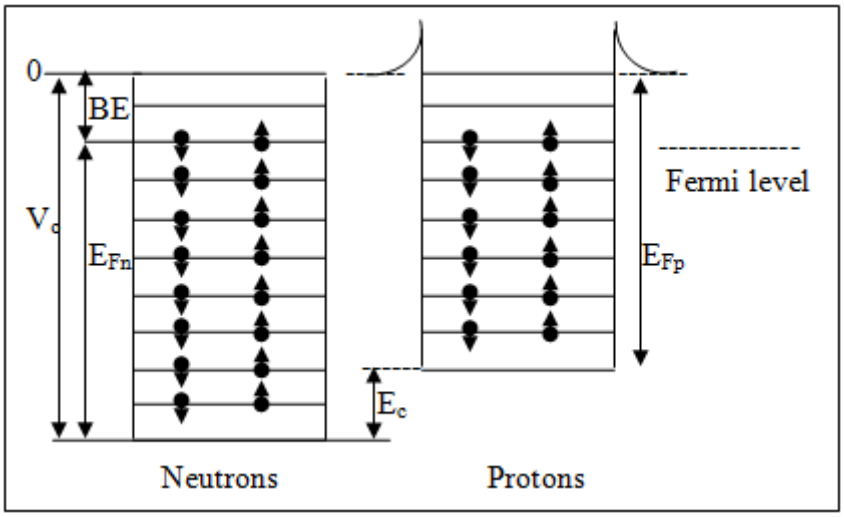

Figure 7.1. Sketch of the nuclear square well potentials and states. The double-degeneracy associated with nucleon intrinsic spin is presented.

Neglecting spin, the state's degeneracy n, i.e., the number of states of protons and neutrons within the spherical nuclear volume V is given by:

$$dn = \frac{4\pi p^2 dp}{(2\pi\hbar)^3} V \qquad 7.1$$

For the low excitation energy (the nucleus in its ground state), called the temperature T=0 limit, the lowest states will be filled pair wise up to a maximum momentum, called the Fermi momentum p_F or Fermi level. The numbers of these states follow from integrating Eq. 7.1:

$$n = \int_0^{p_F} \frac{4\pi p^2 dp}{(2\pi\hbar)^3} V = \frac{V p_F^3}{6\pi^2\hbar^3} \qquad 7.2$$

Since each state can be filled with two nucleons of the same type, then the number of neutrons and protons are:

$$N = \frac{V p_{F,n}^3}{6\pi^2\hbar^3}, \qquad Z = \frac{V p_{F,p}^3}{6\pi^2\hbar^3} \qquad 7.3$$

where $p_{F,n}$ and $p_{F,p}$ are the Fermi momenta of neutrons and protons, respectively. Using our prior knowledge of the nuclear volume $V = \frac{4}{3}\pi R^3 = \frac{4}{3}\pi R_o^3 A, \quad R_o = 1.21\,fm$, we obtain for Z = N = A/2 and equal radius for the two separate potential wells of the protons and the neutrons a Fermi momentum:

$$p_F \cong p_{F,n} \cong p_{F,p} \cong \frac{\hbar}{R_o}\left(\frac{9\pi}{8}\right)^{1/3} \cong \frac{297}{R_o} \approx 250 MeV/c \qquad 7.4$$

The corresponding Fermi kinetic energy which is the energy of the highest occupied nucleon level becomes:

$$E_F \cong \frac{p_{F,N}^2}{2m} \cong \frac{p_{F,p}^2}{2m} \approx 33MeV \qquad 7.5$$

where m denotes the nucleon mass ($m_n \approx m_p$).

The difference BE between the edge of the potential well and the Fermi level is rather constant for different nuclei and equals the average binding energy per nucleon, BE/A ≈ 7 – 8 MeV. Hence, the depth of the potential well, V_o, is approximately independent of A and given by:

$$V_o = E_F + BE \approx 40 \text{ MeV} \qquad 7.6$$

Eq. 7.6 shows that the kinetic and potential energies of the nucleons are of the same order. In this sense, nucleons are rather weakly bound in the nucleus (similar to the case of electrons in a metal).

7.2.2. Nuclear symmetry energy

The neutron potential well is deeper than the proton one, since the former has no Coulomb interaction. On the other hand, for a stable nucleus, the Fermi levels of the protons and the neutrons have to be the same, otherwise it would decay to an energetically more favorable state through a β transition. As a result, there are more neutron states than proton states occupied, which explains the fact that N > Z for heavier stable nuclei.

The binding energy as a function N – Z can be estimated using the Fermi-gas model: the mean kinetic energy per nucleon is.

$$\left\langle E_{kin} \right\rangle = \frac{\int_0^{p_F} E_{kin} p^2 dp}{\int_0^{p_F} p^2 dp} = \frac{3}{5}\frac{p_F^2}{2m} \approx 20MeV \qquad 7.7$$

The total kinetic energy of the nucleus is:

$$E_{kin}(N,Z) = N\left\langle E_{kin,n} \right\rangle + Z\left\langle E_{kin,Z} \right\rangle = \frac{3}{10m}(Np_{F,n}^2 + Zp_{F,p}^2) \quad 7.8$$

Hence, using Eq. 7.3 and 7.4, we get:

$$E_{kin}(N,Z) = \frac{3}{10m}\frac{\hbar^2}{R_o^2}\left(\frac{9\pi}{4}\right)^{2/3}\frac{N^{5/3} + Z^{5/3}}{A^{2/3}} \qquad 7.9$$

Again the radii of the proton and the neutron potential well have been taken as equal.

This result can now be expanded around the symmetric case with N = Z = A/2. This expansion will lead to an expression for the symmetry energy and we shall be able to derive a value for the constant a_{sy}. Taking Z – N = Є, and Z + N = A, we can substitute in Eq. 7.9, Z = A/2(1 +Є/A); N = A/2(1 – Є/A), with Є/A << 1 and inserting the binomial expansion $(1+x)^n = 1 + nx + \frac{n(n-1)}{2}x^2 + ...$ we obtain:

$$E_{kin}(N,Z) = \frac{3}{10m}\frac{\hbar^2}{R_o^2}\left(\frac{9\pi}{4}\right)^{2/3}\left(A + \frac{5}{9}\frac{(N-Z)^2}{A} + ...\right) \qquad 7.10$$

From the above equation it is clear that for fixed A, the kinetic energy has a minimum for N = Z.

The first term corresponds to the volume energy; the second term has exactly the form of the symmetry energy in the Beth-Weizsäcker mass formula**.** Inserting the values of the various constants m, ħ, R_o, π, we obtain the result:

$$\begin{aligned} \langle E(A,Z)\rangle &= \langle E(A,Z=A/2)\rangle + \Delta E_{sym} \\ &= a_V A + a_{sy}\frac{(N-Z)^2}{A} \end{aligned} \qquad 7.11$$

where $a_V \approx 19MeV$, $a_{sy} \approx 11MeV$

The numerical value is, however, about half the value of a_{sy} as determined in the next section. Without discussing this point here in detail, the difference arises from the fact that the nuclear well depth V_o is itself also dependent on the neutron excess N - Z and makes up for the missing contribution to the symmetry energy.

Higher-order terms with a dependence $(N-Z)^4/A^4$… naturally derive from the more general (E(A,Z)) value.

7.3. Liquid Drop Model

The liquid drop model was first proposed by G. Gamow and then developed by N. Bohr (1937). This model also ignores the motion of individual nucleons. The observation is made that nuclear matter is essentially incompressible, which arises from the fact that the interior mass densities are approximately equal, since the radii of nuclei are proportional to $A^{1/3}$, by analogy with a classical model for a liquid drop, where liquid drops of various sizes have the same interior density, the nucleus is assumed to have a

definite surface tension, with nucleons behaving in a manner similar to that of molecules in liquid. The decay of nuclei by the emission of particles is analogous to the evaporation of molecules from the surface of liquid. Nuclear fission is analogous to the division of a large drop of liquid into two smaller ones.

In order to achieve a quantitative and more basic understanding of the binding energy of the nuclei, we use the liquid drop model to derive the *Semi-Empirical Mass Formula* SEMF, in which the binding energy or the mass of the nucleus is expressed as the sum of a number of terms, such as volume term, surface term, coulomb term, symmetry term, and pairing term. Actually, the last two terms are shell model corrections.

7.3.1. Volume term

For a liquid drop, the latent heat of evaporation is proportional to the drop mass and as it is defined as the average energy required to disperse the liquid drop into a gas, so is analogues to the binding energy per nucleon B_v/A:

$$\text{Latent heat} = B_v/A = Q_0 M_m = a_v \qquad 7.12$$

where Q_0 is the heat of evaporation
M_m is the mass of each molecule
A is the number of molecules
a_v is a constant of a volume term

Then for a nucleus of mass number A:

$$B_v = a_v A \qquad 7.13$$

where $a_v = 15.6$ MeV

7.3.2. Surface term

The surface effect takes into account, in a simple way, the fact that nucleons at, or close to, the nuclear surface will have a reduced binding energy since only partial surrounding with nucleons is possible, for a nucleus with a finite radius. Let f_1 be a fraction of the number of molecules (nucleons) surrounding molecules (nucleus) inside the drop and f_2 be the fraction of molecules that are on the surface, then:

$$B = Q_0 M_m A(1 - f_2) + Q_0 M_m A f_1 f_2$$

$$= a_v A(1 - f_2) - a_v A f_1 f_2 \qquad 7.14$$

where $a_v A(1 - f_2)$ is the B.E of interior molecules

$a_v A f_1 f_2$ is the B.E of the molecules on the surface

Rearrange the last equation to get:

$$B = B_v + B_s = a_v A - a_v A f_2 (1 - f_1) \qquad 7.15$$

where $B_s = -a_v A f_2(1 - f_1)$ is the surface term

Now taking $f_1 \approx 2/3$ and $f_2 = V_s / V_t = 3/A^{1/3}$, where $V_s = 4\pi R^2(1.07) = 4\pi(1.07)^3 A^{2/3}$ is the shell volume of thickness 1.07 *fm*, then:

$$-B_s = a_s A^{2/3} \qquad 7.16$$

where a_s =16.8 MeV

Fig. 7.2 is a Pictorial representation of nuclear surface effects on binding energy. Nucleons at or near to the nuclear surface are less strongly bound than a nucleon within the nuclear interior.

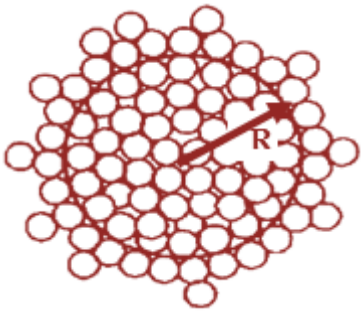

Figure 7.2. A Pictorial representation of a liquid drop.

7.3.3. Coulomb term

Coulomb effects result since a charge of **Ze** is present within the nuclear volume, which make it a negative term.

For a homogeneously charged liquid drop with sharp radius **R** and density ρ_c:

$$\rho_c = \frac{Ze}{\frac{4}{3}\pi R^3} \qquad 7.17$$

One can evaluate the Coulomb contribution to the nuclear binding energy by a classical argument. Fig. 7.3 **(a)** shows the Coulomb energy evaluated by calculating the energy needed to constitute the full nuclear charge in terms of spherical shells d**r** filled in one after the other. While Fig. 7.3**(b)** shows the electrostatic potential energy, calculation is reduced to the Coulomb energy between a

central charge, $\frac{4}{3}\pi r^3 \rho_c$ and the charge in an infinitesimal shell $4\pi r^2 dr \rho_c$.

Therefor, the Coulomb energy needed (work required) to add a spherical shell to the outside of the sphere with radius *r* to give an increment *dr* becomes:

$$U_c' = \frac{1}{4\pi\varepsilon_o}\int_0^R \frac{\frac{4}{3}\pi r^3 \rho_c 4\pi r^2 \rho_c}{r} dr \qquad 7.18$$

Using the above charge density, the integral becomes:

$$U_c^{/} = \frac{3}{5}\frac{Z^2 e^2}{R}\frac{1}{4\pi\varepsilon_0} \qquad 7.19$$

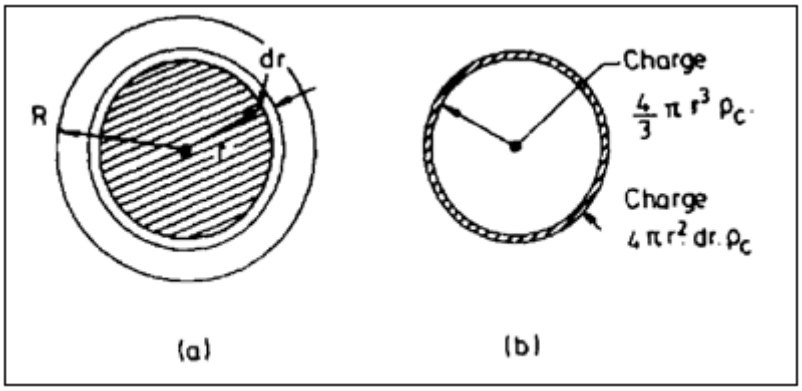

Figure 7.3. Evaluation of the Coulomb energy of a liquid, spherical charged drop.

In the argument used above, we have smoothed out the charge of Z nucleons over the whole nucleus. In this

evaluation, we have counted a self-energy Coulomb interaction which is spurious and we should correct for the effect of *Z* protons. Using the same method as before, but now with the proton smeared charge density:

$$\rho_p = \frac{e}{\frac{4}{3}\pi R^3} \tag{7.20}$$

and self-coulomb energy, for the Z protons, as:

$$U_c^{//} = \frac{3}{5}\frac{Ze^2}{R}\frac{1}{4\pi\varepsilon_0} \tag{7.21}$$

The total coulomb energy correction becomes:

$$U_c = U_c^{/} - U_c^{//} = \frac{3}{5}Z\frac{(Z-1)}{R}\frac{e^2}{4\pi\varepsilon_0} \tag{7.22}$$

and in terms of binding energy B_c, mass number A, and atomic number Z,

$$-B_c = a_c Z(Z-1)A^{-1/3} \tag{7.23}$$

where $a_c = \frac{3}{5}\frac{e^2}{R}\frac{1}{4\pi\varepsilon_0}$ = 0.72 MeV

7.3.4. Symmetry term

It is the increase in energy required by nucleus to have unequal numbers of protons (Z) and neutrons (N). This term is purely quantum mechanical in origin and a shell model correction due to Pauli principle.

In the absence of the Coulomb force, the binding energy of a nucleus of mass number A is minimum when Z = N compared with isobar of different N and Z, i.e., N > Z , then binding energy due to symmetry is negative $-B_{sy}$. This term is important in light stable nuclei for which $Z \approx A/2$. The binding energy of these nuclei will be maxima when nucleons occupy the lowest possible orbital. The Pauli principle (*in a closed system no two identical particles can be in the same energy state*), however, prevents the occupation of a certain orbital by more than two identical nucleons with opposite intrinsic spin orientations. The symmetric distribution $Z = N = A/2$ proves to be the energetically most favored (*if only this term is considered*!).

Any other repartition, $N = (A/2) + \upsilon$, $Z = (A/2) - \upsilon$, will involve lifting particles from occupied into empty orbital. If the average energy separation between adjacent orbital amounts to be Δ, replacing υ nucleons will cost an energy loss of, see Fig. 7.4:

$$\Delta(BE) = \upsilon(\Delta\upsilon/2) \qquad 7.24$$

and with $\upsilon = (N - Z)/2$, this becomes:

$$B_{sy} = (1/8)(N - Z)^2\Delta$$

$$= (A - 2Z)^2 \Delta/8 \qquad 7.25$$

The potential depth V_O, describing the nuclear well does not vary much with changing mean number; for the two extremes ^{16}O and ^{208}Pb, the depth does not change by more than 10% and thus, the average energy spacing between the single particles, Δ, should vary inversely with A, i.e. $\Delta \alpha A^{-1}$.

The final result, expressing the loss of symmetry energy due to the Pauli effect which blocks the occupation of those levels that already contain two identical nucleons, becomes:

$$B_{sy} = a_{sy} (A - 2Z)^2 A^{-1} \qquad 7.26$$

where $a_{sy} = 23.3$ MeV

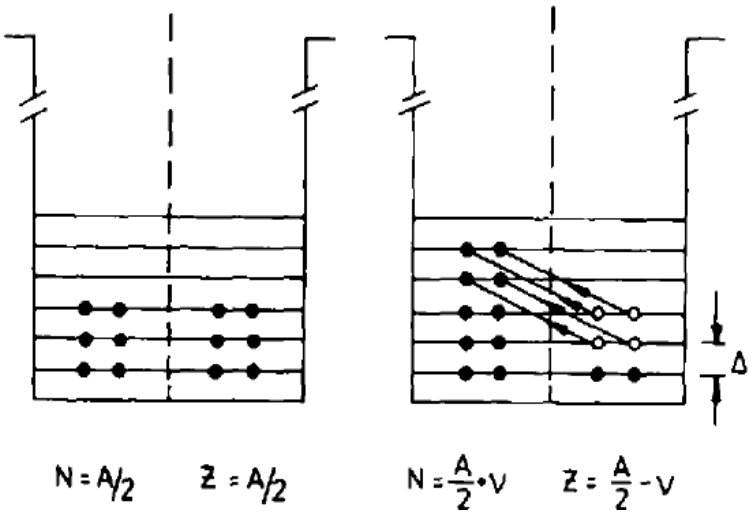

Figure 7.4. Schematic single-particle model description, two different distributions of A nucleons over the proton and neutron orbital with two-fold (spin) degeneracy.

7.3.5. Pairing term

The pairing is the tendency of like nucleons to couple pair wise (proton pair, neutron pair) to a stable configuration in the nucleus under the influence of the short-range nucleon-nucleon attractive force. This effect is best illustrated by studying nucleon separation energies. We can define each of the various separation energies as the energy needed to take a particle out of the nucleus and so this

separation energy becomes equal to the energy with which a particular particle (or cluster) is bound in the nucleus.

For a proton and a neutron, the separation energy becomes:

$$S_p = B_{(A, Z)} - B_{(A-1, Z-1)} \qquad 7.27$$

$$S_n = B_{(A, Z)} - B_{(A-1, Z)} \qquad 7.28$$

The separation energy for α-particle reads:

$$S_\alpha = B_{(A, Z)} - (B_{(A-4, Z-2)} + B_{(4, 2)}) \qquad 7.29$$

In mapping S_p and S_n values, a specific saw-tooth figure results from S_n values. This figure very clearly expresses the fact that it costs more energy (on average ***1.2-1.5*** MeV) to separate a neutron from a nucleus with even neutron number than for the adjacent odd-neutron number nuclei. The above point proves an odd-even effect, showing that even-even nuclei are more bound than odd-even nuclei by an amount which we call **δ**. Proceeding to an odd-odd nucleus, we have to break a pair, relative to the odd-even case and lose an amount **δ** of binding energy. Taking the odd-even nucleus as a reference point, we can then express the extra pairing energy correction B_p as:

$$\begin{aligned} B_p &= +\delta \quad \text{if Z even, N even} \\ B_p &= 0 \quad \text{if Z even, N odd; or Z odd, N even} \\ B_p &= -\delta \quad \text{if Z odd, N odd} \end{aligned} \qquad 7.30$$

The exact form of **δ** used as found by fitting the data is:

$$\delta = a_p A^{-3/4} \qquad \text{where } a_p = 34 \text{ MeV} \qquad 7.31$$

7.3.6. SEMF terms collection

Combining all of the above derived results of the binding energy terms, we obtain a *semi-empirical mass formula* SEMF:

$$B(A, Z) = B_v + B_s + B_c + B_{sy} + B_p$$

$$B(A, Z) = a_v A - a_s A^{2/3} - a_c Z(Z - 1)A^{-1/3}$$

$$- a_{sy}(A - 2Z)^2 A^{-1} + B_p \qquad 7.32$$

Accordingly the binding energy per nucleon B /A is:

$$B/A = a_v - a_s A^{-1/3} - a_c Z(Z - 1)A^{-4/3}$$

$$- a_{sy}(A - 2Z)^2 A^{-2} + B_p A^{-1} \qquad 7.33$$

This is known as the Bethe-Weizsäcker mass equation and the behavior of various terms contribution to the B/A is given in Fig. 7.5. It should be noted from Fig. 7.5 that the surface, asymmetry and Coulomb terms have been plotted so that they subtract from the volume term to give the total SEMF result in the lowest curve.

A simple way to interpret Eq. 7.32 is to regard the first term as a first approximation to the binding energy. That is to say, the binding energy is proportional to the volume of the nucleus or the mass number A. This assumes every nucleon is like every other nucleon. Of course, this is an oversimplification and the remaining terms can be regarded as corrections to this first approximation.

The contribution of the pairing energy (the last term) for the same A may be different for different combinations of Z, N, though it generally decreases with increasing A. The

contribution of the volume energy, which is proportional to A, is a constant. The surface energy makes a negative contribution whose absolute value gives the largest correction for smallest A and decreases with increasing A. The Coulomb energy also makes a negative contribution whose absolute value increases with A as Z and A increase together. The two terms taken together produce a maximum in the ***B /A*** curve, already very close to the region of most strongly bound (per nucleon) nuclei. The symmetry energy makes a negative contribution too, its absolute value increasing with A because Z/A decreases when A increases. Adding together these terms, we see that the mean binding energy increases with A at first, reaching a flat maximum at A ~ 50 and then decreases gradually, as shown in Fig. 7.5.

Using fits of known masses to SEMF, one can determine the five coefficients; a fit by Wabstra-1971 gives the following values in units of MeV/c^2:

$$a_v = 15.6;\ \ a_s = 16.8;\ \ a_c = 0.72;$$

$$a_{sy} = 23.3;\ \ a_p = 34 \qquad 7.34$$

Since the fitting to experimental data is not perfect, one can find several slightly different coefficients in the literature.

The average accuracy of Eq. 7.32 is about 2 Mev except where strong shell effects are present. One can add a term, ~ 1 to 2 Mev, to Eq. 7.32 to represent the shell effects, extra binding for nuclei with closed shells of neutrons or protons.

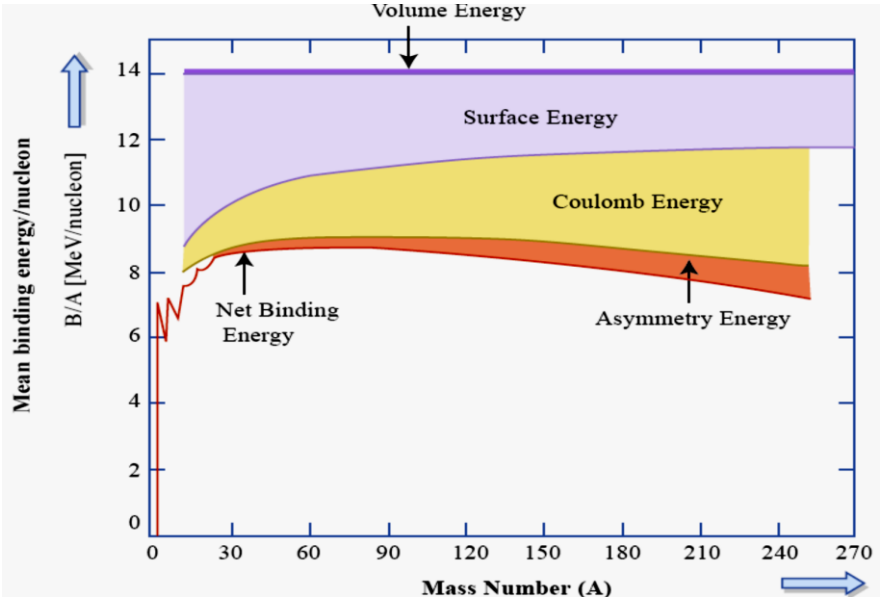

Figure 7.5. Contributions to the B/A as a function of mass number A from various term in the SEMF.

7-3-7. Shell term correction

The Liquid Drop Model (LDM) describes the bulk properties of nuclei with the above five terms. However, although this empirical model can reproduce the average properties of most nuclei, there are significant deviations from this near closed shells, specifically those nuclei corresponding magic numbers: p and/or N = 2, 8, 20, 28, 50, 82, and 126, where the LDM underestimates the binding energy. It is, therefore, necessary to include the shell correction that accounts for the differences of more than 10 MeV of the ground-state masses. Qualitatively, this is because the nucleons are occupying “deeper” orbitals. The shell effects can, therefore, be thought of as arising from fluctuations in the level density around the Fermi surface.

The method for incorporating these effects is called the Strutinsky shell correction (or renormalisation approach).

By expressing the nuclear binding energy B_{tot} as the sum of a liquid drop model part B_{LD} (Eq. 7.32) and a shell correction term $B_{sh} = \eta_{sh}$:

$$B_{tot} = B_{LD} + \eta_{sh} \qquad 7.35$$

η_{sh} in Eq.7.35 consists of proton η_Z and neutron η_N shell terms which represent the mutual support of magic number.

$$\eta_{sh} = \eta_{(Z)} + \eta_{(N)} \qquad 7.36$$

$$with\ \eta_{(Z)} = \left(\frac{2Z}{A}\right)^{2/3} \eta_Z^0,\ and\ \eta_{(Z)} = \left(\frac{2N}{A}\right)^{2/3} \eta_N^0$$

where $\eta_Z^0\ and\ \eta_N^0$ are adjustable parameters.

So η_{sh} derived from the shell model energy with a smooth part subtracted averages to zero over the range of atomic mass number but not the magic numbers. The extra binding energy per nucleon due to shell term for magic numbers of N and Z is about 1 – 2 MeV more binding.

In addition to what we have already mentioned, one can consider another term representing nuclear deformation.

7.4. Shell Model

7.4.1. Introduction

There are similarities between the electronic structure of atoms and nuclear structure. Atomic electrons are arranged in orbits (energy states) subject to the laws of quantum mechanics. The distribution of electrons in these states

follows the Pauli Exclusion Principle. Atomic electrons can be excited up to normally unoccupied states or they can be removed completely from the atom. From such phenomena, one can deduce the structure of atoms. In nuclei, there are two groups of like particles, protons and neutrons. Each group is separately distributed over certain energy states subject to the Pauli Exclusion Principle. Nuclei have excited states and nucleons can be added to or removed from a nucleus.

Electrons and nucleons have intrinsic angular momentum called intrinsic spins. The total angular momentum of a system of interacting particles reflects the details of the forces between particles. For example, from the coupling of electron angular momentum in atoms we infer an interaction between the spin and the orbital motion of an electron in the field of the nucleus (the spin-orbit coupling). In nuclei, there is also a coupling between the orbital motion of a nucleon and its intrinsic spin (but of different origin). In addition, nuclear forces between two nucleons depend strongly on the relative orientation of their spins.

The structure of nuclei is more complex than that of atoms. In an atom the nucleus provides a common center of attraction for all the electrons and inter-electronic forces generally play a small role. The predominant force (Coulomb) is well understood. Nuclei, on the other hand, have no center of attraction; the nucleons are held together by their mutual interactions which are much more complicated than Coulomb interactions.

All atomic electrons are alike, whereas there are two kinds of nucleons. This allows a richer variety of structures. Notice that there are ~ 100 types of atoms, but more than 1000 different nuclides. Neither atomic nor nuclear structures can be understood without quantum mechanics.

7.4.1.1. Experimental basis

It is to be expected that the ideas and concepts that proved so effective in determining the electronic structure of atoms should be carried over into nuclear physics, closed shells structure is one of these ideas because of the stability of the system with the given number of particles, depending on different experimental evidences. *One of these evidences is the isotopes abundance*, the elements of high isotopic abundance, particularly those with Z > 33, for example, ^{88}Sr with N=50 and ^{140}Ce with N=82 have abundance greater than 60%.

Another evidence is *the number of stable isotopes* of a given element; for example, tin $_{50}$Sn of Z=50 and lead $_{82}$Pb of Z=82, have 10 and 4 stable isotopes, respectively, also there are 7 *stable isotones* of nuclides with N=82, these are ^{136}Xe, ^{138}Ba, ^{139}La, ^{140}Ce, ^{141}Pr, ^{142}Nd, and ^{144}Sm.

Fig. 7.6 shows that the abundance of stable isotones (same number of neutrons) is particularly large for nuclei with magic neutron numbers. Specifically, the nuclides with neutron numbers 20, 28, 50 and 82 are more abundant by 5 to 7 times than those with non-magic neutron numbers.

Other evidence for the existence of a *closed shells at N=50, 82 and 126 may be obtained from some fission products called the delayed neutron emitters*, such as ^{87}Kr of N=51 and ^{137}Xe of N=83, in which the last neutron has very small binding energy and can rapidly be emitted to form ^{86}Kr of N=50 and ^{136}Xe of N=82, respectively.

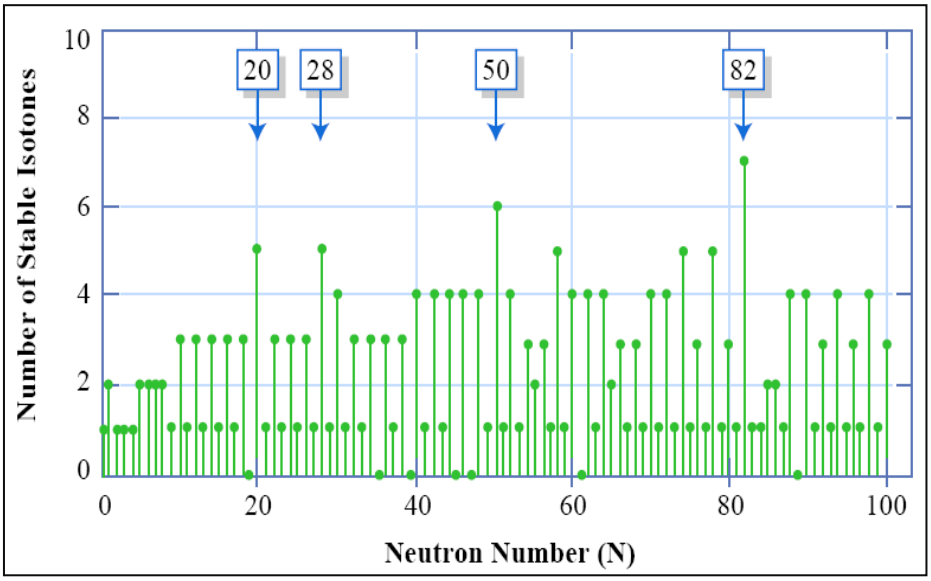

Figure 7.6. Histogram of stable isotones showing number of magic nuclides.

The first excited states of even-even nuclei have higher excitation energy than usual energies at the magic numbers, indicating that the magic nuclei are more tightly bound.

Also nuclei of N=50, 82 and 126 have very small neutrons absorption cross-section, indicating a wider spacing of the energy levels just beyond a closed shell, as shown in Fig. 7.7.

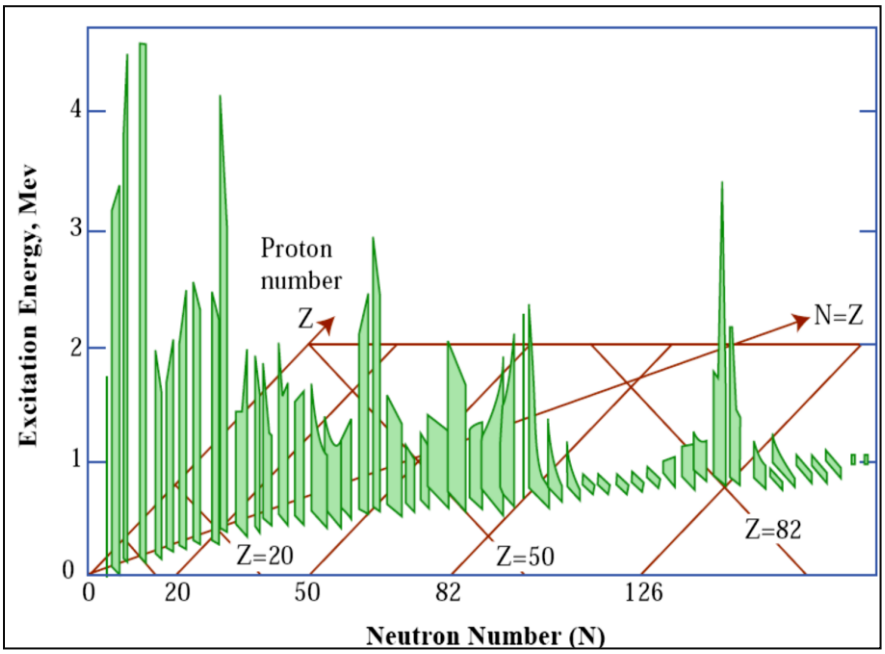

Figure 7.7. First excited state energies of even-even nuclei.

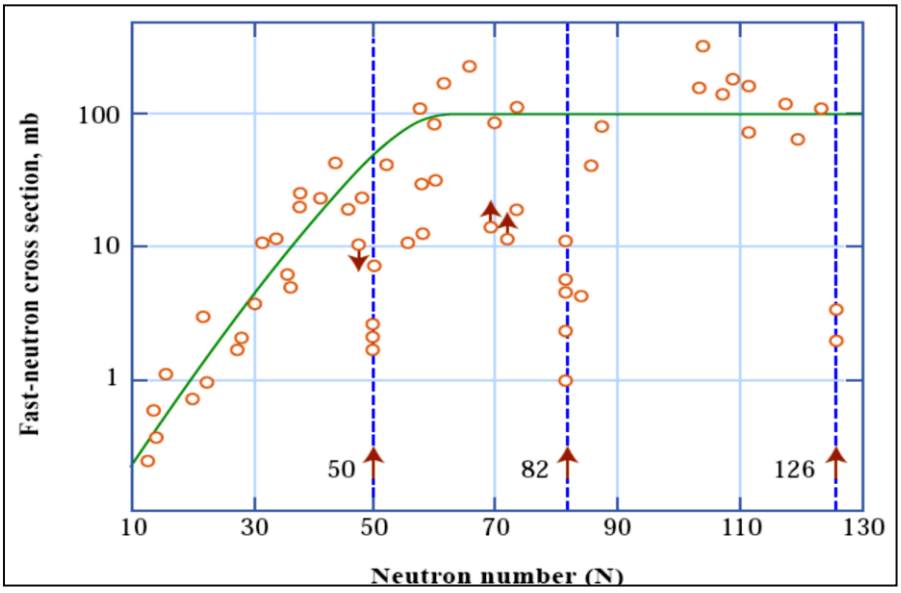

Figure 7.8. Cross sections for capture at 1 MeV.

Also the measured proton and neutron separation energies as compared to the predicted values by the semi-empirical mass formula, as discussed before, show that the separation energy increases gradually with N or Z except for a few sharp drops that occur at the same neutron and proton even numbers. This led to guess that the sharp discontinuities in the separation energy correspond (as in the atomic case) to the filling of major shells.

Fig. 7.9 shows that the neutron separation energy S_n is particularly low for nuclei with one more neutron than the magic numbers, which are more tightly bound.

The nuclear shell model is limited in its application to the ground states and low-lying excited states of nuclei. The present experimental evidence shows that there are closed nuclear shells at neutron and proton numbers 2, 8, 20, 28, 50, 82 and neutron number 126, which are called magic numbers.

The problem then is to determine the order in which these shells are filled as nucleons are added to make heavier nuclei. Quantum mechanical calculation has been made to determine a complete shell structure and the order of filling such shells. The model can account for many crucial nuclear properties as well, and we will, therefore, review several quantum behavior of atomic structure (*the detailed information as connected to the nuclear structure is given in the previous section*) before discussing the model and its application to the nuclear domain.

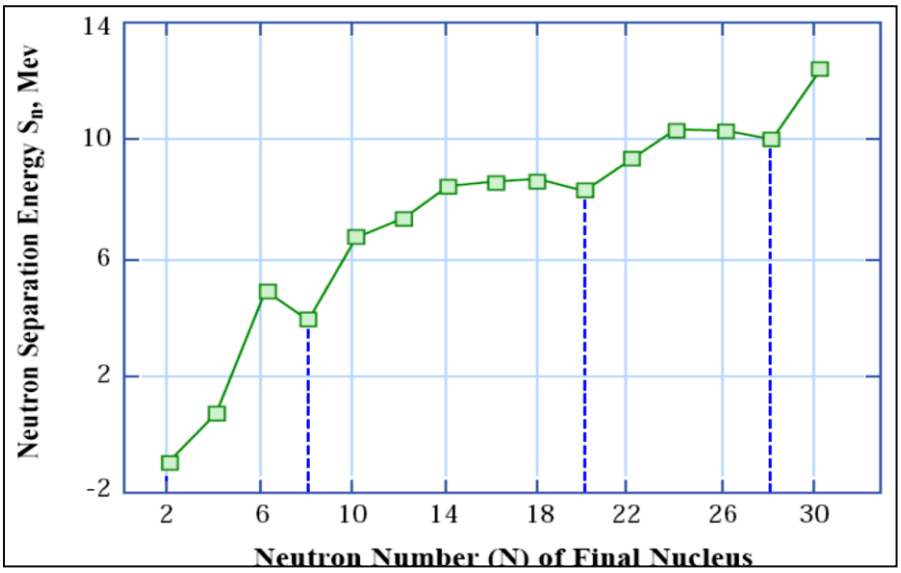

Figure 7.9. Variation of neutron separation energy with neutron number of the final nucleus M(A,Z).

7.4.1.2. Quantum behavior of atomic structure

As we know, the binding of electrons to a nucleus in a complex atom is attributed to the central Coulomb potential. Electron orbits and energy levels for such a quantum system can be obtained by solving the appropriate Schrödinger equation. In general, the solutions are quite complicated because they involve the Coulomb field of the nucleus as well as that of the other electrons, and cannot be obtained in closed analytic form. Nevertheless, certain characteristic features of the motion of an electron in a hydrogen atom have general relevance, which will be first discussed.

The orbits and atomic energy levels that electrons can occupy are labeled by a *principal quantum number n* (this determines the eigenvalue of the energy in the case of hydrogen), which can assume only integral values:

$$n = 1, 2, 3 \ldots\ldots \quad 7.37$$

For any given value of the principal quantum number, there are energy-degenerate levels with *orbital angular momentum quantum number* given by:

$$\ell = 0, 1, 2\ldots (n - 1) \quad 7.38$$

(This restriction follows from the form of the Coulomb potential). For any value of ℓ, there are $(2\ell + 1)$ sub-states with different values of the projection of orbital angular momentum along any chosen axis (the magnetic quantum number):

$$m_\ell = - \ell, - \ell + 1\ldots 0, 1\ldots \ell - 1, \ell \quad 7.39$$

Due to the rotational symmetry of the Coulomb potential, all such sub-states are degenerate in energy. Furthermore, since electrons have an intrinsic spin angular momentum of $\hbar/2$, each of the above states can be occupied by an electron with spin "up" or "down", corresponding to the spin-projection quantum number:

$$m_s = \pm 1/2 \quad 7.40$$

Again, the energy corresponding to either of these spin configurations will be the same.

Thus, any energy eigenstate in a hydrogen atom is labeled by four quantum numbers, namely (n, ℓ, m_ℓ, m_s). For a given value of n, it follows that the number of such degenerate energy states n_{dg} is given by:

$$n_{dg} = 2\sum_{\ell=0}^{n-1}(2\ell+1)$$

$$n_{dg} = 2[2\sum_{\ell=0}^{n-1}\ell + n]$$

$$= 2[2\times\frac{1}{2}n(n-1)+n]$$

$$n_{dg} = 2n^2 \qquad 7.41$$

However, all of these states are degenerate only if there is no preferred direction in space that can break the rotational symmetry of the Coulomb interaction. The high degree of degeneracy can be broken if there is a preferred direction in space, such as that supplied by a magnetic field; the energy of the system can also depend on the m_ℓ and m_s quantum numbers. In particular, spin-orbit interactions in atoms lead to a fine structure in the energy levels that has been well-studied.

Because the effects of such interactions are usually quite small, they are often neglected in elementary discussions of atomic physics; however, as we shall see, they provide a key element in determining the nature of nuclear structure.

The degeneracy in m_ℓ and m_s is not affected greatly, even in more complex atoms. Any shell can still accommodate only $2n^2$ electrons, in consistency with the Pauli principle. It also follows that if a shell or a sub-shell is filled, we have:

$$\sum m_\ell = 0 \qquad 7.42$$

$$\sum m_s = 0 \qquad 7.43$$

In other words, there is a strong pairing effect for closed shells and from the antisymmetric of the fermionic wave function, it can be shown that we get in general:

$$\boldsymbol{L = S = 0}, \qquad 7.44$$

$$\mathbf{J = L + S = 0}. \qquad 7.45$$

For any atom containing a closed shell or a closed sub-shell, all electrons are paired off and consequently no valence electrons are available. As a result, such atoms will be chemically inert. In fact, if we examine the inert elements, we find that they have just such structure with ground state configuration.

For example, both electrons in the He *(Z* =2) atom fill up the shell corresponding to n = 1, $\mathbf{1s^2}$. Similarly, Ne *(Z*=10) has closed shells corresponding to n=1 and n= 2, $\mathbf{1s^2\ 2s^2\ 2p^6}$. *Ar (Z*=18) has closed shells corresponding to n=1, 2, and closed sub-shells corresponding to n =3, ℓ=0, l, **[Ne] $\mathbf{3s^2\ 3p^6}$**. Kr *(Z*=36) fill up shells corresponding to n=1, 2, 3, as well as the sub-shells corresponding to n=4, ℓ=0, 1, **[Ar] $\mathbf{3d^{10}\ 4s^2\ 4p^6}$**. Finally, Xe *(Z*=54) has closed shells corresponding to n=1, 2, 3, and closed sub-shells corresponding to n=4, ℓ = 0, 1, 2, as well as n=5, ℓ=0, 1. (The energies of the oblong n = 4, ℓ=3 levels lie above the more spherical n=5, ℓ= 0, 1 levels; the latter, therefore, get filled first), **[Kr] $\mathbf{4d^{10}\ 5s^2\ 5p^6}$**.

These inert elements are exceedingly stable. In fact, their ionization energies are particularly large, as is consistent with their greater stability. The above atomic numbers, namely, Z = 2, 10, 18, 36, 54, are called the *magic* numbers of atomic physics and correspond to closed shell structures.

7.4.2. Nuclear shell model potential

A simple Coulomb potential is clearly not appropriate for nuclear structure as we need some form that describes the effective potential of all the other nucleons. Since the strong nuclear force is short-ranged, we would expect the potential to follow the form of the density distribution of nucleons in the nucleus. Although, it cannot be attractive for all separations or, otherwise, nuclei would collapse in on them. So at very short ranges, there must be a repulsive core. However, the repulsive core can be ignored in low-energy nuclear structure problems because low-energy particles cannot probe the short-distance behavior of the potential. In lowest order, the potential may be represented dominantly by a central term (i.e. one that is a function only of the radial separation of the particles), although there is also a smaller non-central part. We know from proton–proton scattering experiments that the nucleon–nucleon force is short-range, of the same order as the size of the nucleus, and thus does not correspond to the exchange of gluons, as in the fundamental strong interaction.

A schematic diagram of the resulting potential is shown in Fig. 7.10. In this figure, the distance R is the range of the nuclear force and $\delta << R$ is the distance at which the short-range repulsion becomes important and the depth $V_0 \approx 40$ - 50 MeV. In practice, of course, this strong interaction potential must be combined with the Coulomb potential in the case of protons.

A comparison of n-n and p-p scattering data (after allowing for the Coulomb interaction) shows that the nuclear force is charge-symmetric (p-p = n-n) and almost charge-independent (p-p = n-n = p-n), and evidence for charge-

independence comes from the energy levels of triplets of related nuclei with the same A values.

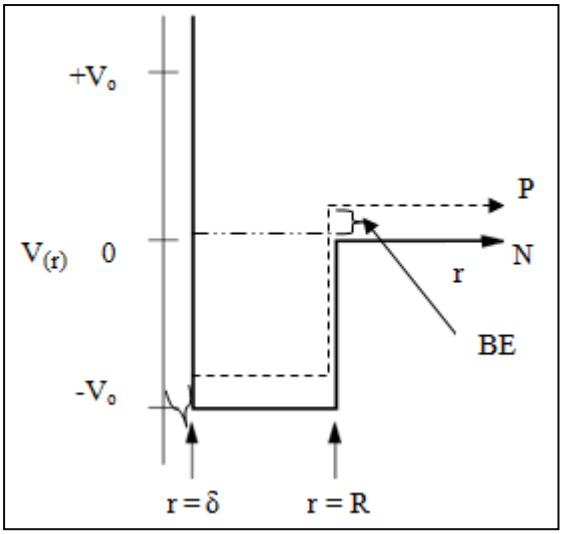

Figure 7.10. Idealized square well representation of the strong interaction nucleon-nucleon potential.

Nucleon–nucleon forces are, however, spin-dependent. The force between a proton and neutron in an overall spin-1 state (i.e. with spins parallel) is strong enough to support a weakly bound state (the deuteron), whereas the potential corresponding to the spin-0 state (i.e., spins antiparallel) has no bound states. Finally, nuclear forces saturate, this describes the fact that a nucleon in typical nucleus experiences attractive interactions only with a limited number of the many other nucleons and is a consequence of the short-range nature of the force. The evidence for this is the form of the nuclear binding energy curve and was discussed in Chapter 2.

7.4.2.1. Simple shell model

As a first step in improving the model, we try to choose a more realistic potential. The basic assumption of the shell model is that the effects of inter-nuclear interactions can be represented by a single-particle potential. One might think that with very high density and strong forces, the nucleons would be colliding all the time and therefore cannot maintain a single-particle orbit. But, because of Pauli exclusion the nucleons are restricted to only a limited number of allowed orbits. A typical shell-model potential is:

$$V(r) = -V_0 / \{1 + \exp[(r - R)/a]\} \qquad 7.46$$

This is sketched in Fig. 7.11. The parameters R and a give, respectively, the mean radius and skin thickness of the nucleus, where typical values for the parameters are $V_0 \approx 57$ MeV, $R \approx 1.25A^{1/3}$ fm, $a \approx 0.65$ fm. In addition, one can consider corrections to the well depth arising from, first symmetry energy from an unequal number of neutrons and protons, with a neutron being able to interact with a proton in more ways than n-n or p-p (therefore n-p force is stronger than n-n and p-p), and second Coulomb repulsion.

For a given spherically symmetric potential V(r), one can examine the bound-state energy levels that can be calculated from Schrödinger equation for a central potential $V(r)$, starting from the general form:

$$-\frac{\hbar^2}{2m}\nabla^2\Psi(\boldsymbol{r}) + V(r)\Psi(\boldsymbol{r}) = E\Psi(\boldsymbol{r}) \qquad 7.47$$

where E is the energy eigenvalue.

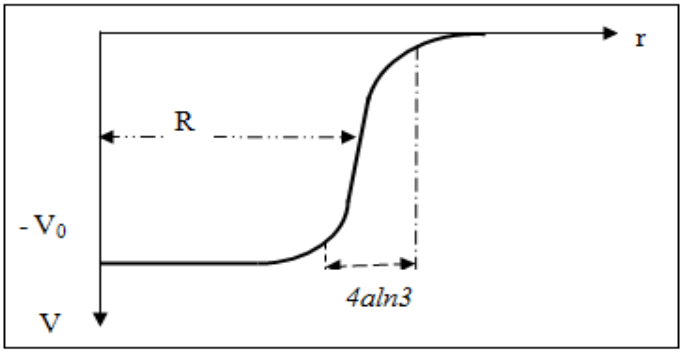

Figure 7.11. A realistic form of the shell model potential.

Because we assume that the potential is spherically symmetric, the energy eigenstates will also be eigenstates of the angular momentum operator. In other words, the system has rotational invariance which gives rise to its angular momentum to be conserved.

When we search for separable solutions, of the form $\Psi(r,\theta,\varphi) = R(r)\ \Theta(\theta)\ \Phi(\varphi)$, the central potential *V(r)* in Eq. 7.47 appears only in the radial part of the separation equation and the angular parts can be solved directly. The differential equation for $\Phi(\varphi)$ is:

$$\frac{d^2\Phi}{d\Phi^2} + m_\ell^2\Phi = 0 \quad \textit{with} \quad \textit{solution} \quad \Phi_{m_\ell}(\varphi) = \frac{1}{\sqrt{2\pi}} e^{im_\ell\varphi} \qquad \mathbf{7.}48$$

where m_ℓ^2 is the separation constant, and:

$$m_\ell = 0, \pm1, \pm2 \ldots\ldots \pm\ell \qquad 7.49$$

and the differential equation for $\Theta(\theta)$ is:

$$\frac{1}{\sin\theta}\frac{d}{d\theta}\left(\sin\theta\frac{d\Theta}{d\theta}\right) + \left[\ell(\ell+1) - \frac{m_\ell^2}{\sin^2\theta}\right]\Theta = 0 \qquad 7.50$$

where ℓ = 0, 1, 2, 3 ….. and m_ℓ = 0, ±1, ±2…±ℓ. The solution $\Theta_{\ell m \ell}(\theta)$ can be expressed as a polynomial of degree ℓ in sinθ or cosθ. Together, and normalized, $\Phi_{m\ell}(\varphi)$ and $\Theta_{\ell m \ell}(\theta)$ give the spherical harmonics $Y_{\ell m \ell}(\theta, \varphi)$.

As a result, the radial wave equation for a particular orbital angular momentum ℓ can be written:

$$-\frac{\hbar^2}{2m}\left(\frac{d^2R}{dr^2}+\frac{2}{r}\frac{dR}{dr}\right)+\left[\frac{\ell(\ell+1)\hbar^2}{2mr^2}+V(r)\right]R=ER \qquad 7.51$$

where the term ℓ (ℓ + 1) is generally written as an addition to the potential, called "centrifugal potential" and it acts like a potential that keeps the particle away from the origin when ℓ >0.

Fig. 7.12 shows the energy levels of the nucleons for an infinite spherical well and a harmonic oscillator potential, $V(r) = m\omega^2 r^2 / 2$. In the spectroscopic notation (n, ℓ), n refers to the number of times the orbital angular momentum state ℓ has appeared. Also in Fig. 7.12, one can see at certain levels the cumulative numbers of nucleons that can be put into all the levels up to the indicated level.

While no simple formulas can be given for the former, for the latter one has the expression:

$$E_n = \hbar\omega\,(\nu + 3/2) = \hbar\omega\,(n_x + n_y + n_z + 3/2) \qquad 7.52$$

where ν = 0, 1, 2… and n_x, n_y, n_z = 0, 1, 2 … are quantum numbers. One should notice the degeneracy in the oscillator energy levels. The quantum number ν can be divided into *radial* quantum number n (1, 2, 3 …) and *orbital* quantum numbers ℓ (0, 1, 3 …) as shown in Fig. 7.12. One can see from these results that a central force potential is able to

account for the first three magic numbers, 2, 8, 20, but not the remaining four, 28, 50, 82, 126. This situation does not change when more rounded potential forms are used. The implication is that something very fundamental about the single-particle interaction picture is missing in the description.

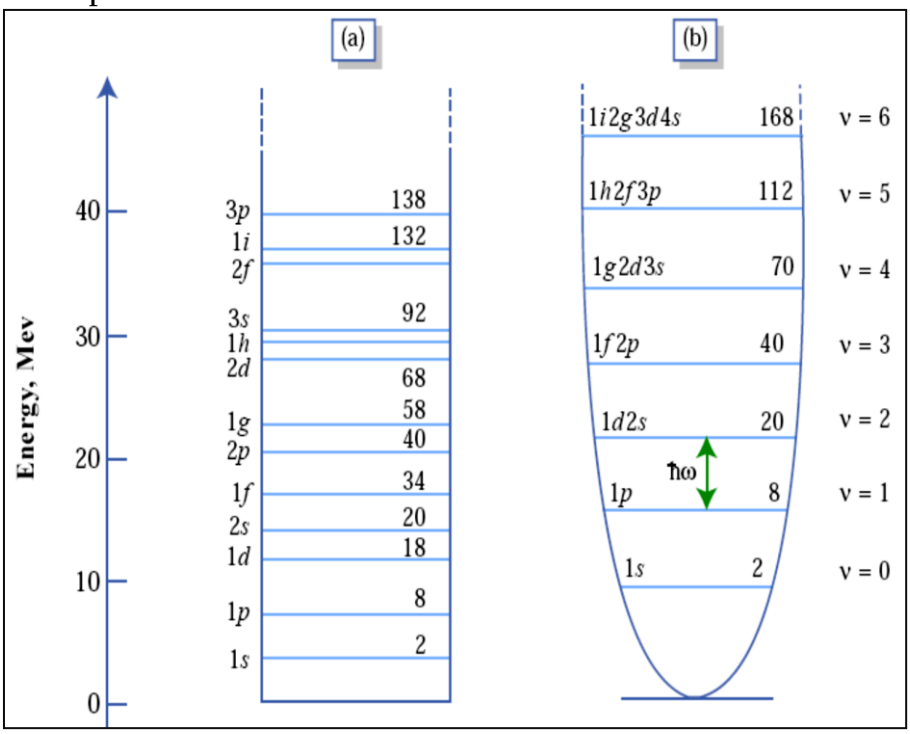

Figure 7.12. Energy levels of nucleons (a) in an infinite spherical well (range R = 8fm) and (b) in a parabolic potential well.

7.4.2.2. Shell model with spin-orbit coupling

It remains for M. G. Mayer and independently Haxel, Jensen, and Suess to show (1949) that an essential missing piece is an attractive interaction between the orbital angular

momentum and the intrinsic spin angular momentum of the nucleon. To take into account this interaction, we add a term to the Hamiltonian H:

$$V_{tot} = V(r) + V_{so}(r)\ \mathbf{S.L} \qquad 7.53$$

where V_{so} is another central potential (known to be attractive).

This modification means that the interaction is no longer spherically symmetric; the potential now depends on the relative orientation of the spin and orbital angular moments. In order to understand the meaning of the results of such calculations (eigenvalues and eigenfunctions), we need to digress somewhat to discuss the addition of two angular momentum operators.

The presence of the spin-orbit coupling term in Eq.7.53 means that we will have a different set of eigenfunctions and eigenvalues for the new description. What are these new quantities relative to the eigenfunctions and eigenvalues we had for the problem without the spin-orbit coupling interaction? We first observe that in labeling the energy levels in Fig. 7.12 we had already taken into account the fact that the nucleon has an orbital angular momentum (it is in a state with a specified ℓ) and that it has an intrinsic spin of ½ (in unit of $\hbar$). For this reason, the number of nucleons that we can put into each level has been counted correctly. For example, in the 1s ground state, one can put two nucleons, for zero orbital angular momentum and two spin orientations (up and down). The number of nucleons that can go into that state is $2(2\ell+1)$. The two angular moments we want to add are obviously the orbital angular momentum operator **L** and the intrinsic spin angular momentum operator **S**, since they are the only angular momentum operators in our problem.

Notice that if we define the total angular momentum as:

$$\boldsymbol{j} = \boldsymbol{S} + \boldsymbol{L} \qquad 7.54$$

we can then write the expectation values as:

$$\boldsymbol{J.J} = (\boldsymbol{S} + \boldsymbol{L}).\ (\boldsymbol{S} + \boldsymbol{L})$$
$$< \boldsymbol{S.L} > = < (\mathbf{j}^{2} - \boldsymbol{S}^{2} - \boldsymbol{L}^{2})/2 > \qquad 7.55$$

So the problem of diagonalizing the formula Eq. 7.51 is the same as diagonalizing j^2, S^2, and L^2. This is then the basis for choosing our representation, denote the new eigenfunctions by $| jm_j\ \ell s>$, which has the following properties:

$$j^{2}\,|jm_j\,\ell s> = j(j+1)\hbar^{2}\,|jm_j\,\ell s>,\ |\ell - s| \le j \le \ell + s \qquad 7.56$$

$$j_z\,|jm_j\,\ell s> = m_j\hbar\,|jm_j\,\ell s>, \qquad -j \le m_j \le j \qquad 7.57$$

$$L^{2}\,|jm_j\,\ell s> = \ell(\ell+1)\hbar^{2}\,|jm_j\,\ell s>,\ \ \ell = 0, 1, 2, \ldots \qquad 7.58$$

$$S^{2}\,|jm_j\,\ell s> = s(s+1)\hbar^{2}\,|jm_j\,\ell s>, \quad s = ½ \qquad 7.59$$

In Eq.7.56, we indicate the values that j can take for given ℓ and s (=1/2 in our discussion), the lower or upper limit corresponds to when **S** and **L** are antiparallel or parallel respectively, as shown in the sketch Fig. 7.13.a.

The expectation values of Eq. 7.55 can be written as:

$$< S.L > = \frac{1}{2}[j(j+1) - \ell(\ell+1) - s(s+1)]\hbar^{2} \qquad 7.60$$

To illustrate the degeneracy of each level, consider a level such as 1f (ℓ=3) level, which has a degeneracy of $2(2\ell+1) = 14$. The possible j values are $\ell \pm 1/2 = 5/2$ or $7/2$. Thus we have the levels $1f_{5/2}$ and $1f_{7/2}$. The degeneracy of each level is (2j + 1), which comes from m_j values. The capacity of $1f_{5/2}$ level is 6 and of $1f_{7/2}$ is 8. For the $1f_{5/2}$ and $1f_{7/2}$ states, which are known as a spin-orbit pair or doublet, there is an energy separation that is proportional to the value of <S.L> for each state. Indeed, for any pair of states with $\ell>0$, we can compute the energy difference using Eq. 7.60:

$$< S.L >_{j=\ell+½} - < S.L >_{j=\ell-½} = \frac{1}{2}(2\ell+1)\hbar^2 \qquad 7.61$$

Returning now to the energy levels of the nucleons in the shell model with spin-orbit coupling we can understand the conventional spectroscopic notation where the value of j is shown as a subscript, Fig. 7.13.b.

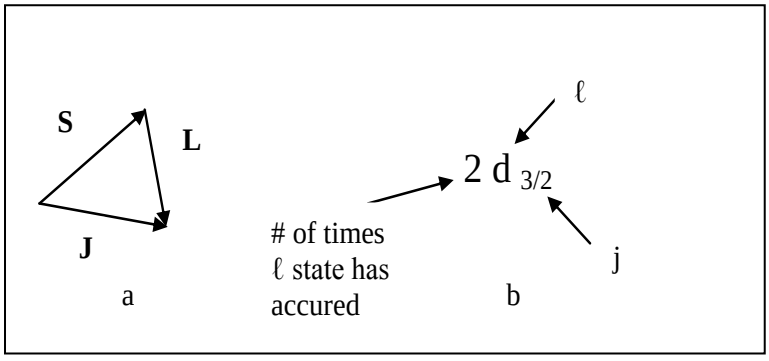

Figure 7.13. Sketch of,
a- vector relationship between **S, L** and **J**,
b- The conventional spectroscopic notation.

This is then the notation in which the shell-model energy levels are displayed in Fig. 7.14.

For a given (n, ℓ, *j)* level, the nucleon occupation number is 2j+1. It would appear that having (2j+1) identical nucleons occupying the same level would violate the Pauli Exclusion Principle. But, this is not the case since each nucleon would have a distinct value of m_j (this is why there are 2j+1 values of mj for a given j).

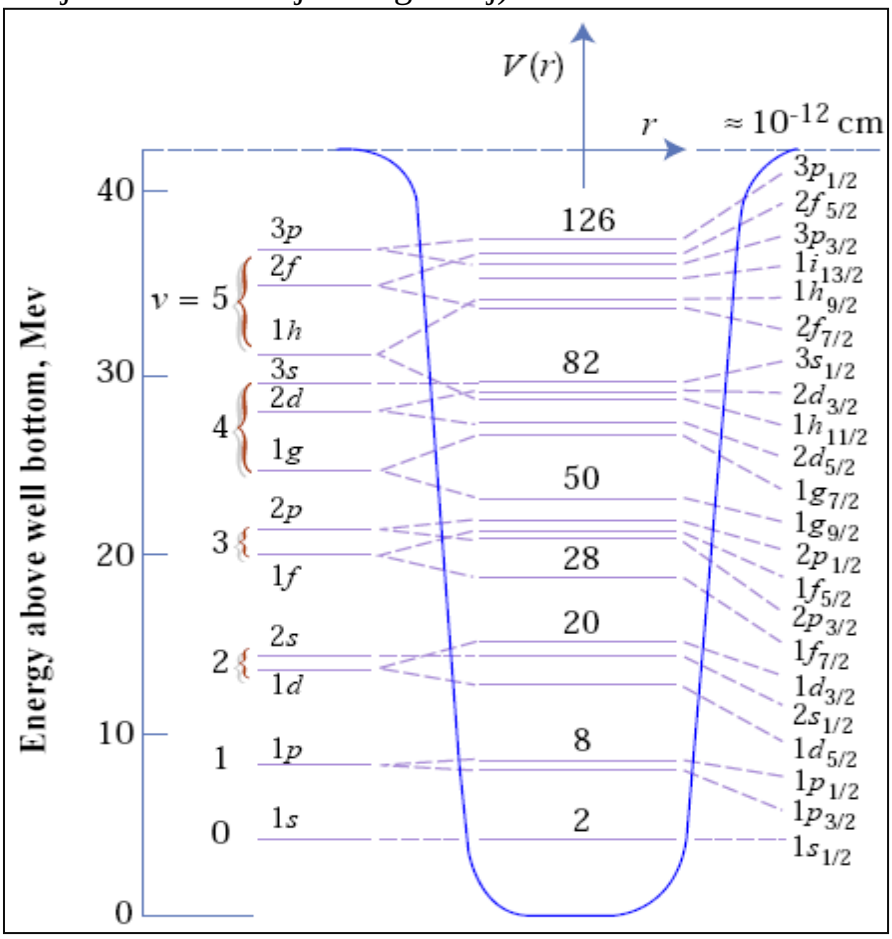

Figure 7.14. Energy levels of nucleons in a smoothly varying potential well with a strong spin-orbit coupling term.

We see in Fig. 7.14 that the shell model with spin-orbit coupling gives a set of energy levels having breaks at the seven magic numbers. This is considered a major triumph of the model, for which Mayer and Jensen were awarded the Noble prize in physics. For our purpose, we will use the results of the shell model to predict the ground-state spin and parity of nuclei. Before going into this discussion, *we should mention the following comments*:

1. The shell model is most useful when applied to closed-shell or near closed-shell nuclei.
2. Away from closed-shell nuclei, collective models taking into account the rotation and vibration of the nucleus are more appropriate.
3. Simple versions of the shell model do not take into account pairing forces, the effects of which are to make two like-nucleons combine to give zero orbital angular momentum.
4. Shell model does not treat distortion effects (deformed nuclei) due to the attraction between one or more outer nucleons and the closed-shell core. When the nuclear core is not spherical, it can exhibit "rotational" spectrum.

7.4.3. Shell model predictions

7.4.3.1. Ground-state spin and parity

The shell model accounts for a wide variety of properties of complex nuclei: For example; the nuclear spin and parity.

There are three general rules for using the shell model to predict the total angular momentum I (spin) and parity of a nucleus in the ground state. These do not always work, especially away from the major shell breaks.

1. Angular momentum of odd-A nuclei I is determined by the angular momentum of the last nucleon in the species (ℓ + s) (neutron or proton) that is odd (j_p or j_n).
2. Even-even nuclei have zero ground-state spin, because the net angular momentum associated with even N and even Z is zero, and even parity.
3. In odd-odd nuclei, the last neutron couples to the last proton with their intrinsic spins in parallel orientation, i.e., $\mathbf{I}=\mathbf{j}_p+\mathbf{j}_n$. Therefore, to determine the possible ground state spin, the above vectore coupling can be written as:

$$|j_p - j_n| \leq I \leq j_p + j_n \qquad 7.62$$

To illustrate how these rules work, we consider an example for each case:

1- Consider the odd-A nuclide ^{9}Be which has 4 protons and 5 neutrons. With the last nucleon being the fifth neutron, we see in Fig. 7.14 that this nucleon goes into the state $1p_{3/2}$ (ℓ =1, j=3/2). Thus we would predict the spin and parity of this nuclide to be $3/2^-$, i.e., the 4 neutrons should be completely paired off, while the 5 neutrons should fill the following shells:

$$(1s_{1/2})^2\,(1p_{3/2})^3$$

2- For an even-even nuclide, we can take ^{36}A, with 18 protons and neutrons, or ^{40}Ca, with 20 protons and neutrons. For both cases, we would predict spin and parity of 0^+. Since both protons and neutrons should be completely paired off as:

$$(1s_{1/2})^2\,(1p_{3/2})^4\,(1p_{1/2})^2\,(1d_{5/2})^6\,(2s_{1/2})^2\,(1d_{3/2})^2 \quad \text{for } ^{36}\text{A}$$

$$(1s_{1/2})^2\,(1p_{3/2})^4\,(1p_{1/2})^2\,(1d_{5/2})^6\,(2s_{1/2})^2\,(1d_{3/2})^4 \quad \text{for } ^{40}\text{Ca}$$

3- For an odd-odd nuclide, we take ^{38}Cl, which has 17 protons and 21 neutrons. In Fig. 7.14, we see that the 17th proton goes into the state $1d_{3/2}$ (ℓ =2, j=3/2), while the 21st neutron goes into the state 1 $f_{7/2}$ (ℓ =3, j=7/2), i.e., protons and neutrons fill, respectively, the following shells:

$$(1s_{1/2})^2\,(1p_{3/2})^4\,(1p_{1/2})^2\,(1d_{5/2})^6\,(2s_{1/2})^2\,(1d_{3/2})^1$$

$$(1s_{1/2})^2\,(1p_{3/2})^4\,(1p_{1/2})^2\,(1d_{5/2})^6\,(2s_{1/2})^2\,(1d_{3/2})^4\,(1f_{7/2})^1$$

From the ℓ and j values, we know that for the last proton the orbital and spin angular moments are pointing in opposite direction (because j = ℓ -1/2). For the last neutron, the two moments are pointing in the same direction (j = ℓ +1/2). Now the rule tells us that the two spin moments are parallel, *therefore, the orbital angular momentum of the odd proton is pointing in the opposite direction from the orbital angular momentum of the odd neutron*, with the latter in the same direction as the two spins. Adding up the four angular moments, we have +3+1/2+1/2-2 = 2. Thus, the total angular momentum (nuclear spin) is I = 2. One can come out to the same conclusion by introducing the total angular momentum of both last proton 3/2 and last neutron 7/2 as in Eq. 7.62. As $|7/2 - 3/2| \leq I \leq 7/2 - 3/2$ to get I = 2, 3, 4, 5. Again the most likely I = 2.

What about the parity? The parity of the nuclide is the product of the two parities, one for the last proton and the other for the last neutron as $\pi = (-1)^{\ell p+\ell n}$.

Recall that the parity of a state is determined by the orbital angular momentum quantum number ℓ, $\pi = (-1)^{\ell}$. So with the proton in a state with ℓ = 2, its parity is even, while the neutron in a state with ℓ = 3 has odd parity. The parity of

the nucleus is therefore odd. Our prediction for ^{38}Cl is then 2^-. The student can verify, using for example the Nuclide Chart, the foregoing predictions are in agreement with experiment.

However, certain spin-parity assignments of the shell model do not agree with observation. For example, the 25 neutrons in ^{47}Ti would be expected to fill the levels as:

$$(1s_{1/2})^2 (1p_{3/2})^4 (1p_{1/2})^2 (1d_{5/2})^6 (2s_{1/2})^2 (1d_{3/2})^4 (1f_{7/2})^5$$

Leading to a ground state spin-parity of $(7/2)^-$, whereas the experimental value is $(5/2)^-$. Such discrepancies can be remedied by slightly modifying the assumptions of the single-particle shell model to allow pairing between all "valence" nucleons, namely between any nucleons that occupy unfilled levels.

7.4.3.2. Magic nuclei

In fact, although the binding energy per nucleon varies smoothly on a broad scale, a close examination shows peaks corresponding to specific values of nucleon numbers:

$$\begin{aligned} &N = 2, 8, 20, 28, 50, 82, 126 \\ &Z = 2, 8, 20, 28, 50, 82 \end{aligned} \qquad 7.63$$

Nuclei with either proton or neutron number corresponding to any of these magic values appear to be particularly stable and are referred to as *magic nuclei.* Nuclei where both the proton and the neutron numbers are magic (e.g., ^{4}He, ^{16}O, ^{208}Pb) are known as *doubly magic*, and have even greater stability, as mentioned earlier with experimental evidences in the beginning of this section.

7.4.3.3. Nuclear magnetic moment μ

The shell model can also be used to calculate magnetic moments of nuclei. As measurements show, *the proton and the neutron have intrinsic dipole moments of 2.792847* μ_N *and -1.910427* μ_N, respectively, where μ_N is nuclear magneton. Thus, we expect the intrinsic magnetic moment of any unpaired nucleon to contribute to the total magnetic moment of the nucleus. In addition, since protons are charged, the orbital motion of any unpaired proton can also contribute to the magnetic moment of the nucleus, while any unpaired neutron has zero orbital motion contribution, just intrinsic spin contribution.

For the even–odd nuclei, we would expect all the paired nucleons to contribute zero net magnetic moment, for the same reason that they do not contribute to the nuclear spin. Predicting the nuclear magnetic moment is then a matter of finding the correct way to combine the orbital μ_ℓ and spin μ_s components of magnetic moment of the single unpaired nucleon. As shown in section 2.9, we can write Eq. 2.29 in terms of the nuclear magnetic moment as:

$$\mu = g_I \, I \, \mu_N \qquad 7.64$$

where g_I is the nuclear (gyromagnatic ratio) g-factor and I is the nuclear spin quantum number equal to the total angular quantum number of the last unpaired nucleon j. It is beyond the scope of this book to go deep in details, the simplified resultant formula are as follows:

$$I \, g_I = g_\ell \, j + g_s/2 \qquad \text{for } j = \ell + 1/2 \qquad 7.65a$$

and

$$I\, g_I = g_\ell\, j[1+1/(2\ell+1)] - g_s\, j[1/(2\ell+1)] \quad \text{for } j=\ell-1/2 \qquad 7.65b$$

Since the g-factor due to orbital angular momentum, $g_\ell = 1$ for a proton and 0 for a neutron, while that due to spin g_s = +5.585694 for the proton and = -3.826084 for the neutron. Eq. 7.65 yield the following results for the unpaired (odd) proton and neutron:

$$\begin{aligned}
\mu_{proton} &= [j + \frac{1}{2}\times 5.6]\mu_N = [j+2.3]\mu_N \qquad for \quad j = \ell + 1/2 \\
\mu_{proton} &= \left[j(1+\frac{1}{2\ell+1}) - 5.6\times j(\frac{1}{2\ell+1}) \right]\mu_N = \left[j - \frac{2.3j}{j+1} \right]\mu_N \; for \quad j = \ell - 1/2 \\
\mu_{neutron} &= [-\frac{1}{2}\times 3.8]\mu_N = -1.9\mu_N \qquad for \quad j = \ell + 1/2 \\
\mu_{neutron} &= \left[3.8\times j(\frac{1}{2\ell+1}) \right]\mu_N = \left[\frac{1.9j}{j+1} \right]\mu_N \; for \quad j = \ell - 1/2
\end{aligned} \qquad 7.66$$

Accurate values of magnetic dipole moments are available for a wide range of nuclei and plots of a sample of measured values for a range of odd-Z and odd-N nuclei across the whole periodic table are shown in Fig. 7.15. It is seen that for a given j, the measured moments usually lie somewhere between the $j = \ell - 1/2$ and the $j = \ell + 1/2$ values (the so-called Schmidt lines), but beyond that the model does not predict the moments accurately. *The only exceptions are a few low-A nuclei* where the numbers of nucleons are close to magic values.

For the deuteron, for example, if we assume that the proton and the neutron are in $1s_{1/2}$ states, then, without orbital angular momentum for the proton ($\ell = 0$), we expect the magnetic moment of the deuteron μ_d to be the sum of the intrinsic dipole moments of the proton and the neutron:

$$\mu_d = 2.792847\ \mu_N - 1.9130427\ \mu_N = 0.8854273\ \mu_N \qquad 7.67$$

The observed magnetic moment of the deuteron is 0.86 μ_N, which is in fair agreement with expectation.

The nucleus of tritium (^{3}H) has two neutrons and one proton, all in the $ls_{1/2}$ state. Since the neutrons are paired, they should not contribute to the magnetic moment. The unpaired proton, having ℓ=0, will have no contribution from its orbital motion. Consequently, the total magnetic moment of ^{3}H should be the same as that of the unpaired proton, namely 2.792847 μ_N, which is in good agreement with measured value of 2.98 μ_N.

For ^{3}He, the unpaired nucleon is a neutron in an $lS_{1/2}$ state. Consequently, the total magnetic moment should be the same as that of the neutron, which is -1.91 μ_N. Again, close to the observed value of -2.13 μ_N, ^{4}He (α-particle) has a closed shell structure (in fact, it is doubly magic) and the shell model would, therefore, predict no spin and no magnetic moment, which is indeed experimentally correct.

In ^{10}B, the five protons and the five neutrons have the same level structure, namely:

$$(1s_{1/2})^2 (1p_{3/2})^3$$

Thus, there is one unpaired proton and one unpaired neutron. The unpaired proton will be in an ℓ = 1 state, and therefore the orbital motion will contribute $\mu = \mu_N$ to the total magnetic moment, which will yield a value:

$$\mu_B = 2.792847\mu_N - 1.9130427\mu_N + \mu_N = 1.8542738\ \mu_N. \quad 7.68$$

This compares quite well with the measured value of 1.80 μ_N.

We see, therefore, that the shell model, in addition to providing the known magic numbers, also describes other important properties of light nuclei. For heavy nuclei,

however, there is marked difference between the predictions of the shell model and the measured quantities.

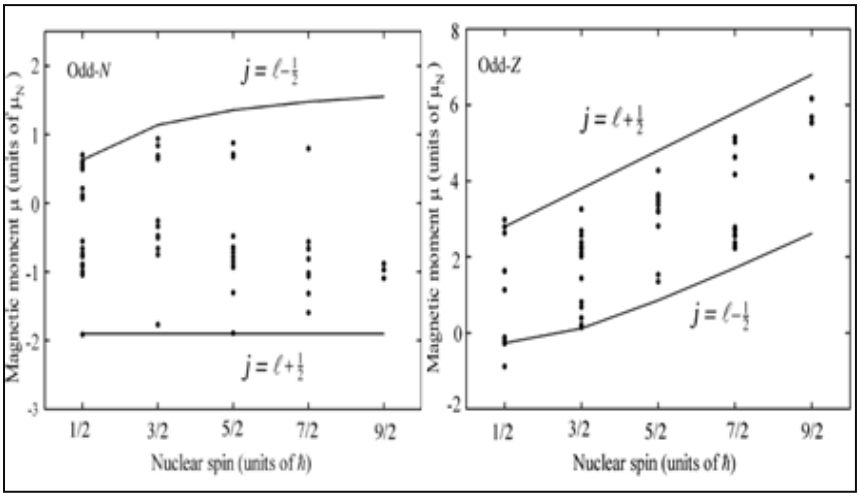

Figure 7.15. Magnetic moments for odd-N, even-Z nuclei (left diagram) and odd-Z, even-N (right diagram) as functions of nuclear spin compared with the predictions of the single-particle shell model (the Schmidt lines).

7.4.3.4. Symmetry and Coulomb interactions correction

The qualitative features of the potential wells for neutrons and protons can be summarized by following: If we exclude the Coulomb interaction for the moment, the well for a proton is known to be deeper than that for a neutron. The *reason is that* in a given nucleus there are usually more neutrons than protons, especially for the heavy nuclei, and the n-p interactions can occur in more ways than either the n-n or p-p interactions on account of the Pauli exclusion principle. The difference in well depth ΔV_{sy} is called the

symmetry energy; as has been described in liquid drop model, it is approximately given by:

$$\Delta V_{sy} = \pm 27\ (N - Z)/A\ \text{MeV} \qquad 7.69$$

where the (+) and (–) signs are for protons and neutrons, respectively. If we now consider the Coulomb repulsion between protons, its effect is to raise the potential for a proton. In other words, the Coulomb effect is a positive contribution to the nuclear potential which is larger at the center than at the surface and extends beyond it; this potential can be estimated as follows:

If all positive charge Ze is concentrated at the center of the nucleus of a sharp edge at $r = R_0$, the electric field E(r) is:

$$\begin{aligned} E(r) &= \frac{Ze^2}{4\pi\varepsilon_0 r^2} \qquad for \qquad r > R_0 \\ E(r) &= \frac{r}{R_0}\frac{Ze^2}{4\pi\varepsilon_0 R_0^2} \qquad for \qquad r \le R_0 \end{aligned} \qquad 7.70$$

The coulomb potential $V_C(r)$ is:

$$V_C(r) = \int_{\infty}^{r} E(r)dr = \int_{\infty}^{R_0} \frac{Ze^2}{4\pi\varepsilon_0 r^2}\,dr + \int_{R_0}^{r} \frac{Ze^2}{4\pi\varepsilon_0 R_0^2}\frac{r}{R_0}\,dr$$

$$\therefore \quad V_C(r) = \begin{cases} \dfrac{Ze^2}{4\pi\varepsilon_0 R_0}\left[1 + \dfrac{1}{2}\left(1 - \left(\dfrac{r}{R_0}\right)^2\right)\right] & for \quad r \le R_0 \\ \dfrac{Ze^2}{4\pi\varepsilon_0 r} & for \quad r > R_0 \end{cases} \qquad 7.71$$

This potential is, therefore, half times larger at the center ($r < R_0$) of the nucleus than that at the edge ($r > R_0$).

Combining the symmetry and the Coulomb effects, we have a sketch of the potential for a neutron and a proton as indicated in Fig. 7.16. One can also estimate the well depth in each case using the Fermi Gas Model. One assumes that the nucleons of a fixed kind behave like a fully degenerate gas of fermions (degeneracy here means that the states are filled continuously starting from the lowest energy state and there are no unoccupied states below the occupied ones), so that the number of states occupied is equal to the number of nucleons in the particular nucleus.

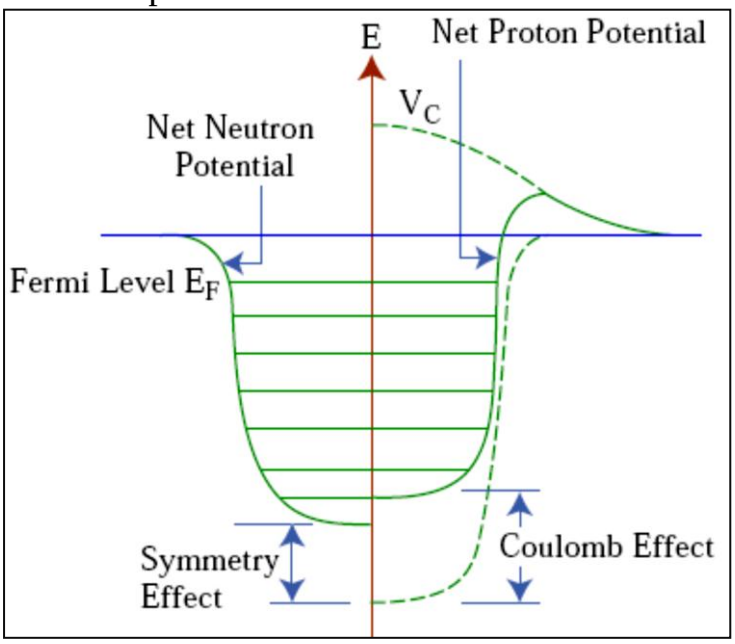

Figure 7.16. Schematic diagram showing the effects of symmetry and Coulomb interactions on the potential for a neutron and a proton.

This calculation is carried out separately for neutrons and protons. The highest energy state that is occupied is called the Fermi level, and the magnitude of the difference between this state and the ground state is called the *Fermi energy* E_F.

It turns out that E_F is proportional to $n^{2/3}$, where n is the number of nucleons of a given kind, therefore, E_F (neutron) > E_F (proton). The sum of E_F and the separation energy of the last nucleon provide an estimate of the well depth (The separation energy for a neutron or proton is about 8 MeV for many nuclei). Based on these considerations, Fig. 7.17 shows the nuclear potential wells for neutrons and protons according to the Fermi-Gas Model, with the mean binding energy per nucleon to be 8 MeV, the mean relative nucleon admixture to be N/A ~ 1/1.8, Z/A ~ 1/2.2, and a range of 1.4 fm(a) and 1.1 fm(b**)**.

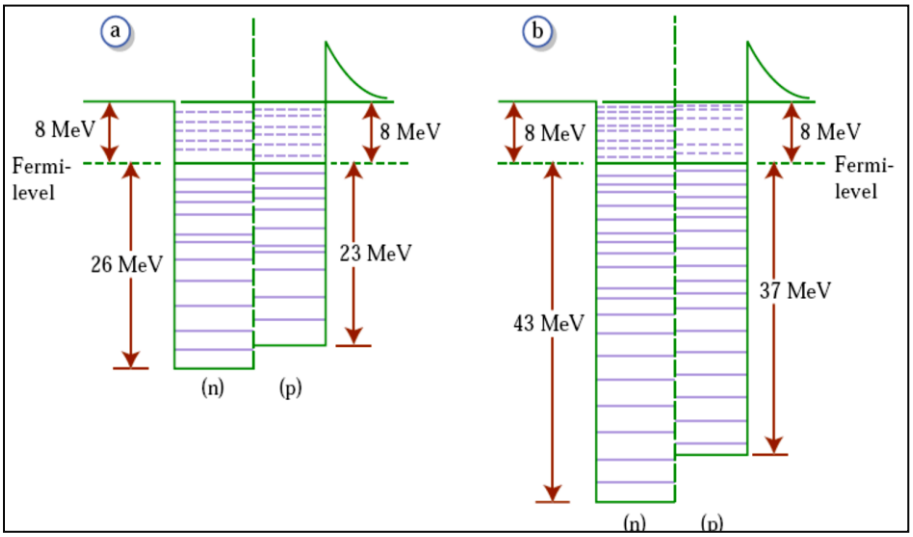

Figure 7.17. Nuclear potential wells for neutrons and protons according to the Fermi-Gas Model.

7.4.3.5. Excited states

In principle, the shell model's energy level structure can be used to predict nuclear excited states. This works quite well for the first one or two excited states when there is only

one possible configuration of the nucleus. However, for higher states the spectrum becomes very complicated because several nucleons can be excited simultaneously into a superposition of many different configurations to produce a given nuclear spin and parity. When trying to predict the first one or two excited states using a filling diagram like Fig. 7.14, we are looking for the configuration that is nearest to the ground state configuration. This will normally involve either moving an unpaired nucleon to the next highest level, or moving a nucleon from the sub-shell below the unpaired nucleon up one level to pair with it. Thus it is necessary to consider levels just above and below the last nucleons (protons and neutrons).

As an example, consider the case of ^{17}O. Its ground-state configuration is:

$$(1s_{1/2})^2 (1p_{3/2})^4 (1p_{1/2})^2 \qquad \text{for the protons}$$

$$(1s_{1/2})^2 (1p_{3/2})^4 (1p_{1/2})^2 (1d_{5/2})^1 \text{ for the neutrons}$$

All the proton sub-shells are filled, and all the neutrons are in filled sub-shells except for the last one, which is in a sub-shell on its own. There are three possibilities to consider for the first excited state:

1. Promote one of the $1p_{1/2}$ protons to$1d_{5/2}$, giving a configuration of $(1p_{1/2})^{-1}(1d_{5/2})^1$, where the superscript -1 means that the shell is one particle short of being filled;
2. Promote one of the $1p_{1/2}$ neutrons to $1d_{5/2}$, giving a configuration of $(1p_{1/2})^{-1}(1d_{5/2})^2$;
3. Promote the $1d_{5/2}$ neutron to the next level, which is probably $2s_{1/2}$ (or the nearby $1d_{3/2}$), giving a configuration of $(1d_{5/2})^{-1} (1s_{1/2})^1$ or $(1d_{5/2})^{-1} (1d_{3/2})^1$.

The above three possibilities can be represented schematically as in Fig. 7.18.

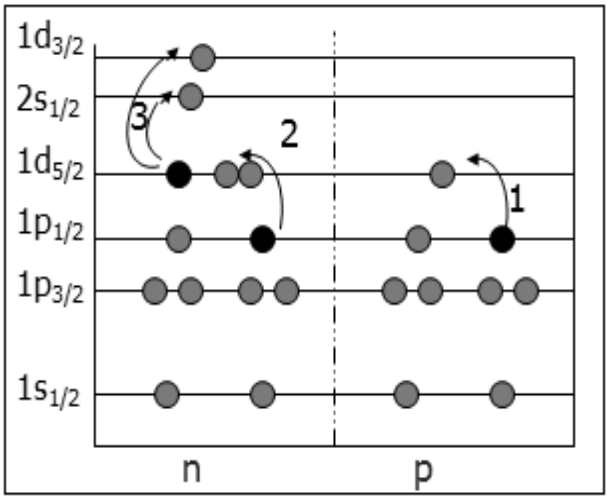

Figure 7.18. Illustration of the three possibilities for the first excited state of ^{17}O.

Following the diagram of Fig. 7.14, the third of these possibilities would correspond to the smallest energy shift, so it should be favored over the others. The next excited state might involve moving the last neutron up a further level to$1d_{3/2}$, or putting it back where it was and adopting configurations (1) or (2). Option (2) is favored over (1) because it keeps the excited neutron paired with another, which should have a slightly lower energy than creating two unpaired protons. When comparing these predictions with the observed excited levels, it is found that the expected excited states do exist, but not necessarily in precisely the order predicted.

The shell model has many limitations, most of which can be traced to its fundamental assumption that the nucleons move independently of one another in a spherically

symmetric potential. The latter, for example, is only true for nuclei that are close to having doubly-filled magnetic shells and predicts zero electric quadruple moments, whereas in practice, many nuclei are deformed and quadruple moments are often substantial. We discuss this important observation in the next section.

7.5. Collective Model

For heavy nuclei, many predictions of the single-particle shell model do not agree quantitatively with experiment. The discrepancies are particularly severe for magnetic dipole moments. Also, the shell model predicts vanishingly small quadrupole moments for closed shells and quadrupole moments of opposite sign for neighboring nuclei with atomic numbers $Z \pm 1$. Although this agrees qualitatively with experiments, the measured values of quadrupole moments are very different from the predictions. In fact, some heavy nuclei appear to have large permanent electric quadrupole moments, suggesting a non-spheroid in the shape of these nuclei. This is certainly not consistent with the assumptions of the shell model, where rotational symmetry plays a crucial role.

In a revival of the liquid drop model, A. Bohr noted that many properties of heavy nuclei could be attributed to a surface motion of the nuclear liquid drop. Furthermore, James Rainwater showed that excellent agreement between the expected and measured values of magnetic dipole, and electric quadrupole moments could be obtained under the assumption that the liquid drop had a spherical shape. These successes presented somewhat of a dilemma because the liquid drop model and the single-particle shell model had fundamentally opposite viewpoints about the nature of

nuclear structure. Individual particle characteristics, such as intrinsic spin and orbital angular momentum, play no role in a liquid drop picture, where collective motion that involves the entire nucleus has prime importance. On the other hand, individual nucleon properties, especially of the valence nucleons, are crucial to the success of the independent-particle shell model. The shell model had yielded too many important nuclear features to be abandoned outright and reconciliation between the two extreme views was needed.

The reconciliation was brought about by *A. Bohr, Ben Mottelson and James Rainwater who proposed a collective model for the nucleus* to provide many features that were not present in the shell or the liquid drop model. In what follows, we describe this model only qualitatively. *Its basic assumption is that a nucleus consists of a hard core of nucleons in the filled shells, and outer valence nucleons that behave like the surface molecules in a liquid drop.* The surface motion (rotation) of the valence nucleons introduces a non-spheroid in the central core, which in turn affects the quantum states of the valence nucleons. In other words, one can think of the surface motion as a perturbation that causes the quantum states of the valence nucleons to change from the unperturbed states of the shell model. This adjustment accounts for the difference in predictions for dipole and quadrupole moments from those given by the shell model.

Physically, one can view the collective model as a shell model with a potential that is not spherically symmetric. Spherically symmetric nuclei are, of course, insensitive to rotations, and consequently rotational motion cannot produce additional (rotational) energy levels in such nuclei. Spherical nuclei, on the other hand, can have additional energy levels because of the presence of rotational and

vibrational degrees of freedom. These types of effects modify the predictions of the simple shell model.

In particular, large non-spheroid in nuclei can provide large permanent dipole and quadrupole moments. Mathematically, these ideas can be incorporated as follows. For simplicity, we assume the nucleus to be an ellipsoid defined by the form:

$$ax^2 + by^2 + z^2/ab = R^2 \qquad 7.72$$

where a and *b* are parameters related to the deformation from a spherical shape of radius *R*. The mean potential for nuclear motion can then be chosen as:

$$V(x, y, z) = \begin{cases} 0 \text{ for } ax^2 + by^2 + 4 < R^2 \\ \infty \text{ otherwise.} \end{cases} \qquad 7.73$$

Needless to say, more realistic calculations in the collective model provide even better descriptions of nuclear properties, but they also become far more complicated.

One of the important predictions of the collective model is the existence of rotational and vibrational levels in a nucleus. These levels can be derived much the same way as is done for the case of molecules. Thus, we can add an additional term to the spherically symmetric nuclear potential of the shell model, to account the centrifugal contribution of the form $\ell(\ell + 1)\hbar^2/2I_m$ (where the effective moment of inertia of the nucleus $I_m = mr^2$ is a function of the nuclear shape). As a result, the well becomes narrower and shallower for the higher orbital angular momentum states, and an attractive spin-orbit contribution. Its effect comes from the fact that when a nucleon is moving near the surface

of the nucleus, where the density of nucleons is decreasing, it will pass more nucleons on the inside of its orbit than on the outside. Therefore, there will be a net potential energy decrease, if **S** is parallel to **L**, and a net increase, if S is antiparallel to **L**. The effects are illustrated in Fig. 7.19 and Fig. 7.20). Notice that for $\ell = 0$ both are absent.

Finally, the collective model accommodates quite naturally the decrease of the spacing between the first excited state and the ground level in even-even nuclei with increasing *A*, since the moment of inertia grows with *A*, which decreases the energy eigenvalue of the first excited rotational state. Also the fact that the spacing is largest for nuclei with closed shells should be taken into account. This is due to the fact that a nucleus with a closed shell should not have a rotational level because such a nucleus would tend to be spherical. On the other hand, such a nucleus can have vibrational excitations. However, vibrational excitations involve the entire core and not just the surface. The core being much more massive implies that the energy level for vibration will lie far higher, and the spacing between the ground state and the first excited state will be much greater.

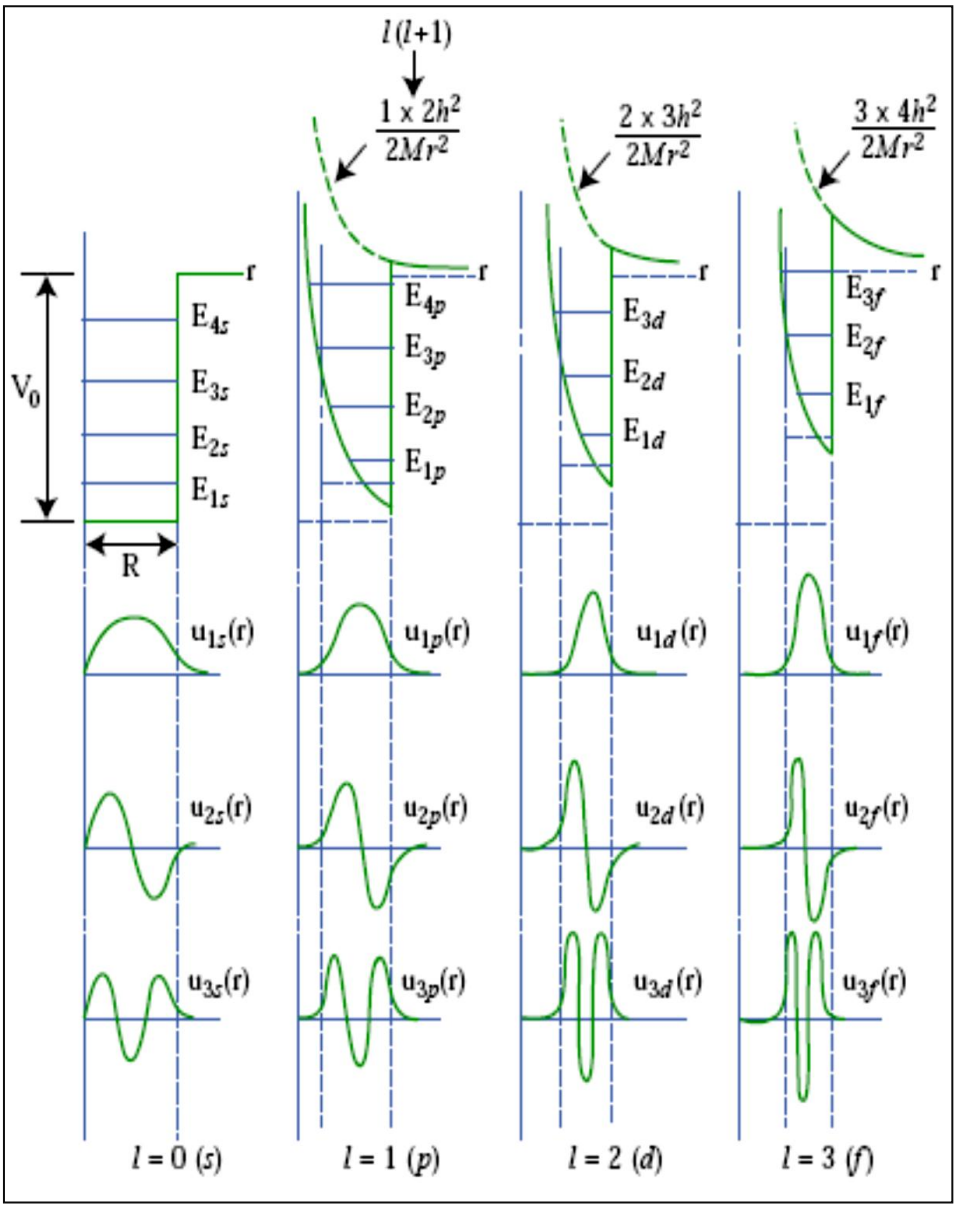

Figure 7.19. Energy levels and wave functions for a square well for ℓ = 0, 1, 2, and 3.

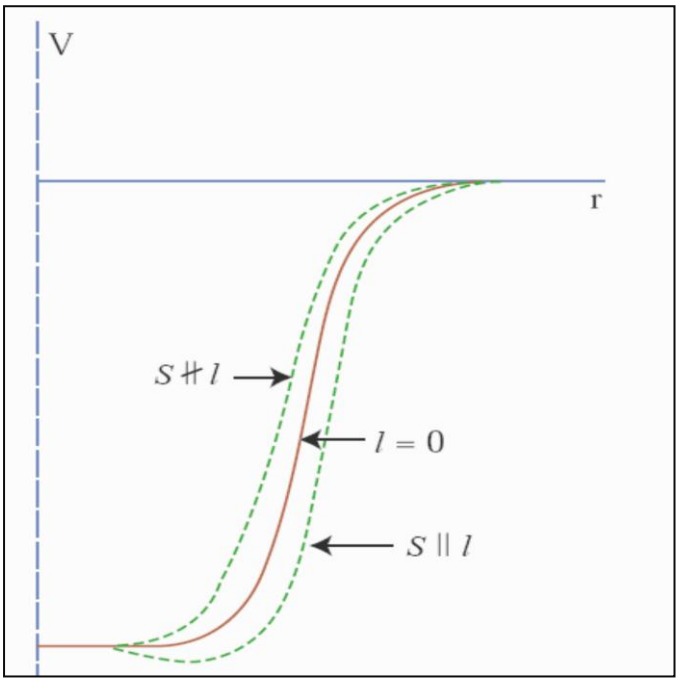

Figure 7.20. The effect of spin-orbit interaction on the shell-model potential.

We conclude this chapter with the remark that in addition to the bound states in the nuclear potential well there exists also virtual states (levels) which are positive energy states in which the wave function is large within the potential well. This can happen if the de Broglie wavelength is such that approximately standing waves are formed within the well. (Correspondingly, the reflection coefficient at the edge of the potential is large). A virtual level is, therefore, not a bound state; on the other hand, there is a non-negligible probability that inside the nucleus a nucleon can be found in such a state. See Fig. 7.21.

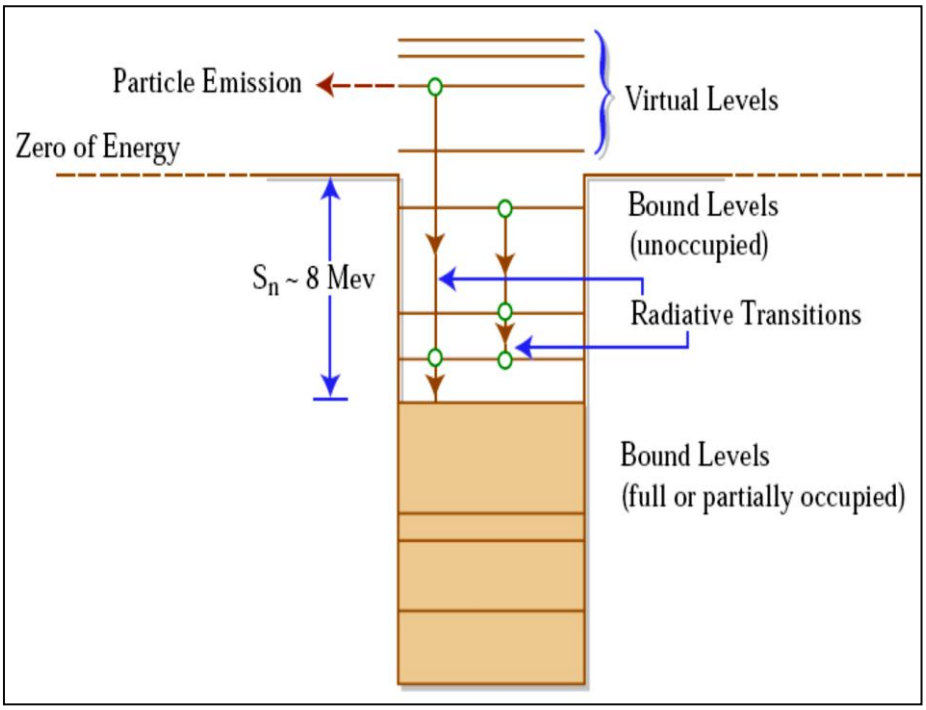

Figure 7.21. Schematic representation of nuclear levels.

Problems:

7-1. Derive in details the total kinetic energy of the nucleus (Eq. 7.9). Then expand your derivation to get the symmetry energy (Eq.7.11).

7-2. For each of the following nuclei, use the semiempirical mass formula to compute the total binding energy and the Coulomb energy. $^{21}_{10}Ne$, $^{57}_{26}Fe$, $^{209}_{83}Bi$.

7-3. The nuclear binding energy may be approximated by the empirical expression (Eq. 7.32)

a- Explain the various terms in this expression.

b- Considering a set of isobaric nuclei (nuclides that have the same mass number A), derive a relationship between A and Z for naturally occurring nuclei.

c- Use a Fermi gas model to estimate the magnitude of a_{sy}. You may assume that $A \neq 2Z$ and the nuclear radius is $R = R_o A^{1/3}$.

7-4. Use the formula derived in the problem7-3-b to find the most stable isobar of A = 25.

7-5. Use the semiempirical mass formula to estimate the α-decay energy of $^{242}_{98}Cf$ and compare it with the calculated value from Eq. 3.15.

7-6. The numbers of protons and neutrons are roughly equal for stable lighter nuclei; however, the number of neutrons is substantially greater than the number of protons for stable heavy nuclei. For light nuclei, the energy required to remove a proton or a neutron from the nucleus is roughly the same; however, for heavy nuclei, more energy is

required to remove a proton than a neutron. Explain these facts, assuming that the specific nuclear forces are exactly equal between all pairs of nucleons.

7-7.

a- Calculate the electrostatic energy of a charge Q distributed uniformly throughout a sphere of radius R.

b- Since $^{27}_{14}Si$ *and* $^{27}_{13}Al$ are "mirror nuclei", their ground states are identical except for charge. If their mass difference is 6 MeV, estimate their radius (neglecting the proton-neutron mass difference).

7-8. The nucleus $^{27}_{14}Si$ decays to its "mirror" nucleus $^{27}_{13}Al$ by positron emission. The maximum (kinetic energy+m_ec^2) energy of the positron is 3.48 MeV. Assume that the mass difference between the nuclei is due to the Coulomb energy. Assume that the nuclei to be uniformly charged spheres of charge Ze and radius R. Assuming that the radius is given by $r_oA^{1/3}$, use the above data to estimate r_o.

7-9. The binding energy of $^{90}_{40}Zr$ is 783.916 MeV. The binding energy of $^{90}_{39}Y$ is 782.410 MeV. Estimate the excitation energy of the lowest T = 6 isospin state in ^{90}Zr.

7-10. Consider a Fermi-gas model for atomic nuclei (containing protons and neutrons) in which the repulsive Coulomb force acting inside the nucleus gives rise to an approximate but constant Coulomb potential energy term. Thereby, we consider the nucleus as a homogeneously charged sphere with radius $R = r_oA^{1/3}$(with r_o = 1.2 fm). Show that the following expression between the proton and neutron numbers exists: $N = \left(Z^{2/3} + bZ^2A^{1/3}\right)^{3/2}$.

Determine the constant value of ***b***, using the Fermi-gas-model parameters only. Replace $Z\,(Z-1) \rightarrow Z^2$: use values of the various constants.

7-11. The spin-parity of ^{9}Be and ^{9}B are both $3/2^-$. Assuming in both cases that the spin and parity are characteristic only of the odd nucleon, show how it is possible to obtain the observed spin-parity of ^{10}B (3^+). What other spin-parity combinations could also appear? (These are observed as excited states of ^{10}B.)

7-12. Give the expected shell model spin and parity assignments for the ground states of (a) ^{7}Li, (b) ^{11}B, (c) ^{15}C, (d) ^{17}F, (e) ^{31}P, (f) ^{141}Pr.

7-13. The low-lying levels of ^{13}C are ground state, $1/2^-$; 3.09 MeV, $1/2^+$; 3.68 MeV, $3/2^-$; 3.85 MeV, $5/2^+$. The next states are about 7 MeV and above. Interpret these four states according to the shell model.

7-14. Fig. 7.18 illustrates the three possibilities for the first excited state of ^{17}O. Compute the energies values of the levels to prove the related conclusion.

7-15. In an odd-odd nucleus, the last neutron and proton go into a $1d_{3/2}$ and a $1g_{9/2}$ level, respectively. Use the shell model to predict the spin and parity of this nucleus.

7-16.

a- What spin-parity and isospin would the shell model predict for the ground states of $^{13}_{5}B$, $^{13}_{6}C$, *and* $^{13}_{7}N$?

b- Order the above isobaric triad according to mass with the lowest mass first. Briefly justify your order.
c- Indicate how you could estimate rather closely the energy difference between the two lowest-mass members of the above triad.

7-17. The level scheme of Fig. 7.14 would lead us to expect $I^{\pi} = 11/2^{-}$ for the ground state of $^{203}_{81}TI$, while the observed value is $1/2^{+}$. A similar case occurs in $^{207}_{82}Pb$ (N = 125) and $^{199}_{80}Hg$ (N = 119), where $13/2^{+}$ is expected but $1/2^{-}$ is observed. Given that the pairing force increases strongly with ℓ, give the shell-model configurations for these nuclei that are consistent with the observed spin-parity assignments.

7-18. In the single particle shell model, the ground state of a nucleus with an odd proton and an odd neutron is determined from the coupling of the proton and neutron shell model states: $I = j_p + j_n$. Consider the following nuclei: $^{16}_{7}N - 2^{+}; {}^{12}_{5}B - 1^{+}; {}^{34}_{15}P - 1^{+}; {}^{28}_{13}Al - 3^{+}$. Draw simple vector diagram illustrating these couplings, then replace j_p and j_n, respectively by $\ell_p + s_p$ and $\ell_n + s_n$. Examine your four diagrams and deduce an empirical rule for the relative orientation of s_p and s_n in the ground state. Finally, use your empirical rule to predict the I^{π} assignments of $^{26}_{11}Na \text{ and } {}^{28}_{11}Na$.

7-19. If the energy of a single-particle state in the absence of spin-orbit splitting is E_o, find the energies of the two members of the spin-orbit doublet whose difference is given by Eq. 7.61. Then, show that the center of gravity of the doublet is E_o.

7-20. Illustrate the degeneracy of each energy level from s to g and their corresponding spin-orbit pair. Then, compute the energy difference of each spin-orbit pair in MeV.

7-21. Consider a nuclear level corresponding to a closed shell plus a single proton in a state with the angular momentum quantum numbers l and j. Of course $j = l \pm 1/2$. Let g_p be the empirical gyromagnatic ratio of the free proton. Compute the gyromagnatic ratio for the level in question, for each of the two cases $j = l + 1/2$ and $j = l - 1/2$.

7-22. The low-lying levels of ^{17}O and ^{19}O differ primarily in the presence of states of $I^{\pi} = 3/2^{+}$ and $9/2^{+}$ in ^{19}O; these two states have no counterparts in ^{17}O. Show that these two states could result from the configuration $(d_{5/2})^3$ and thus are not expected in ^{17}O.

7-23. Among the energy levels of a central force potential is a level labeled 1d. Suppose we now add a spin-orbit interaction term to the Hamiltonian such as in the shell model. Using the spectroscopic notation, label the new levels that evolve from this 1d level. Specify how many nucleons can go into each of the new levels, and explicitly write out the quantum numbers specifying the wave function of each nucleon.

CHAPTER 8

INTERACTION OF CHARGED PARTICLES WITH MATTER (DIRECT IONIZING RADIATION)

The interactions of radiations with an external matter allow us to observe radiation and its effect, and to determine the nature of transition inside the nucleus. The interaction of radiation with matter is also the cause of chemical, physical and biological changes that concern the public at large.

8.1. Ionizing Radiation

Ionizing radiation is radiation with enough energy so that during an interaction with an atom, it can remove tightly bound electrons from the orbit of an atom, causing the atom to become charged or ionized.

All radiation can be divided into two main categories, ionizing radiation and non-ionizing radiation. Charged particles (hadrons and leptons), heavy ions and photons are considered ionizing radiation, as they can ionize an atom through electromagnetic interactions. Radiation such as infrared, microwave, long radio wave, and visible light and other neutral hadrons that do not ionize atoms or molecules on its path are called non-ionizing radiation.

Ionizing radiation consists of alpha, beta, protons, X-rays, cosmic rays and gamma rays that are energetic enough to detach electrons from atoms or molecules, ionizing them. The occurrence of ionization depends on the energy of the impinging individual particles or waves, not

on their number. An intense flood of particles or waves will not cause ionization if these particles or waves do not carry enough energy to be ionizing. Roughly speaking, particles or photons with energies above a few electron volts (eV) are ionizing.

Alpha and beta particles are considered directly ionizing because they carry a charge and can, therefore, interact directly with atomic electrons through coulombic forces (i.e., like charges repel each other; opposite charges attract each other).

Gamma and X rays, which are electromagnetic, are indirectly ionizing radiation because they are electrically neutral (as are all electromagnetic radiations) and do not interact with atomic electrons through coulombic forces.

Strictly speaking, neutrons do not cause ionization. However, they induce radioactivity and eventually lead to ionization. The neutron is an indirectly ionizing particle because it does not carry an electrical charge. Because of the interesting properties of neutrons in science and technology, a separate chapter will devoted to this topic.

8.2. Reaction Cross-Section

It is generally only possible to measure the probability of the interaction of radiation with atoms. In such circumstances, it is natural to introduce the statistical concept of “cross-section” for a given interaction.

Since interactions in a reaction take place with individual target nuclei independently of each other, it is useful to refer the probability of nuclear reaction to one target nucleus. We need neither assume that a nucleus is spherical in shape nor that it behaves as a solid elastic sphere of radius R toward projectiles particle. We sometimes talk of the "geometrical"

cross section given by πR^2, where R is the radius of the nucleus given by Eq.1.28. However, a more useful concept is the cross section of a nucleus for a given process such as the cross section for the scattering of charged particles, or for the absorption of certain particles or radiation such as gamma rays.

To follow such concept experimentally, assume a sufficiently thin slab of target material of area A and thickness δx (say one atomic layer thick) containing N_t nuclei as a spheres of radius R_c (also called impact parameter) is struck by a monoenergetic beam consisting of N_o free particles, as shown in Fig. 8.1. A certain fraction of the beam particles will interact with the target nuclei, either scattering into a new direction or reacting in a way that particles are created or destroyed. A point-like particles impinging upon the slab at a random position will have a probability δP of hitting one of the nuclei that is equal to the fraction of the surface area covered by a nuclei.

$$\delta P = \frac{N_t \pi R_c^2}{A} = \sigma n \delta x \qquad \sigma = \pi R_c^2 \tag{8.1}$$

Here, $N_t = n \times A \times \delta x$, where n is the number of nuclei per unit volume.

In the mean time, if N_i is the number of particles that are lost due to the interaction with the target nuclei, then:

$$\delta P = \frac{N_i}{N_o} \qquad or \qquad N_i = N_o \sigma n \delta x \tag{8.2}$$

from which:

$$\sigma = \frac{N_i}{N_o n \delta x} \qquad 8.3$$

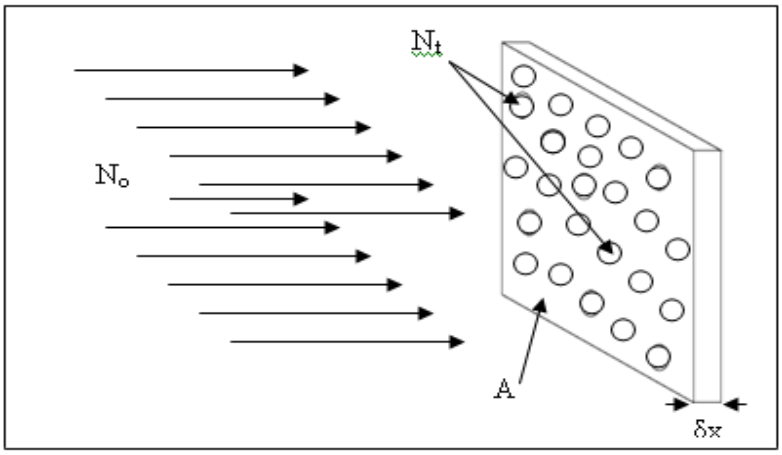

Figure 8.1. A monoenergetic beam of N_o particles incident normally upon a thin target of *n* nuclei per unit volume. Each circle represents the cross section σ associated with a target entity such as an atom.

Eq. 8.3 can be used to determine the nuclear reaction cross section from empirical data.

Since the nuclear radius is roughly 10^{-12} cm, the geometrical cross sectional area is of the order of 10^{-24} cm^2. Hence, we might expect that nuclear cross sections (σ) are of the same order of 10^{-24} cm^2, without misleading the geometrical nuclear geometrical cross sectional area. Since σ can be much larger (or smaller) than the geometrical cross section of the nucleus due to resonance effects, this in turn, are a consequence of the quantum mechanical nature of the particle and the nucleus. It has been found convenient to use a separate name for this area. The name adopted is barn (b); that is, 1 b = 10^{-24} cm^2.

The above discussion can be applied to any type of nuclear reaction. Thus, σ_s may denote the cross section for scattering of a given kind of incident particle, σ_a refer to absorption cross section and $\sigma(x,y)$ indicate individual reactions.

The expression for the number of processes of a given kind of reaction, say the i^{th} kind, contains the product $n\sigma_i$. This product represents the cross section, for the i^{th} process, of all the atoms in a cubic centimeter of material. It is sometimes called the *macroscopic cross section* which has a unit of cm^{-1}, and dented by Σ, while σ is called *microscopic cross section*:

$$\Sigma_i = n\sigma_i \qquad 8.4$$

Accordingly, the usual procedure for dealing with mixtures and compounds is to assume that each atom scatters independently. This represents the macroscopic cross section of the mixture. If the cross section for element j summed over all the interaction processes of interest is denoted by σ_j, the cross section per molecule is the sum of the cross sections for all the atoms in the molecule. If the volume of the compound V contains a total mass $M = \rho V$ and the mass of each element is M_j, the mass fraction is $w_j = M_j/M$. The total number of atoms of species j in volume V (number density) is $n_j = \frac{M_j N_A}{A_j V} = \frac{w_j}{A_j}\rho N_A$, where N_A is Avogadro's number.

The mass fraction of element j in a compound containing a_j atoms per molecule with atomic mass A_j is $w_j = a_j A_j / A_{mol}$, where A_{mol} is the molecular weight. Therefore:

$$\sum_j n_j \sigma_j = \left(\sum_j \frac{a_j \sigma_j}{A_{mol}} \right) \rho N_A$$
$$= \left(\sum_j a_j \sigma_j \right) \frac{\rho N_A}{A_{mol}} = \sigma_{mol} n_{mol} = \sum_{mol} \quad 8.5$$

Where the factor $n_{mol} = \rho N_A / A_{mol}$ is the number of molecules per unit volume. When a target entity (molecule) consists of a collection of sub-entities (atoms), we can say that, in this approximation (all sub-entities interacting independently), the cross section per entity is the sum of the cross sections for each sub-entity. For example, for the molecule CH_4, the total molecular cross section is

$4\sigma_{hydrogen} + \sigma_{carbon}$ and the molecular weight is

$A_{mol} = [(4 \times 1) + 12] = 16$ g mol^{-1}.

8.2.1. Attenuation cross section

The attenuation of a beam of particles or electromagnetic ray with identical energies, all traveling in the same direction, is described by an exponential law. This exponential attenuation law follows from the fact that, over any short distance, the probability of losing a particle from the beam is proportional to the number of particles left.

The transmission method for the experimental determination of cross section is based on measurements of the attenuation of the monoenergetic radiation beam after passing through a slab of target material of finite thickness. Suppose a collimated beam of particles strikes perpendicularly a specified area of material of appreciable thickness as in Fig. 8.2. Consider a thin layer, of thickness *dx*, parallel to the surface; then it follows that $n\sigma dx$ is the fraction of the particles falling on this layer. This may be set

equal to $-d\Phi/\Phi$, where Φ is the beam flux (number of particles per unit area per sec) and $-d\Phi$ is the decrease in the particles per unit area as the result of passing though the thickness dx of target material. Consequently,

$$-\frac{d\Phi}{\Phi} = n\sigma dx \qquad 8.6$$

and integration over the thickness x of the material gives:

$$\begin{aligned}\Phi_x &= \Phi_o e^{-n\sigma x} \\ &= \Phi_o e^{-\Sigma x}\end{aligned} \qquad 8.7$$

where Φ_o is the incident flux or number of incident particles falling on a particular area and Φ_x is the numbers which succeed in passing through x cm of the material over the same area. The cross section determined in this manner is the total cross section (absorption, scattering) $\sigma = \sum\sigma_i$.

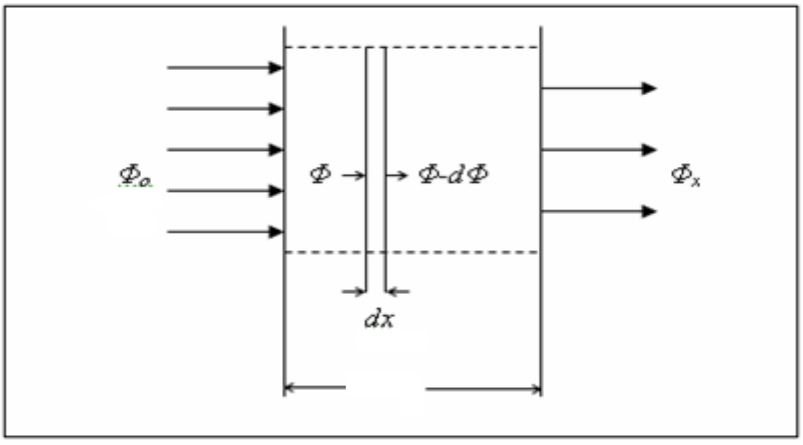

Figure 8.2. Attenuation of a collimated particle beam in passage through a slab.

8.2.2. Differential scattering cross section

It is frequently useful to introduce a generalization of the concept of a particle cross section characterizing the scattering cross section. In such reactions, the incident particle will usually experience a change in both directions of motion and energy in the scattering event, (just imagine a billiard-ball collision). The microscopic scattering cross section will describe the probability that such a scattering collision occurs. However, it provides no information about the change in particle direction or energy that occurs in such a collision. This latter information is very important in certain types of neutron-nucleus interactions. To characterize it, we must introduce the concept of the *differential scattering cross section*.

To describe cross sections characterizing changes in particle energy and direction, one must utilize a bit of vector notation. The natural choice would be the particle velocity $\boldsymbol{v}$. Then the cross section we wish to define would describe the probability that a particle incident with a velocity $\boldsymbol{v}$ would be scattered by an atomic electron or nucleus to a new velocity $\boldsymbol{v}'$. It is essential to decompose the particle velocity vector into two components, one variable characterizing the particle speed or kinetic energy (more convenient in neutron-nucleus interaction, will be discussed in chapter 10) and a second variable for the particle direction of motion.

To specify the direction of particle motion, we introduce a unit vector $\boldsymbol{\Omega} = \boldsymbol{v} / |\boldsymbol{v}|$ in the direction of particle velocity.

To know the probability that particles are scattered from an incident direction $\boldsymbol{\Omega}$ to a final direction $\boldsymbol{\Omega}'$, $\sigma(\Omega \rightarrow \Omega')$ we have to consider the probability that they are scattered into a small solid angle $d\boldsymbol{\Omega}$, Fig. 8.3. In this case $\sigma(\Omega \rightarrow \Omega')$, can be written as the differentiation of $\sigma(\Omega) = \sigma$:

$$\sigma(\Omega \to \Omega')d\Omega = \frac{d\sigma}{d\Omega}d\Omega \quad or \quad \sigma(\theta)d\Omega \tag{8.8}$$

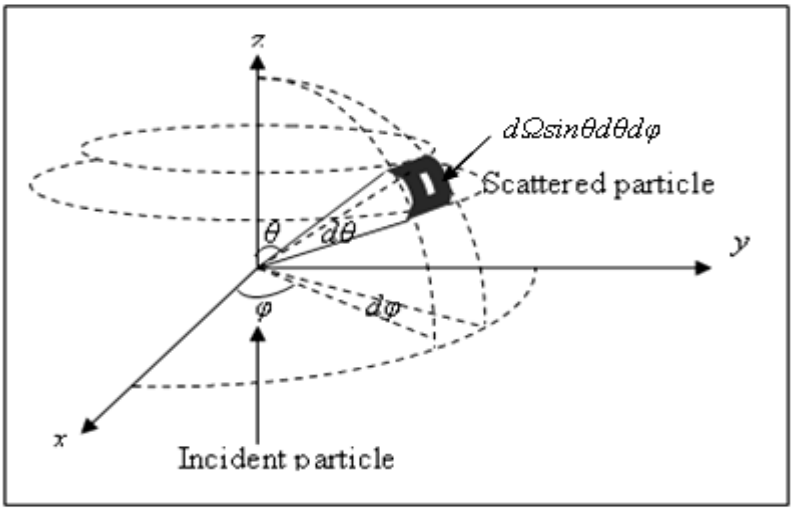

Figure 8.3. The scattered particle within a solid angle $d\Omega = \sin\theta\, d\theta\, d\varphi$ surrounds the direction defined by angles θ and φ.

The differential cross section $\sigma(\Omega \to \Omega')$ is related to our earlier microscopic cross section by integration over all final directions:

$$\sigma = \int_{4\pi} \frac{d\sigma}{d\Omega} d\Omega = \int_0^{2\pi} d\varphi \int_0^{\pi} \sin\theta d\theta \frac{d\sigma}{d\Omega}(\theta, \varphi) \tag{8.9}$$

It should be mentioned that the dependence of the scattering cross section $\sigma(\Omega)$ on the incident particle direction is usually ignored; it depends on the scattering angle θ, or more conveniently, the cosine of this scattering angle $\mu_0 = \cos\theta$. In other words, the cross section has no φ dependence, then the integration over φ can be carried out

and $d\Omega = 2\pi \sin\theta \, d\theta$, Fig. 8.3. While if the target or beam particles are polarized, it can be a function of the azimuthal angle φ.

8.2.3. Mean free path

As particles pass through material, they undergo collisions that may change their direction of motion. The average distance between these collisions is, therefore, a measure of the probability of a particular interaction. This distance, generally known as the mean free path, is inversely proportional to the cross section and the density of the material, which is:

$$\lambda = \frac{1}{n\sigma} = \frac{1}{\Sigma} \qquad 8.10$$

Note that the definition of the mean free path depends on the type of cross section used in the calculation. For example, if scattering cross section is used, the mean free path would correspond to just the scattering process. However, in most instances, such as when calculating the shielding required in a radiation environment, one uses total cross section, which gives the total mean free path.

8.3. Interactions of Charged Particles

It is natural when a free charged particle, with a certain kinetic energy passes through material; it faces the atoms and their constituents (negative electrons and positive nucleus). Three possible interaction processes may take place with different probability of each process; interaction

with the electrons of the atom, interaction with the nucleus, or radiation due to deceleration of the particle.

The basic mechanism for the interaction of a moving charged particle is Coulombic interactions between the particle and electrons in the medium. This is common to all charged particles. The particle loses on the average not more than a few electron volts of kinetic energy; ionization and excitation of atoms give the greatest energy loss per unit path length of the particle.

While in the interaction with the nucleus (nuclear interaction), the loss of kinetic energy would be much larger, but the probability of such collision are extremely rare compared to atomic interaction. Roughlyit is in proportion to the area of cross section of nucleus compared to that of the atom ($10^{-26}cm^2$ / $10^{-18}cm^2$= 10^{-8}). Hence, the interactions with nuclei do not contribute appreciably to the overall energy loss.

For kinetic energies larger than the rest mass energy of the particle, m_oc^2, energy loss by emission of electromagnetic radiation becomes increasingly important. The radiation is called Bremsstrahlung-breaking (decelerating radiation). It is caused by the same mechanism as the emission of continuous X-ray. The basic process can be understood classically. According to Maxwell's equations, any accelerated charge radiates electromagnetic radiation. If a charged particle passes close to a nucleus, its velocity vector will be rapidly changed (at least in direction if not in magnitude), so that the particle undergoes an acceleration and hence it radiates. Radiation is only important for electrons and occurs in a certain fraction of the elastic electron scatterings from the target nucleus. Nuclear scattering causes a fairly large change in the electron acceleration and consequently its energy.

If we ignore nuclear forces and consider only the interactions arising from Coulomb forces, we can speak of four principal types of charged-particle interactions:

1- *Inelastic Collision with Atomic Electrons*. This is the principal process of energy transfer, particularly if the particle velocity is below the level where Bremsstrahlung is significant. It leads to the excitation of the atomic electrons (still bound to the nucleus) and to ionization (electron stripped off the nucleus). Inelastic here refers to the excitation of electronic levels.
2- *Inelastic Collision with a Nucleus*. This process can leave the nucleus in an excited state or the particle can radiate (Bremsstrahlung).
3- *Elastic Collision with Atomic Electrons*. The process is elastic deflection which results in a small amount of energy transfer. It is significant only for charged particles that are low-energy electrons.
4- *Elastic Collision with a Nucleus*. This process is known as Rutherford scattering. There is no excitation of the nucleus, nor emission of radiation. The particle loses energy only through the recoil of the nucleus.

In general, interaction of type (1), which is sometimes simply called collision, is the dominant process of energy loss, unless the charged particle has a kinetic energy exceeding its rest mass energy, in which case the radiation process, type (2), becomes important.

8.3.1. Energy-Loss mechanisms: Stopping power

Each interaction of a charged particle with atomic electron usually causes only a slight decrease in the particle's energy, and it is convenient to follow the charged particle along its path.

It is convenient to speak of how much energy the charged particle loses per unit path length, the *stopping power* and roughly its *range* (the total distance it travels before losing all its energy). The stopping power is the expectation value of the amount of kinetic energy T lost by the projectile per unit path length, denoted by S. The *mass stopping power* is the stopping power divided by the density of the stopping material (often we will say stopping power when we actually mean mass stopping power):

$$S = -\frac{dT}{dx}, \qquad \frac{S}{\rho} = -\frac{1}{\rho}\frac{dT}{dx} \tag{8.11}$$

There are quantum mechanical as well as classical theories for calculating this basic quantity. One wants to express $-dT/dx$ in terms of the properties specifying the incident charged particle, such as its mass M, velocity υ and charge ze, the properties pertaining to the atomic medium, the charge of the atomic nucleus Ze, the density of atoms n, and the average ionization potential I.

We consider only a crude, approximate derivation of the formula for $-dT/dx$. We begin with an estimate of the energy loss suffered by an incident charged particle when it interacts with a free and initially stationary electron. Fig. 8.4 shows a collision cylinder whose radius is the impact parameter b and whose length is the small distance traveled dx. If F be the coulomb force exerted on the electron, we see that the net momentum transferred to the electron P_e as the particle moves from one end of the cylinder to the other end is essentially entirely directed in the perpendicular direction (because F_x changes sign, so the net momentum along the horizontal direction vanishes) along the negative y-axis.

$$\int F_x(t)dt \approx 0$$
$$\int F_y(t)dt = P_e \qquad 8.12$$

If the impact parameter of the collision is b and the speed of the particle υ, P_e can be estimated from the time of the impact $dt = dx/\upsilon$:

$$P_e = \int_{-\infty}^{\infty} \frac{ze^2}{x^2 + b^2} \frac{b}{(x^2 + b^2)^{1/2}} \frac{dx}{\upsilon}$$

$$\cong \frac{ze^2 b}{\upsilon} \int_{-\infty}^{\infty} \frac{dx}{\left(x^2 + b^2\right)^{3/2}} = \frac{2ze^2}{\upsilon b} \qquad 8.13$$

here, $e = 4.8\times10^{-10}$ *esu*.

The smaller the impact parameter is, the greater the momentum transfers to the electron. The kinetic energy acquired by the electron (transferred to the electron) is therefore:

$$W = \frac{P_e^2}{2m_e} = \frac{2(ze^2)^2}{m_e b^2 \upsilon^2} \qquad 8.14$$

Note that *W* does not depend on the mass of the projectile, but only on its speed. As the speed becomes less, the energy transfer becomes greater, because the projectile takes longer to move past the electron and the force is exerted for a longer time (as long as the time is still short enough so that the impulse approximation remains valid).

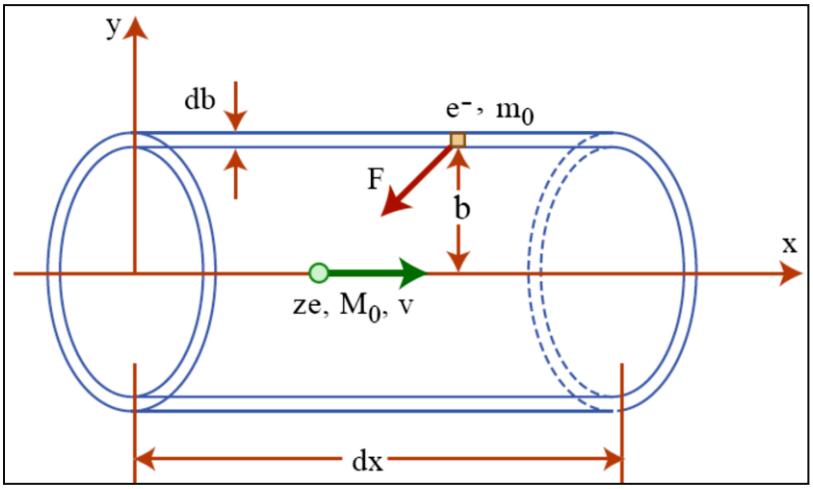

Figure 8.4. Collision cylinder for deriving the energy loss to an atomic electron by an incident charged particle.

If there are *n* atoms per unit volume (number density) each with *Z* electrons, in a path length *dx*, there will be *nZ (2πb dbdx)* electrons within a distance b to b + db from the path of the particle. To each of these electrons, the particle losses an amount of energy given by expression (Eq. 8.13) so that the total energy loss per unit path will be the result of multiplication:

$$S = -\frac{dT}{dx} = \int_{b_{\min}}^{b_{\max}} nZ\,2\pi b db \frac{2}{m_e}\left(\frac{ze^2}{\upsilon b}\right)^2$$

$$= \frac{4\pi (ze^2)^2 nZ}{m_e \upsilon^2} \ln\left(\frac{b_{\max}}{b_{\min}}\right) \qquad 8.15$$

Where b_{max} and b_{min} are the maximum and minimum impact parameters which one should specify according to the physical description he wishes to treat.

This expression is an approximate, since for nearly head-on collisions, Eq. 8.14 is not valid. In reality, the atomic electrons are rotating in certain orbits (not free electrons), so the charged particle must transfer at least an amount of energy equal to the first excited state of the atom. If we take the time interval of energy transfer to be $\Delta t \approx b / \upsilon$, the maximum time of impact $(\Delta t)_{max}$ must not be longer than the period of rotation of a typical electron in its orbit $1/\nu$, where ν is the frequency of rotation, i.e., $(\Delta t)_{max} \sim 1/\nu = b_{max}/\upsilon$, then:

$$b_{\max} = \frac{\upsilon}{\nu} \qquad 8.16$$

Since $h\nu \approx \bar{I}$ is the mean ionization potential. This gives an estimate of the maximum impact parameter:

$$b_{\max} \approx \frac{h\upsilon}{\bar{I}} \qquad 8.17$$

Values of $\bar{I}$ have been calculated theoretically and also derived from measurements of the stopping power. They range from 14.8 eV for hydrogen to 884 eV for uranium. The value 14.8 eV is greater than the ground-state energy of hydrogen, 13.6 eV, because the ejected electron has some average kinetic energy. An empirical expression for $\bar{I}$ is $\bar{I} \approx kZ$, with k ~ 19 eV for H and ~ 10 eV for Pb.

Next we estimate b_{min} by using the uncertainty principle to say that the electron position cannot be specified more

precisely than its de Broglie wavelength (in the relative coordinate system of the electron and the charged particle). Since electron momentum in the relative coordinate system is $m_e v$, we have:

$$b_{\min} \approx \frac{h}{m_e \upsilon} \qquad 8.18$$

Combining these two estimates we obtain:

$$S = -\frac{dT}{dx} = \frac{4\pi z^2 e^4 nZ}{m_e \upsilon^2} \ln\left(\frac{2m_e \upsilon^2}{\bar{I}}\right) \qquad 8.19a$$

or

$$S = -\frac{dT}{dx} = D\left(\frac{Z}{A}\right)\rho \frac{z^2}{\beta^2} \ln\left(\frac{2m_e \upsilon^2}{\bar{I}}\right) \qquad 8.19b$$

In Eq. 8.19b, $D = 4\pi N_A e^4/m_e c^2 = 0.32$ MeV.cm^{-1} and $\beta = \upsilon/c$. By introducing numerical values of the constants and if the target matter is of mass density ρ and consists of atoms of atomic number Z, atomic mass $M(Z)$, the number of electrons per unit volume is $(\rho N_A/M(Z))Z$ and the medium number density $n = \rho N_A/M(Z) \approx \rho N_A/A$.

In Eq. 8.19, we have inserted a factor of 2 in the argument of the logarithm; this is to make our formula agree with the result of quantum mechanical calculation which was first carried out by H. Bethe using the Born approximation.

Eq. 8.19 is a relatively simple expression, yet one can gain much insight into the factors that govern the energy loss of a charged particle by collisions with the atomic electrons. We can see why the usual neglect of the contributions due to collisions with nuclei is justified. In a collision with a nucleus, the stopping power would increase

by a factor Z, because of the charge of the target nuclei with which the incident charged particle is colliding and decrease by a factor of $m_e/M(Z)$. The decrease is a result of the larger mass of the recoiling target. Since Z is always less than 10^2 whereas $M(Z)$ is at least a factor 2000 greater than m_e (for ^{1}H as a medium, $m_e/M_H \approx 1/1837$), the mass factor always dominates over the charge factor. On the other hand, scattering from the weakly-bound atomic electrons (and ionization) represents an inelastic process that requires energy transfer. Consequently, the dependence of energy loss in Eq. 8.19b on the inverse of the mass of the target supports our previous contention that, ignoring strong nuclear collisions, small-angle scattering from atomic electrons is the dominant mechanism of energy deposition for massive charged particles traversing matter.

Another useful observation is that (Eq. 8.18) is independent of the mass of the incident charged particle. This means that nonrelativistic electrons and protons of the same velocity would lose energy at the same rate or, equivalently, the stopper power of a proton at energy T is about the same as that of an electron at energy ~ $T/2000$.

Eq. 8.19 describes the energy loss due to particle collisions in the nonrelativistic regime. One can include relativistic effects by replacing the logarithm in Eq.8.19 and introducing the velocity of the particle relative to the speed of light, $\beta = v/c$ and $\gamma = \left(1 - v^2/c^2\right)^{-1/2}$:

$$S = -\frac{dT}{dx} = \frac{4\pi z^2 e^4 nZ}{m_e c^2 \beta^2}\left[\ln\left(\frac{2m_e c^2 \gamma^2 \beta^2}{\bar{I}}\right) - \beta^2\right] \qquad 8.20$$

This correction can be important in the case of high energetic particles (produced in accelerator experiments),

electrons and positrons. The above expression for S has been confirmed for different kinds of media and various types of particles, over a wide range of energies.

In light of the previous arguments, the relativistic factors that govern the energy loss of a charged particle can be discussed. Because of the β^{-2} dependence in Eq. 8.20, at low particle velocities, the ionization loss is quite sensitive to particle energy. In fact, this dependence on υ^{-2} suggests that particles of different rest mass (M_o) but same momentum *(p)* can be distinguished because of their different rates of energy loss. Although S has no explicit dependence on particle mass, for any fixed momentum, the effect of mass comes in through:

$$S \propto \frac{1}{\upsilon^2} = \frac{M^2\gamma^2}{P^2} \qquad 8.21$$

Consequently, at low velocities ($\gamma \approx 1$), particles of the same momentum but different mass will display significantly different energy loss. Independent of particle mass, the stopping power decreases with increasing particle velocity and S displays a rather shallow minimum when $\gamma\beta << 3$ ($\upsilon << 0.96c$ or $T << 3Mc^2$) that is, the minimum occurs at higher momenta for more massive particles. This minimum in Eq. 8.20 is due to the convolution of the decrease in S caused by the β^{-2} dependence (β saturates at $\beta \approx 1$or $\upsilon = c$ at high energies) and the rise caused by the $\ln\gamma^2$ term that is due to relativistic effects. When the stopping power is displayed as a function of $\gamma\beta$ or P/Mc, S is almost independent of M, and we can, therefore, say that S "scales as" $\gamma\beta$ or P/Mc, see Fig. 8.5.

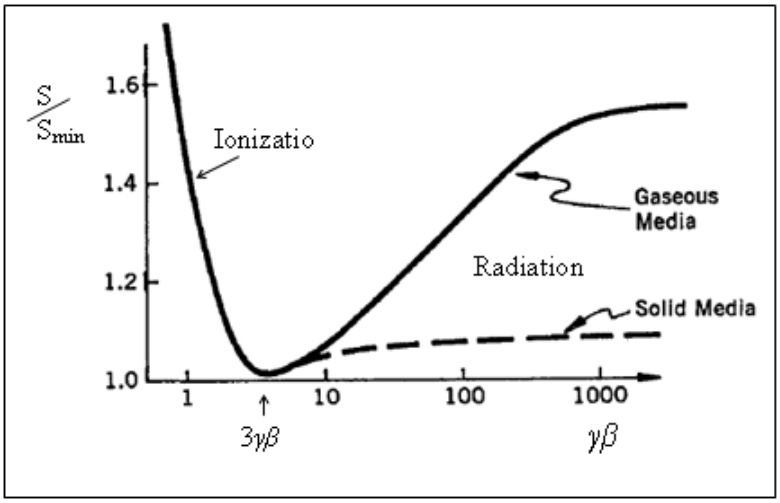

Figure 8.5. Stopping power relative to its minimum value as a function of $\gamma\beta$ or P/Mc.

The relativistic β^2 rise in S for $\gamma\beta > 3$ ($T > 3Mc^2$) eventually plateaus (saturates) because of the presence of long-range inter-atomic screening effects (ignored in the Bethe-Bloch calculation). The total increase in ionization is rarely greater than 50% beyond the value measured for a "minimum-ionizing" particle, namely a particle that has $\upsilon << 0.96c$ ($T << 3Mc^2$). The relativistic rise is best observed in gaseous media and is only a several percent effect for dense materials. Nevertheless, this can be used to distinguish different particle types through their small differences in energy loss in gaseous detectors for energies corresponding to $\gamma\beta > 3$.

At very high energies, after the saturation of the relativistic rise, ionization loss becomes an energy-independent constant rate and it is, therefore, not possible to distinguish particle-types purely on the basis of ionization. Except in gaseous media, the stopping power at high

energies can be approximated quite adequately by the value when $\gamma\beta \approx 3$.

When $\gamma\beta \approx 3$ (β = 0.9), the minimum value of the stopping power S_{min} for a particle can be evaluated approximately from Eq. 8.20 after inserting the values of constants *and* $\bar{I} \approx 10Z$.

$$
\begin{aligned}
S_{\min} &= \frac{4\pi z^2 e^4 N_A \left(\frac{\rho Z}{A}\right)}{m_e c^2 \beta^2} \ln\left(\frac{2m_e c^2 \gamma^2 \beta^2}{\bar{I}}\right) \\
&\approx \frac{0.32\,(\mathrm{MeV.cm^{-1}})}{0.9} z^2 \left(\frac{\rho Z}{A}\right) \ln\left(\frac{2 \times 0.51(MeV) \times 9}{10 \times 10^{-6}(MeV) Z}\right) \\
&\approx 0.35 z^2 \left(\frac{\rho Z}{A}\right)[13.7 - \ln Z] MeV.cm^{-1}
\end{aligned}
$$

The ln$Z$ term is relatively small (< 4.5) for the heaviest elements and it varies slowly with Z. Let us, therefore, use $Z \approx 20$ to get an approximate result:

$$
\begin{aligned}
S_{\min} &\approx 3.5 z^2 \left(\frac{\rho Z}{A}\right) Mev.cm^{-1} \\
&\approx 3.5 z^2 \frac{Z}{A} MeV.cm^2.g^{-1}
\end{aligned}
\qquad 8.22
$$

As we mentioned before, Eq. 8.22 can also be used as a high-energy approximation for ionization loss in most media.

We should also point out that, at very low energies, the stopping power in Eq. 8.20 becomes unphysical (negative), reflecting the fact that ionization loss is very small when the velocity of the particle is small. In this regime, the details of

the atomic-structure of the medium become important, and the incident particle can even capture electrons from the medium to form atomic systems of its own.

As physics is an experimental science, experiments provide the foundation for our understanding of nature and physical laws. In these sub-atomic domains, scattering of particles from each other provides the primary source of information. To be more confident, we support the above discussion by experimental results. Fig. 8.6 shows an experimentally determined energy loss curve *S* for a heavy charged particle (proton) in air, on two energy scales. (a) An expanded low-energy region where, the Bethe formula applies down to $T \sim 0.3$ MeV with $I \sim 80$ eV. The stopping power decreases smoothly with increasing kinetic energy of the charged particle *T* below a certain peak centered about 0.1 MeV. Below this range charge loss energy due to electron capture causes the stopping power to reach a peak and starts to decrease. (b) A more compressed high-energy region where the stopping power reaches a broad minimum around 10^3 MeV. Notice also a slight upturn as one goes to higher energies past the broad minimum which we expect is associated with relativistic corrections.

Experimentally, the collision energy loss is measured through the number of ion pairs formed along the trajectory path of the charged particle. Suppose a heavy charged particle loses on the average an amount of energy W (Eq. 8.14) in producing an ion pair, an electron and a positive ion. Then the number of ion pairs produced per unit path is:

$$i = \frac{1}{W} S \qquad 8.23$$

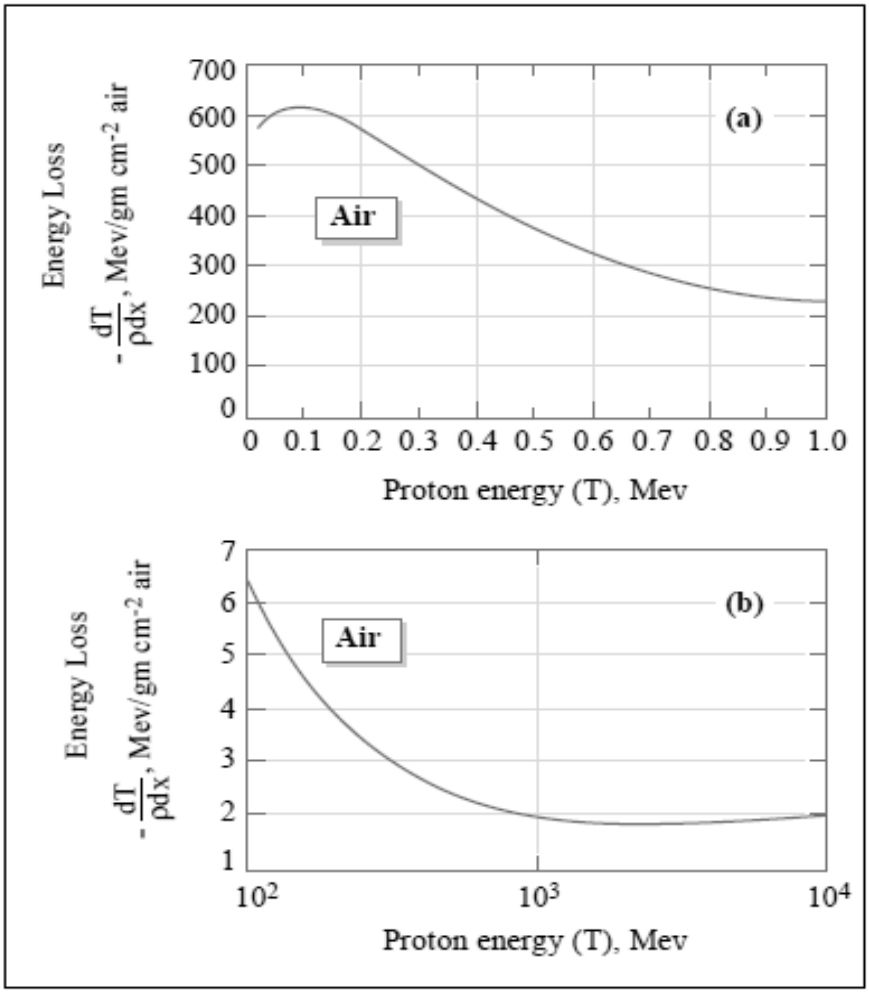

Figure. 8.6. The experimentally determined stopping power for protons in air, (a) low-energy region, (b) high-energy region.

8.3.2. Range of charged particles

As particles entering a matter with the same energy, it is normal to assume that all particles travel about the same

distance before coming to rest. This distance is called the *range*. Roughly, the range is the total distance the particle travels before losing all its energy.

We can estimate the range from the stopping power as it represents an average energy loss per unit path length. The actual energy loss fluctuates about the mean values given by the stopping power. If these fluctuations are neglected and the projectiles are assumed to lose energy continuously along their tracks at a rate equal to the stopping power, one is making the *continuous slowing-down approximation* (CSDA). In this approximation, one can calculate the range, the distance a particle with initial energy T_o travels before coming to rest or reaching some very small final kinetic energy $T_f \approx 0$:

$$R = \int_0^R dx = \int_{T_f}^{T_o} \frac{dT}{dT/dx} = \int_{T_o}^{T_f} \frac{dT}{S} \qquad 8.24$$

The CSDA range is not directly measurable. The range of a single particle may be slightly larger or smaller than expression 8.20 because there are statistical variations in the amount of energy lost per unit path length and in the total number of ions pairs formed. This is called *straggling* as shown in Fig. 8.7.

Measurements of the fraction $F(R)$ of monoenergetic particles in a beam that passes through an absorber of thickness R gives a curve like that of Fig. 8.7. Various ranges can be defined using this curve. The most easily measured range is the median range R_{50}, corresponding to an absorber thickness that transmits 50% of the incident particles. The extrapolated range R_{ex} is obtained by extrapolating the linear portion of the curve to the abscissa. The maximum range R_m is the thickness that just stops all of

the particles; it is, of course, very difficult to measure. If $F(R)$ is known accurately, one can define a *mean range* $<R>$.

$$< R >= \int R\left(-\frac{dF}{dR}\right)dR \Big/ \int\left(-\frac{dF}{dR}\right)dR \qquad 8.25$$

The range is expressed in g cm^{-2}; that is, the range in cm multiplied by the density of the matter. Like mass stopping power, the range in g cm^{-2} applies to all materials of similar atomic composition.

For two heavy charged particles of rest masses and charge M_1, z_1 and M_2, z_2 at the same initial speed β, the ratio of their ranges can be simply determined by scaling low:

$$\frac{R_1(\beta)}{R_2(\beta)} = \frac{z_2^2 M_1}{z_1^2 M_2} \qquad 8.26$$

If particle number 2 is a proton ($M_2 = 1$ and $z_2 = 1$), the range R of the other particle is given with respect to the range of proton $R_p(\beta)$ by:

$$R(\beta) = R_p(\beta)\frac{M}{z^2} \qquad 8.27$$

Another useful relation, Bragg and Kleeman gave a formula to compute the range of a particle in a medium if its range is known in another medium.

$$\frac{R_1}{R_0} = \frac{\rho_0\sqrt{A_1}}{\rho_1\sqrt{A_0}} \qquad 8.28$$

Here, ρ and A represent the density and atomic mass of the materials. If we have a compound material, a molecular weight (as in section 8.2) is given by, $A_{mol} = \sum_i \frac{a_i A_i}{w_i}$.

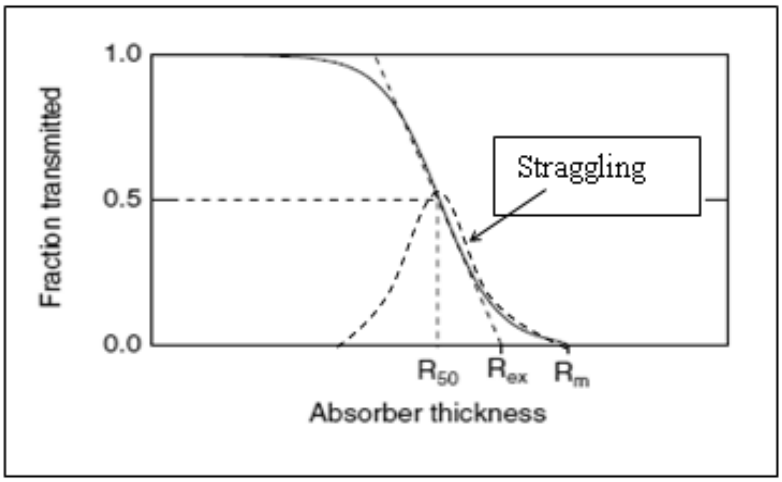

Figure 8.7. The ranges of charged particles, the median range R_{50}, extrapolated range R_{ex}, and maximum range R_m.

8.3.3. Newtonian dynamics of the collision

In non-relativistic Newtonian dynamics, when a projectile object (particle or ion) of mass *M* of a velocity *v* hits a stationary object (orbital electron or nucleus) of mass *m* head-on, the laws of dynamics predict the energy lost by the incident particle (transferred to the electron or nucleus).

As discussed in Chapter 3, the maximum possible energy transferred W_{max} to the target, can be calculated using conservation of energy and momentum.

$$W_{\max} = \frac{4mMT}{(M+m)^2} \qquad 8.29$$

where $T = \frac{1}{2}M\upsilon^2$ is the initial kinetic energy of the incident particle.

The incident particle can scatter from stationary nuclei, while the following assumptions of ionization or excitation of atomic electrons are required:

1. The particle moves rapidly compared with the electron.
2. For maximum energy transfer, the collision is head-on.
3. The energy transferred is large compared with the binding energy of the electron in the atom.
4. Under these conditions, the electron is considered to be initially free and at rest, and the collision is elastic.

The energy transferred is a very small fraction of the incident particle's energy when a massive particle collides with a much lighter particle, the atomic electron. However, when $M = m$ (case of incident electron), all the kinetic energy is transferred to the target electron ($T_e = T$) and the projectile electron stops.

This result is strictly true only for particles traveling with speeds much less than that of light (non-relativistic speeds) but similar results are obtained also for relativistic particle speeds. When the collision is not head-on, the energy transfer to the target is less and, of course, the energy loss of the incident particle is correspondingly less.

8.4. Classification of Charged Particles

Although the above fundamental mechanism operates for all kinds of charged particles, there are considerable differences in the overall patterns of energy loss and scattering between the passage of light particles (electrons and positrons), heavy particles (muons, protons, alpha particles and light nuclei), and heavy ions (partially or fully ionized atoms of high *Z* elements). Most of these differences arise from the dynamics of the collision process. In general, when a massive particle collides with a much lighter particle, the laws of energy and momentum conservation predict that only a small fraction of the massive particle's energy can be transferred to the less massive particle. The actual amount of energy transferred will depend on how closely the particles approach and restrictions imposed by quantization of energy levels. The largest energy transfers occur in head-on collisions.

8.4.1. Heavy charged particles

A charged particle is called ‘heavy’ if its rest mass is large compared to the rest mass of the electron, $m_e c^2$ or a particle with $A \geq 1$. Thus, mesons, protons, α -particles, atomic nuclei from particle accelerators and, of course, fission fragments, are all heavy charged particles. The reason for differentiating between heavy and light charged particles is that the former, due to their heavier mass and higher charge, experience stronger Coulomb force of nuclei than the latter. Furthermore, if they come close enough to nuclei, they can also be affected by the strong nuclear force, which on lighter particles, such as electrons, does not act. Consequently, the heavy charged particles behave quite

differently in matter than the light charged particles. The moving heavy charged particle exerts electromagnetic forces on atomic electrons and imparts energy to them. The energy transferred may be sufficient to ionize the atom or it may leave the atom in an excited, non-ionized state. A heavy charged particle can transfer only a small fraction of its energy in a single electronic collision. Its deflection is negligible. All heavy charged particles travel essentially straight paths in matter. At low to moderate energies the most important type of interaction for heavy charged particles is the so called Rutherford scattering.

As discussed before, section 8.3.1, the energy loss mechanism shows a minimum when $\gamma\beta \sim 3$ ($\upsilon \sim 0.96c$) or $T \sim (3Mc^2 \approx M_o c^2)$, which differentiate the collisions with orbital electrons from radiation processes. For heavy particles, radiation occurs only at kinetic energies, $\sim 10^3$ MeV for proton and greater than that for the heaviest ones that it is of no practical interest for almost all heavy charged particles. The main interactions of heavy charged particles then are ionization and excitation of the atoms of the medium.

The stopping power of a medium is determined using Eq.8.19. Born and Bethe have shown that the stopping power of heavy charged particles in a medium is proportional to the followings:

1. The mass $M(Z)$, of the atoms in the medium, thus, a medium consisting of heavy atoms has high stopping power.
2. The square of atomic number z^2, of the incident charged particle, therefore, for example, the stopping power of α particle is four times higher than that of proton of the same kinetic energy in the same type of media.

3. The stopping power is inversely proportional to the energy of the particle, since $\beta = (2T/Mc^2)^{1/2}$. A fast moving particle deposits less energy per unit length on its track. High stopping power results in generating high ion pair density.

Accordingly, the Born-Bethe formula for energy loss of charged particles can be written as:

$$S = -\frac{dT}{dx} = C\frac{m(Z)z^2}{T} \qquad 8.30$$

where C is constant.

The stopping power of the medium is relatively small at the time when a heavy charged particle enters the medium because its energy is high. As it travels through the medium, it loses energy and the stopping power increases because the energy of the particle decreases. Thus, the ion pair's density generated along the paths of a particle is low at the time when it enters the medium and increases to a maximum called *Bragg peak* just before it stops. A plot of ion density as a function of the distance in the medium is called *a Bragg curve*. Such curve has a general shape as shown in Fig. 8.8.

Heavy particles lose energy in a medium at a faster rate than light particles. Thus, they generate higher ion-pair densities on their tracks. Alpha particles generate denser ion-pair densities than protons of the same kinetic energy in the same type of media.

Several empirical and semi-empirical formulae have been proposed to compute range of α-particles in air.
For example:

$$R_\alpha^{air}(mm) = \begin{cases} 0.56T_\alpha & for T_\alpha < 4MeV \\ 1.24T_\alpha - 2.62 & for\ 4MeV \le T_\alpha < 8MeV \end{cases} \quad 8.31$$

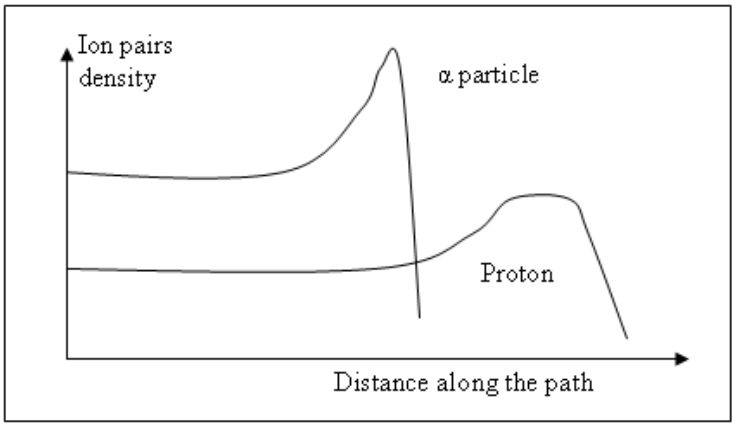

Figure 8.8. Ion pair density along the path of heavy charged particles in a medium.

Similarly, the range of proton in air can be computed by:

$$R_p^{air} = \left(\frac{T_p}{9.3}\right)^{1.8} \qquad for T_p < 200MeV \quad 8.32$$

To compute the range in some other material, Eq. 8.28 can be used. For example, at normal pressure and temperature, the range of α-particles in any material x can be determined from:

$$R_\alpha^x = 3.37 \times 10^{-4} R_\alpha^{air} \frac{\sqrt{A_x}}{\rho_x} \quad 8.33$$

8.4.2. Light charged particles

Particles with masses comparable to those of electrons are *light charged particles*. Essentially, they are high-speed beta particles, positron and electrons. Their rest mass is only *1/1850* u (*0.511 MeV*), much lighter than those of protons.
As compared to heavy charged particles, electrons behave quite differently when passing through matter. The main reason for this difference is, of course, the very small mass of electrons as compared to heavy charged particles. Due to their low mass, electrons travel so fast that their velocity may become very close to the velocity of light. A large deflection can occur with each interaction, resulting in many path changes (very tortuous) in an absorbing medium, since its mass is equal to that of an electron.

The theory of relativity must be considered for a proper calculation of the velocity or speed of a high-energy electron. The mass, *m*, of 1 MeV beta particle is actually 1.51 MeV, rather than 0.51 MeV (rest mass of electron). In general, for a β particle of kinetic energy *T*, its mass in *u* is, $m = \frac{T + o.511}{931.5} u$ .The velocity, *v*, is then calculated by Eq.1.11:

$$v = \sqrt{1 - (\frac{m_o}{m})^2}\, c = \sqrt{1 - (\frac{0.51}{1.51})^2}\, 3 \times 10^8 = 2.82 \times 10^8 \text{ m/s}$$

where *c* is the velocity of light, and m_o is the rest mass of the electron. The velocity is 94% the speed of light. Therefore the computations become more complicated than for the heavy charged particles.

In certain situations, an electron may even attain a velocity greater than the velocity of light in the same material. If this happens, a special kind of radiation, called

Cherenkov radiation, with a specific cone signature is emitted. As electrons pass through matter, they rapidly lose energy and hence decelerate. This deceleration gives rise to another type of radiation called *Bremsstrahlung*.

Whenever an electron beam passes through a material, the individual electrons in the beam can interact with the target atoms or molecules mainly by collision (ionization or excitation) and radiation. Fig. 8.9 shows the contributions of both types of interactions on the stopping power of a high-Z medium like lead for electrons of various energies in addition to the proton, for comparison. It is interesting to note that except for the ionization process, the Bremsstrahlung remains the dominant mode of interaction from moderate to high energies. Therefore, the radiative component of the stopping power cannot be neglected in case of electrons.

Radiation yield, Y, is defined as *the average fraction of its energy that a beta particle radiates as Bremsstrahlung in slowing down completely.* Radiation yield increases with electron kinetic energy *T* and with the atomic number of the absorber *Z.*

$$Y = \frac{6\times10^{-4}\,ZT}{1+6\times10^{-4}\,ZT} \qquad 8.34$$

An estimate of Y gives an indication of the potential Bremsstrahlung hazard of a beta-particle source. To limit *Y*, low *Z* materials (e.g., Al) should be used as shielding for β and electrons since *Y* increases with *Z.* At very high energies, the dominance of radiative over collisional energy losses gives rise to electron-photon cascade showers. High-energy β particles emit high-energy photons. These, in turn, produce Compton electrons and electron-positron pairs,

which also produce in turn, additional Bremsstrahlung photons.

At low to moderate energies, the collisional energy loss of electrons is quite significant and up to certain energy is higher than the radiative energy loss. Hence, the stopping power of a material for electrons consists of two components: collisional and radiative.

$$S_e = S_{col.} + S_{rad.} \qquad 8.35$$

The analytic forms of the collisional and radiative components of the total stopping power for electrons, derived from Eq. 8.20 in terms of kinetic energy, can be written as:

$$S_{col} = -\frac{dT}{dx} = \frac{2\pi e^4 nZ}{m_e c^2 \beta^2}\left[\ln\left(\frac{m_e c^2 \gamma^2 T}{\bar{I}^2}\right) - \beta^2\right] \qquad 8.36$$

$$S_{rad} = -\frac{dT}{dx} = \frac{Z(Z+1)e^4 nT}{137 m_e^2 c^4}\left[4\ln\left(\frac{2T}{m_e c^2}\right) - \frac{4}{3}\right] \qquad 8.37$$

From these two equations, we can deduce that the rate of energy loss of an electron through the collisional and radiative processes can be approximately expressed in terms of proportionality as:

$$S_{col} \alpha \ln(T) \quad \text{and} \quad S_{rad} \alpha T \qquad 8.38$$

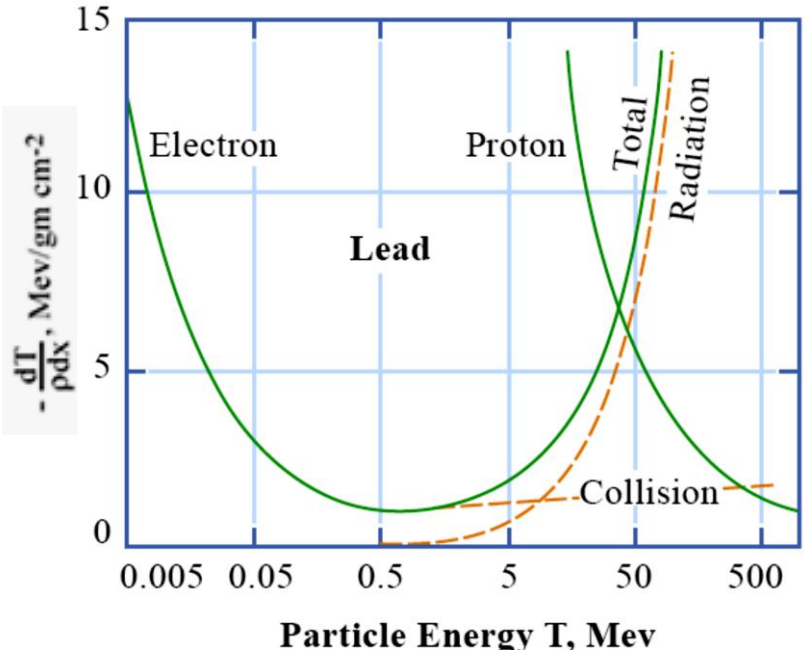

Figure 8.9. Stopping power verses particle energy, showing the contributions from collisions and radiation.

This implies that the losses due to radiative effects such as Bremsstrahlung increase more rapidly than the losses due to collisional effects such as ionization. This can also be seen from Fig. 8.9, where the two effects have been plotted for electrons traveling through a slab of lead. The energy at which these two types of losses become equal is called the *critical energy*. A number of attempts have been made to develop a simple relation for this critical energy, the most notable of which is the one that uses the approximate ratio of Eq. 8.36 and 8.37 given by:

$$\frac{S_{rad}}{S_{col}} \approx \frac{(Z+1)T(MeV)}{800} \qquad 8.39$$

This equation clearly shows that, for materials with low atomic numbers and low incident electron energies, the collisional component of the stopping power dominates. Hence, most of the electrons in a beam of low energy electrons passing through a gas will loose their energy through collisions with the gas molecules. But for the same electrons passing through a high Z material (such as Lead), the radiative losses will be significant.

The comparison of the energy dependent interactions of light and heavy charged particles with different target materials is shown in Table 8.1. The table shows the values of W_{max} for representative projectiles and targets along with the percentage of the stopping power due to nuclear collisions. For electrons, it also shows the percentage of the stopping power due to radiative transitions. Electrons can scatter from nuclei, but the amount of recoil energy transferred to the nucleus is very small. Although electrons undergo a great deal of nuclear scattering, which results in a tortuous path through material, they lose very little energy in a nuclear scattering. The heavier projectiles can lose relatively more energy in each nuclear collision than in each electron collision. For a given kind of projectile, nuclear stopping is more important at lower energies, because less energy can be transferred to an electron. The heavier the projectile for a given energy, the more important the nuclear term becomes, for the same reason.

The collision of electrons with electrons is a special case. Eq. 8.29 gives $W_{max} = T$. Consider the collision of two billiard balls of the same mass. If the projectile misses the target, it continues straight ahead with its original energy and $W = 0$. If it hits the target head on, it comes to rest and the target travels in the same direction with the same energy that the projectile had "a situation indistinguishable from the

complete miss". It is customary (but arbitrary) in the case of identical particles to say that the particle with higher energy is the projectile, so $W_{max} = T/2$. This adjustment has been made in Table 8.1 for electrons on electrons and protons on protons.

Table 8.1. Comparison of relative importance of nuclear and radiative interactions for various projectiles and targets.

Projectile	Target	Nuclear W_{max} (eV)	Electron W_{max} (eV)	S_n/S	S_r/S
Electron, 100 keV	Hydrogen	240	50,000		0.01%
	Carbon	20	50,000		0.09%
	Lead	1	50,000		2.2%
Electron, 1 MeV	Hydrogen	4,300	500,000		0.13%
	Carbon	360	500,000		0.65%
	Lead	20	500,000		11.5%
Proton, 10 keV	Hydrogen	5,000	20	1.7%	
	Carbon	2,800	20	1.6%	
	Lead	200	20	1.5%	
Proton, 100 keV	Hydrogen	50,000	220	0.17%	
	Carbon	28,400	220	0.15%	
	Lead	1,900	220	0.24%	
Proton, 1 MeV	Hydrogen	500,000	2,200	0.11%	
	Carbon	280,000	2,200	0.07%	
	Lead	19,000	2,200	0.09%	
α particle, 10 keV	Hydrogen	6,400	5	27%	
	Carbon	7,500	5	12%	
	Lead	700	5	10%	
α particle, 100 keV	Hydrogen	64,000	50	1.6%	
	Carbon	75,000	50	1.1%	
	Lead	7,400	50	1.8%	
α particle, 1 MeV	Hydrogen	640,000	500	0.13%	
	Carbon	750,000	500	0.12%	
	Lead	74,000	500	0.20%	

The range of a beam of monoenergetic electrons (all have the same kinetic energy) is not a well defined quantity compared to those of heavy charged particles, then there is more *range straggling*. In spite of the severe range straggling, kinetic energies of electrons can be estimated approximately by means of extrapolation. The extrapolation and the range straggling as seen from the plot of their intensity I (*number of particles/cm^2.sec*) after they pass an absorber of thickness $\boldsymbol{x}$ is shown in Fig. 8.10. The measurement of the attenuation intensity of a beam of monoenergetic electrons has been seen to follow an exponential curve given by Eq. 8.7. $I_x = I_o e^{-\Sigma x}$ where I_o is the incident intensity and $\Sigma = n\sigma$ is the total macroscopic cross section or absorption coefficient of the material for the electrons and is also a function of the electron energy. In such a case the real range actually corresponds to the endpoint energy R_e and the straggling length of electrons from a radioactive source.

The absorption coefficient can be related to the endpoint energy E_{max} of the β spectrum by an empirical formula:

$$\Sigma(cm^2 g^{-1}) = 0.17 E_{\max}^{-1.14} \qquad 8.40$$

The measurements of the attenuation of the β spectrum from a newly discovered (or unknown) isotope can be used to identify the energy of the *β-decay*. Also the attenuation of strong sources can be used to monitor the thickness of the shielding materials during manufacturing processes.

Electrons have a greater range than protons if they all have the same kinetic energy, but the intensity drops gradually as the thickness increases. In contrast, the intensity of heavy particles remains essentially constant as the

thickness increases until the thickness is approximately equal to the range.

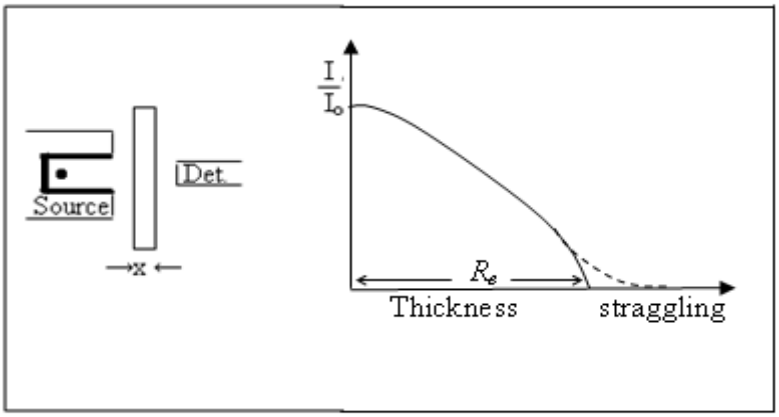

Figure 8.10. A schematic attenuation curve for a monoenergetic electron beam in a solid material.

Although the best way to determine the range of electrons in a material is to perform an experiment as described above, however, it may not be always practical to do so. Fortunately enough, the range of electrons in any material can be fairly accurately determined from the following simple empirical formulae:

$$R(gcm^{-2}) = \begin{cases} 0.512T^{1.27-0.0954\ln T} & \text{for } 0.01 \le T \le 2.5\,MeV \\ 0.530T - 0.106 & \text{for } T > 2.5\,MeV \end{cases} \quad 8.41$$

According to the above equation, one can calculate the energy of the electron beam from the range:

$$\begin{aligned} &\ln T = 6.63 - 3.24(3.29 - \ln R)^{1/2} && \text{for } 0.01 \le T \le 2.5\,MeV \\ &T = 1.89R + 0.2 && \text{for } T > 2.5\,MeV \end{aligned} \quad 8.42$$

Fig. 8.11 shows the ranges in g cm^{-2} of protons, alpha particles, and electrons in water or muscle (virtually the same), bone, and lead. For a given proton or alpha energy, the range in g cm^{-2} is greater in Pb than in H_2O, consistent with the smaller mass stopping power of Pb, while for electron, the range deviates from this behavior at electron energy greater than about 20 MeV due to the fact of domination of radiation interaction.

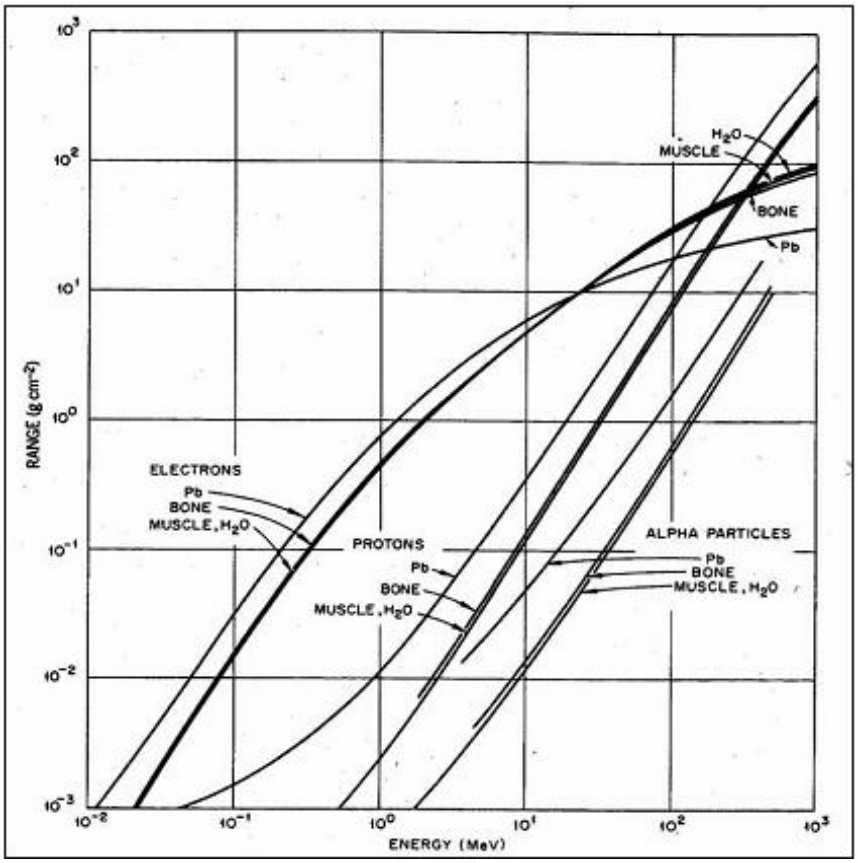

Figure 8.11. Ranges of protons, alpha particles, and electrons in water, muscle, bone and lead, expressed in cm^{-2}.

Problems

8-1. Show that the classical cross section for elastic scattering of point particles from an infinitely massive sphere of radius R is isotropic.

8-2. Evaluate the stopping power of beryllium metal for $^{18}O^{8+}$ ion with a kinetic energy 540 MeV (E/A=30 MeV) using a Bethe formula. The density of the beryllium metal is 1.85 g/cm^3 and Z = 4.

8-3. Which can transfer more energy to an electron in a single collision – a proton or an alpha particle? Explain.

8-4. Astatine–211 is an alpha-emitting isotope that is used in radiation therapy by attaching it to a monoclonal antibody. The energy of the ^{211}At alpha particle is 6.87 MeV.

a- What is the stopping power (– dE/dx) of water for the ^{211}At alpha?

b- What is the range in water?

8-4. What thickness of Lucite (density 1.19 g cm^{-3}) would be required to completely shield the beta radiation from phosphorus-32 (1.7 MeV maximum energy).

8-5. An electron emerges normally from a 7 mm-thick Lucite slab (density 1.19 g cm^{-3}) with energy of 1.2 MeV. What was its energy when it entered the slab?

8-6. Assume that the *W* values for protons and carbon-recoil nuclei are both 30 eV ip-1 in C_2H_4 gas. What is the

maximum number of ion pairs that can be produced by a 3 MeV neutron interacting elastically with (a) H or (b) C?

8-7. A ^{210}Po source is placed in an air ionization chamber and a saturation current of 8 x 10^{-12} A is observed. Assume all ionizations are due to 3.5 MeV alpha particles stopping completely in the chamber. How many particles per second are stopped in the chamber?

8-8. A proton and an alpha particle with the same velocity are incident on a water target. Which will penetrate to a greater depth? Explain.

8-9. What is the rate of energy loss of an 8 MeV α-particle in air? Assume air is 21% oxygen 79% nitrogen.

8-10. A proton of kinetic energy 2.5 GeV passes through a sheet of lead 15 mm thick. The density of lead is 11.4×10^3 kg.m^{-3}. Estimate the energy lost by the proton.

8-11. The energy loss of a heavy charged particle (charge Ze) of speed v in a material with n atom per unit volume can be derived from Eq. 8.20. Show that this expression passes through a minimum as υ is varied and find the approximate kinetic energy of the particle at that speed. Relativistic expression must be used.

8-12. Omitting the two speed terms ($-ln\gamma^2 - \beta^2$) in the derived expression in problem 8-11, calculate the energy loss of 10 MeV alpha particle in aluminum, for which $\bar{I}$ = 150 eV.

8-13. You can make a rough estimate of the range of (kinetic energy) 300 MeV muons moving through air by using the energy loss rate at minimum ionization. This rate is 0.2 $MeV.m^2.kg^{-1}$ and so the range is 300 MeV/0.2 $MeV.m^2.kg^{-1}$ = 1500 $kg.m^{-2}$. The density of air is 1 $kg.m^{-3}$. How far will the muon travel? Is this an overestimate or an underestimate of the range?

8-14. Assuming that the energy loss equation for protons and for nonrelativistic electrons are identical, at what kinetic energy does an electron have the same energy loss as a proton of 10 MeV?

8-15. Use the graphs of Fig.8.9 to determine the dominant energy loss mechanism for electrons travelling through lead with energy (a) 100 keV, (b) 1 MeV, (c) 10 MeV and (d) 100 MeV.

8-16. Estimate the minimum the value of the relativistic factor γ at which an electron will emit Cherenkov radiation when it is travelling through (a) water, (b) crown glass and (c) air. n_{water} = 1.33, n_{glass} = 1.52, n_{air}=1.0003.

8-17.
a- Explain why "Bremsstrahlung" is a more important energy loss mechanism for electrons than for protons travelling through matter.
b- Explain why energy loss rate by "Bremsstrahlung" is greater for electrons travelling through lead than for electrons travelling through water.

CHAPTER 9

INTERACTION OF GAMMA RAY WITH MATTER (INDIRECT IONIZING RADIATION)

Gamma-rays as an electromagnetic wave are an important source of information about nuclear energy levels. The emission of γ-rays was regarded simply as a means by which a nucleus can pass from an excited state to a less excited one. Gamma-decay is in itself a subject of great theoretical and practical importance.

9.1. Attenuation of Gamma-ray

As discussed before, gamma radiation (γ emission) is a process of de-excitation of the atomic nucleus through the emission of a γ photon. The energy spectrum of γ radiation is discrete (linear). Since γ is one type of radioactive radiation, γ radiation is often considered a type of radioactive decay. However, in the case of γ emission, the composition of the atomic nucleus does not change (i.e., there is no change in the proton and neutron number). γ emission is a burst of very high energy as electromagnetic radiation of a very high frequency (wavelengths of 10^{-10} m).

Since γ-ray is typically a photon, where photons are electromagnetic radiation with zero mass, zero charge, and a velocity that is always c, with energies in the range of ~ 0.1–10 MeV, the interaction of γ-ray with matter is markedly different from that of charged particles such as

α or β-particles. Because they are electrically neutral, they do not steadily lose energy via columbic interactions with atomic electrons. In fact, photons are the carriers of electromagnetic force and can interact with matter in a variety of ways that lead to ionization of atoms and to energy deposition in a medium. The difference is apparent in the much greater penetrating power of γ-rays and in the absorption laws. Photons travel some considerable distance before undergoing a more "catastrophic" interaction leading to partial or total transfer of the photon energy to electron energy. These electrons will ultimately deposit their energy in the medium.

As a beam of photons propagate through any material, the intensity of the beam will decrease as the photons, that interact, are removed but the energy of all the non-interacting photons remains constant. The photons will interact in ways that predominantly release fast moving electrons, low energy photons will interact only once and give rise to a single electron, while energetic photons can interact several times and give rise to a few electrons. The most energetic photons can create a matter-antimatter pair of electrons that induces a cascade of electrons.

The energy of the non-interacting photons remains constant so that the probability that a photon will interact in a fixed thickness of material will also remain constant regardless of the photon energy. This leads immediately to a characteristic exponential attenuation of electromagnetic radiation that is called the Beer-Lambert law and consequently have no definite range such as the one found in charged particles. Charged particles, especially heavy ones, lose their energy during the course of a large number of collisions with atomic electrons. The energy loss occurs in

many small steps and the particle gradually slows down until it is stopped altogether and absorbed.

When a beam of γ-ray photons is incident on a thin absorber, however, each photon that is removed from the beam is removed individually in a single event. The event may be an actual absorption process, in which case the photon disappears or the photon may be scattered out of the beam. The one shot nature of the removal process is reasonable for the exponential absorption.

The derivation of the exponential attenuation law is similar to the derivation of the exponential decay law of radioactive nuclei, as shown in section 4.3 alone. The analogy is that the probability of radioactive decay is constant in a given time interval.

The general expression for the attenuation of photon is (see section Fig. 8.2 above):

$$I_x = I_o e^{-\mu x} \qquad 9.1$$

The interaction is expressed through the *total linear attenuation coefficient* μ (cm^{-1}) which does not depend on x but does depend on the energy of the incident gamma. By attenuation we mean either scattering or absorption. Since either process will remove the gamma from the beam, the probability of penetrating a distance x is the same as the probability of traveling a distance x without any interaction, $e^{-\mu x}$. The attenuation coefficient is, therefore, the *probability per unit path* of interaction; it is what we would call the macroscopic cross section $\Sigma = n\sigma$ in the case of neutron interaction.

As in the case of other statistical processes, such as radioactive decay, we can define a half-thickness, $x_{1/2}$, as the thickness of material that photons must traverse in order for

their intensity to fall to half of the original value. This can be related to μ by equating $I_x=I_{1/2}=I_o/2$ in Eq. 9.1, to get:

$$x_{1/2} = \frac{\ln 2}{\mu} = \frac{0.693}{\mu} \qquad 9.2$$

Since photons interact with individual atoms, the probability that a photon will interact somewhere within a slab of matter depends on the total number of atoms ahead of it along its path. So the attenuation of radiation depends on the amount of material in the beam's path and not on how it is distributed. It is useful, therefore, to describe the attenuation process in a way that does not depend on the density of material, only on what kind of stuff it is. We can achieve that by defining the *mass attenuation coefficient*, μ/ρ, which is related to the linear attenuation coefficient by dividing μ by the density ρ of the material, usually expressed in cm^2g^{-1}. This means that the mass attenuation coefficient is the same for ice, liquid water and steam whereas the linear attenuation coefficients will differ greatly.

If $x_{1/2}$ is expressed in *cm*, μ must have units of cm^{-1}, and when $x_{1/2}$ is given in terms of $g.cm^{-2}$, μ has units of $cm^2.g^{-1}$. The value of μ^{-1} is just the *mean free path* for absorption or the average distance through which a beam of photons will propagate before their number drops to *1/e* of the initial value.

There are several different processes of gamma interaction. Each process can be treated as occurring independently of the others; for this reason μ is the sum of the individual contributions. These contributions, of course, are not equally important at any given energy. Each process has its own energy variation as well as dependence on the atomic number of the absorber. We will focus our

discussions on the three most important processes of gamma interaction, *Compton scattering, photoelectric effect, and pair production*. These can be classified by the object with which the photon interacts and the type of process (absorption or scattering).

9.2. Photoelectric Effect

Photoelectric is the absorption of a photon followed by the ejection of an atomic electron.

In the photoelectric process, all the energy $h\nu_o$ of the incident photon is transferred to a bound electron which is ejected from the atom with a kinetic energy $T_e = h\nu_o - B_e$, where B_e is the magnitude of the binding energy of the electron and depends on which shell the electron was in. Therefore, it is labeled B_K, B_L, and so forth; it represents the ionization potential of the electron in that atomic shell. The cross section for the photoelectric effect, τ, is a sum of terms for each shell: $\tau = \tau_K + \tau_L + \tau_M + \ldots$.

As the energy of a photon beam is decreased, the photoelectric cross section increases rapidly. Because photon energies are too small to remove an electron from the *K* shell, the cross section for the *K*-shell photoelectric effect is zero. Even though photons do not have enough energy to remove an electron from the *K* shell, they may have enough energy to remove *L*-shell electrons. The cross section for *L* electron photoelectric effect is much smaller than that for *K* electrons, but it increases with decreasing energy until its threshold energy is reached. This energy dependence is shown for lead in Fig. 9.1, which plots the cross section for the photoelectric effect. The *K absorption edge* for the photoelectric effect is seen. The photoelectric effect below

the *K* absorption edge is due to *L*, *M* . . . electrons; above this energy the *K* electrons also participate.

Formulas for the probability that a photon of energy $E_\gamma = h\nu_o$ will undergo photoelectric absorption have been derived by quantum mechanical methods. The cross section for this reaction has a strong Z dependence, the probability of photoelectric effect increases rapidly with atomic number of the target atom. In addition, it also has a strong inverse relationship with energy of the incident photon. Specifically, this dependence can be expressed as:

$$\begin{aligned} \tau &\propto \frac{Z^5}{E_\gamma^{3.5}} \qquad for\ E_\gamma < (m_e c^2 = 0.511 MeV) \\ \tau &\propto \frac{Z^{4.5}}{E_\gamma} \qquad for\ E_\gamma > (m_e c^2 = 0.511 MeV) \end{aligned} \tag{9.3}$$

Photoelectric effect takes place predominantly in the K atomic shell and therefore generally the cross section related to K-shell interaction is used to estimate the total photoelectric cross section. The K-shell photoelectric cross section per atom is given by:

$$\tau = 4\sqrt{2}\left(\frac{1}{137}\right)^4 \sigma_{Th} Z^5 \left(\frac{m_e c^2}{E_\gamma}\right)^{7/2} \tag{9.4}$$

where

$$\sigma_{Th} = \frac{8\pi}{3} r_e^2 = 6.65 \times 10^{-25} cm^2 \tag{9.5}$$

is the Thompson scattering cross section. Thompson scattering is an elastic scattering process between a free electron and a photon of *low energy*. Low energy means the

energy at which the quantum effects are not significant, and $r_e = \frac{e^2}{m_e c^2} = 2.82 \times 10^{-13} cm$ is the classical electron radius.

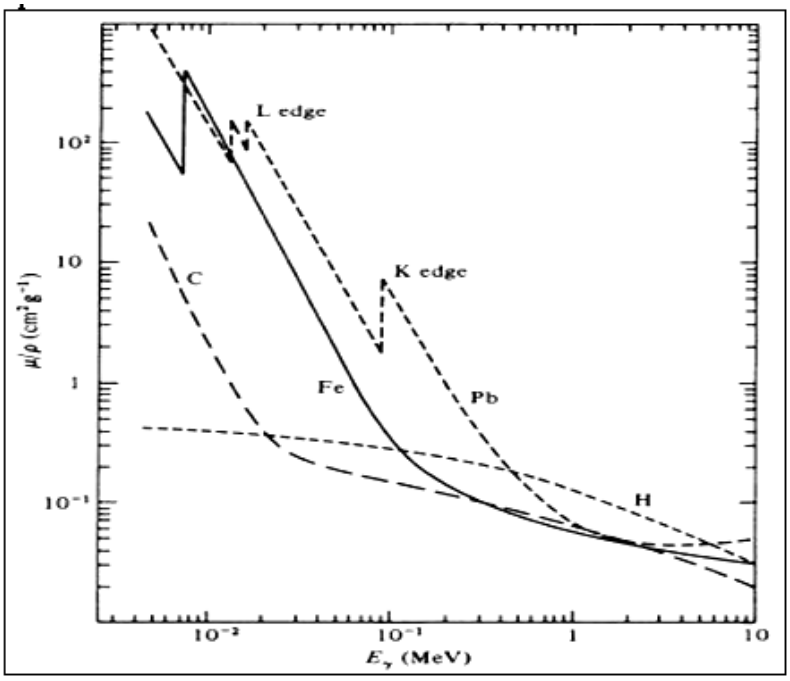

Figure 9.1. Photoelectric cross sections or mass attenuation coefficient as a function of energy for hydrogen, carbon, iron and lead. The K and L absorption edge in lead while only K absorption edge in iron.

An interesting aspect of photoelectric effect is that if the incident photon has sufficient energy to overcome the binding energy of an inner shell electron, that electron might get ejected leaving a vacancy behind. This vacancy can then be filled by an outer shell electron to stabilize the atom. Such a transition would emit a photon with energy equal to the difference of the two energy levels; see Eq.1.9. These

photons are generally in the x-ray region of electromagnetic spectrum and are called *fluorescence photons*. An x-ray photon emitted as a consequence of photoelectric effect can also knock off another orbital electron provided that its energy is equal to the binding energy of that electron. This electron is called *Auger electron*. The process is essentially radiationless because the excess energy of the atom is used and taken away by the Auger electron. An example of these processes is shown graphically in Fig. 9.2. Here, an incident photon knocks off the K-shell electron, creating a vacancy. For the atom to be stable again, another electron from the M-shell fills this gap but releases a photon of energy equal to the difference between the two energy levels. This photon may knock off another electron called Auger electron

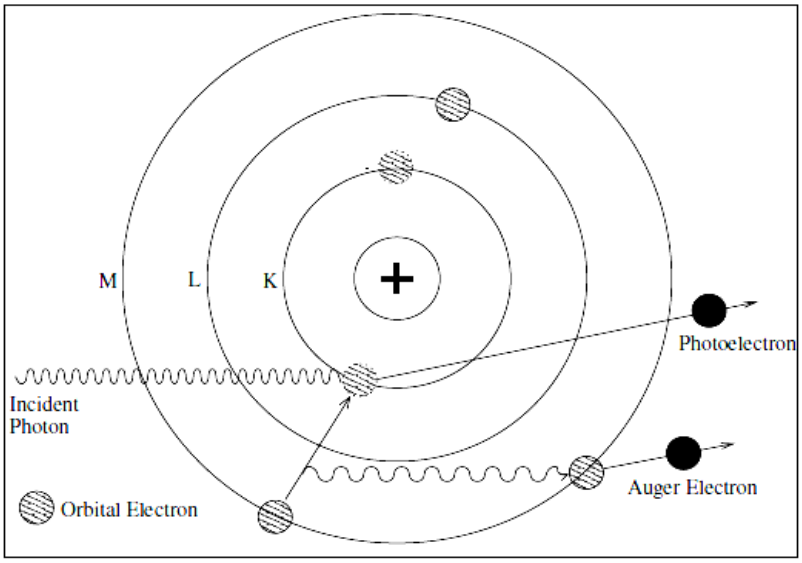

Figure 9.2. Depiction of photoelectric effect in a free atom.

9.3. Compton scattering

Compton scattering replaces the photoelectric effect as the energy of the radiation increases. In this process the incident photon is scattered inelastically by one of the free or loosely bound atomic electrons which are ejected from its atom. The photon moves off at an angle with its original direction and with less energy than it had initially. The change of direction serves to remove the photon from the incident γ-ray beam.

The main features of Compton scattering that were first discovered and studied by Compton in 1923 will be discussed. The theoretical treatment of the Compton Effect involves Einstein's quantum theory of light as well as some of the ideas of relativity theory.

During a scattering experiment, he found out that the wavelength of the scattered light was different (longer wavelength) from that of the incident light. He successfully explained this phenomenon by considering light to consist of quantized wave packets or photons.

To account for the presence of the scattered component and the amount of the scatter, Compton assumed that the scattering process could be treated as an elastic collision between a photon of energy $h\upsilon_0$ and a *free electron*, and that in this collision, energy and momentum are conserved. Fig. 9.3 shows this process for a bound electron where some of the energy of the incident photon goes into knocking the orbital electron out of its orbit. We may recall that the binding energies of low Z elements are on the order of a few hundred eV, while the γ-ray sources used in laboratories have energies in the range of hundreds of keV. Therefore the bound electron can be considered almost free and at rest with respect to incident photons. In general, for orbital

electrons, the Compton Effect is more probable than photoelectric effect if the energy of the incident photon is higher than the binding energy of the innermost electron in the target atom.

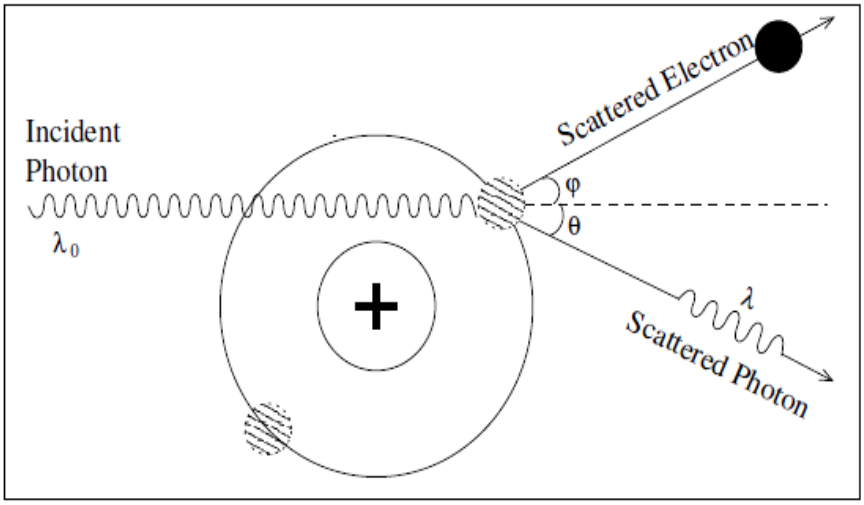

Figure 9.3. Compton scattering of a photon having energy $h\nu_0 = hc/\lambda_0$ from a bound electron.

In order for that momentum to be conserved, the electron which scatters the photon must recoil with a momentum equal to the vector difference between that of the incident and that of the scattered photon, as in the schematic diagram Fig. 9.4. The energy of the recoiling electron is taken from that of the primary photon, leaving a scattered photon which has less energy and hence a lower frequency, or longer wavelength than that of the incident photon. The relativistic kinetic energy of the electron must be used because the velocity of the electron may be great enough for relativistic effect to be significant. The requirement that momentum be

conserved gives two equations, one for the x-component of the momentum, and one for the y-component.

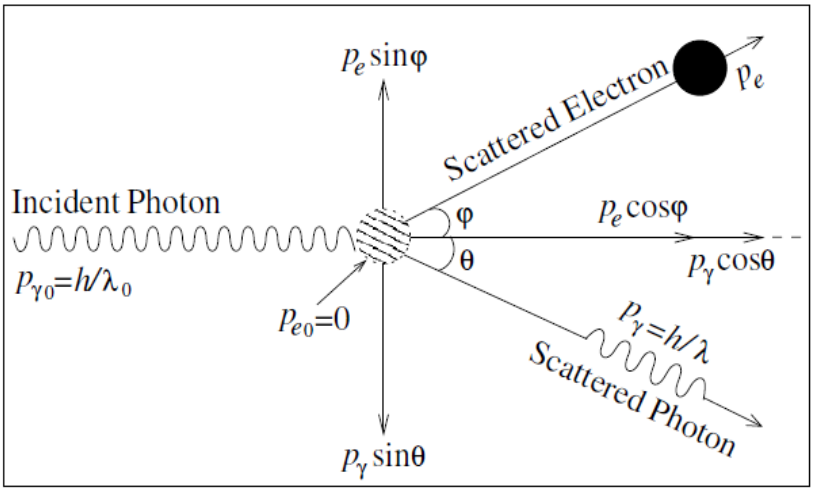

Figure 9.4. A schematic diagram of the Compton scattering.

The x-component of the momentum, see Fig. 9.4, is:

$$P_{\gamma 0} = P_\gamma \cos\theta + P_e \cos\varphi$$

or

$$\frac{h}{\lambda_0} = \frac{h}{\lambda}\cos\theta + \frac{m_o \upsilon}{\sqrt{1-\beta^2}}\cos\varphi \qquad 9.6$$

The y-component of the momentum is:

$$0 = P_\gamma \sin\theta - P_e \sin\varphi$$

or

$$0 = \frac{h}{\lambda}\sin\theta - \frac{m_0 \upsilon}{\sqrt{1-\beta^2}}\sin\varphi \qquad 9.7$$

Application of the conservation of energy to the scattering process:

$$E_{\gamma 0} + E_{e0} = E_{\gamma} + T_e$$

or

$$h\frac{c}{\lambda_0} + m_0 c^2 = h\frac{c}{\lambda} + \frac{m_0 c^2}{\sqrt{1-\beta^2}} \qquad 9.8$$

where we have used the energy-wavelength relation $E_\gamma = hc/\lambda$ for initial, $E_{\gamma 0}$ and final E_γ γ energies, respectively, and $m_0c^2 = E_{e0}$ for the electron.

Now, rearranging and squaring of Eq. 9.6 and Eq. 9.7, and combining with Eq. 9.8, the required relation of the difference in wavelength $\Delta\lambda$ between the scattered and incident photons can be written as:

$$\Delta\lambda = \lambda - \lambda_0 = \frac{h}{m_0 c}(1-\cos\theta) \qquad 9.9$$

Inserting the values of constants, h =6.624×10^{-27}erg.sec, m = 0.9107×10^{-27}g and c = 3×10^{10}cm/sec, then:

$$\Delta\lambda = \lambda - \lambda_0 = 0.0243\times10^{-8}(1-\cos\theta)cm \qquad 9.10$$

In terms of incident and scattered photon energies, Eq. 9.9 can be written as:

$$E_{\gamma} = E_{\gamma 0}\left[1 + \frac{E_{\gamma 0}}{m_0 c^2}(1-\cos\theta)\right]^{-1} \qquad 9.11$$

This relation shows that energy of the scattered photon depends not only on the incident photon energy but also on

the scattering angle. In other words, the scattering process is in no way isotropic.

It is worthwhile to see the dependence of scattered photon energy on three extreme angles: 0^0, 90^0, and 180^0.

1. At $\theta = 0^0$: In this case, $\cos\theta = 1$ and therefore Eq. 9.11 gives $E_\gamma = E_{\gamma max} = E_{\gamma 0}$. That is, the scattered photon continues in the same direction as the incident photon and carries with it all of its energy. Of course, this implies that the photon has not actually interacted with the electron and therefore this should not be regarded as a scattering process at all. However, it should be noted that this case gives us the upper bound of the scattered photon energy.
2. At $\theta = 90^0$: In this situation, the incident photon flies away at right angles to its original direction of motion after interacting with the electron. We can find the energy it carries away by the scattered photon and the change in photon's wavelength as:

$$E_\gamma = E_{\gamma 0}\left[1+\frac{E_{\gamma 0}}{m_0c^2}\right]^{-1} \text{ and } \Delta\lambda = \lambda - \lambda_0 = 2430\ fm$$

3. At $\theta = 180^0$: It is obvious from Eq. 9.11 that a photon scattered at $\theta = 180^0$ will carry the *minimum possible energy* called backscattering (since $1-\cos\theta=2$ is maximum). In this case:

$$E_{\gamma\min} = E_{\gamma 0}\left[1+\frac{2E_{\gamma 0}}{m_0c^2}\right]^{-1} \quad or \quad E_{\gamma\min} = \frac{m_0c^2}{2}\left[1+\frac{m_0c^2}{2E_{\gamma 0}}\right]^{-1}$$

To obtain a numerical result independent of the incident photon energy, let us assume that the incident photon

energy is much higher than half the electron rest mass energy, such as $E_\gamma >> m_0c^2/2$. There is nothing magic about half the electron rest mass energy. It has been chosen because we want to eliminate the term containing $m_0c^2/2E_{\gamma 0}$. In this situation, the above equation is reduced to $E_{\gamma \min} \approx \frac{m_0c^2}{2} = 255keV$. This is a very interesting result because it tells us that the electron will carry the maximum energy it could at any angle. This process resembles the simple head-on collision of two point masses in which the incident body completely reverses its motion and the target body starts moving forward. To determine the energy of the recoiling electron, we assume that most of the energy of the incident photon is distributed between the scattered photon and the recoil electron with kinetic energy $T_e = E_{\gamma 0} - E_\gamma$:

$$T_e = E_{\gamma 0}\frac{(1-\cos\theta)\alpha}{1+\alpha(1-\cos\theta)} \qquad where\,\alpha = \frac{E_{\gamma 0}}{m_0c^2} \qquad 9.12$$

Hence the maximum energy of the scattered electron can be calculated from the above equation:

$$T_{e\max} = E_{\gamma 0} - 255 \quad keV\,.$$

This implies that in a γ-ray spectroscopy experiment, one should see a peak at the energy Eγ − 255 keV. Such a peak is actually observed and is so prominent that it has gotten a name of its own; the Compton edge (see Fig. 9.5). A consequence of this observation is that our assumption that even though the scattering is inelastic, the energy imparted to the atom is not significantly high.

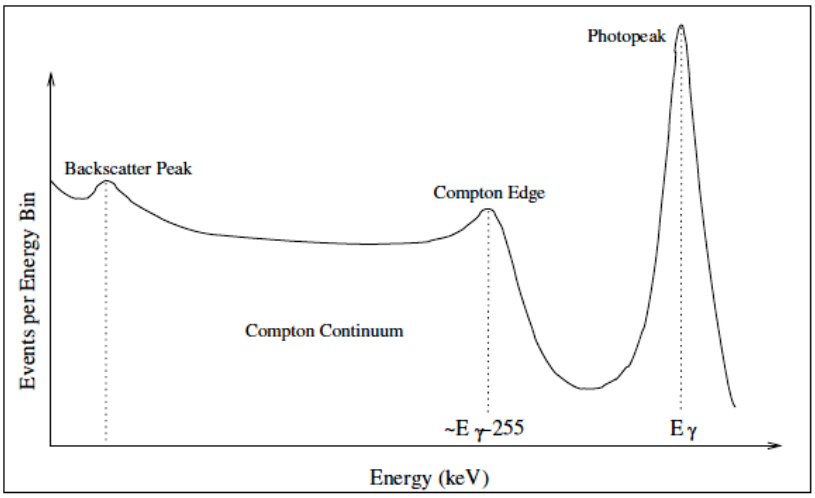

Figure 9.5: Typical γ-ray spectrum obtained by a detector surrounded by heavy shielding (such as lead).

The discussion so far refers only to a single Compton scattering process. In order to treat the contribution of the Compton effect to the attenuation of a beam of γ-rays in matter, it is necessary to calculate the probability that such a scattering process will occur. This probability was calculated on the basis of *relativistic quantum mechanics* by Klein and Nishina. Although the details of the theory are complicated and beyond the scope of this book, the results may be expressed in straightforward formulas with which calculations can be made quite easily.

We will simply quote the formula of the dependence of the Compton scattering cross section σ on the scattering angle θ and discuss some of its implications. The differential cross section for Compton scattering can be fairly accurately written as:

$$\frac{d\sigma}{d\Omega} = \frac{r_e^2}{2}(1+\cos^2\theta)\left(\frac{1}{1+\alpha(1-\cos\theta)}\right)^2\left[1+\frac{\alpha^2(1-\cos\theta)^2}{(1+\cos^2\theta)\left[1+\alpha(1-\cos\theta)\right]}\right] \quad 9.13$$

The behavior of $d\sigma/d\Omega$ is shown in Fig. 9.6. Notice that at any given α, the angular distribution is peaked in the forward direction. As α increase, the forward peaking becomes more pronounced. The deviation from Thomson scattering is largest at large scattering angles; even at $E_\gamma = h\nu \sim 0.1$ MeV the assumption of Thomson scattering is not valid. In practice, the Klein-Nishina cross section has been found to be in excellent agreement with experiments at least to $h\nu = 10\ m_e c^2$.

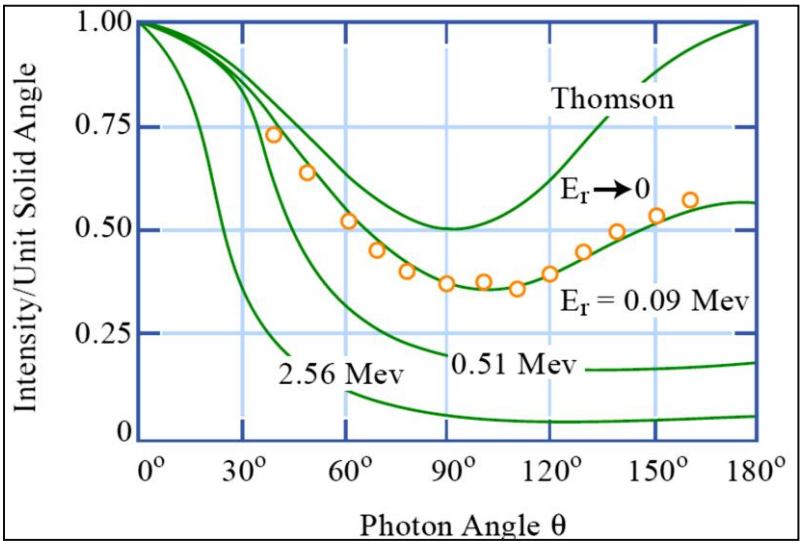

Figure 9.6. Angular distribution of Compton scattering at various incident energies E_γ. All curves are normalized at 0^o

To find the total cross section per electron for Compton scattering σ_c^e, one can integrate Eq. 9.13 over solid angles. A formula was obtained for the total cross section per

electron for the *removal* of photons from the incident beam by scattering:

$$\sigma_c^e = \frac{3}{4}\sigma_{Th}\left\{\frac{1+\alpha}{\alpha^2}\left[\frac{2(1+\alpha)}{1+2\alpha} - \frac{1}{\alpha}\ln(1+2\alpha)\right] + \frac{1}{2\alpha}\ln(1+2\alpha) - \frac{1+3\alpha}{(1+2\alpha)^2}\right\} \quad 9.14$$

Where, again, $\alpha = E_{\gamma 0}/m_0c^2$ and σ_{Th} is Thompson cross section given by Eq. 9.5. When σ_c^e is multiplied by the number of electrons per unit volume $nZ \approx \rho N_A\ (Z/A)$, the result is the Compton absorption coefficient (cross section) σ (cm^{-1}):

$$\sigma(cm^{-1}) = \rho N_A \frac{Z}{A}\sigma_c^e \quad 9.15$$

The total Compton coefficient σ is actually a measure of the probability that a photon is scattered out of the beam per centimeter of absorber σ_s. Since the beam is initially homogeneous, σ is also a measure of the total amount of energy removed (absorbed by the recoil electrons) from the beam per centimeter of absorber σ_a:

$$\sigma = \sigma_s + \sigma_a \quad 9.16$$

The amount of energy carried off by the scattered photons may be expressed in terms of the Compton scattering cross section *per electron* for the energy of the scattered photon σ_s^e, which is given by:

$$\sigma_s^e = \frac{3}{8}\sigma_{Th}\left[\frac{1}{\alpha^3}\ln(1+2\alpha) + \frac{2(1+\alpha)(2\alpha^2-2\alpha-1)}{\alpha^2(1+2\alpha)^2} + \frac{8\alpha^2}{3(1+2\alpha)^3}\right] \quad 9.17$$

Therefore, the Compton scattering cross section *per electron* for the energy absorbed by the recoil electron σ_a^e can be found by subtraction Eq. 9.17 from Eq. 9.14, since the coefficient σ_c^e is simply the sum of the two:

$$\sigma_c^e = \sigma_s^e + \sigma_a^e \qquad 9.18$$

In analogy with Eq. 9.15, we can write:

$$\begin{aligned} \sigma_s(cm^{-1}) &= \rho N_A \frac{Z}{A}\sigma_s^e \\ \sigma_a(cm^{-1}) &= \rho N_A \frac{Z}{A}\sigma_a^e \end{aligned} \qquad 9.19$$

Eqs. 9.14 and 9.17 show that the Compton scattering per electron is independent of *Z*, so that the scattering per atom is *proportional to Z*. The mass scattering cross section is then given by:

$$\frac{\sigma}{\rho}(cm^2 g^{-1}) = N_A \frac{Z}{A}\sigma_c^e \qquad 9.20$$

For light elements, *Z/A* is closely equal to *1/2*, so that for a given photon energy, *σ/ρ* is practically constant for these elements. The total scattering coefficient per electron σ_c^e decreases with increasing photon energy. The decrease is quite slow at low values of the energy and for energies above 0.5 MeV, σ_c^e is roughly proportional to $(E_\gamma)^{-1}$. Thus Compton scattering decreases much more slowly with increasing energy than does photoelectric absorption; even

in heavy elements, it is the most important process in the energy range from about 0.6 to 2.5 MeV.

9.4. Pair Production

This process, which has no analogy in classical physics, may be accepted as a strictly experimental phenomenon.

In this process, which can occur only when the energy of the incident γ exceeds 1.02 MeV, the photon is absorbed in the vicinity of the nucleus, a particle–antiparticle pair: a negative electron and a positive electron or *positron* is produced, and the atom is left in an excited state. Since photon has no rest mass, while both the electron and the positron do, we can say that this process converts energy into mass according to Einstein's mass energy relation $E = mc^2$. Conservation of energy requires that:

$$E_{\gamma 0} = \underbrace{T_- + m_0c^2}_{electron} + \underbrace{T_+ + m_0c^2}_{positron} = T_+ + T_- + 2m_0c^2 \qquad 9.21$$

Since the rest energy (m_0c^2) of an electron or positron is 0.51 MeV, pair production is energetically impossible for photons below $2m_0c^2$ = 1.02 MeV.

One can show, using $hv_0 = pc$ for the photon, that momentum is not conserved by the positron and electron if Eq. 9.21 is satisfied. However, pair production always takes place in the Coulomb field of another particle (usually a nucleus) that recoils to conserve momentum. The actual threshold energy for the process in the vicinity of a heavy nucleus of mass M is given by:

$$E_{\gamma,tresh.} \geq 2m_0c^2 + \frac{2m_0^2c^2}{M}$$

or

$$E_{\gamma,tresh.} \geq 2m_0c^2\left[1 + \frac{m_0}{M}\right] \qquad 9.22$$

The cross section for this (γ, e^+e^-) reaction involving the nucleus is κ_n. Now, since the mass of a nucleus is much greater than the mass of an electron (M >> m_0), we can neglect the second term in the parenthesis on the right hand side and get the threshold condition we derived earlier, such as:

$$E_{\gamma,\ thresh} \geq 2m_0c^2 \qquad 9.23$$

Pair production with excitation or ionization of the recoil atom can take place at energies that are only slightly higher than the threshold.

The pair production can also occur in the vicinity of lighter particles, such as electrons. The process in the vicinity of an electron is, generally, referred to as *triplet pair production* and can be written as:

$$\gamma + e \rightarrow e + e^+ + e \qquad 9.24$$

The cross section for this reaction, denoted κ_e, does not become appreciable until the incident photon energy exceeds $4m_0c^2$ = 2.04 MeV, the threshold for pair production in which a free electron (rather than a nucleus) recoils to conserve momentum. Since there are only a few radioactive sources that emit γ-rays having energies higher than this threshold, this process is not of much significance in usual radiation measurements.

The cross section for both processes is $\kappa = \kappa_n + \kappa_e$. The energy dependence of κ starts from zero for photon energies less than 1.02 MeV and increases slowly at first, then more rapidly. It is proportional to Z^2, so that for a given photon energy, pair formation increases quite rapidly with atomic number. This means that for heavy elements, the pair production cross section is significantly higher than that for lighter elements. The actual cross section can be written as:

$$\kappa(cm^2 / atom) = 4\alpha r_e^2 Z^2 \left[\frac{7}{9} \ln\left(\frac{183}{Z^{1/3}} \right) - \frac{1}{54} \right] \qquad 9.25$$

A natural question to ask is what happens to the positrons that are created in the conversion of photons in matter? Because positrons are the antiparticles of electrons, they traverse matter after production, much as electrons do, and deposit their energies through ionization or through bremsstrahlung. Once a positron loses most of its kinetic energy, it captures an electron to form a hydrogen-like atom, referred to as positronium, where the proton is replaced by a positron. Unlike hydrogen, positronium atoms are unstable and decay (annihilate) with lifetimes of about 10^{-10} sec to form two photons. The process of annihilation produces photons of equal energy, back-to-back in the laboratory. To conserve momentum-energy, each photon carries away exactly 0.511 MeV. Thus, pair annihilation provides a very clean signal for detecting positrons, as well as for calibrating the low-energy response of detectors. These processes, pair absorption and pair annihilation, are shown graphically in Fig. 9.7.

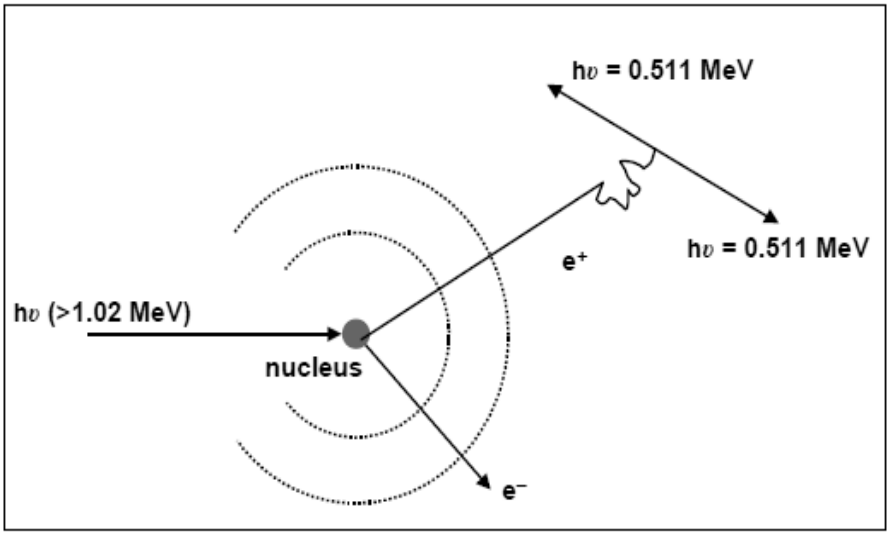

Figure 9.7. Schematic diagram of pair production by a photon having energy $h\nu > 1.02$ MeV in the vicinity of the nucleus and the annihilation of the created positron.

9.5. Bulk Behavior of Photons in an Absorber

So long as the different processes of photon interaction are not correlated, the total linear attenuation coefficient μ for γ -interaction can be taken as the sum of contributions from Compton scattering, photoelectric effect, and pair production.

$$\mu = \tau + \sigma + \kappa \qquad 9.26$$

With $\mu = n\sigma$ and n being the number of atoms per cm^3. Since $n = N_A \rho / A$, where N_A is Avogadro's number and ρ the mass density of the absorber, it is again useful to express the interaction in terms of the *mass attenuation coefficient* μ / ρ. As discussed in previous sections, this quantity is

essentially independent of the density and physical state of the absorber. Recall our observation in the case of charged particle interactions that *Z/A* is approximately constant for all elements. Here we see that in the product $(n\,\mu)$ we get a factor of *1/A* from *n*, and we can get a factor of *Z* from any of the three cross sections ($\tau + \sigma + \kappa$), so we can also take advantage of Z/A being roughly constant in describing photon interaction. We can rewrite Eq. 9.1 in terms of mass attenuation coefficient:

$$I_x = I_o e^{-\frac{\mu}{\rho}\rho x} \qquad 9.27$$

The quantity μ/ρ ($cm^2.g^{-1}$) is the mass attenuation coefficient. The product ρx ($g.cm^{-2}$), the *area density* (mass per area) of a thickness *x* of the attenuating material, is also called the *density-thickness*. It is often quoted instead of the geometrical thickness *x* (cm). Each of the components, τ, σ and κ can be expressed as mass attenuation coefficients.

$$\frac{\mu}{\rho} = \frac{\tau}{\rho} + \frac{\sigma}{\rho} + \frac{\kappa}{\rho} \qquad 9.28$$

where:

$$\frac{\tau}{\rho} = \frac{N_A}{A}\tau, \quad \tau \sim \frac{Z^5}{E_\gamma^{3.5}} \qquad \text{per atom}$$

$$\frac{\sigma}{\rho} = \frac{N_A}{A} Z\sigma_c^e, \quad \sigma_c^e \sim \frac{1}{E_\gamma} \qquad \text{per electron}$$

$$\frac{\kappa}{\rho} = \frac{N_A}{A}\kappa, \quad \kappa \sim Z^2 \ln\left(2h\upsilon / m_0c^2\right) \quad \text{per atom}$$

It should be quite clear by now that the three processes we have studied are not equally important for a given region of Z and $h\nu$. Generally speaking, photoelectric effect is important at low energies and high Z, Compton scattering is important at intermediate energies (~ 1 – 5 MeV) and all Z, and pair production dominates at higher energies and high Z. This is illustrated in Fig. 9.8.

We also show several mass attenuation coefficients in Figs. 9.9 and 9.10. One should make note of the magnitude of the attenuation coefficients, their energy dependence and the contribution associated with each process. In comparing theory with experiment, the agreement is good to about 3 %, for all elements at $h\nu < 10m_0c^2$. At higher energies, disagreement sets in at high Z (can reach ~ 10% for Pb), which is due to the use of Born approximation in the calculation of κ. If one corrects this approximation, an agreement to within ~ 1% is obtained out to energies ~ 600 m_0c^2.

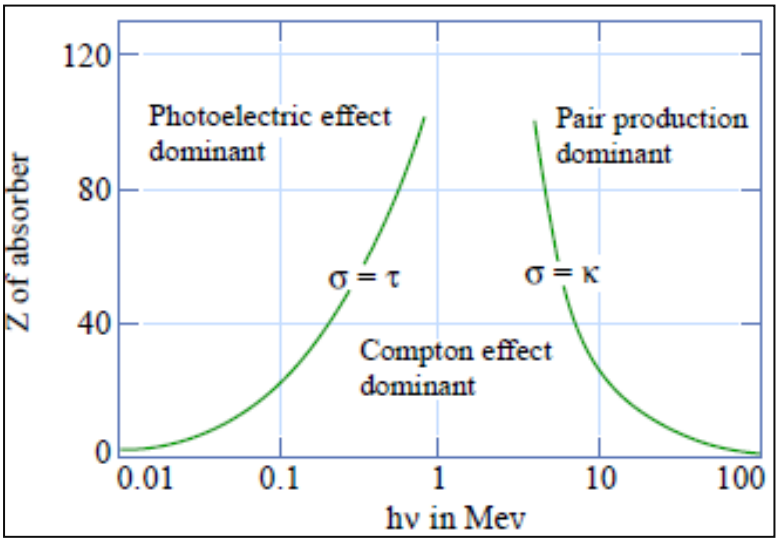

Figure 9.8. Regions where one of the three γ - interactions dominates over the other two.

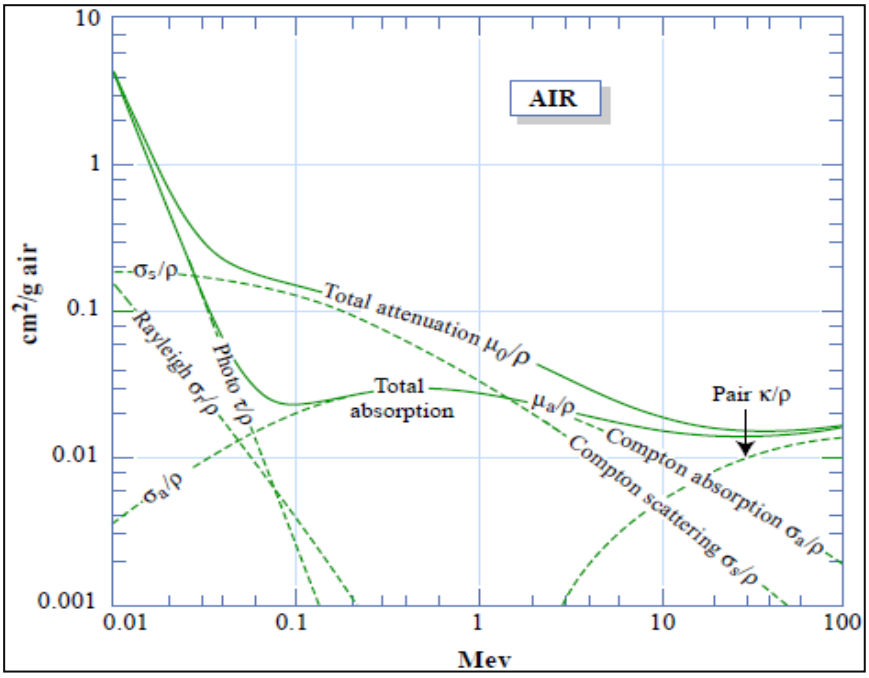

Figure 9.9. The 3 energy transfer processes in air, each depends differently on E_γ.

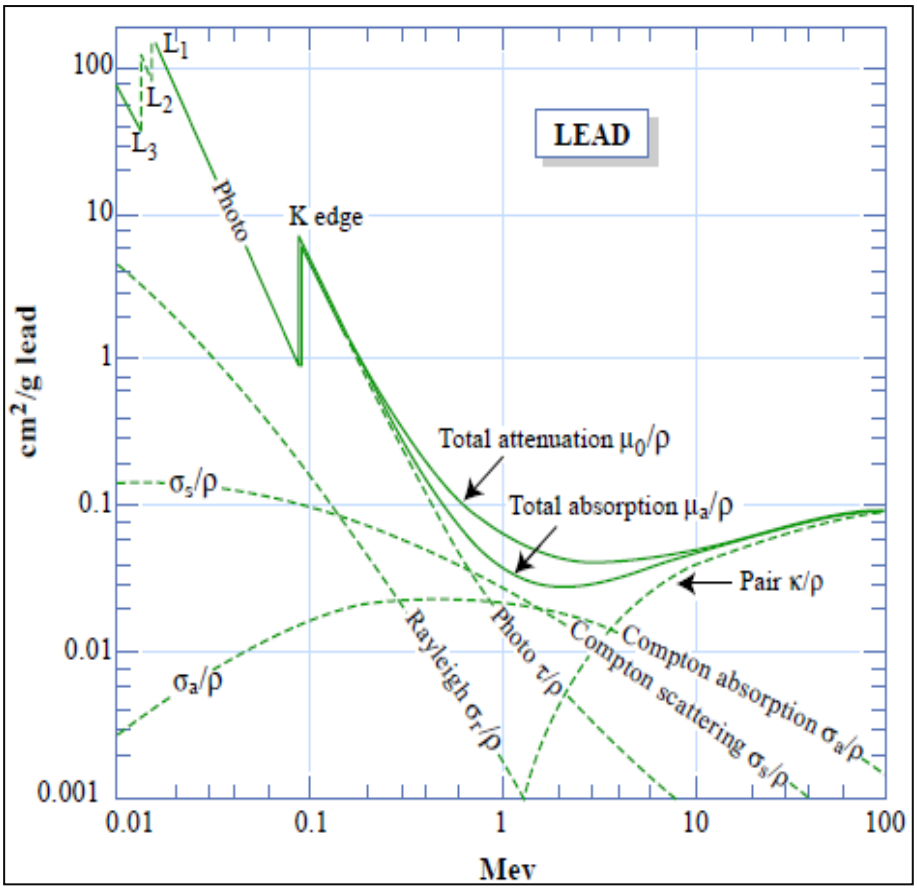

Figure 9.10. The 3 energy transfer processes in lead, each depends differently on E_γ.

Problems

9-1. A narrow beam of 10^8 photons per second is normally incident on a 6 mm aluminum sheet. The beam consists of equal numbers of 200 keV photons and 2 MeV photons.

a- Calculate the number of photons per second of each value of energy that are transmitted without interaction through the sheet.

b- Calculate the transmitted intensities for the same two photon beams striking a lead sheet of the same thickness.

c- Calculate the atomic cross sections of aluminum and lead for the 200 keV and the 2 MeV photons.

9-2. What is the fractional attenuation of a beam of 1 MeV photon in 2.5 cm of Pb?

9-3. Prove that a photon of $E_\gamma > 1.022$ MeV cannot go pair production in free space.

9-4. Lead is thought to be a better absorber than aluminum. At what gamma ray energy is the mass absorption coefficient of lead greater than that of aluminum? Why?

9-5. A narrow beam of 200 keV photons strikes a target consisting of a 1.4 cm-thick sheet of aluminum followed by a 2 mm-thick sheet of lead.

a- What fraction of the incident photons penetrates both sheets without interacting?

b- Would there be any difference if the photons came from the other direction, entering the lead first and then the aluminum?

9-6. A 1 MeV photon undergoes Compton scattering through angles 0^o, 90^o, and 180o. What is the energy of the scattered photon in each case?

9-7. An experiment is carried out with monoenergetic photons in "good" geometry. The relative count rate of the detector is measured with different thicknesses *x* of tin (Sn) used as absorber. The following data are measured:

x(cm)	0	0.50	1.0	1.5	2.0	3.0	5.0
Relative count rate	1.00	0.861	0.735	0.621	0.538	0.399	0.210

a- What is the value of the linear attenuation coefficient?
b- What is the value of the mass attenuation coefficient?
c- What is the atomic cross section?
d- What is the photon energy?

9-8. For gamma rays of energy *E*, the linear attenuation coefficient in material A is twice that in material B. Given that 80% of the gamma rays penetrate a given thickness of A, what fraction will penetrate the same thickness of B?

9-9. The mass attenuation coefficient of 1 MeV photons in aluminum is 0.0065 $m^2.kg^{-1}$. The density of aluminum is 2.7×10^3 $kg.m^{-3}$.

a- What is the linear attenuation coefficient of 1 MeV gamma rays in aluminum?
b- What fraction of incident 1 MeV gamma radiation penetrates 30 mm of aluminum?

9-10. The total radiation penetrating to a given depth in a material is sometimes greater than that predicted using the known attenuation coefficient. This is known as "build-up". Use an example to explain what is happening.

9-11. What is the mean free path of a 0.1, 1.0, and a 3.0 MeV photon in water and in NaI?

9-12. How much lead shielding will it take to reduce the radiation exposure level to <10 mrem/h 1 foot from a 5 mCi ^{60}Co source?

9-13. The mass attenuation coefficients for 10 MeV photons in lead are:-

μ (Pe) = 6×10^{-5} $m^2.kg^{-1}$; μ (C) = 1.2×10^{-3} $m^2.kg^{-1}$;
μ (Pp) = 0.005 $m^2.kg^{-1}$.

a- Which process of attenuation is dominant for 10 MeV photons?
b- What is the total attenuation coefficient for 10 MeV photons?
c- Which of the mass attenuation coefficients μ (Pe), μ (C), μ (Pp), increase and which decrease if the photon energy is increased to 20 MeV?

9-14. Suppose you have a sample that contains radionuclides that emits 1MeV β-particles and 1MeV γ-rays. Device an attenuation technique that would allow you to count γ-rays without interference from the β-particles.

CHAPTER 10

NEUTRON PHYSICS AND INTERACTIONS
(INDIRECT IONIZING RADIATION)

When hearing the word 'nuclear physics' or 'neutron physics' most people will think of two things: nuclear bombs and nuclear reactors. Because of these two aspects, nuclear physics was probably the part of science with the biggest impact on politics in the 20th century, just think of the entire cold war. Today's mainstream nuclear physics research has very little to do with bombs and reactors.

10.1. Neutrons Properties

The neutron was the last of the basic atomic constituents to be discovered mainly because of their almost identical mass to protons and no electrical charge. A British scientist, James Chadwick, discovered these particles in 1932. Like protons, they are also composite particles made up of three quarks. However, they are not as stable outside the nucleus (free) as protons and decay within about 15 minutes.

Neutrons, because they are uncharged heavy particle, have properties which make them especially interesting and important in contemporary science and technology. The many nuclear reactions induced by neutrons are the available source of information about the nucleus and have produced many new nuclear species. Neutrons do not cause ionization. However, they induce radioactivity and eventually lead to ionization by charged particles, which are

produced during collisions with atomic nuclei, or via nuclear reaction.

Neutrons have direct uses as research tools and have applications in other branches of science, such as chemistry, biology and medicine. The most striking use of neutrons is in the chain reactions involving fissile materials. The opening epoch of nuclear power was in military applications (nuclear bombs) and in nuclear power plants where they were used to initiate and sustain chain fission reactions necessary to create heat and thus generate electricity. Another important application of neutrons is also being extensively used in radiation therapy to destroy cancerous tumor cells in the body.

The wide uses of neutrons and applications of neutron physics depend on knowledge of the properties of neutrons and on an understanding of their sources and interactions with matter.

10.2. Sources of Neutrons

Neutrons are very valuable particles because of their ability to penetrate deeper in matter as compared to charged particles. Production of free neutrons is, therefore, of high research significance. Neutrons are generated over a wide range of energies by a variety of different processes based on nuclear reactions. Their main interaction mechanism with other particles is through collisions and absorption, releasing other detectable particles and/or electromagnetic rays. In this section, we will have a look at the most important of the neutron sources available today.

10.2.1. Isotopic neutron sources

(α, n) nuclear reactions on light elements which led to the discovery of the neutron are still used to produce these particles. However, it is also possible to generate neutrons by bombarding light elements with high energy charged particles, such as protons. This nuclear reaction can be accomplished by exciting nuclei such that they emit neutrons during the process of de-excitation. Fortunately, for such a process to occur, it is not always necessary that the target particle carries a very high energy. In fact, incident particles coming out of radioactive sources or a small particle generator are more than sufficient to cause neutron emission from some materials. In general, such sources are made of a radioactive material acting as the source of incident particles mixed in a target material.

A common example of (α, n) reaction is the plutonium-beryllium source, which produces neutrons of a continuous energy spectrum (neutrons have energies from about 1 MeV to 12 MeV) used to provide neutrons to "start" reactors. Plutonium-238 emits α-particles of energy around 5.48 MeV with a half life of about 87.4 years. One curie of plutonium mixed with powdered beryllium yields about 10^6 n/sec. *The yield is the number of neutrons per second from 1 gram of target at 1 cm from 1 curie of the source*. The reaction can be represented by the following sequence:

$$
\begin{aligned}
&{}^{238}_{94}Pu \rightarrow {}^{234}_{92}U + \alpha \\
\alpha + {}^{9}_{4}Be &\rightarrow {}^{13}_{6}C^{*} \\
&{}^{13}_{6}C^{*} \rightarrow {}^{12}_{6}C + n
\end{aligned}
$$

Another common example of an (α , n) neutron source, similar to ^{238}Pu – Be, is ^{241}Am − Be. Americium-241 has a half life of 433 years. It decays by α emission with a mean energy of 5.48 MeV. This long half life makes it suitable for long time storage in laboratories.

An example of the production of neutrons by bombarding lithium target by high energy protons is:

$$p + {}^{7}_{3}Li \rightarrow {}^{7}_{4}Be + n$$

In addition, photoneutron sources are used frequently. In this process atomic nucleus is disintegrated by high-energy photon with an emission of a neutron from the nucleus that has been raised to an excited state by the absorption of this photon. Neutrons produced by photodisintegration are practically monoenergetic. Most of these sources are based on the $^{9}Be(\gamma, n)^{8}Be$ and the $^{2}H(\gamma, n)^{1}H$ reactions. The binding energy of the last neutron is particularly low in ^{9}Be and ^{2}H, and the (γ, n) reactions have low thresholds, 1.67 MeV for the beryllium reaction and 2.23 MeV for the deuterium reaction. A common example of such γ-emitting nuclides is antimony-124 ($^{124}_{51}Sb$). It emits a number of γ-rays, the most probable of which has energy of around 603 keV. If these photons are then allowed to interact with beryllium nuclei, it may result in the emission of a neutron. Antimony-beryllium neutron sources are commonly used in laboratories.

10.2.2. Spallation sources

Spallation is a violent reaction in which a target is bombarded by very high energy particles (normally from high accelerators). The incident particle, such as a proton, alpha or light ions, disintegrates the nucleus through

inelastic nuclear reactions. The result is the emission of protons, neutrons, α-particles, and other light and heavy particles. The neutrons produced in such a reaction can be extracted and used in experiments. A general spallation reaction with a proton as the incident particle can be written as:

$$p + ST \rightarrow SF1 + SF2 + ... + SFm + (k)n \qquad 10.1$$

Where p is the accelerated particle, ST is the spallation target and SF represents m spallation fragments. The number k of neutrons produced in this reaction depends on the type of the target and the energy of the incident particle. The targets used in spallation sources are generally high Z materials such as lead, tungsten, silver or bismuth.

A big advantage of spallation sources is that they produce neutrons with a wide spectrum of energies ranging from a few eV to several GeV. Another advantage is their ability to generate neutrons continuously or in short pulses. The pulses could be as short as a nanosecond.

10.2.3. Fusion sources

We have seen that the plot of binding energy per nucleon (section 2.4 and Fig. 2.4) has a maximum at $A \approx 56$ (close to iron) and slowly decreases for heavier nuclei. For lighter nuclei, the decrease is much quicker, so that with the exception of magic nuclei, lighter nuclei are less tightly bound than medium size nuclei. Thus, in principle, energy could be produced by combining (fusing) two light nuclei to produce a heavier in an excited state. This nucleus releases neutrons and photons to reach its ground state to be more tightly bound nucleus. This process as a potential source of

power is called *nuclear fusion*. However, since lighter nuclei contain fewer nucleons, the total energy released per fusion is smaller than that released in fission. On the other hand, since there is an abundance of light and stable nuclei in nature, fusion provides an attractive alternative for generating power. Fusion is, in fact, the mechanism responsible for energy generation in the interior of the sun, through the proton-proton cycle and of other stars, through carbon or CNO cycle.

The fusion reaction can therefore be used to produce neutrons. To initiate a fusion reaction practically, a fair amount of energy must be supplied through some external means because the nuclei are repelled by electromagnetic force between the protons. This energy can be provided by several means, such as through charged particle accelerators. These sources are more efficient in terms of neutron yield. The main fusion process producing neutrons is called Deuterium Cycle.

$$
\begin{aligned}
{}^{2}_{1}H + {}^{2}_{1}H &\rightarrow {}^{3}_{2}He + n + 3.3\ MeV \\
{}^{2}_{1}H + {}^{3}_{1}H &\rightarrow {}^{3}_{1}H + p + n + 4.0\ MeV \\
{}^{2}_{1}H + {}^{3}_{1}H &\rightarrow {}^{4}_{2}He + n + 17.6\ MeV
\end{aligned}
$$

Just as for fission, the energy released comes from the difference in the binding energies of the initial and final states. Thus, fusion offers enormous potential for power generation, *if the huge practical problems could be overcome*.

The first practical problem in obtaining a controlled fusion, whether in power production or more generally, has its origin in the Coulomb repulsion (coulomb barrier), which inhibits two nuclei getting close enough together to fuse.

However, for this to happen, the Coulomb barrier between the two nuclei has to be overcome. The value of the repulsive Coulomb energy is a maximum when the two nuclei are just touching, and has the form:

$$V_{Coul} = \frac{ZZ'e^2}{R + R'} \qquad 10.2$$

where Z and Z' are the atomic numbers of the two nuclei, and R and R' are their respective radii. Recalling Eq.1.28, we can rewrite this as:

$$\begin{aligned} V_{Coul} &= \frac{e^2}{\hbar c}\frac{\hbar c ZZ'}{1.2\left(A^{1/3} + A'^{1/3}\right) fm} \\ &= \frac{1}{137}\frac{197\ MeV.fm}{1.2\ fm}\frac{ZZ'}{A^{1/3} + A'^{1/3}} \\ &\approx \frac{ZZ'}{A^{1/3} + A'^{1/3}} \approx \frac{1}{8}A^{5/3}MeV \end{aligned} \qquad 10.3$$

where A and A' are the nucleon numbers of the two light nuclei and the final expression is obtained by setting $A \approx A' \approx 2Z \approx 2Z'$. Thus, the Coulomb barrier between two nuclei of $A \approx 8$ is about 4 MeV. Consequently, for fusion to take place, we must provide kinetic energies of the order of a few MeV to overcome the Coulomb barrier (clearly, the exact value depends on the specific nuclear masses and charges). It would, therefore, appear that a natural way to achieve fusion is by colliding two energetic beams of light nuclei. In such a process, however, most of the nuclei get scattered elastically and, as a result, this turns out to be an inefficient way of inducing fusion.

An alternative and Practical method is to heat a confined mixture of the nuclei to supply enough thermal energy to overcome the Coulomb barrier as in *thermonuclear bomb*. The temperature necessary may be estimated from the relation $E=k_BT$, where k_B is Boltzmann constant. For energy of *4 MeV*, this implies a temperature of about 10^{10} *K*.

It is also the major hurdle that the nuclei must be confined close enough to allow them to fuse (density $n \sim 2-3 \times 10^{20}$ m^{-3}) and the confinement must be sufficiently long ($t \sim 1-2$ sec). To date, no device has yet succeeded in achieving such conditions. Experience with fission power reactors suggests that it will probably take decades of further technical development before fusion power becomes a practical reality.

10.2.4. Radioactive Sources

There are no known naturally occurring isotopes that emit significant number of neutrons. Perhaps the most extensively used sources of neutrons are some artificial heavy nuclei of atomic number greater than 92, called transuranium elements. Among them, californium-252 was found to have two decay modes: α-emission (96.9%) and *spontaneous fission* (3.1%). A *spontaneous fission* is a common decay mode resulting in the emission of neutrons. During this process, a heavy nucleus spontaneously splits into two lighter nuclides called fission fragments and emits several neutrons. The general equation for spontaneous fission process cannot be written as there are a number of modes in which a nucleus may fission. That is, there is generally a whole spectrum of nuclides in which a decaying nucleus may split. Also, the number of neutrons emitted is variable and depends on the particular mode of decay,

normally 2–4 neutrons per fission. As an example, californium-252 may result 4 neutrons:

$$^{252}_{98}Cf \rightarrow ^{94}_{38}Sr + ^{154}_{60}Nd + 4n$$

1 mg of ^{252}Cf emits around 2.3×10^9 neutrons per second with average neutron energy of 2.1 MeV. It also emits a large number of γ-ray photons but the intensity is an order of magnitude lower than that of the neutrons. It, therefore, does not pose much problem for applications requiring a moderately clean neutron beam. Table 10.1 lists some of the common sources of neutrons and their decay modes.

10.2.5. Neutrons from nuclear reactors

The most powerful sources of neutrons are those associated with nuclear reactors. Many neutrons are produced in a chain reacting assembly of a fissile material and a moderator. The neutrons resulting from the *induced fission* of uranium atoms are fast and are slowed down to thermal energy by scattering process in the moderator (the details of the fission process will be given in the next section). Although most of these neutrons are used up to induce more fission reactions, still a large number of neutrons manage to escape the nuclear core.

For some purposes, as for the production of artificial radionuclides or for any nuclear experimental research, the mixture of neutrons with different energies can be used. These neutrons can be obtained by designing of suitable columns made of metal (vertical or horizontal columns) extended from outside the reactor to definite locations of the reactor core or the moderator to get a desired neutron flux

and desired neutron energy. These neutrons inside channel can be used to bombard targets exposed there or they can be allowed to escape through a hole, forming a beam of neutrons which can be used outside the channel.

Table 10.1
Common neutron sources and their decay modes.

Source	Isotopes	Reaction Type
Californium	$^{252}_{98}Cf$	Spontaneous Fission
Deuterium-Helium	$^{2}_{1}D$-$^{3}_{2}He$	Nuclear Fusion
Tritium-Helium	$^{3}_{1}T$-$^{4}_{2}He$	Nuclear Fusion
Uranium	$^{235}_{92}U$	Nuclear Fission
Lithium	$^{7}_{3}Li$	Spallation
Beryllium	$^{9}_{4}Be$	Spallation
Plutonium-Beryllium	$^{238}_{94}Pu$-Be	(α, n)
Plutonium-Beryllium	$^{239}_{94}Pu$-Be	(α, n)
Americium-Beryllium	$^{241}_{95}Am$-Be	(α, n)
Americium-Boron	$^{241}_{95}Am$-B	(α, n)
Americium-Fluorine	$^{241}_{95}Am$-F	(α, n)
Americium-Lithium	$^{241}_{95}Am$-Li	(α, n)
Radium-Beryllium	$^{226}_{88}Ra$-Be	(α, n)
Antimony-Beryllium	$^{124}_{51}Sb$-Be	(γ, n)

10.3. Interaction of neutrons with matter

As we have already mentioned, neutrons are in most respects very similar to protons. They are the constituents of nuclei, and have essentially the same mass, same nucleon number and spin as protons. They are, however, electrically neutral, and consequently, just like photons, cannot interact directly through the Coulomb force. Although neutrons have small magnetic dipole moments, these do not provide substantial interactions in media. This enables them to move swiftly through large open atomic spaces without interacting with atoms. However, if they pass near the nuclei, they encounter strong nuclear force. In such a situation, they can interact with the nuclei in different ways depending on their energy.

Neutron-nuclei reactions, formulated in a manner very similar to that given in Chapter 3, are generally accompanied by either absorption or emission of energy calculated by the theory of relativity, $Q=\Delta mc^2$, where Δm is the mass difference between the interacting particles before and after the collision. Obviously, nuclear reaction is exothermic, i.e., the reaction Q-value >0.

There are a wide variety of possible neutron-nuclei reactions. The reactions of most interest especially in the analysis of a nuclear fission reactor include:

1. Nuclear fission (n, fission):

$$ {}_0^1n+{}_Z^AX \rightarrow ({}_Z^{A+1}X^*)\rightarrow {}_{Z1}^{A1}FF_1+{}_{Z2}^{A2}FF_2+(\upsilon)n+200\ MeV \quad 10.4 $$

2. Scattering (n,n) or (n,n'):

$$
\begin{aligned}
&{}_0^1n+{}_Z^AX\rightarrow{}_Z^AX+{}_0^1n \qquad [elastic\ \ scattering\ \ (n,n)]\\
&\rightarrow({}_Z^AX^*)+{}_0^1n \quad [inelastic\ \ scattering\ \ (n,n')]\\
&\rightarrow{}_Z^AX+{}_0^1n+\gamma \quad [inelastic\ \ scattering\ \ (n,n')]
\end{aligned}
\qquad 10.5
$$

3. Radiative capture (n, γ):

$$
{}_0^1n+{}_Z^AX\rightarrow({}_Z^{A+1}X^*)\rightarrow{}_Z^{A+1}X+\gamma \qquad 10.6
$$

4. Transmutation:

$$
\begin{aligned}
&{}_0^1n+{}_Z^AX\rightarrow({}_Z^{A+1}X^*)\rightarrow{}_{Z-2}^{A-4}Y+{}_2^4\alpha+{}_0^1n\\
&{}_0^1n+{}_Z^AX\rightarrow({}_Z^{A+1}X^*)\rightarrow{}_{Z-1}^{A-1}Z+{}_1^1p+{}_0^1n
\end{aligned}
\qquad 10.7
$$

The importance of the fission reaction to nuclear reactor operation is obvious. Both radiative capture and scattering are also extremely important since they influence the neutron economy and hence the controlling chain reaction. We will discuss each process more quantitatively.

10.3.1. Nuclear fission

Nuclear fission is a process in which an unstable heavy nucleus splits up into two lighter nuclides and emits neutrons. Two types of fission reactions are possible: spontaneous fission and induced fission. We saw earlier that spontaneous fission occurs in some radionuclides, at least one of which, i.e., californium-252, occurs naturally. These radionuclides are extensively used as neutron sources.

Induced fission, caused by the absorption of a neutron, occurs with certain nuclei of high atomic (or mass) number, called fissionable nuclides. With increasing atomic number, the electrostatic repulsion between protons varies as Z^2, and hence becomes an important contributory factor. When fission takes place, the excited compound nucleus formed after absorption of a neutron breaks up into two lighter nuclei, called fission fragments. The two fission fragments generally have unequal masses with mass numbers in the range of roughly 72 to 161, especially if the neutron is of low kinetic energy (slow neutron) but in a sample of many fissionable atoms, some of the fragments are always of equal mass. Most of these fission fragments are unstable and go through a series of nuclear decays before transforming into stable elements (see Fig. 10.1 for an example of uranium-233, uranium-235, and plutonium-239 fission fragments spectrum).

- Neutrons released:

Number of neutrons (called prompt neutrons) released immediately (the fission takes place in a time of the order $t = \hbar/\Gamma \approx 10^{-14}$sec, since the measured widths of low-energy resonance of fissionable nuclides is about $\Gamma \approx 0.1$ eV, refer to section 3.3.3) from those fission fragments, each of which has too many neutrons for stability, as well as the excess (excitation) energy of about 6 to 8 MeV required for the expulsion of a neutron, refer to Fig. 2.1.

The reaction can be written as in Eq.10.4, where X represents fissionable material (such as uranium-235), υ is the number of neutron released per fission (normally between 2 to 3), n is the neutron, and FF_1 and FF_2 are the two fission fragments.

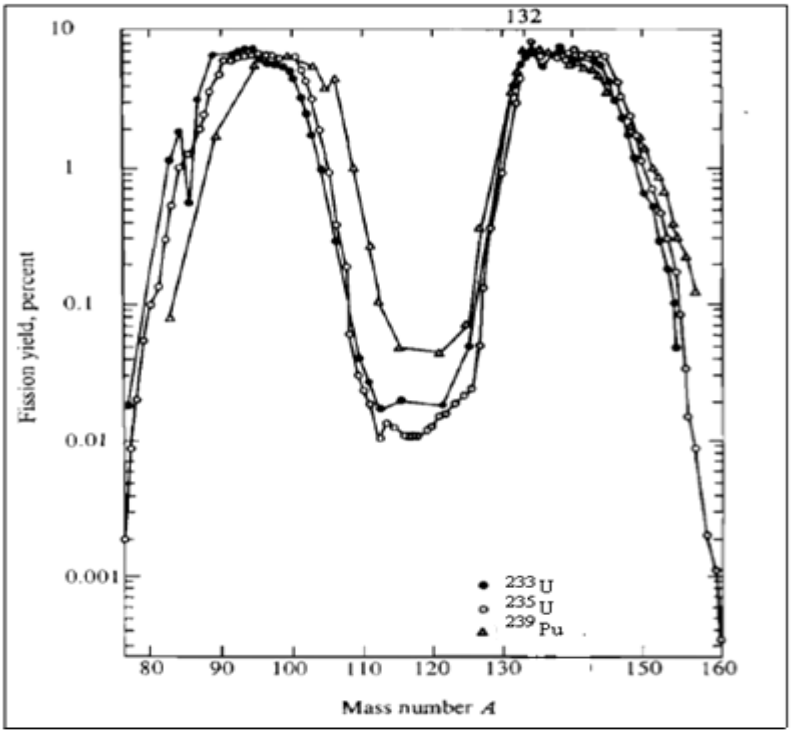

Figure 10.1. Fission yield as a function of mass number of the fission products.

- **Fissionable nuclides:**

Only three heavy nuclides of odd mass number, having sufficient stability to permit storage for a long time, namely, uranium-233, uranium-235, plotonium-239, are fissionable by neutrons of all energies, from thermal values (0.25 eV, or less) to millions of electron volts. They are referred to as *fissile nuclides*. Of these nuclides, uranium-235 is the only one which occurs in nature; the other two are produced artificially from thorium-232 and uranium-238, respectively, by neutron capture followed by two stages of radioactive decay. Moreover, since thorium-232 and uranium-238 can

be converted into the fissile species, both of them are called *fertile nuclides*.

As an example, let us have a look at how uranium-235 fissions. The following equation shows the process for two of the most probable fission fragments:

$$n + {}^{235}_{92}U \rightarrow {}^{236}_{92}U \rightarrow {}^{137}_{53}I + {}^{96}_{39}Y + 3n \qquad 10.8$$

where ${}^{236}_{92}U$, is an unstable compound isotope of $n + {}^{235}_{92}U$ that eventually breaks up in fragments and releases 3 neutrons. These two fission fragments are unstable and go through the following β-decays:

$$\begin{aligned}
&{}^{137}_{53}I \rightarrow {}^{137}_{54}Xe + \beta^- + \bar{\upsilon}_e \qquad t_{1/2} = 24.5\,\text{sec} \\
&{}^{137}_{54}Xe \rightarrow {}^{137}_{55}Cs + \beta^- + \bar{\upsilon}_e \qquad t_{1/2} = 3.818\,\text{min} \\
&{}^{137}_{55}Cs \rightarrow {}^{137}_{56}Ba + \beta^- + \bar{\upsilon}_e \qquad t_{1/2} = 30.1\,yr \\
&{}^{96}_{39}Y \rightarrow {}^{96}_{40}Zr + \beta^- + \bar{\upsilon}_e \qquad t_{1/2} = 5.34\,\text{sec}
\end{aligned}$$

or, the process can be written globally as:

$$n + {}^{235}_{92}U \rightarrow {}^{137}_{56}Ba + {}^{96}_{40}Zr + 3n + 4\beta^- + 4\bar{\upsilon}_e \qquad 10.9$$

These fission fragments are themselves unstable and go through a series of β-decays till they transmute into stable elements. Iodine-137 eventually decays into xenon-137 which, in turn, decays to cesium-137, then to barium-137 (stable), while yttrium-96 decays into zirconium-96 (stable). Because of their high β-yields, these fission fragments and their daughters are regarded as extremely hazardous and special precautions must be taken while handling them.

- Fission energy:

The amount of energy released when a nucleus undergoes fission can be calculated by determining the net decrease in mass from the known isotopic masses, and utilizing the Einstein mass-energy relation. A simple, but instructive although less accurate, alternative procedure is by disregarding the neutrons involved, since they have a negligible effect on the present calculation. The fission reaction may be represented approximately by:

$$\text{Uranium-235} \rightarrow \text{FF1} + \text{FF2} + \text{energy}.$$

In uranium-235, the mean binding energy per nucleon is about 7.6 MeV (refer to section 2.4-4), so that it is possible to write:

$$92p + 143n \rightarrow \text{uranium-235} + (235 \times 7.6)\ \text{MeV}.$$

Here, p and n represent protons and neutrons, respectively. The mass numbers of the two fission product nuclei, FF1 and FF2, are mostly in the range of roughly 95 to 140 (as shown in Fig. 10.1), where the binding energy per nucleon is about 8.5 MeV, taking tin-120 as an average; hence:

$$92p + 143n \rightarrow \text{FF1} + \text{FF2} + (235 \times 8.5)\ \text{MeV}.$$

Upon subtracting the above two binding energy expressions, the result is:

$$\text{Uranium-235} \rightarrow \text{FF1} + \text{FF2} + 210\ \text{MeV}.$$

The fission of a single uranium-235 (or similar) nucleus is thus accompanied by the release of about 200 MeV (32×10^{-12} J) of energy. This may be compared with about 4 eV (6.4×10^{-19} J) released by the combustion of an atom of

carbon-12. Now, one kilogram of any element contains $N_A \times 10^3/A$ atoms, where N_A is Avogadro's number, and one kilogram of ^{235}U contains, therefore, about $6.02\times10^{26}/235 \approx 2.6\times10^{24}$ atoms. Accordingly the complete fission of one kg of ^{235}U can yield a total energy of:

$$32\times10^{-12}\ (\text{J/atom}) \times 2.6\times10^{24}\ (\text{atoms}) \approx 8.2\times10^{13}\ \text{J}$$

Since 1 J is equivalent to 1 watt-second (W.sec) or equal to 1.16×10^{-11} megawatt-days (MW.d), the 8.2×10^{13} J produced by the complete fission of 1kg of fissile material is equivalent to $(8.2\times10^{13})(1.16\times10^{-11}) = 951$ MW.d. A rough approximation is that the fission of 1.08 kg of fissile material will produce 1000 MW.d of thermal energy. Consequently, 1 kg of uranium-235 will produce energy equivalent to combustion of about 2700 metric tons of coal (3.0×10^4 kJ/kg, 1.3×10^4 Btu/lb).

The analysis of Eq.10.8 shows that the most of the released energy is contained in the initial kinetic energies of the two fission fragments. The kinetic energy of each heavy fragment at the time of fragmentation is of the order of 75 MeV, with initial velocities of roughly 10^7 m.sec^{-1}. Given their large masses, their ranges are very small, about 10^{-6} m. The stopping process transforms the kinetic energy to thermal energy.

On average, the various components take the following energies:

Kinetic energy of fragments	165 ± 5 MeV
Energy of prompt photons	7 ± 1 MeV
Kinetic energy of neutrons	5 ± 0.5 MeV
Energy of β decay electrons	7 ± 1 MeV
Energy of β decay antineutrinos	10 MeV
In addition to energy of photons	6 ± 1 MeV
Total	200 ± 6 MeV

Of the ~ 200MeV, only 190 ± 6 MeV are useful, since the neutrinos escape and do not heat the medium.

The neutrons produced will maintain chain reactions in induced fission processes. For ^{236}U (i.e. for the fission of ^{235}U induced by a neutron), the mean number of produced neutrons is $\upsilon = 2.47$.

The energy distribution of these neutrons is peaked around $E_n = 0.7$ MeV. The mean energy is $<E_n> \sim 2$MeV.

- Fission mechanism, fission barrier:

The complexity of fission seems out of reach of a detailed theoretical description. However, as early as 1939, the liquid droplet model of Bohr and Wheeler gave a good qualitative description (see section 7.3).

The process starts as a compound nucleus (more or less spherical) formed from the absorption of a neutron by a target nucleus Fig. 10.2, A. Let us follow the potential energy of the system as a function of variation of the distance *r* between the two fragments FF1 and FF2, as illustrated in Fig. 10.2.

The excitation energy of the compound nucleus will be equal to the binding energy of the neutron plus any kinetic energy the neutron may have before its capture. As a result of this excess energy, the compound nucleus may be considered to undergo a series of oscillations, in the course of which it passes through a phase similar to Fig. 10.2, B, where *r* increases, the nucleus becomes deformed, its surface area increases compared to the initial shape. Therefore, this deformation *increases* the surface tension energy. On the other hand, the increase in the distance *FF1 −FF2* means a decrease of the *Coulomb repulsion* energy between *FF1* and *FF2*. There is a competition between the

nuclear forces and the Coulomb repulsion. At some point, as r varies between r_0 (initial shape of the nucleus) and infinity (separated fragments *FF1* and *FF2*, Fig 10.2, D), the potential energy of the system has a maximum value.

In other words, there is a potential barrier, called the *fission barrier* that must be crossed in order for the process to permit the compound nuclei to deform into the state C of Fig. 10.2. One calls *activation energy* E_A (also called *critical energy*), the difference between the maximum of the barrier and the energy of the initial nucleus in its ground state. For nuclei with $A \sim 240$, this energy turns out to be of the order of 6 MeV.

In order for the compound nucleus to decay by spontaneous fission, the barrier must be crossed by the quantum tunnel effect. To get an idea of the factors that determine the difficulty of tunneling through the barrier, it is interesting to compare the surface term and Coulomb term energies of a spherical nucleus as predicted by the Bethe-Weizsäcker semi-empirical mass Eqs. 7.16, 7.23, and 7.33:

$$\frac{B_c}{B_s} = \frac{0.72Z(Z-1)A^{-\frac{1}{3}}}{16.8A^{\frac{2}{3}}} \approx \frac{Z^2/A}{25} \qquad 10.10$$

The activation energy E_A for fission should decrease as the value of Z^2/A increases. A qualitative argument leading to this conclusion is that repulsion between the nucleons, which favors fission, varies as Z^2, (representing Coulomb energy) whereas the attraction is approximately proportional to A (as surface energy), so that fission should occur more easily as Z^2/A increases. Accordingly, nuclei with $Z^2/A < 25$ would be expected to have large barriers so that neutrons (or other particles) of very high energy would be required to

cause fission. But for nuclei with $Z^2/A > 25$, where the Coulomb energy dominates the surface energy, the E_A is decreased in such a way as to have very small barriers of about 6 MeV or less. In fact, this is of the order of magnitude of the binding energy of a neutron and hence of the excitation energy that will accompany the capture of a low-energy neutron.

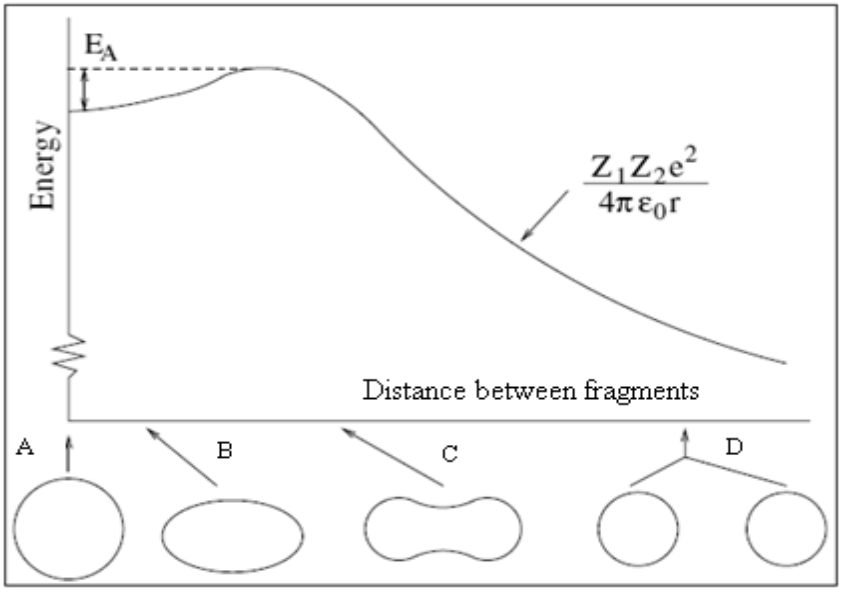

Figure 10.2. Liquid drop model of fission and variation of the energy of a deformed nucleus as a function of the distortion stages.

10.3.2. Scattering (n, n) or (n, n′)

In scattering reaction of neutron with atomic nuclei, the final result is merely an exchange of energy between the two colliding particles, and a neutron remains free after the interaction. As mentioned before, neutrons are generated over a wide range of kinetic energies, in the MeV range, and

so they are called *fast neutrons*. However, after a sufficient number of scattering collisions with various nuclei of the medium, the speed of a neutron is reduced to such an extent that it has approximately the same *average* kinetic energy as the atoms or molecules of the scattering medium. The energy depends on the temperature of the medium, and so it is called *thermal energy*. Neutrons whose energies have been reduced to this extent are called *thermal neutrons*. At ordinary temperature, the average energy of such neutrons is less than 0.04 eV. A typical grouping of neutron energies is:

- Thermal: $E_n < 1$ eV (0.025 eV)
- Epithermal: 1 eV $< E_n <$ 10 keV
- Fast: $E_n >$ 10 keV

The ways of scattering of neutrons depend mainly on their energy.

- Elastic scattering (n, n):

Elastic scattering is the principal mode of interaction of neutrons with atomic nuclei. In this process, the target nucleus remains in the same state after interaction. The (n, n) reaction is written as the first formula of Eq.10.5. Elastic scattering is possible with all nuclei, free or bound, and neutrons of *all energies*.

The elastic scattering process of neutrons with nuclei can occur in two different modes: potential elastic and resonance elastic.

1. Potential elastic scattering: the one of major interest in nuclear reactor systems. It occurs with neutrons having energies up to a few MeV and for nuclei of low mass number. Potential scattering refers to the process in which the neutron is acted on by the short range nuclear

forces of the nucleus and as a result, it scatters without touching the particles, in other words, there is no compound nucleus formation.

2. Resonance elastic scattering: In the resonance mode, also called compound nucleus scattering, a neutron with the right amount of energy is absorbed by the nucleus, forming a compound nucleus, with the subsequent emission of another neutron leaving the target nucleus in its ground state but usually with a different (larger) kinetic energy such that the kinetic energy of the system is conserved.

As a general rule in situations of present interest, elastic scattering can be treated as a "billiard ball" type of collision. The behavior can then be analyzed by means of the familiar laws of classical mechanics, based on the principles of the conservation of kinetic energy and of momentum (see Chapter 3).

The neutron elastic cross section will be discussed later.

- Inelastic Scattering (n, n′):

Unlike elastic scattering, the inelastic scattering leaves the target nucleus in an excited state. The reaction is written as given by the last two formulas in Eq.10.5.

In such a process, the incoming neutron is absorbed by the nucleus forming an excited compound nucleus. The compound nucleus is unstable and quickly emits a neutron of lower kinetic energy, leaving the target nucleus in an excited state. In other words, in an inelastic scattering collision, some (or all) of the kinetic energy of the neutron is converted into excitation (internal) energy of the target nucleus. This excess energy is subsequently emitted as one or more photons of gamma radiation, i.e., the excited

nucleus goes through one or more γ-decays to return to the ground state. Therefore, for inelastic scattering to occur, the initial kinetic energy of the incident neutron must exceed the minimum excitation energy of the target nucleus which depends on mass number.

For elements of low mass number, the excitation energy of even the first (lowest) excited state above the ground state is large, of the order MeV. Hence, only neutrons with kinetic energy exceeding several MeV can be inelastically scattered as a result of nuclear excitation. For elements of moderate and high mass number, the minimum excitation energy will be lower, usually ranging from (~ 0.1 MeV to less than 1 MeV). Magic nuclides are exceptional in this respect, as discussed in Chapter 7.

10.3.3. Radiative capture

Radiative capture is a very common reaction involving neutrons. In such a reaction, a nucleus absorbs the neutron forming a compound nucleus which is evidently raised to one of its excited states. To return to stable state, the nucleus emits γ-ray photon. In this case, no transmutation occurs; however, the isotopic form of the element changes due to the increase in the number of neutrons. The reaction is represented by Eq.10.6 or A(n, γ)A + 1.

Radiative capture has been observed with a great many elements, particularly the heavier ones. In most cases, the isotopes formed by the capture of a neutron have been found to be radioactive, so (n, γ) reaction is generally used to produce radioisotopes in a so-called activation analysis, mainly in nuclear reactors, such as cobalt-60:

$$n + {}^{59}_{27}Co \rightarrow ({}^{60}_{27}Co^{*}) \rightarrow {}^{60}_{27}Co + \gamma$$

followed by

$${}^{60}_{27}Co \rightarrow {}^{60}_{28}Ni + \beta^{-} + \bar{\upsilon} \qquad t_{1/2} = 5.26\,yr \qquad 10.11$$

Another typical case is gold-198:

$$n + {}^{197}_{79}Au \rightarrow ({}^{198}_{79}Au^{*}) \rightarrow {}^{198}_{79}Au + \gamma$$

followed by

$${}^{198}_{79}Au \rightarrow {}^{198}_{80}Hg + \beta^{-} + \bar{\upsilon} \qquad t_{1/2} = 2.7\,days \qquad 10.12$$

10.3.4. Transmutation

It is a reaction in which an element changes into another one. Neutrons of all energies are capable of producing transmutations. In one type of reaction, (n, α) reaction, the capture of a slow neutron results in the emission of an alpha particle as in Eq.10.7. Two such cases that have been studied extensively are:

$$\begin{aligned} n + {}^{6}_{3}Li &\rightarrow ({}^{7}_{3}Li^{*}) \rightarrow {}^{3}_{1}H + {}^{4}_{2}\alpha \\ n + {}^{10}_{5}B &\rightarrow ({}^{11}_{5}B^{*}) \rightarrow {}^{7}_{3}Li + {}^{4}_{2}\alpha \end{aligned} \qquad 10.13$$

The (n, α) reaction with boron-10 is widely used in control rods of nuclear reactors as neutrons absorber and in neutron detectors, particularly in ionization chamber work.

When fast neutrons are captured by heavier nuclei, resulting in the emission of an alpha particle, the product nucleus is usually radioactive. Some typical reactions are:

$$n + {}^{23}_{11}Na \rightarrow ({}^{24}_{11}Na^{*}) \rightarrow {}^{20}_{9}F + {}^{4}_{2}\alpha$$

followed by

$$ {}^{20}_{9}F \rightarrow {}^{20}_{10}Ne + \beta^{-} + \overline{\upsilon} \qquad t_{1/2} = 10.7\,\text{sec} \qquad 10.14$$

and

$$n + {}^{27}_{13}Al \rightarrow ({}^{28}_{13}Al^{*}) \rightarrow {}^{24}_{11}Na + {}^{4}_{2}\alpha$$

followed by

$$ {}^{24}_{11}Na \rightarrow {}^{24}_{12}Mg + \beta^{-} + \overline{\upsilon} \qquad t_{1/2} = 15.0\,hr$$

The capture of a neutron may sometimes result in the emission of a proton by the compound nucleus; see Eq.10.7. This (n, p) process has been observed with slow neutrons in the case of nitrogen-14 in the reaction:

$$n + {}^{14}_{7}N \rightarrow ({}^{15}_{7}N^{*}) \rightarrow {}^{14}_{6}C + {}^{1}_{1}H$$

followed by 10.15

$$ {}^{14}_{6}C \rightarrow {}^{14}_{7}N + \beta^{-} + \overline{\upsilon} \qquad t_{1/2} = 5730\,yr$$

The above equation is assumed to be the source of the ^{12}C found in nature. This reaction undoubtedly takes place in the atmosphere where nitrogen nuclei are bombarded by neutrons produced by the interaction of cosmic rays with other particles in the atmosphere.

Other (n, p) reactions with fast neutrons have usually resulted in the production of nuclei that are radioactive, emitting beta particles. For example:

$$n + {}^{32}_{16}S \rightarrow ({}^{33}_{16}N^{*}) \rightarrow {}^{32}_{15}P + {}^{1}_{1}H$$

followed by 10.16

$$ {}^{32}_{15}P \rightarrow {}^{32}_{16}S + \beta^{-} + \overline{\upsilon} \qquad t_{1/2} = 14.3\,days$$

The above reactions have several interesting consequences. It will be noticed that the bombarded nucleus and the final stable nucleus are identical, whereas the incident neutron has been transformed, apparently, into a proton, an electron and an antineutrino. If the mass of the intermediate radioactive nucleus-for example, ^{32}P-is equal to the mass of the initial ^{32}S, the energy available for the disintegration must come from the mass difference between a neutron and a hydrogen atom plus the initial energy of the neutron. If slow neutrons are used as bombarding particles, the energy available is equivalent to 0.000842 u or 0.784 MeV. Now the end point energy of the beta-ray spectrum is equal to the disintegration energy. If this end-point energy is less than 0.784 MeV, slow neutrons will be effective in producing the above reaction, as in the case of ^{14}N. But if the end-point energy exceeds 0.784 MeV, the additional energy must come from the kinetic energy of the incident neutrons; hence only fast neutrons can be effective in producing this reaction. For example, the end point energy of the beta-ray spectrum from ^{32}P is 1.7 MeV; hence only fast neutrons bombarding ^{32}S will be effective in producing this reaction, Eq.10.16. This reaction can then be used to differentiate between slow and fast neutrons.

Another interesting conclusion is that if the mass of the nucleus formed in an (n, p) reaction exceeds the mass of the bombarded nucleus by more than 0.000842 u, only fast neutrons will be effective in producing this reaction.

10.4. Neutron Cross Section

The probability that a neutron-nucleus reaction will occur is characterized by a quantity called a *nuclear cross section*. The empirical data in section 8.2 showed in Eq. 8.3,

$\sigma = \frac{N_i}{N_o n \delta x}$, that the nuclear reaction cross section and N_o are the number of a monoenergetic beam of free neutrons incident on the target containing N_t nuclei. This can be written as:

$$N_t = n \times A \times \delta x \qquad 10.17$$

where n is the number of nuclei per unit volume, δx is the target thickness and N_i is the number of neutrons that are lost due to the interaction with the target nuclei.

In this case, we would expect that the rate of neutron-nuclear reactions, $Rate = N_i / A$ (reaction/$cm^2 sec$), in the target will be proportional to both the incident neutron beam intensity (neutron flux) $I = N_o / A$ (*in units of number of neutrons/*cm^2*.sec*) and the number of target atoms per unit surface area $N_s = N_t / A = n \times \delta x$ (atom/cm^2). We can write the rate at which reactions occur per unit area on the target as:

$$Rate\left(\frac{reaction}{cm^2.\text{sec}}\right) = \sigma\left(cm^2\right) \times I\left(\frac{neutron}{cm^2.\text{sec}}\right) \times N_s\left(\frac{atom}{cm^2}\right) \qquad 10.18$$

We can define a microscopic cross section for each type of neutron-nuclear reaction and each type of nuclide; see section 8.2. For example, the appropriate cross sections characterizing the four types of reactions we discussed earlier, fission, scattering, radiative capture and transmutation, are denoted by σ_f, σ_s, σ_γ, and $\sigma_{n,\alpha}$, respectively.

We can also assign separate cross sections to characterize elastic scattering σ_e in which the target nucleus remains in its ground state and inelastic scattering σ_{in} in which the target nucleus is left in an excited state. Since cross sections are

related to probabilities of various types of reactions, it is apparent that:

$$\sigma_s = \sigma_e + \sigma_{in} \qquad 10.19$$

The microscopic scattering cross section will describe the probability that such a scattering collision occurs. However, it provides no information about the change in neutron direction or energy that occurs in such a collision. This information is very important in a certain type of nuclear reactor studies. To characterize it, we introduce the concept of the *differential scattering cross section*. A full mathematical detail for the variable characterizing neutron direction of motion is given in section 8.2.2, Fig. 8.3, while the component characterizing the neutron speed, $\sigma_s(T_i \rightarrow T_f)$, will be given in the next section.

In a similar sense, we can define the *absorption* cross section characterizing those events in which a nucleus absorbs a neutron σ_a:

$$\sigma_a = \sigma_f + \sigma_\gamma + \sigma_{n,\alpha} + \cdots \qquad 10.20$$

Finally, we can introduce the concept of the *total* cross section σ_t characterizing the probability that any type of neutron-nuclear reaction will occur. Obviously:

$$\sigma_t = \sigma_s + \sigma_a \qquad 10.21$$

Accordingly, the macroscopic cross sections (see section 8.2, $\Sigma_i = n\sigma_i$) define the macroscopic cross section for any specific reaction as just the microscopic cross section for the reaction of interest multiplied by the number density n characterizing the material of interest. For example:

$\Sigma_f = n\sigma_f$ is the macroscopic fission cross section
$\Sigma_s = n\sigma_s$ is the macroscopic scattering cross section
$\Sigma_a = n\sigma_a$ is the macroscopic absorption cross section
$\Sigma_t = n\sigma_t$ is the total macroscopic cross section
Notice also that:

$$\Sigma_t = \Sigma_s + \Sigma_a \qquad 10.22$$

It should be stressed that while one can formally define such macroscopic cross sections for specific reactions, our earlier discussion of attenuation of the monoenergetic radiation beam (charged particle, electromagnetic ray) after passing through a thick target slab, given in section 8.2, applies to the total macroscopic cross section of neutron penetration as well, the concept of macroscopic cross section can also be generalized to homogeneous mixtures of different nuclides as given in Eq. 8.5. Also we can calculate the average distance a neutron travels before interacting with a nucleus in the target sample (*mean free path*) in the same manner given in section 8.2.3, $\lambda = 1/\Sigma_t = 1/n\sigma_t$.

10.5. Analyses of Neutron Cross Sections

There are two aspects involved in the analysis of neutron cross sections. The first is the *dynamics of nuclear reactions*. Second is the *kinematics of two-body collisions* that is the application of the laws of conservation of momentum and energy to such elastic collisions.

10.5.1. Dynamic of nuclear reactions

The dynamic of nuclear reactions is concerned with the fundamental physical mechanisms involved in such collision events. The two mechanisms of most interest are:

First, *potential scattering*; in this mechanism the neutron merely bounces off of the force field of the nucleus without actually penetrating the nuclear surface. The neutron scatters elastically off the nuclear potential without ever penetrating the nucleus itself, very similar to billiard balls. The cross section for such a reaction is essentially just the geometrical cross section of the nucleus. Potential cross sections are characterized by rather flat energy dependence from about 1 eV up to the MeV range.

Second, *compound nucleus formation*; as discussed in section 3.2, compound nucleus formation occurs in many neutron-nuclear reactions of interest, including radiative capture, fission, inelastic scattering and elastic resonance scattering (refer to Eqs. 10.4 to 10.7). The formation of a compound nucleus actually corresponds to the so called *resonance reaction*, in which the incident neutron energy matches one of the excited energy levels in the compound nucleus.

The energy available for such reaction is the center of mass (CM) energy $T_C = [M/(m+M)]T$, where m is the neutron mass, M is the nuclear mass, and T is neutron kinetic energy in the LAB system. The actual energy of the excited level of the compound nucleus E_{ex} is much higher due to the additional binding energy of the added neutron E_b. If $T_C + E_b$ is very close to the excited energy level of the compound nucleus ${}^{A+1}_{Z}X$, one expects that the probability for compound nucleus formation will be much larger than if $T_C + E_b$ does not match this energy level. Hence, we expect that

the cross sections for such compound nuclear reactions will exhibit sharp peaks or resonances at those neutron energies T for which this energy matching occurs of the form:

$$\sigma_t \sim \frac{A}{(T - E_o)^2 + (\Gamma/2)^2} \qquad 10.23$$

where E_o is the energy at which the resonance occurs (that is, the energy T_C at which $T_C + E_b$ *match or equal* E_{ex}) and Γ is the total line width of the resonance that essentially characterizes the width of the energy level and the full width at half-maximum (FWAM) of the resonance. In nuclear physics, these resonances are excited states of nuclei that decay rapidly (Γ *(eV)* $= \hbar/\tau$) by dissociation or photon-emission. Where τ is the mean lifetime of a neutron in the beam and it is equal to the mean free path λ divided by the beam velocity v:

$$\tau = \frac{\lambda}{v} = \frac{1}{n\sigma_t v} = \frac{1}{reaction \quad Rate} \qquad 10.24$$

We have shown this resonance situation schematically for neutron capture in ^{6}Li, as an example, in Fig. 10.2. The first excited state of ^{6}Li decays to the ground state via photon emission while the higher excited states decay to ^{6}Li(n,t)^{4}He (t stand for tritium ^{3}H). The fourth and higher excited states can also decay to ^{6}Li(n,n)^{6}Li. The fourth excited state of the compound nucleus ^{7}Li (7.459MeV) appears prominently as a resonance in ^{6}Li(n,n)^{6}Li elastic scattering and in the exothermic ^{6}Li(n,t)^{4}He reaction. The resonance is seen at the neutron kinetic energy $T \sim 200$ keV in Fig. 10.3. Neutron elastic scattering, (n,n), has a relatively gentle energy dependence while the neutron capture, (n,γ)

and ^{6}Li(n,t)^{4}He have a 1/*v* dependence at low energy. The reaction ^{6}Li(n,p)^{6}Be has an energy threshold. The fourth excited state of ^{7}Li (Fig. 10.2) appears as a prominent resonance in ^{6}Li(n,n)^{6}Li elastic scattering and in ^{6}Li(n, t)^{4}He.

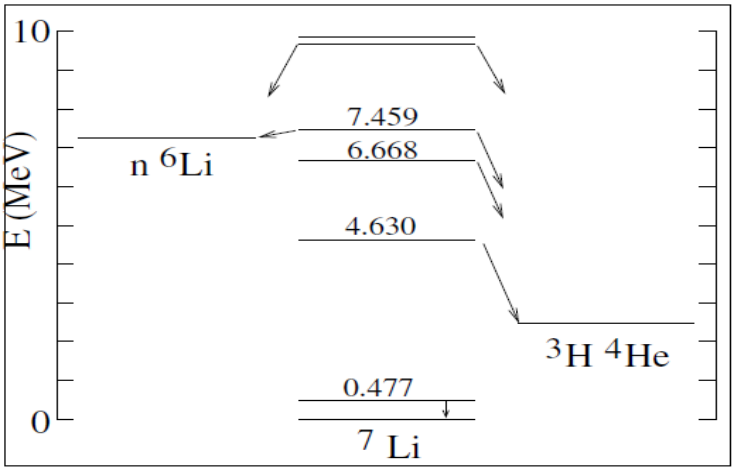

Figure 10.2. The energy levels of ^{7}Li and two dissociated states ^{6}Li(n,n)^{6}Li and ^{6}Li(n, t)^{4}He.

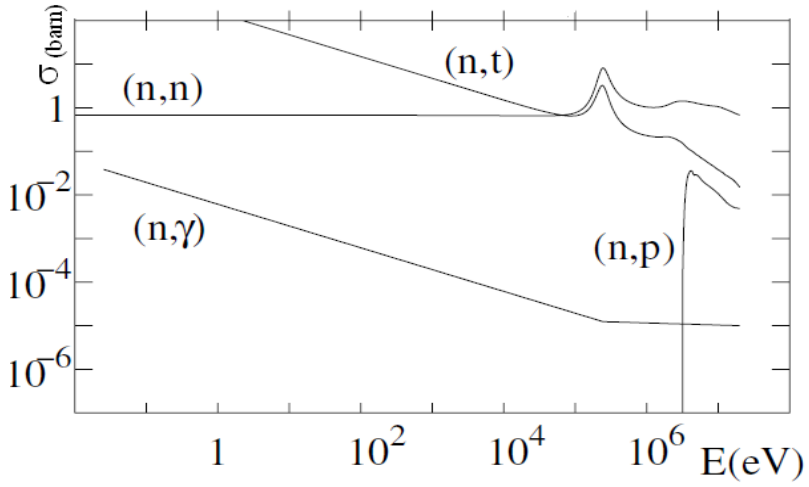

Figure 10.3. Neutron reaction cross-sections on ^{6}Li.

More spectacular examples are the multitude of highly excited states of heavy nuclei that have sufficient energies to decay by dissociation. The cases of ^{236}U and ^{239}U are shown in Fig. 10.4 where these states appear as resonances in the scattering of neutrons on ^{235}U and ^{238}U. Fig. 10.4 shows the neutron-induced fission cross-sections and Radiative capture for ^{235}U and ^{238}U. The fission cross-section on ^{238}U has an effective threshold of ~ 1.2MeV while the cross-section on ^{235}U is proportional, at low energy, to the inverse neutron velocity (1/*v* behavior), as expected for exothermic reactions. Both fission and absorption cross-sections have resonances in the energy range 1 eV < E < 10 keV.

In order to see how resonances (i.e. energy levels) come about in quantum mechanics, we introduce the description of the energy dependence of the absorption cross section by a very simple expression known as the Breit-Wigner single-level resonance formula:

$$\sigma_a(T_C) = \sigma_o \frac{\Gamma_\gamma}{\Gamma}\left(\frac{E_o}{T_C}\right)^{1/2} \frac{1}{1+y^2}, \quad y = \frac{2}{\Gamma}(T_C - E_o) \qquad 10.25$$

Here, Γ_γ is the radioactive line width essentially characterizing the probability that the compound nucleus will decay via gamma emission. σ_o is the value of the total cross section $\sigma_t(E)$ at the resonance energy E_o and can be written in terms of the reduced neutron wavelength $\lambda\!\!\!^{-}_o$ at E_o as:

$$\sigma_o = 4\pi\lambda\!\!\!^{-2}_o \frac{\Gamma_n}{\Gamma} g = 2.608\times10^6 \frac{(A+1)^2}{A^2 T(eV)} \frac{\Gamma_n}{\Gamma} g \qquad 10.26$$

where

$$g = \frac{(2J+1)}{2(2I+1)} \qquad 10.27$$

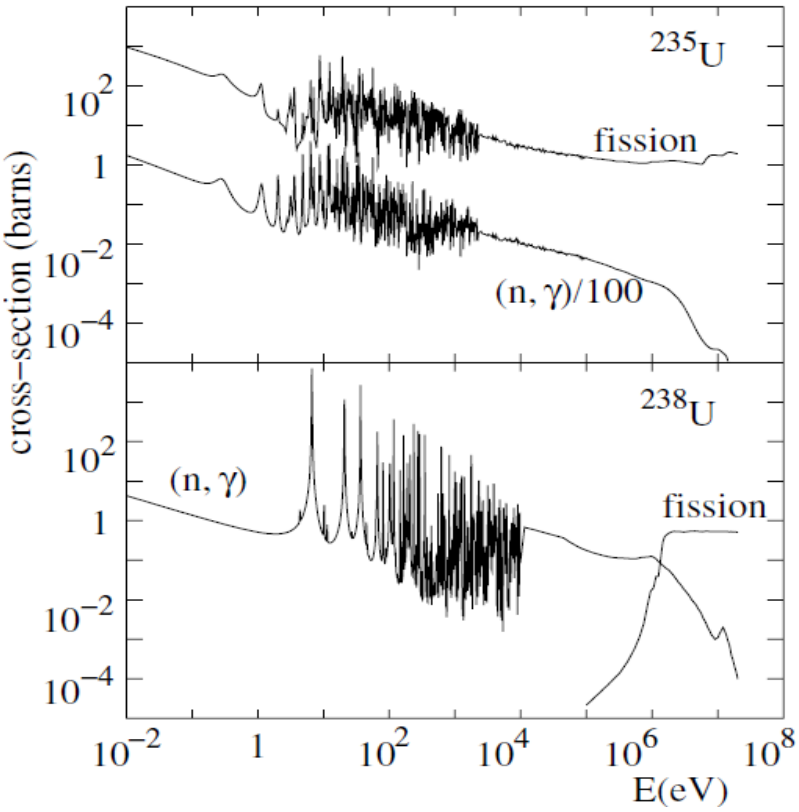

Figure 10.4. Neutron-induced fission and radiative capture cross-sections for ^{235}U and ^{238}U as a function of the incident neutron energy.

is a statistical spin factor given in terms of the nuclear spin I and total angular momentum J. Γ_n is the neutron line width and varies in energy as:

$$\Gamma_n = \Gamma_n^o \sqrt{T} \qquad 10.28$$

It should be noted from the above three equations that since resonance absorption is primarily of importance in heavy nuclei, one can usually approximate $T_C \sim T$. Then for low neutron energy $T << E_o$, the cross section behaves as essentially $1/T^{1/2}$ or $1/v$. it is also important to note that such absorption cross sections are largest at low energies.

Nuclear fission cross sections exhibit a resonance structure very similar to that characterizing radiative capture, since both processes proceed via compound nucleus which then decays with the mode relatively independent of the formation mechanism. This is certainly the case of ^{233}U, ^{235}U and ^{239}Pu nuclei.

The *elastic scattering* is the simplest nuclear interaction with the nucleus called *potential scattering*. Such billiard-ball collisions characterized by essentially energy independent cross section σ_p which is of the order of magnitude of the geometric cross section of the nucleus for low and intermediate neutron energies:

$$\sigma_p = 4\pi R^2, \quad R \sim 1.25 A^{1/3} \, fm \qquad 10.29$$

As one finds with most compound nucleus reactions, there is again a resonance behavior in the corresponding scattering cross section for fast neutrons, as for ^{6}Li in Fig. 10.3. In such a case, the resonance elastic scattering may interfere (in a quantum mechanical sense) with potential scattering. The appropriate modification of the Breit-Wigner formula to account for scattering interference is:

$$\sigma_s(T_C) = \sigma_o \frac{\Gamma_n}{\Gamma} \frac{1}{1+y^2} + \sigma_o \frac{2R}{\lambda\!\!\!^{-}_o} \frac{y}{1+y^2} + \sigma_p \qquad 10.30$$

Resonance scattering, *Interference scattering,* *Potential scattering*

Finally, an *inelastic scattering* is also the process of forming a compound nucleus, which then decays by reemitting a neutron. However, the final nucleus is left in an excited state. Such reactions usually occur only for relatively very fast neutrons, say above 10 MeV, since the neutron kinetic energy must exceed certain threshold energy in order to excite the first excited state of the compound nucleus.

10.5.2. Kinematics of neutron scattering

The kinematics of any two body reaction in the laboratory system (LAB) is given in section 3.2.

The process of neutron scattering can be simplified very considerably when analyzed within the center-of-mass (CM) coordinate frame. Even though the reader should be familiar with introductory courses in mechanics or modern physics, we will review such kinematics calculations in brief to be in consistent with our attempt to make this presentation as self-contained as possible.

The collision event before and after the collision in both the LAB and CM coordinate frames are sketched in Fig 10.5. Here, lower-case notation corresponds to the neutron and upper-case notation to the nucleus, while the subscripted L and C refer to LAB and CM frames, respectively.

The velocity of the CM frame is defined by:

$$\upsilon_{CM} = \frac{1}{m+M}(m\upsilon_L + MV_L) = \left(\frac{1}{1+A}\right)\upsilon_L \qquad 10.31$$

where, as in section 3.2, we have assumed that the initial nucleus velocity V_L is zero and that the nucleus-neutron ratio *M/m* is essentially just the nuclear mass number *A*.

Fig. 10.5 and Eq.10.31show that the neutron and nucleus velocities in the CM frame can be written as:

$$\upsilon_C = \upsilon_L - \upsilon_{CM} = \left(\frac{A}{A+1}\right)\upsilon_L$$
$$V_C = -\upsilon_{CM} = -\left(\frac{1}{A+1}\right)\upsilon_L \qquad 10.32$$

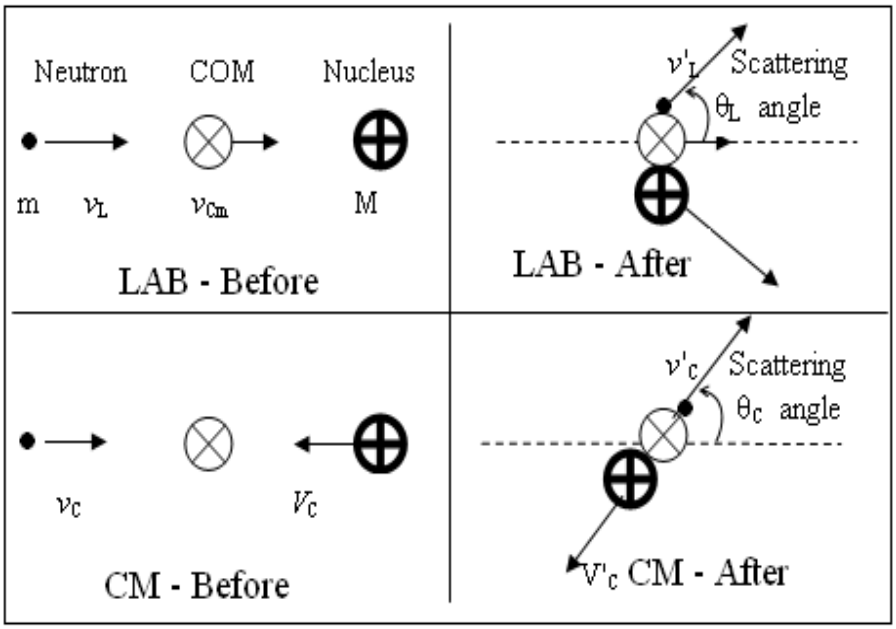

Figure 10.5. Definition of collision coordinates in LAB and CM systems.

Then, it is apparent that the total momentum in the CM frame is zero, as it must be.

We can write the total kinetic energies in the LAB and CM frames by computing:

$$\begin{aligned} LAB: \quad & T_L = \frac{1}{2} m \upsilon_L^2 + 0 \\ CM: \quad & T_C = \frac{1}{2} m \upsilon_C^2 + \frac{1}{2} M V_C^2 + \frac{1}{2} \mu \upsilon_L^2 \end{aligned} \qquad 10.33$$

Where, we introduced the *reduced mass* $\mu = Mm/(M+m)$. Hence, we find the important relation between the energy in the CM and LAB frames as:

$$T_C = \frac{M}{M+m} T_L = \frac{A}{A+1} T_L \qquad 10.34$$

Using conservation of momentum and energy, it is easy to demonstrate that the magnitudes of the CM velocities do not change in the collision, *i.e.*, $\upsilon'_C = \upsilon_C$ and $V'_C = V_C$, but their velocity vectors are rotated through the CM scattering angle θ_C. This fact allows one to relate the scattering angles in the LAB and CM frames. Fig. 10.6 illustrates the velocity vectors and scattering angles in these two frames, from which we conclude the following useful relation:

$$\tan\theta_L = \frac{\upsilon'_C \sin\theta_C}{\upsilon_{CM} + \upsilon'_C \cos\theta_C} = \frac{\sin\theta_C}{\frac{1}{A} + \cos\theta_C} \qquad 10.35$$

This relationship is particularly useful since cross sections are usually calculated in the CM system, but are measured and used in the Lab system.

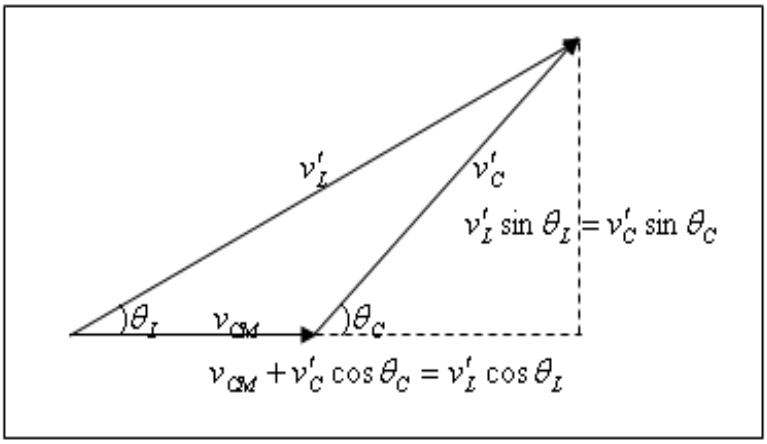

Figure 10.6. Trigonometric relationship between the scattering angles in the LAB and CM frames.

If we denote the differential scattering cross sections characterizing scattering through angle θ_L and θ_C in the LAB and CM frames, $\sigma_L(\theta_L)$ and $\sigma_C(\theta_C)$, respectively. We can use:

$$\sigma_L(\theta_L)\sin\theta_L d\theta_L = \sigma_{CM}(\theta_C)\sin\theta_C d\theta_C \qquad 10.36$$

to relate the LAB and CM differential scattering cross sections by:

$$\sigma_L(\theta_L) = \sigma_{CM}(\theta_C)\frac{\left(\frac{1}{A^2}+\frac{2}{A}\cos\theta_C+1\right)^{3/2}}{1+\frac{1}{A}\cos\theta_C} \qquad 10.37$$

Returning to the vector diagram in Fig. 10.6 and using the law of cosines, the following equation can be found:

$$\cos(180-\theta_C)=\frac{\upsilon_C'^2+\upsilon_{CM}^2-\upsilon_L'^2}{2\upsilon_C\upsilon_{CM}} \qquad 10.38$$

Now, using Eq.10.31 and 10.32 with $\upsilon'_C = \upsilon_C$, we can find the kinetic energy relationship in both frames:

$$\frac{\frac{1}{2}mv_L'^2}{\frac{1}{2}mv_l^2}=\frac{T_f}{T_i}=\frac{A^2+1+2A\cos\theta_C}{(A+1)^2} \qquad 10.39$$

where, T_f and T_i are the final (after collision) and initial (before collision) neutron energies. Rearranging the final equation by introducing a parameter related to the nuclear mass number A, the final neutron energy after collision can be written as:

$$T_f=\left[\frac{(1+\alpha)+(1-\alpha)\cos\theta_c}{2}\right]T_i \qquad 10.40$$
$$where \quad \alpha=\left(\frac{A-1}{A+1}\right)^2$$

One can analyze this equation to find that the energy transfer from the neutron to the stationary nucleus is directly related to the scattering angle in the CM system. The neutron energy after collision is always less than the energy before collision, except in case of $\theta_C=0$, the neutron will lose no energy ($T_f=T_i$) which corresponds to no collision at all. The maximum energy loss occurs in a backscattering $\theta_C=180^o$. In this case, $T_f=\alpha T_i$. Hence, the maximum energy that a neutron can lose in an elastic scattering collision with a stationary nucleus is $(1-\alpha)T_i$. For example, in scattering collisions with hydrogen nuclei (A=1), the neutron could

conceivably lose all of its energy, while in a collision with a heavy nucleus, such as ^{238}U it could lose at most 2% of its incident energy.

The concept of a differential scattering cross section $\sigma(\mathbf{\Omega})$ describing the probability of neutron direction of motion is given in section 8.2.2. Similarly we will now proceed to introduce the concept of a cross section that characterizes the probability that a neutron is scattered from an initial energy T_i to a final energy T_f.

There is a very simple relationship between the differential scattering cross section $\sigma_s(T_i \rightarrow T_f) = d\sigma_s(T)/dT$, in unit $cm^2.eV^{-1}$, and our earlier definition of the microscopic scattering cross section $\sigma_s(T)$. If we recognize that the latter quantity is just related to the probability that a neutron of incident energy T_i will suffer a scattering collision, regardless of the final energy to which it is scattered, it is apparent that $\sigma_s(T_i)$ is just the integral of the differential scattering cross section $\sigma_s(T_i \rightarrow T_f)$ over all final energies E_f.

$$\sigma_s(T_i) = \int_0^\infty dT_f \, \sigma_s(T_i \rightarrow T_f) \qquad 10.41$$

Thus far, we have developed the concept of differential scattering cross sections that characterize the probability of scattering from energy to another or one direction to another. By combining these two concepts by double differential scattering cross section that characterizes scattering from an incident energy T_i, direction $\mathbf{\Omega}$ to a final energy T_f in dT and $\mathbf{\Omega}'$ in $d\mathbf{\Omega}'$.

$$\sigma_s(T_i \rightarrow T_f, \mathbf{\Omega} \rightarrow \mathbf{\Omega}') = d^2\sigma/dTd\mathbf{\Omega} \qquad 10.42$$

We can again relate the double differential scattering cross section to the differential scattering cross section or scattering cross section by integration over energy or angle or both:

$$\sigma_s(T_i \to T_f') = \int_{4\pi} d\Omega' \sigma_s(T_i \to T_f, \Omega \to \Omega') \qquad 10.43$$

or

$$\sigma_s(T_i, \Omega \to \Omega') = \int_0^\infty dT_f \sigma_s(T_i \to T_f, \Omega \to \Omega') \qquad 10.44$$

or

$$\sigma_s(T_i) = \int_{4\pi} d\Omega' \int_0^\infty dT_f \sigma_s(T_i \to T_f, \Omega \to \Omega') \qquad 10.45$$

We can go one step further and actually calculate the differential scattering cross section $\sigma_s(T_i \to T_f)$ depending on the energy transfer in CM system. To do so, let us first decompose the $\sigma_s(T_i \to T_f)$ into two factors:

$$\sigma_s(T_i \to T_f') = \sigma_s(T_i) P(T_i \to T_f) \qquad 10.46$$

where $\sigma_s(T_i)$ is our earlier scattering cross section and $P(T_i \to T_f)$ is the scattering probability distribution, accordingly we define:

$P(T_i \to T_f)dT_f \equiv$ probability that a neutron scattering with initial energy T_i will emerge with a new T_f in the interval T_f to $T_f + dT_f$.

This quantity can be explicitly calculated for the situation in which neutrons of moderate energies (T<1MeV) via potential scattering from stationary nuclei of low mass number A.

Eq.10.43 defines the relationship between the neutron energy transfer and the scattering angle. Then, the probability of scattering through an angle θ_C into $d\theta_C$ about θ_C is just given by:

$$P(\theta_C)2\pi\sin\theta_C d\theta_C = \frac{\sigma_{CM}(\theta_C)}{\sigma_s}2\pi\sin\theta_C d\theta_C \qquad 10.47$$

Hence we can equate to the probability of scattering with energy T_f.

$$P(T_i \to T_f)dT_f = \frac{\sigma_{CM}(\theta_C)}{\sigma_s}2\pi\sin\theta_C d\theta_C \qquad 10.48$$

If we differentiate Eq.10.40 with respect to θ_C:

$$dT_f = -\frac{T_i(1-\alpha)\sin\theta_C d\theta_C}{2} \qquad 10.49$$

Now, substitute this into Eq.10.48, we find the following very important result:

$$P(T_i \to T_f) = \begin{cases} \dfrac{4\pi\sigma_{CM}(\theta_C)}{(1-\alpha)T_i\sigma_s}, & \alpha T_i \le T_f \le T_i \\ 0, & otherwise \end{cases} \qquad 10.50$$

where $\sigma_{CM}(\theta_C)$ is the differential scattering cross section in CM system and can be calculated by quantum mechanics and the detailed nuclear physics of the interaction. Fortunately, we can avoid such considerations since the scattering in the CM system is isotropic in most interactions (with energy T_i < 10 MeV) and for light nuclei (A about 12), do not depend on θ_C. That is:

$$\sigma_{\mathrm{CM}}(\theta_C) = \frac{\sigma_s}{4\pi} \qquad 10.51$$

For heavier nuclei, there will tend to be some mild angular dependence of $\sigma_{\mathrm{CM}}(\theta_C)$.

Then, using Eq.10.51 in Eq.10.50, we find that the scattering probability distribution for isotropic elastic scattering from stationary nuclei has the form:

$$P(T_i \to T_f) = \begin{cases} \dfrac{1}{(1-\alpha)T_i}, & \alpha T_i \le T_f \le T_i \\ 0, & \textit{otherwise} \end{cases} \qquad 10.52$$

Again, notice in particular that the probability of scattering from an incident energy T_i to a final energy T_f is independent of the final energy T_f.

Using this probability distribution, we can compute the average final energy of a neutron suffering an elastic collision as:

$$\overline{T}_f = \int dT_f T_f P(T_i \to T_f) = \left(\frac{1+\alpha}{2}\right) T_f \qquad 10.53$$

Hence, the average energy loss in each collision is:

$$\overline{\Delta T} = T_i - \overline{T}_f = \left(\frac{1-\alpha}{2}\right) T_i \qquad 10.54$$

Accordingly, neutrons suffering scattering collisions in hydrogen (α=0) will lose, on average, half of their original energy in each collision. While in a scattering collision with

a ^{238}U nucleus, they will lose, on average, less than 1% of their original energy.

Finally, we can write the differential scattering cross section characterizing elastic scattering from stationary nuclei by substituting Eq.10.52 into Eq.10.46:

$$\sigma_s(T_i \to T_f) = \begin{cases} \dfrac{\sigma_s(T_i)}{(1-\alpha)T_i}, & \alpha T_i \le T_f \le T_i \\ 0, & \textit{otherwise} \end{cases} \qquad 10.55$$

It should be mentioned that there are two instances where thermal motion of the nuclei must be taken into account. First, if the neutron speeds are comparable to the nuclear speeds, of course one can no longer treat the nuclei as stationary. This occurs in thermal energy (T<1eV), second, when the cross sections exhibit sharp resonance of width much less than 1 eV.

10.6. Nuclear Reactor Criticality

As soon as the discovery of nuclear fission was announced in early 1939, a lot of laboratory works were done to analyze the fission process, number of neutrons (on average υ = 2.43 neutron per fission) and energy released (~200 MeV per fission). It was immediately apparent that these neutrons could be utilized, under proper conditions, to produce fission of other fissile nuclei and thus a *chain reaction* could be initiated that could result in the release of tremendous amount of energy. The first successful nuclear reactor was constructed in Chicago and operated on December 2, 1942. Since then, many other nuclear reactors

of various designs and purposes have been built throughout the world.

The *nuclear reactor* is thus a device or assembly in which controlled nuclear fission chain reactions can be maintained. Generally speaking, the reactor assembly consists of:

1- reactor core; is a main part of the reactor that contains *fuel* of fissile materials such as ^{235}U or ^{239}Pu, fertile materials such as ^{238}U, *moderator* to slowdown the fast neutrons released from fissions, mainly by elastic scattering, such as light water H_2O, heavy water D_2O,graphite or beryllium and *control elements* as neutron absorber such as boron, cadmium and gadolinium)

2- reflector; the core is surrounded by a neutron *reflector* of a material characterized by low absorption cross section, such as light water or graphite, used to decrease the loss of neutrons from the core by scattering.

The reactor is said to be *critical* when a steady state chain reaction is maintained, on average, exactly one of the several neutrons ($\upsilon = 2.43$) emitted in the fission process causes another nucleus to fission. The power output of the assembly is then constant. The other fission neutrons are either absorbed without fission or else escape from the system. Criticality thus depends upon geometrical factors as well as the distribution and kinds of the material present. If an average of *more than one* fission neutron produces fission of another nucleus, the assembly is said to be *supercritical* and the power output increases. If *less than one* fission occurs per fission neutron produced, the unit is *subcritical*.

Criticality is determined by the extent of neutron multiplication as successive generations are produced. If N_i

thermal neutrons are present in a system, their absorption will result in a certain number N_{i+1} of next-generation thermal neutrons. The *effective multiplication factor* is defined as:

$$k_{eff} = \frac{N_{i+1}}{N_i} \qquad 10.56$$

The system is: critical if $k_{\text{eff}} = 1$;
supercritical if $k_{\text{eff}} > 1$;
subcritical if $k_{\text{eff}} < 1$.

It is useful to discuss k_{eff} independently of the size and shape of an assembly. Therefore, we introduce the *infinite multiplication factor*, k_∞, for a system that is infinite in extent. For a finite system one can then write:

$$k_{\text{eff}} = P_{nl}\, k_\infty \qquad 10.57$$

where P_{nl} is the probability that a neutron will not escape.

The value of k_∞ will depend on several factors. Of N_i total thermal neutrons present in the i^{th} generation in an infinite system, the average number of fast neutrons liberated per neutron absorbed in fission and other reactions in the fissile material is the reproduction factor (η) where:

$$\eta = \upsilon \frac{\Sigma_f}{\Sigma_a} = \frac{\sum_j n_j (\sigma_f)_j}{\sum_j [n_j (\sigma_f)_j + n_j (\sigma_\gamma)_j]} \qquad 10.58$$

where the summation of the absorption cross-section on j^{th} isotopes in the system consist of fission and radioactive capture cross-sections, while the upper summation consists only the fissionable elements, in the case of reactor, only

^{235}U. In the case where the fuel contains several fissionable materials, it is necessary to account for each material. In the case of a reactor core containing both uranium-235 and uranium-238, the reproduction factor would be calculated as shown below:

$$\eta = \upsilon^{235} \frac{n^{235}\sigma_f^{235}}{n^{235}\sigma_a^{235}+n^{238}\sigma_a^{238}} \qquad 10.59$$

Table 10.2 lists values of υ and η for fission of several different fissionable materials by thermal neutrons and fast neutrons.

Table 10.2
Average number of neutrons librated in fission.

Fissile Nucleus	Thermal Neutrons		Fast Neutrons	
	ν	η	ν	η
Uranium-233	2.49	2.29	2.58	2.40
Uranium-235	2.42	2.07	2.51	2.35
Plutonium-239	2.93	2.15	3.04	2.90

Hence, (N_i η) fast fission neutrons will be produced. At neutron energies greater than 1 MeV, most of the fast neutron fission will be of ^{238}U because of its larger proportion in the fuel. Since more than one neutron is produced in each fast-fission, there will be an increase in the number of neutron available. Now introducing the *fast fission factor*, denoted by ε, and defined as the ratio of the total number of fast neutrons slowing down past the fission

threshold of ^{238}U to the number produced by thermal neutron fission. The mathematical expression is:

$$\varepsilon = \frac{number\ of\ fast\ neutrons\ produced\ by\ all\ fissions}{number\ of\ fast\ neutrons\ produced\ by\ thermal\ fissions} \quad 10.60$$

Hence, the number of neutrons produced is ($N_i\ \eta\ \varepsilon$) fast neutrons. ε is very close to unity in a homogenous reactors, but can be as high as 1.1 in certain heterogeneous reactors. In several natural-uranium, graphite-moderator reactors, ε = 1.03, therefore for a homogeneous distribution of fuel and moderator it is acceptable to approximate, $\varepsilon \sim 1$.

While being slowed down, neutrons may be removed in nonfission processes. Many materials have resonances in the (n,γ) cross section at energies of several hundred eV and downward. Letting p represent the *resonance escape probability* (i.e., the probability that a fast neutron will slow down to thermal energies without radioactive capture or escaping the resonance cross section region), hence, the number of neutrons that reach thermal region is (($N_i\ \eta\ \varepsilon\ p$). This ratio can be written as:

$$p = \frac{number\ of\ neutrons\ that\ reach\ thermal\ energy}{number\ of\ neutrons\ that\ start\ to\ slow\ down} \quad 10.61$$

Generally, but depending on the particular circumstances, p ranges from ~0.7 to ~1 for enriched systems. In most natural-uranium, graphite-moderator reactors, p = 0.75. For pure ^{235}U, p = 1. For natural uranium metal, p = 0; and so such a system, even of infinite extent, will never be critical.

Finally, when the neutrons are thermalized, they will diffuse for a time in the infinite system until they are ultimately absorbed by fuel, by moderator, or by other

materials present in the reactor. Of the thermal neutrons, therefore, a fraction *f*, called the *thermal utilization factor*, will be absorbed in fuel material; the value of *f* is thus a fraction of thermal neutrons absorbed in fuel to the total thermal neutrons absorbed by all materials.

According to Eq.10.18, the rate at which thermal neutrons are absorbed in a unit volume per unit time is equal $\Sigma_a I$ (neutrons.cm^{-3}.sec^{-1}), where $\Sigma_a = n\sigma_a$ (cm^{-1}) is the appropriate macroscopic absorption cross section and I (neutrons.cm^{-2}.sec^{-1}) is the thermal flux. The rate of absorption in a volume V will then be $V\Sigma_a I$ per unit time. Accordingly, in a *heterogeneous reactor*, the general expression for the thermal utilization factor is thus:

$$f = \frac{V_F \Sigma_{aF} I_F}{V_F \Sigma_{aF} I_F + V_M \Sigma_{aM} I_M + V_P \Sigma_{aP} I_P} \qquad 10.62$$

where the subscripts *F*, *M*, and *P* indicate fuel, moderator, and parasitic absorbers (control rods, coolant, structure, fission products, and poison).

In a *homogenous reactor*, the volume V terms are identical as are the neutron flux. Eq.10.62 can then be simplified as:

$$f = \frac{\Sigma_{aF}}{\Sigma_{aF} + \Sigma_{aM} + \Sigma_{aP}} \qquad 10.63$$

We, therefore, obtain for the total number N_{i+1} of thermal neutrons in the next generation and we can write:

$$N_{i+1} = N_i \, \eta \, \varepsilon \, p \, f \qquad 10.64$$

From the definition and Eq.10.56, it follows that the infinite-system multiplication factor is given by:

$$k_\infty = \eta\ \varepsilon\ p\ f \qquad 10.65$$

The right-hand side of Eq.10.65 is called the *four-factor formula*, describing the multiplication factor for an infinitely large system. The four factors depend on the composition and enrichment of the fuel and its physical distribution in the moderator.

Problems

10-1. A sample containing 62 grams of ^{31}P (100% abundant) is exposed to 2×10^{11} thermal neutrons cm^{-2} sec^{-1}. If the thermal neutron absorption cross section is 0.19 barns, for how long must the sample be irradiated to produce 3.7×10^{10} Bq of ^{32}P?

10-2. A narrow beam of 100 MeV neutrons, with a fluency of 10^5 $n/cm^2.sec$, is normally incident on an aluminum plate. The elastic scattering cross section of aluminum for 100 MeV neutrons is 0.95 barns. The density of aluminum is 2.7 g/cm^3.

a- How thick must the aluminum plate be in order to reduce the number of unscattered neutrons emerging from the plate by three orders of magnitude?

b- How much would this plate attenuate a narrow beam of 100 MeV photons? Knowing that $\mu/\rho = 0.025$ cm^2/g.

10-3. A gold foil weighing 3.500 mg is irradiated with thermal neutrons for exactly 10 minutes. Forty-eight hours after the end of the irradiation, the foil is placed in a gamma spectrometer with 100% counting efficiency and an activity of 2750 Bq is recorded. Given:

^{197}Au (100% abundance)

Thermal neutron capture cross section, $\sigma = 98.8$ barns

$^{197}Au + n \rightarrow {}^{198}Au$

^{198}Au $t_{½} = 2.7$ days

a- What was the thermal neutron flux (neutrons/cm^2/sec) to which the foil was exposed?

b- What would be the saturation activity of this gold foil when exposed to this neutron flux?

10-4. Estimate (order of magnitude) the ratio of the energy released when 1 g of uranium undergoes fission to the energy released when 1 g of TNT explodes.

10-5. What are the particular fission fragments resulting from an even split of ^{235}U, with 4 neutrons and 2 beta particles emitted instantaneously?

10-6. An alloy is composed of 95% aluminum and 5% silicon (by weight). The density of the alloy is 2.66 g/cm^3. Properties of aluminum and silicon are shown below:

Element	Gram Atomic Weight	σ_a (b)	σ_s (b)
Aluminum	26.9815	0.23	1.49
Silicon	28.0855	0.16	2.20

a- Calculate the atom densities for the aluminum and silicon.
b- Determine the absorption and scattering macroscopic cross sections for thermal neutrons.
c- Calculate the mean free paths for absorption and scattering.

10-7. The absorption cross section of ^{113}Cd for certain neutrons is 20800 barns. Taking the density of this material to be 8.67 g/cm^3, calculate the macroscopic cross section and the thickness of ^{113}Cd required to reduce the intensity of the neutron beam to 1% of its original value.

10-8. Calculate and compare the collision and absorption mean free paths for neutrons in graphite, knowing that $\sigma_s = 4.7$ b, $\sigma_a = 0.0045$ b and density $\rho = 1.6$ g/cm^3.

10-9. Calculate the macroscopic scattering cross sections of a certain energy in H_2O, assuming that $\sigma_s(H) = 20.5$ b and $\sigma_s(O) = 3.8$ b.

10-10. If a one cubic centimeter section of a reactor has a macroscopic fission cross section of 0.1 cm^{-1}, and if the thermal neutron flux is 10^{13} $n/cm^2.sec$, what is the fission rate in that cubic centimeter?

10-11. A reactor operating at a flux level of $3x10^{13}$ $n/cm^2.sec$ contains 10^{20} atoms of uranium-235 per cm^3. The reaction rate is 1.29×10^{12} $fission/cm^3$. Calculate Σ_f and σ_f.

10-12. A beryllium target was bombarded with α-particles accelerated to a kinetic energy of 21.7 MeV in a cyclotron. It was reported that four groups of protons were observed corresponding to Q-values of -6.92, -7.87, -8.57 and -10.74 MeV, respectively.

a- What are the energies of the proton groups observed at an angle 90^o with the incident beam?
b- Which of the Q-values corresponds to the ground state of the product nucleus and how does it compare with the value calculated from the atomic masses?
c- To which levels of the product nucleus do the different proton groups correspond?
d- What are the threshold energies for the excitation of the different states of the product nucleus?

10-13. The reaction ^{13}C (d, p) ^{14}C has a resonance at a deuteron energy of 2.45 MeV. At what α-particle energy does this datum lead you to predict a resonance level for the reaction ^{11}B (α, n) ^{14}N?

10-14. The nucleus ^{14}N has an excited state at energy 12.8 MeV above the ground level. At what energy of the incident particle would you expect a resonance to occur in each of the following reactions:
a- ^{10}B (α, n) ^{13}N; b- ^{12}C (d, p) ^{13}C?

10-15. A tantalum foil 0.02 cm thick and with a density of 16.6 g/cm^3 is irradiated for 2 hours with a beam of thermal neutrons of flux 10^{12} neutrons/cm^2.sec. The radionuclide ^{182}Ta, with a half-life of 114 days, is formed as a result of the radiation ^{181}Ta (n, γ) ^{182}Ta and the foil has an activity of 12.3 rad/cm^2 immediately after the irradiation. Find:
a- The number of atoms of ^{182}Ta produced.
b- The cross section for the reaction ^{181}Ta (n, γ) ^{182}.

10-16. A sample of lead was bombarded with thermal neutrons and the capture γ-rays were analyzed with a gamma spectrometer. Two γ-rays were observed, one with energy of 6.734 MeV, the second with energy of 7.380 MeV. What reactions were responsible for these rays?

10-17. The reaction ^{9}Be (α, n) ^{12}C with polonium α-particles with energy of 5.3 MeV is a useful source of neutrons. Calculate:
a- The Q-value of the reaction.
b- The energy of the neutrons which emerge at angles 0^o, 90^o, and 180^o with the direction of the incident beam.

10-18. Assume a uranium nucleus breaks up spontaneously into two roughly equal parts. Estimate the reduction in electrostatic energy of the nuclei. What is the relationship of this to the total change in energy? (Assume uniform charge distribution; nuclear radius= 1.2×10^{-13} $A^{1/3}$ cm)

10-19. Calculate the reproduction factor for a reactor that uses 10% enriched uranium fuel. The microscopic absorption cross section for uranium-235 is 694 barns. The absorption cross section for uranium-238 is 2.71 barns. The microscopic fission cross section for uranium-235 is 582 barns. The atom density of ^{235}U is 4.83 x 10^{21} atoms/cm^3. The atom density of ^{238}U is 4.35 x 10^{22} atoms/cm^3.

10-20. Calculate the thermal utilization factor for a homogeneous reactor. The macroscopic absorption cross section of the fuel is 0.3020 cm^{-1}, the macroscopic absorption cross section of the moderator is 0.0104 cm^{-1} and the macroscopic absorption cross section of the poison is 0.0118 cm^{-1}.

10-21. Calculate k_∞ for a homogeneous, natural uranium-graphite-moderated assembly which contains 300 moles of graphite per mole of uranium. Assume natural uranium to contain one part of 235U to 139 parts of 238U, and use these constants: $\sigma_a(^{235}U)$ = 694 b, : $\sigma_a(^{238}U)$ = 2.71 b, $\sigma_a(M)$ = 0.0032 b, : $\sigma_f(^{235}U)$ = 582 b, p = 0.705.

10-22. Repeat the calculations of problem 10-21 for heavy water-moderated assembly with N_m/N_u = 50, p = 0.842 and for D_2O σ_a = 0.00092 b. Comment on the result.

10-23. Calculate k_∞ for an enriched uranium-graphite-moderated assembly using 400 mole of graphite to 1 mole of uranium and a $^{238}U/^{235}U$ ratio of 70, which is about twice the natural concentration, p = 0.75.

Appendix I

CODATA RECOMMENDED VALUES OF THE FUNDAMENTAL PHYSICAL CONSTANTS

NIST SP 961 (Dec/2005) Values from: P. J. Mohr and B. N. Taylor, Rev. Mod. Phys.77,1(2005). A more extensive listing of constants is available in the above reference and on the NIST Physics Laboratory Web site physics.nist.gov/constants.

Quantity	Symbol	Value
speed of light in vacuum	c	2.99792458×10^{8} m/s
gravitational constant	G	6.67259×10^{-11} $m^3/(kg\ s^2)$
electron charge, elementary charge	e, e_0	$1.60217733 \times 10^{-19}$ C
permittivity constant of free space or Electric constant	$\epsilon_o = (\mu_0 c^2)^{-1}$	$8.854187817 \times 10^{-12}$ F/ m
permeability of free space or magnetic constant	μ_0	$4\pi \times 10^{-7}$ N/A^2 $12.566370614\times10^{-7}$ N/A^2
Planck's constant in eV s	h	$6.6260755 \times 10^{-34}$ J·s $4.135\ 66743 \times 10^{-15}$eV.s
Planck's constant in eV s	$\hbar=h/2\pi$	$1.05457266 \times 10^{-34}$ J ·s $6.58211915 \times 10^{-16}$ eV. s
Avogadro's number	N_A	6.0221367×10^{23} mol^{-1}
Faraday constant	$F = N_A e_0$	9.6485309×10^{4} C/mol
electron mass in atomic mass unit energy equivalent	m_e	$9.1093897 \times 10^{-31}$ kg $5{:}4857990945\times 10^{-4}$ u 0.51099906 MeV
Rydbeg constant	$R_\infty=(2h)^{-1}m_e c\alpha^2$	$1.0973731534 \times 10^{7}$ m^{-1}
fine-structure constant	$\alpha = e_0^2(2\varepsilon_0 hc)^{-1}$ α^{-1} $1/(4\pi\varepsilon_0)$	$7.29735308 \times 10^{-3}$ 137.0359895 8.99×10^{9} $N.m^2/C^2$
electron radius	$r_e = \hbar\,(m_e c)^{-1}\alpha$	$2.81794092 \times 10^{-15}$ m
e^--Compton wavelength	$\lambda_C = h(m_e c)^{-1}$	$2.42631058 \times 10^{-12}$ m
Bohr radius	$a_0 = r_e\alpha^{-2}$	$5.29177249 \times 10^{-11}$ m
atomic mass unit	u = 1/12 $m(^{12}C)$	$1.6605402 \times 10^{-27}$ kg

proton mass in atomic mass unit energy equivalent	m_p	$1.6726231 \times 10^{-27}$ kg 1.00727646688 u 938.27231 MeV
neutron mass in atomic mass unit energy equivalent	m_n	$1.6749286 \times 10^{-27}$ kg 1:00866491560 u 939.56563 MeV
magnetic flux quantum	$\phi_0 = h(2e_0)^{-1}$	$2.06783461 \times 10^{-15}$ Wb
specific electron charge	$-e_0 m_e^{-1}$	$-1.75881962 \times 10^{11}$ C/kg
Bohr magneton	$\mu_B = e_0\hbar\ (2m_e)-1$	9.2740154 × 10−24 J/T
magnetic moment of electron	μ_e	9.2847701 × 10−24 J/T
nuclear magneton	$\mu_N = e_0\ \hbar\ (2m_p)^{-1}$	5.0507866 × 10−27 J/T
magnetic moment of proton	μ_p	2:792847351 μ_N $1.41060761 \times 10^{-26}$ J/T
magnetic moment of neutron	μ_n	-1.91304273 μ_N $-0.96623645 \times 10^{-26}$ J/T
deuteron mass energy equivalent	m_d	2.01355321270 u 1875.61282 MeV
magnetic moment of deuteron	μ_d	0.8574382329 μ_N $0.433073482 \times 10^{-26}$ J/T
gyromagnatic ratio	γ_p	2.67522128×10^8 rad/sT
quantum Hall resistance	R_H	25812.8056 Ω
universal gas constant	R	8.314510 J/(mol K)
Boltzmann constant	k, $k_B = RN_A^{-1}$	1.380658×10^{-23} J/K
Stefan-Boltzmann constant	$\sigma = \pi^2 k_B^4 (60\ \hbar^3 c^2)^{-1}$	5.67051 × 10−8 W/m^{2}K^4
Wien's constant	$b = \lambda_{max} T$	2.897756×10^{-3} m · K

Appendix II

TABLE OF ELEMENTAL AND ISOTOPIC PROPERTIES

Explanation of Table

Column 1:

Nuclides (Z, El) (in **bold face**) are listed in order of increasing atomic number (Z). The names and symbols for elements (El) are those adopted by the International Union of Pure and Applied Chemistry (2004).

Column 2:

Elemental atomic weight in atomic mass unit (u)

Column 3:

Atomic valance

Column 4:

Isotopes mass number (in **bold face**) are listed in order of increasing mass number (A)

Column 5, Jπ:

Nuclear spin and parity assignments, without and with parentheses, are based upon strong and weak arguments respectively.

Column 6:

Mass defect, $\Delta = M–A$, of isotopes is given in MeV

Column 7:

Half-life $t_{1/2}$ and natural Abundance of Isotopes (in **bold face**) is shown followed by their units ("%" symbol).

Column 8:

Decay modes are given in decreasing strength from left to right. The various modes of decay are given below:

β–, β^- decay. β+, β^+ decay. ε, electron capture
2β–, double β^-. β–x, delayed x (n, p, α) following β^-.
IT, isomeric transition. SF, spontaneous fission.
n, p, α, neutron, proton and alpha decay.

Element Z El	Atomic Weight u	Valance	A	J^{π}	Δ MeV	$t_{1/2}$, Γ or Abundance	Decay Mode
0 n	1.008665		**1**	1/2+	8.071	10.24 m	β^-
1H	1.00794 7	1	**1**	1/2+	7.289	**99.985%**	
			2	1+	13.136	**0.015%**	
			3	$1/2^+$	14.950	12.32 y	β^-
			4	2^-	25.9	4.6 MeV	n
2He	4.002602	0	**3**	1/2+	14.931	**0.000137%**	
			4	0+	2.425	**9.999863%**	
			5	3/2–	11.39	0.60 MeV	α, n
			6	0–	17.595	806.7 ms	β^-
			7	3/2–	26.10	150 keV	n
			8	0+	31.598	119.0 ms	β– , β–n
3Li	6.941 2	1	**4**	2–	25.3	6.03 MeV	p
			5	3/2–	11.68	≈1.5 MeV	α, p
			6	1+	14.087	**7.59%**	
			7	3/2–	14.908	**92.41%**	
			8	3+	20.947	838 ms	β– , β–α
			9	3/2–	24.954	178.3 ms	β– , β–n
4Be	9.012182	2	**6**	0+	18.375	92 keV	p , α
			7	3/2–	15.770	53.22 d	ε
			8	0+	4.942	6.8 eV	α
			9	3/2–	11.348	**100%**	
			10	0+	12.607	1.51×10^{6} y	β–
			11	1/2+	20.174	13.81 s	β– , β–α
			12	0+	25.08	21.49 ms	β– , β–n
			13	1/2–	33.25	2.7×10^{-21}s	n
5B	10.811	3	**7**	3/2–	27.87	1.4 MeV	p , α
			8	2+	22.921	770 ms	ε , εα
			9	3/2–	12.416	0.54 keV	p
			10	3+	12.051	**19.8%**	
			11	3/2–	8.668	**80.2% 3**	
			12	1+	13.369	20.20 ms	β–,β–3α
			13	3/2–	16.562	17.33 ms	β–
			14	2–	23.66	12.5 ms	β– , β–n
6C	12.0107	2,3,4	**9**	3/2–	28.910	126.5 ms	ε,εp,εα
			10	0+	15.699	19.26 s	ε
			11	3/2–	10.650	20.334 m	ε
			12	0+	0.000	**98.89%**	
			13	1/2–	3.125	**1.11%**	
			14	0+	3.020	5700 y	β–
			15	1/2+	9.873	2.449 s	β–
			16	0+	13.694	0.747 s	β–,β–n
			17		21.04	193 ms	β–,β–n
			18	0+	24.93	92 ms	β–,β–n

Element Z El	Atomic Weight u	Valance	A	J^{π}	Δ MeV	$t_{1/2}$, Γ or Abundance	Decay Mode
7 N	14.0067	3,5	**11m**	1/2+	24.62	1.58 MeV	p
			12	1+	17.338	11.00 ms	ε
			13	1/2–	5.345	9.965 m	ε
			14	1+	2.863	**99.634%**	
			15	1/2–	0.101	**0.366%**	
			16	2–	5.684	7.13 s	β–, β–α
			17	1/2–	7.87	4.173 s	β–, β–n
			18	1–	13.11	624 ms	β–n,β–α
			19		15.86	271 ms	β– , β–n
8 O	15.9994	2	**13**	3/2–	23.112	8.58 ms	ε , εp
			14	0+	8.007	70.641 s	ε
			15	1/2–	2.856	122.24 s	ε
			16	0+	–4.737	**99.762%**	
			17	5/2+	–0.809	**0.038%**	
			18	0+	–0.781	**0.200%**	
			19	5/2+	3.335	26.88 s	β–
			20	0+	3.797	13.51 s	β–
			21	5/2+	8.060	3.42 s	β–
			22	0+	9.280	2.25 s	β–, β–n
9 F	18 .9984	1	**16**	0–	10.680	40 keV	P
			17	5/2+	1.952	64.49 s	ε
			18	1+	0.874	1.8291 h	ε
			19	1/2+	–1.487	**100%**	
			20	2+	–0.017	11.07 s	β–
			21	5/2+	–0.048	4.158 s	β–
			22	4+	2.790	4.23 s	β–, n
			23	3/2,5/2+	+ 3.33	2.23 s	β–
			24	(1,2,3)+	7.560	400 ms	β–, β–
10Ne	20.17976	0	**17**	1/2–	16.46	109.2 ms	ε, εp, εα
			18	0+	5.317	1672 ms	ε
			19	1/2+	1.751	17.22 s	ε
			20	0+	–7.042	**90.48%**	
			21	3/2+	–5.732	**0.27%**	
			22	0+	–8.025	**9.25%**	
			23	5/2+	5.154	37.24 s	β–
			24	0+	5.951	3.38 m	β–
			25	3/2+	–2.11	602 ms	β–
			26	0+	0.43	192 ms	β–, β–n
11Na	22.98977	1	**20**	2+	6.848	447.9 ms	ε , εα
			21	3/2+	–2.184	22.49 s	ε
			22	3+	–5.182	2.6027 y	ε
			23	3/2+	–9.530	**100%**	
			24	4+	8.418	14.951 h	β–
			25	5/2+	–9.358	59.1 s	β–

Element Z El	Atomic Weight u	Valance	A	J^{π}	Δ MeV	$t_{1/2}$, Γ or Abundance	Decay Mode
11Na	22.98977	1	**26**	3+	–6.862	1.077 s	β–
			27	5/2+	–5.517	301 ms	β–n
			28	1+	–0.990	30.5 ms	β–, β–n
12Mg	24.3050	2	**21**	5/2+	10.910	122 ms	ε , εp
			22	0+	–0.397	3.8755 s	ε
			23	3/2+	–5.474	11.317 s	ε
			24	0+	–13.934	**78.99%**	
			25	5/2+	–13.193	**10.00%**	
			26	0+	–16.215	**11.01%**	
			27	1/2+	–14.587	9.458 m	β–
			28	0+	–15.019	20.915 h	β–
			29	3/2+	–10.62	1.30 s	β–
			30	0+	–8.911	335 ms	β–
13Al	26.98154	3	**25**	5/2+	–8.916	7.183 s	ε
			26	5+	–12.210	7.17×10^{5} y	ε
			26m	0+	–11.982	6.3452 s	ε
			27	5/2+	–17.197	**100%**	
			28	3+	–16.850	2.2414 m	β–
			29	5/2+	–18.215	6.56 m	β–
			30	3+	–15.87	3.60 s	β–
			31	3/2,5/2+	–14.95	644 ms	β–
			32	1+	–11.06	33 ms	β–
14Si	28.0855	4	**25**	5/2+	3.82	220 ms	ε , εp
			26	0+	–7.145	2.234 s	ε
			27	5/2+	–12.384	4.16 s	ε
			28	0+	–21.493	**92.230%**	
			29	1/2+	–21.895	**4.683%**	
			30	0+	–24.433	**3.087%**	
			31	3/2+	–22.949	157.3 m	β–
			32	0+	–24.081	132 y	β–
			33	3/2+	–20.49	6.18 s	β–
			34	0+	–19.96	2.77 s	β–
			34		–14.36	0.78 s	β–
15P	30.97376	3,5	**27**	1/2+	–0.72	260 ms	ε , εp
			28	1/2+	–7.159	270.3 ms	ε , εp, εα
			29	3+	–16.953	4.142 s	ε
			30	1+	–20.201	2.498 m	ε
			31	1/2+	–24.441	**100%**	
			32	1+	–24.305	14.262 d	β–
			33	1/2+	–26.337	25.34 d	β–
			34	1+	–24.558	12.43 s	β–
			35	1/2+	–24.858	47.3 s	β–
			36	4–	–20.25	5.6 s	β–
			37		–18.99	2.31 s	β–

Element Z El	Atomic Weight u	Valance	A	J^{π}	Δ MeV	$t_{1/2}$, Γ or Abundance	Decay Mode
16S	32.060	2,4,6	**31**	1/2+	–19.045	2.572 s	ε
			32	0+	–26.016	**95.02%**	
			33	3/2+	–26.586	**0.75%**	
			34	0+	–29.932	**4.21%**	
			35	3/2+	–28.846	87.51 d	β–
			36	0+	–30.664	**0.02%**	
			37	7/2–	–26.896	5.05 m	β–
			38	0+	–26.861	170.3 m	β–
			39	(3/2,5/2 ,7/2)–	–23.16	11.5 s	β–
			40	0+	–22.9 8	8.8 s	β–
			41	7/2–	–19.0 1	1.99 s	β–, β–n
17Cl	35.453	1,3,5,7	**33**	3/2+	–21.003	2.511 s	ε
			34	0+	–24.440	1.5264 s	ε
			34m	3+	–24.293	32.00 m	ε. IT
			35	3/2+	–29.014	**75.77%**	
			36	2+	–29.522	3.01×10^{5} y	β–, ε
			37	3/2+	–31.761	**24.23%**	
			38	2–	–29.798	37.24 m	β–
			38m	5–	–29.127	715 ms	IT
			39	3/2+	–29.800	55.6 m	β–
			40	2–	–27.56	1.35 m	β–
			41	1/2,3/2+	–27.31	38.4 s	β–
			42		–24.9	6.8 s	β–
18Ar	39.94	0	**34**	0+	–18.377	844.5 ms	ε
			35	3/2+	–23.047	1.775 s	ε
			36	0+	–30.232	**0.3365%**	
			37	3/2+	–30.948	34.95 d	ε
			38	0+	–34.715	**0.0632%**	
			39	7/2–	–33.242 –	269 y	β–
			40	0+	35.040	**99.6003%**	
			41	7/2–	–33.068	109.61 m	β–
			42	0+	–34.423	32.9 y	β–
			43	5/2–	–32.010	5.37 m	β–
			44	0+	–32.673	11.87 m	β–
19K	39.0983	1	**37**	3/2+	–24.800	1.226 s	ε
			38	3+	–28.801	7.636 m	ε
	42 2– –		**38m**	0+	–28.670	924.2 ms	ε
	35.022		**39**	3/2+	–33.807	**93.258%**	
	12.321 h		**40**	4–	–33.535	1.248×10^{9} y	β⁻89.3%
	25 β–					**0.0117%**	ε 10.7%
	43 3/2+ –		**41**	3/2+	–35.559	**6.7302%**	
	36.593		**42**	2–	–35.022	12.321 h	β–
	22.3 h 1 β–		**43**	3/2+	–36.593	22.3 h	β–

Element Z El	Atomic Weight u	Valance	A	J^{π}	Δ MeV	$t_{1/2}$, Γ or Abundance	Decay Mode
20Ca	40.078	2	**38**	0+	–22.059	440 ms	ε
			39	3/2+	–27.274	859.6 ms	ε
			40	0+	–34.846	$>3.0\times10^{21}$y	2ε
						96.94%	
			41	7/2–	–35.138	1.02×10^{5}y	ε
			42	0+	–38.547	**0.647%**	
			43	7/2–	–38.409 –	**0.135%**	
			44	0+	41.468	**2.09%**	
			45	7/2–	–40.812	162.61 d	β–
			46	0+	–43.135	0.28×10^{16}y	$2\beta^{-}$
						0.004%	
			47	7/2–	–42.340	4.536 d	β–
			48	0+	–44.214	2.3×10^{19} y	$2\beta^{-}$84%
						0.187%	β^{-}<25%
			49	3/2–	–41.289	8.718 m	β–
			50	0+	–39.571	13.9 s	β–
21Sc	44.9559	3	**41**	7/2–	–28.642	596.3 ms	ε
			42	0+	–32.121	681.3 ms	ε
			42m	7+	–31.505	61.7 s	ε
			43	7/2–	–36.188	3.891 h	ε
			44	2+	–37.816	3.97 h	ε, I
			44m	6+	–37.545	58.61 h	IT
			45	7/2–	–41.068	**100%**	
			45m	3/2+	–41.056	318 ms	IT
			46	4+	–41.757	83.79 d	β–
			46m	1–	–41.615	18.75 s	IT
			47	2–	–44.332	3.3492 d	β–
			48	6+	–44.496	43.67 h	β–
			49	7/2–	–46.552	57.2 m	β–
22Ti	47.867	4	**43**	7/2–	–29.321	509 ms	ε
			44	0+	–37.549	60.0 y	ε
			45	7/2–	–39.006	184.8 m	ε
			46	0+	–44.123	**8.25%**	
			47	5/2–	–44.932	**7.44%**	
			48	0+	–48.488	**73.72%**	
			49	7/2–	–48.559 –	**5.41%**	
			50	0+	51.427	**5.18%**	
			51	3/2–	–49.728	5.76 m	β–
			52	0+	–49.465	1.7 m	β–
			53	3/2–	–46.8	32.7 s	β–
			54	0+	–45.6	1.5 s	β–
			55	3/2–	–41.7	1.3 s	β–
			56	0+	–38.9	200 ms	β– , β–n
			57		–33.5	60 ms	β– , β–n

Element Z El	Atomic Weight u	Valance	A	J^{π}	Δ MeV	$t_{1/2}$, Γ or Abundance	Decay Mode
23V	50.9415	5	**46**	0+	–37.073	422.50 ms	ε
			47	3/2–	–42.002	32.6 m	ε
			48	4+	–44.475	15.9735 d	ε
			49	7/2–	–47.957	329 d	ε
			50	6+	–49.222	1.4×10^{17}y	ε 83%,
						0.250%	β^- 17%
			51	7/2–	–52.201	**99.750%**	
			52	3+	–51.441	3.743 m	β–
			53	7/2–	–51.849	1.60 m	β–
			54	3+	–49.89	49.8 s	β–
			55	7/2–	–49.2	6.54 s	β–
			56	1+	–46.1	216 ms	β–, β–n
			57	3/2–	–44.2	0.35 s	β–, β–n
			58	1+	–40.2	185 ms	β–
24Cr	51.9961	2,3,6	**47**	3/2–	–34.56	500 ms	ε
			48	0+	–42.819	21.56 h	ε
			49	5/2–	–45.331	42.3 m	ε
			50	0+	–50.259	$>1.3\times10^{18}$y	2ε
						4.345%	
			51	7/2–	–51.449	27.7025 d	ε
			52	0+	–55.417	**83.789%**	
			53	3/2–	–55.285	**9.501%**	
			54	0+	–56.932	**2.365%**	
			55	3/2–	–55.107	3.497 m	β–
			56	0+	–55.281	5.94 m	β–
			57	3/2,7/2–	–52.524	21.1 s	β–
			58	0+	–51.8	7.0 s	β–
25Mn	54.93805	1to4,6,7	**53**	7/2–	–54.688	3.74×1^{06}y	ε
			54	3+	–55.555	312.12 d	ε , β–
			55	5/2–	–57.711	**100%**	
			56	3+	–56.910	2.5789 h	β–
			57	5/2–	–57.487	85.4 s	β–
			58	1+	–55.91	3.0 s	β–
			58m	4+	–55.83	65.2 s	β–, IT
26Fe	55.845	2,3,4,6	**53**	7/2–	–50.945	8.51 m	ε
	59 3/2–9		**53m**	19/2–	–47.905	2.526 m	IT
	β–		**54**	0+	–56.252	**5.845%**	
	60 0+ 3 β–		**55**	3/2–	–57.479	2.737 y	ε
	61 3/2–		**56**	0+	–60.605	**91.754%**	
	,5/2–6 β–		**57**	1/2–	–60.180	**2.119%**	
			58	0+	–62.153	**0.282%**	
			59	3/2–	–60.663	44.495 d	β–
			60	0+	–61.412	1.5×106 y	β–
			61	3/2,5/2–	–58.92	5.98 m	β–

Element Z El	Atomic Weight u	Valance	A	J^{π}	Δ MeV	$t_{1/2,\ \Gamma\ or}$ Abundance	Decay Mode
27Co	58.9332	2,3	**57**	7/2–	–59.344	271.74 d	ε
			58	2+	–59.846	70.86 d	ε
			58m	5+	–59.821	9.04 h	IT
			59	7/2–	–62.228	**100%**	
			60	5+	–61.649	1925.28 d	β–
			60m	2+	–61.590	10.467 m	IT, β–
			61	7/2–	–62.898	1.650 h	β–
			62	2+	–61.43	1.50 m	β–
			62m	5+	–61.41	13.91 m	β–, IT
			63	7/2–	–61.84	27.4 s	β–
			64	1+	–59.79	0.30 s	β–
28Ni	58.693	0 to 3	**56**	0+	–53.90	6.075 d	ε
			57	3/2–	–56.082	35.60 h	ε
			58	0+	–60.228	**68.077%**	
			59	3/2–	–61.156	7.6×10^{4} y	ε
			60	0+	–64.472	**26.223%**	
			61	3/2–	–64.221	**1.140%**	
			62	0+	–66.746	**3.634%**	
			63	1/2–	–65.513	100.1 y	β–
			64	0+	–67.099	**0.926%**	
			65	5/2–	–65.126	2.5172 h	β–
			66	0+	–66.006	54.6 h	β–
29Cu	63.546	1,2	**60**	2+	–58.344	23.7 m	ε
			61	3/2–	–61.984	3.333 h	ε
			62	1+	–62.798 –	9.67 m	ε
			63	3/2–	65.579	**69.17%**	
			64	1+	–65.424 –	12.700 h	ε
			65	3/2–	67.264	**30.83%**	
			66	1+	–66.258	5.120 m	β–
			67	3/2–	–67.319	61.83 h	β–
			68	1+	–65.567	31.1 s	β–
			68m	6–	–64.845	3.75 m	IT, β–
30Zn	65.39	2	**62**	0+	–61.17	9.186 h	ε
			63	3/2–	–62.213	38.47 m	ε
			64	0+	–66.004	$>2.8\times10^{16}$y	ε
						48.63%	
			65	5/2–	–65.912	243.66 d	ε
			66	0+	–68.899	**27.90%**	
			67	5/2–	–67.880	**4.10%**	
			68	0+	–70.00	**18.75%**	
			69	1/2–	–68.418	56.4 m	β^{-}
						0.62%	
			69m	9/2+	–67.979	13.76 h	IT, β–
			70	0+	–69.565	$>1.3\times10^{16}$y	β–

Element Z El	Atomic Weight u	Valance	A	J^{π}	Δ MeV	$t_{1/2}$, Γ or Abundance	Decay Mode
31Ga	69.723	2,3	**67**	3/2–	–66.880	3.2623 d	ε
			68	1+	–67.086	67.71 m	ε
			69	3/2–	–69.328	**60.108%**	
			70	1+	–68.910	21.14 m	β–, ε
			71	3/2–	–70.140	**39.892%**	
			72	3–	–68.589	14.095 h	β–
			73	3/2–	–69.699	4.86 h	β–
			74	3–	–68.050	8.12 m	β–
			74m	0+	–67.990	9.5 s	IT, β–
32Ge	72.64	2,4	**68**	0+	–66.980	270.95 d	ε
			69	5/2–	–67.101	39.05 h	ε
			70	0+	–70.563	**20.37%**	
			71	1/2–	–69.908	11.43 d	ε
			72	0+	–72.586	**27.31%**	
			73	9/2+	–71.298	**7.76%**	
			73m	1/2–	–71.231	0.499 s	IT
			74	0+	–73.422	**36.73%**	
			75	1/2–	–71.856	82.78 m	β–
			75m	7/2+	–71.717	47.7 s	IT, β–
			76	0+	–73.213	1.2×10^{25} y	$2\beta^-$
						7.83%	
			77	7/2+	–71.214	11.30 h	β–
			77m	1/2–	–71.054	52.9 s	β–, IT
33As	74.921	3,5	**72**	2–	–68.230	26.0 h	ε
			73	3/2–	–70.957	80.30 d	ε
			74	2–	–70.860	17.77 d	ε, β–
			75	3/2–	–73.032	**100%**	
			76	2–	–72.289	1.0942 d	β–
			77	3/2–	–73.917	38.83 h	β–
			78	2–	–72.817	90.7 m	β–
			79	3/2–	–73.636	9.01 m	β–
			80	1+	–72.16	15.2 s	β–
34Se	78.96	2,4,6	**73**	9/2+	–68.22	7.15 h	ε
			73m	3/2–	–68.19	39.8 m	IT, ε
			74	0+	–72.213	**0.89%**	
			75	5/2+	–72.169	119.779 d	ε
			76	0+	–75.252	**9.37%**	
			77	1/2–	–74.600	**7.63%**	$2\beta^-$
			77m	7/2+	–74.438	17.36 s	IT
			78	0+	–77.026	**23.77%**	
			79	7/2+	–75.918	2.95×10^{5}y	β–
			79m	1/2–	–75.822	3.92 m	IT, β–
			80	0+	–77.760	**49.61%**	
			81	1/2–	–76.390	18.45 m	β–

34Se	78.96	2,4,6	**81m**	7/2+	–76.286	57.28 m	IT, β–
			82	0+	–77.594	9.1×10^{19}y	2β–
						8.73%	
			83	9/2+	–75.341	22.3 m	β–
			83m	1/2–	–75.112	70.1 s 4	β–
35Br	79.904	1,3,5,7	**77**	3/2–	–73.235	57.036 h	ε
			77m	9/2+	–73.129	4.28 m	IT
			78	1+	–73.452	6.46 m	ε , β–
			79	3/2–	–76.068	**50.69%**	
			79m	9/2+	–75.861	4.86 s	IT
			80	1+	–75.890	17.68 m	β–, ε
			81	3/2–	–77.975	**49.31%**	
			82	5–	–77.496	35.282 h	β–
			82m	2–	–77.451	6.13 m	IT, β–
			83	3/2–	–79.009	2.40 h	β–
			84	2–	–77.80	31.80 m	β–
			84m	6–	–77.48	6.0 m	β–
36Kr	83.80	0	**77**	5/2+	–70.169	74.4 m	ε
			78	0+	–74.180	$\geq2.3\times10^{20}$y	2ε
						0.35%	
			79	1/2–	–74.443	35.04 h	ε
			79m	7/2+	–74.313	50 s	IT
			80	0+	–77.893	**2.28%**	
			81	7/2+	–77.694	2.29×10^{5}y	ε
			81m	1/2–	–77.503	13.10 s	IT , ε
			82	0+	–80.590	**11.58%**	
			83	9/2+	–79.982	**11.49%**	
			83m	1/2–	–79.940	1.83 h	IT
			84	0+	–82.431	**57.00%**	
			85	9/2+	–81.480	3916.8 d	β–
			85m	1/2–	–81.175	4.480 h	β–
			86	0+	–83.266	**17.30%**	
			87	5/2+	–80.709	76.3 m	β–
37Rb	85.4678	1	**83**	5/2–	–79.075	86.2 d	ε
			84	2–	–79.750	33.1 d	ε, β–
			84m	6–	–79.286	20.26 m	IT
			85	5/2–	–82.167	**72.17%**	
			86	2–	–82.747	18.642 d	β^-
			86m	6–	–82.191	1.017 m	IT , β–
			87	3/2–	–84.598	4.97×10^{10}y	β–
						27.83%	
			88	2–	–82.609	17.773 m	β–
			89	3/2–	–81.713	15.15 m	β–
			90	0–	–79.362	158 s	β–
			90m	3–	–79.255	258 s	β–, IT
			91	3/2–	–77.745	58.4 s	β–

Element Z El	Atomic Weight u	Valance	A	J^{π}	Δ MeV	$t_{1/2}$, Γ or Abundance	Decay Mode
38Sr	87.62	2	**83**	7/2+	–76.80	32.41 h	ε
			83m	1/2–	–76.54 –	4.95 s	IT
			84	0+	80.644	**0.56%**	
			85	9/2+	–81.103	64.84 d	ε
			85m	1/2–	–80.864	67.63 m	IT , ε
			86	0+	–84.524	**9.86%**	
			87	9/2+	–84.880	**7.00%**	
			87m	1/2–	–84.492	2.815 h	IT , ε
			88	0+	–87.922	**82.58%**	
			89	5/2+	–86.209	50.57 d	β–
			90	0+	–85.942	28.90 y	β–
39Y	88.90585	3	**86**	4–	–79.28	14.74 h	ε
			86m	8+	–79.07	48 m	IT, ε
			87	1/2–	–83.019	79.8 h	ε
			87m	9/2+	–82.638	13.37 h	IT, ε
			88	4–	–84.299	106.616 d	ε
			89	1/2–	–87.702	**100%**	
			89m	9/2+	–86.793	15.28 s	IT
			90	2–	–86.488	64.053 h	β–
			90m	7+	–85.806	3.19 h	IT, β–
			91	1/2–	–86.345	58.51 d	β–
40Zr	91.224	4	**89**	9/2+	–84.869	78.41 h	ε
			89m	1/2–	–84.281	4.161 m	IT, ε
			90	0+	–88.767	**51.45%**	
			90m	5–	–86.448	809.2 ms	IT
			91	5/2+	–87.890 –	**11.22%**	$2\beta^-$
			92	0+	88.454	**17.15%**	
			93	5/2+	–87.117	1.53×10^{6} y	β–
			94	0+	–87.267	**17.38%**	
			95	5/2+	–85.658	64.032 d	β–
			96	0+	–85.443	$>3.9\times10^{20}$y	β–
						2.80%	
			97	1/2+	–82.947	16.744 h	β–
41Nb	92.90638	2,3,4?,5	**91**	9/2+	–86.632	6.8×10^{2} y	ε
			91m	1/2–	–86.528	60.86 d	IT, ε
			92	7+	–86.448	3.47×10^{7}y	ε, β–
			92m	2+	–86.313	10.15 d	ε
			93	9/2+	–87.208	**100%**	
			93m	1/2–	–87.177	16.13 y	IT
			94	6+	–86.365	2.03×10^{4} y	β–
			94m	3+	–86.324	6.263 m	IT, β–
			95	9/2+	–86.782	34.991 d	β–
			95m	1/2–	–86.546	3.61 d	IT, β–
			96	6+	–85.604	23.35 h	β–

Element Z El	Atomic Weight u	Valance	A	J^{π}	Δ MeV	$t_{1/2}$, Γ or Abundance	Decay Mode
42Mo	95.94	2 to 6	**91**	2+	–82.20	15.49 m	ε
			91m	1/2–	–81.55	64.6 s	ε, IT
			92	0+	–86.805	**14.84%**	
			93	5/2+	–86.803	4.0×10^{3} y	ε
			93m	21/2+	–84.379	6.85 h	IT, ε
			94	0+	–88.410	**9.25%**	
			95	5/2+	–87.707	**15.92%**	
			96	0+	–88.790	**16.68%**	
			97	5/2+	–87.540	**9.55%**	
			98	0+	–88.112	**24.13%**	
			99	1/2+	–85.966	2.7489 d	β–
			100	0+	–86.184	0.78×10^{19} y	2β–
						9.63%	
			101	1/2+	–83.511	14.61 m	β–
			102	0+	–83.56	11.3 m	β–
43Tc	Non stable isotopes	0,2,4 to 7	**93**	9/2+	–83.603	2.75 h	ε
			93m	1/2–	–83.211	43.5 m	IT, ε
			94	7+	–84.154	293 m	ε
			94m	2+	–84.079	52.0 m	IT, ε
			95	9/2+	–86.017	20.0 h	ε
			95m	1/2–	–85.978	61 d	IT, ε
			96	7+	–85.817	4.28 d	ε
			96m	4+	–85.783	51.5 m	IT, ε
44Ru	101.07	0 to 8	**95**	5/2+	–83.45	1.643 h	ε
			96	0+	–86.072	**5.54%**	
			97	5/2+	–86.112	2.791 d	ε
			98	0+	–88.225	**1.87%**	
			99	5/2+	–87.617	**12.76%**	
			100	0+	–89.219	**12.60%**	
			101	5/2+	–87.950	**17.06%**	
			102	0+	–89.098	**31.55%**	
			103	3/2+	–87.259	39.26 d	β–
			104	0+	–88.089	**18.62%**	
			105	3/2+	–85.928	4.44 h	β–
			106	0+	–86.322	373.59 d	β–
45Rh	102.9055	3	**101**	1/2–	–87.41	3.3 y	ε
			101m	9/2+	–87.25	4.34 d	ε, IT
			102	1–,2–	–86.775	207 d	ε, β–
			102m	6+	–86.634	≈2.9 y	ε ,IT
			103	1/2–	–88.022	**100%**	
			103m	7/2+	–87.982	56.114 m	IT
			104	1+	–86.950	42.3 s	β–, ε
			104m	5+	–86.821	4.34 m	IT, β–
			105	7/2+	–87.846	35.36 h	β–

Element Z El	Atomic Weight u	Valance	A	J^{π}	Δ MeV	$t_{1/2,\ \Gamma\ or}$ Abundance	Decay Mode
46Pd	106.42	2 to 4	**101**	5/2+	–85.43	8.47 h	ε
			102	0+	–87.925	**1.02%**	
			103	5/2+	–87.479	16.991 d	ε
			104	0+	–89.390	**11.14%**	
			105	5/2+	–88.413	**22.33%**	
			106	0+	–89.902	**27.33%**	
			107	5/2+	–88.368	6.5×10^{6}y	β–
			108	0+	–89.524	**26.46%**	
			109	5/2+	–87.607	13.7012 h	β–
			109m	11/2–	–87.418	4.696 m	IT
			110	0+	–88.35	**11.72%**	
			111	5/2+	–86.00	23.4 m	β–
47Ag	107.868	1	**106**	1+	–86.937	23.96 m	ε, β–
			106m	6+	–86.847	8.28 d	ε
			107	1/2–	–88.402	**51.839%**	
			107m	7/2+	–88.309	44.5 s	IT
			108	1+	–87.602	2.37 m	β–, ε
			108m	6+	–87.492	438 y	ε, IT
			109	1/2–	–88.723	**48.161%**	
			109m	7/2+	–88.635	38.0 s	IT
48Cd	112.411	2	**106**	0+	–87.132	$\geq2.6\times10^{17}$y	2ε
						1.25%	2ε
			107	5/2+	–86.985	6.50 h	ε
			108	0+	–89.252	$>1.0\times10^{18}$y	2ε
						0.89%	
			109	5/2+	–88.508	461.4 d	ε
			110	0+	–90.353	**12.49%**	
			111	1/2+	–89.257	**12.80%**	
			111m	11/2–	–88.861	48.50 m	IT
			112	0+	–90.580	**24.13%**	β–
			113	1/2+	–89.049	7.7×10^{15}y	
						12.22%	2β–
			114	0+	–90.021	$>6.4\times10^{18}$y	β–
						28.73%	β–
			115	1/2+	–88.090	53.46 h	$2\beta^{-}$
			115m	11/2–	–87.910	44.56 d	
			116	0+	–88.719	3.1×10^{19}y	
						7.49%	
49In	114.81	1 to 3	**112**	1+	–87.996	14.97 m	ε, β–
			113	9/2+	–89.370	**4.29%**	
			114	1+	–88.572 +	71.9 s	β–, ε
			115	9/2+	–89.537	4.41×10^{14}y	β^{-}
						95.71%	
			115m	1/2–	–89.200	4.486 h	IT, β–

Element Z El	Atomic Weight u	Valance	A	J^{π}	Δ MeV	$t_{1/2}$, Γ or Abundance	Decay Mode
50Sn	118.710	2,4	**112**	0+	–88.661	**0.97%**	
			113	1/2+	–88.333	115.09 d	ε
			113m	7/2+	–88.256	21.4 m	IT, ε
			114	0+	–90.561	**0.66%**	
			115	1/2+	–90.036	**0.34%**	
			116	0+	–91.528	**14.54%**	
			117	1/2+	–90.400	**7.68%**	
			117m	11/2–	–90.085	13.76 d	IT
			118	0+	–91.656	**24.22%**	
			119	1/2+	–90.068	**8.59%**	
			119m	11/2–	–89.979	293.1 d	
			120	0+	–91.105	**32.58%**	
			121	3/2+	–89.204	27.03 h	β–
			122	0+	–89.946	**4.63%**	
			123	11/2–	–87.821	129.2 d	β–
			124	0+	–88.237	**5.79%**	
			125	11/2–	–85.898	9.64 d	β–
51Sb	121.76	0,±3,5	**120**	1+	–88.424	15.89 m	ε
			121	5/2+	–89.595	**57.21%**	
			122	2–	–88.330	2.7238 d	β–, ε
			122m	8–	–88.167	4.191 m	
			123	7/2+	–89.224	**42.79%**	
			124	3–	–87.620	60.11 d	β–
52Te	127.60	2,4,6	**120**	0+	–89.405	$>2.2\times10^{16}$y	2ε
						0.09%	
			121	1/2+	–88.55	19.16 d	ε
			122	0+	–90.314	**2.55%**	
			123	1/2+	–89.172	$>9.2\times10^{16}$y	ε
						0.89%	
			124	0+	–90.524	**4.74%**	
			125	1/2+	–89.022	**7.07%**	
			126	0+	–90.065	**18.84%**	
			127	3/2+	–88.281	9.35 h	β–
			128	0+	–88.992	8.8×10^{18}y	2β–
						31.74%	
			130	0+	–87.351	$>5\times10^{23}$y	2β–
						34.08%	
53I	126.9	1,3,5,7	**125**	5/2+	–88.836	59.400 d	ε
			126	2–	–87.910	12.93 d	ε, β–
			127	5/2+	–88.983	**100%**	
			128	1+	–87.738	24.99 m	β–, ε
			129	7/2+	–88.503	1.57×10^{7}y	β–
			130	5+	–86.932	12.36 h	β–
			131	7/2+	–87.444	8.0207 d	β–

Element Z El	Atomic Weight u	Valance	A	J^{π}	Δ MeV	$t_{1/2,\ \Gamma}$ or Abundance	Decay Mode
54Xe	131. 293	0	**124**	0+	–87.660	$\geq 1.1\times10^{17}$y	2ε
						0.095%	
			125	1/2+	–87.192	16.9 h	ε
			126	0+	–89.169	**0.089%**	
			127	1/2+	–88.321	36.4 d	ε
			128	0+	–89.860	**1.910%**	
			129	1/2+	–88.697	**26.40%**	
			130	0+	–89.882	**4.071%**	$2\beta^{-}\geq 0\%$
			131	3/2+	–88.415	**21.232%**	2β–
			132	0+	–89.281	**26.909%**	
			133	3/2+	–87.644	5.243 d	β–
			134	0+	–88.124	$>5.8\times10^{22}$y	2β–
						10.436%	
			135	3/2+	–86.417	9.14 h	β–
			136	0+	–86.425	$>2.4\times10^{21}$y	2β–
						8.857%	
55 Cs	132.905	1	**131**	5/2+	–88.060	9.689 d	ε
			132	2+	–87.156	6.480 d	ε, β–
			133	7/2+	–88.071	**100%**	
			134	4+	–86.891	2.0652 y	β– , ε
			134m	8–	–86.753	2.912 h	IT
			135	7/2+	–87.582	2.3×10^{6}y	β–
56 Ba	137.327	2	**130**	0+	–87.262	$\geq 3.5\times10^{14}$y	2ε
						0.106%	
			131	1/2+	–86.684	11.50 d	ε
			132	0+	–88.435	$>3.0\times10^{21}$y	2ε
						0.101%	
			133	1/2+	–87.553	3841 d	ε
			133m	11/2–	–87.265	38.9 h	IT, ε
			134	0+	–88.950	**2.417%**	
			135	3/2+	–87.851	**6.592%**	
			136	0+	–88.887	**7.854%**	
			136m	7–	–86.856	0.3084 s	IT
			137	11/2–	–87.721	**11.232%**	IT
			137m	3/2+	–87.060	2.552 m	
			138	0+	–88.262	**71.698%**	
57 La	138.9055	3	**136**	1+	–86.04	9.87 m	ε
			137	7/2+	–87.10	6×104 y	ε
			138	5+	–86.525	1.02×10^{11}y	ε , β–
						0.090%	
			139	7/2+	–87.231	**99.910%**	
			140	3–	–84.321	1.6781 d	β–
			141	7/2+	–82.938	3.92 h	β–
			142	2–	–80.035	91.1 m	β–

Element Z El	Atomic Weight u	Valance	A	J^{π}	Δ MeV	$t_{1/2,}$ Γ or Abundance	Decay Mode
58 Ce	140.116	3,4	**136**	0+	–86.47	$>0.7\times10^{14}$y	2ε
						0.185%	
			137	3/2+	–85.88	9.0 h	ε
			137m	11/2–	–85.62	34.4 h	IT, ε
			138	0+	–87.57	$\geq0.9\times10^{14}$y	2ε
						0.251%	
			139	3/2+	–86.952	137.641 d	ε
			140	0+	–88.083	**88.450%**	
			141	7/2–	–85.440	32.508 d	β–
			142	0+	–84.538	$>2.6\times10^{17}$y	2β–
						11.114%	
59 Pr	140.907	3	**139**	5/2+	–84.823	4.41 h	ε
			140	1+	–84.695	3.39 m	ε
			141	5/2+	–86.021	**100%**	
			142	2–	–83.793	19.12 h	β–, ε
			143	7/2+	–83.074	13.57 d	β–
60 Nd	144.24	3	**142**	0+	–85.955	**27.2%**	
			143	7/2–	–84.007	**12.2%**	
			144	0+	–83.753	2.29×10^{15}y	α
						23.8%	
			145	7/2–	–81.437	**8.3%**	
			146	0+	–80.931	**17.2%**	
			147	5/2–	–78.152 –	10.98 d	β–
			148	0+	77.413	**5.7%**	
			149	5/2–	–74.381	1.728 h	β–
			150	0+	–73.690	0.79×10^{19}y	2β–
						5.6%	
61Pm	Non stable isotopes	3	**144**	5–	–81.421	363 d	ε
			145	5/2+	–81.274	17.7 y	ε, α
			146	3–	–79.460	5.53 y	ε, β–
			147	7/2+	–79.048	2.6234 y	β–
62Sm	150.36	2,3	**144**	0+	–81.972	**3.07%**	
			145	7/2	–80.658	340 d	ε
			146	0+	–81.002	10.3×10^{7}y	α
			147	7/2–	–79.272	1.06×10^{11}y	α
						14.99%	
			148	0+	–79.342	7×10^{15}y	α
						11.24%	
			149	7/2–	–77.142	**13.82%**	
			150	0+	–77.057	**7.38%**	
			151	5/2–	–74.582	90 y	β–
			152	0+	–74.769	**26.75%**	
			153	3/2+	–72.566	46.284 h	β–
			154	0+	–72.462	**22.75%**	

Element Z El	Atomic Weight u	Valance	A	J^{π}	Δ MeV	$t_{1/2}$, Γ or Abundance	Decay Mode
63 Eu	151.964	2,3	**150**	5–	–74.797	36.9 y	ε
			151	5/2+	–74.659	**47.81%**	
			152	3–	–72.895	13.506 y	ε, β–
			152m	0–	–72.849	9.3116 h	β–, ε
			153	5/2+	–73.373	**52.19%**	
			154	3–	–71.744	8.590 y	β–
64 Gd	157.25	3	**152**	0+	–74.714	1.08×10^{14}y	α
						0.20%	
			153	3/2–	–72.890	240.4 d	ε
			154	0+	–73.713	**2.18%**	
			155	3/2–	–72.077	**14.80%**	α
			156	0+	–72.542	**20.47%**	
			157	3/2–	–70.831	**15.65%**	2β–
			158	0+	–70.697	**24.84%**	
			159	3/2–	–68.568	18.479 h	β–
			160	0+	–67.949	$>3.1\times10^{19}$y	β–
						21.86%	
			161	5/2–	–65.513	3.66 m	β–
65 Tb	158.92	3,4	**158**	3–	–69.477	180 y	ε, β–
			158m	0–	–69.367	10.70 s	IT, β–,ε
			159	3/2+	–69.539	**100%**	
			160	3–	–67.843	72.3 d	β–
			161	3/2+	–67.468	6.906 d	β–
66 Dy	162.50	3	**155**	3/2–	–69.16	9.9 h	ε
			156	0+	–70.530	**0.06%**	
			157	3/2–	–69.428	8.14 h	ε
			158	0+	–70.412	**0.10%**	
			159	3/2–	–69.174	144.4 d	ε
			160	0+	–69.678	**2.34%**	
			161	5/2+	–68.061	**18.91%**	
			162	0+	–68.187	**25.51%**	
			163	5/2–	–66.386	**24.90%**	
			164	0+	–65.973	**28.18%**	
			165	7/2+	–63.618	2.334 h	β–
67 Ho	164.930	3	**163**	7/2–	–66.384	4570 y	ε
			165m	1/2+	–66.086	1.09 s	IT, ε
			164	1+	–64.987	29 m	ε, β–
			165	7/2–	–64.905	**100%**	
			166	0–	–63.077	26.83 h	β–
			167	7/2–	–62.287	3.003 h	β–
68 Er	167.259	3	**162**	0+	–66.343	**0.139%**	
			163	5/2–	–65.174	75.0 m	ε
			164	0+	–65.950	**1.601%**	
			165	5/2–	–64.528	10.36 h	ε

Element Z El	Atomic Weight u	Valance	A	J^{π}	Δ MeV	$t_{1/2}$, Γ or Abundance	Decay Mode
68 Er	167.259	3	**166**	0+	–64.932	**33.503%**	
			167	7/2+	–63.297	**22.869%**	
			168	0+	–62.997	**26.978%**	
			169	1/2–	–60.929	9.392 d	β–
			170	0+	–60.115	**14.910%**	
			171	5/2–	–57.725	7.516 h	β–
69Tm	168.934	3	**167**	1/2+	–62.548	9.25 d	ε
			168	3+	–61.318	93.1 d	ε
			169	1/2+	–61.280	**100%**	
			170	1–	–59.801	128.6 d	β–, ε
			171	1/2+	–59.216	1.92 y	β–
70 Yb	173.04	2,3	**167**	5/2–	–60.594	17.5 m	ε
			168	0+	–61.575	**0.13%**	ε
			169	7/2+	–60.370	32.018 d	
			169m	1/2–	–60.346	46 s	IT
			170	0+	–60.769	**3.04%**	
			171	1/2–	–59.312	**14.28%**	
			172	0+	–59.260	**21.83%**	
			173	5/2–	–57.556	**16.13%**	β–
			174	0+	–56.950	**31.83%**	2β–
			175	7/2–	–54.701	4.185 d	
			176	0+	–53.494	$\geq 1.6\times10^{17}$y	
						12.76%	
71 Lu	174.967	3	**174**	1–	–55.575	3.31 y	ε
			174m	6–	–55.404	142 d	IT, ε
			175	7/2+	–55.171	**97.41%**	
			176	7–	–53.387	3.76×10^{10}y	β–
						2.59%	
			177	7/2+	–52.389	6.6475 d	β–
72 Hf	178.49	4	**174**	0+	–55.847	2.0×10^{15} y	α
						0.16%	
			175	5/2–	–54.484	70 d 2	ε
			176	0+	–54.577	**5.26%**	
			177	7/2–	–52.890	**18.60%**	
			178	0+	–52.444	**27.28%**	
			179	9/2+	–50.472	**13.62%**	
			180	0+	–49.788	**35.08%**	
			181	1/2–	–47.412	42.39 d	β–
73 Ta	180.9479	2?,3,4?,5	**180**	1+	–48.936	8.154 h 6	ε, β–
			180m	9–	–48.859	$>1.2\times10^{15}$y	2ε ?
			181	7/2+	–48.442	**100%**	
			182	3–	–46.433	114.43 d	β–
			182m	5+	–46.417	283 ms	IT
			183	7/2+	–45.296	5.1 d	β–

Element Z El	Atomic Weight u	Valance	A	J^{π}	Δ MeV	$t_{1/2}$, Γ or Abundance	Decay Mode
74 W	183.84	2 to 6	**180**	0+	–49.645	1.8×10^{18} y	α
						0.12%	
			181	9/2+	–48.254	121.2 d	ε
			182	0+	–48.248	$>8.3\times10^{18}$y	α
						26.50%	
			183	1/2–	–46.367	$>1.3\times10^{19}$y	α
						14.31%	
			184	0+	–45.707	$>2.9\times10^{19}$y	α
						30.64%	
			185	3/2–	–43.390	75.1 d	β–
			186	0+	–42.509	$>2.7\times10^{19}$y	α
						28.43%	
			187	3/2–	–39.905	23.72 h	β–
75 Re	186.207	4,6,7	**185**	5/2+	–43.822	**37.40%**	
			186	1–	–41.930	3.7186 d	β–, ε
			187	5/2+	–41.216	4.12×10^{10}y	β–
						62.60%	
			188	1–	–39.016	17.003 h	β–
76 Os	190.23	0 to 8	**184**	0+	–44.256	$>5.6\times10^{13}$y	α
						0.02%	
			185	1/2–	–42.809	93.6 d	ε
			186	0+	–43.000	2.0×10^{15}y	α
						1.59%	
			187	1/2–	–41.218	**1.6%**	
			188	0+	–41.136	**13.29%**	
			189	3/2–	–38.985	**16.21%**	
			190	0+	–38.706	**26.36%**	
			191	9/2–	–36.394	**4**15.4 d	β–
			192	0+	–35.881	**0.93%**	
				3/2–	–33.393	30.11 h	β–
77 Ir	192.217	3,4	**191**	3/2+	–36.706	**37.3%**	
			192	4+	–34.833	73.827 d	β–, ε
			193	3/2+	–34.534	**62.7%**	
			194	1–	–32.529	19.28 h	β–
78 Pt	195.078	1?,2,3	**190**	0+	–37.323	6.5×10^{11}y	α
						0.014%	
			191	3/2–	–35.698	2.862 d	ε
			192	0+	–36.293	**0.782%**	
			193	1/2–	–34.477	50 y	ε
			194	0+	–34.763	**32.967%**	
			195	1/2–	–32.797	**33.832%**	
			196	0+	–32.647	**25.242%**	
			197	1/2–	–30.422	19.8915 h	β–
			198	0+	–29.908	**7.163%**	

Element Z El	Atomic Weight u	Valance	A	J^{π}	Δ MeV	$t_{1/2,\ \Gamma}$ or Abundance	Decay Mode
79 Au	196.966	1,3	**196**	2–	–31.140 –	6.1669 d	ε, β–
			196m	5+	31.055	8.1 s	IT
			197	3/2+	–31.141	**100%**	
			198	2–	–29.582	2.6956 d	β–
			199	3/2+	–29.095	3.139 d	β–
80 Hg	200.5	1,2	**196**	0+	–31.827	**0.15%**	
			197	1/2–	–30.541	64.14 h	ε
			198	0+	–30.954	**9.97%**	
			199	1/2–	–29.547	**16.87%**	
			200	0+	–29.504	**23.10%**	
			201	3/2–	–27.663	**13.18%**	
			202	0+	–27.346	**29.86%**	
			203	5/2–	–25.269	46.595 d	β–
			204	0+	–24.690	**6.87%**	
			205	1/2–	–22.288	5.14 m	β–
81 Tl	204.383	1,3	**201**	1/2+	–27.18	72.912 h	ε
			202	2–	–25.98	12.23 d	ε
	208 5(+)		**203**	1/2+	–25.761	**29.524%**	
			204	2–	–24.346	3.78 y	β–, ε
			205	1/2+	–23.821	**70.476%**	
			206	0–	–22.253	4.200 m	β–
			207	1/2+	–21.034	4.77 m	β–
			208	5+	–16.750	3.053 m	β–
82 Pb	207.21	2,4	**204**	0+	–25.110	$\geq 1.4\times10^{17}$ y	α
						1.4%	
			205	5/2–	–23.770	1.73×10^{7} y	ε
			206	0+	–23.785	**24.1%**	
			207	1/2–	–22.452	**22.1%**	
			207m	13/2+	–20.819	0.806 s	IT
			208	0+	–21.749	**52.4%**	
			209	9/2+	–17.614	3.253 h	β–
			210	0+	–14.728	22.20 y	β– , α
83 Bi	208.9804	3,5	**208**	5+	–18.870	3.68×10^{5} y	ε
			209	9/2–	–18.258	1.9×10^{19}y	α
						100%	
			210	1–	–14.792	5.012 d	β–, α
			211	9/2–	–11.858	2.14 m	α, β–
			212	1–	–8.117	60.55 m	β–, α
84 Po	Non stable isotopes	2,3?,4,6	**207**	5/2–	–17.146	5.80 h	ε, α
			208	0+	–17.469	2.898 y	α , ε
			209	1/2–	–16.366	102 y	α , ε
			210	0+	–15.953	138.376 d	α
			211	9/2+	–12.432	0.516 s	α
			212	18+	**–7.447**	45.1 s	α

Element Z El	Atomic Weight u	Valance	A	J^{π}	Δ MeV	$t_{1/2}$, Γ or Abundance	Decay Mode
85 At	Non stable isotopes	1,3,5,7	**208**	6+	–12.49	1.63 h 3	ε, α
			209	9/2–	–12.880	5.41 h	ε, α
			210	5+	–11.972	8.1 h	ε, α
			211	9/2–	–11.647	7.214 h	ε, α
			212	1–	–8.621	0.314 s	ε, α
86 Rn	Non stable isotopes	0	**220**	0+ 0+	10.613	55.6 s 2.4 h	α
			221	7/2+	14.472	25.7 m	α, β–
			222	0+	16.374	3.8235 d	α
			223	7/2	20.3 ?	24.3 m	β–
			224	0+	22.4 ?	107 m	β–
87 Fr	Non stable isotopes	1	**222**	2–9/2–	16.35	14.2 m	β–, ^{14}C
			223	3/2–	18.384	22.00 m	β–, α
			224	1–	21.66	3.33 m	β–
			225	3/2–	23.81	4.0 m	β–
88 Ra	Non stable isotopes	2	**223**	3/2+	17.235	11.43 d	α
			224	0+	18.827	3.6319 d	α
			225	1/2+	21.994	14.9 d	β–
			226	0+	23.669	1600 y	α
			227	3/2+	27.179	42.2 m	β–
			228	0+	28.942	5.75 y	β–
89 Ac	Non stable isotopes	3	**226**	1 ?	24.310	29.37 h	β–, ε
			227	3/2–	25.851	21.772 y	β–
			228	3+	28.896	6.15 h	β–
			229	3/2+	30.75	62.7 m	β–
90Th	232.0380	2?,3?,4	**231**	5/2+	33.817	25.52 h	β–, α
			232	0+	35.448	1.405×10^{10}y **100%**	α
			233	1/2+	38.733	21.83 m	β–
			234	0+	40.614	24.10 d	β–
91 Pa	Non stable isotopes	4,5	**230**	2–	32.174	17.4 d	ε, β–, α
			231	3/2–	33.426	3.276×10^{4}y	α, SF
			232	2–	35.948	1.31 d	β– , ε
			233	3/2–	37.490	26.975 d	β–
92 U	238.0289	2 to 6	**232**	0+	34.611	68.9 y	α
			233	5/2+.	36.920	1.592×10^{5}y	α , SF
			234	0+	38.147	2.455×10^{5}y **0.0054%**	α, SF
			235	7/2–	40.921	7.04×10^{8} y **0.7204%**	α
			236	0+	42.446	2.342×10^{7}y	α , SF
			237	1/2+	45.392	6.75 d	β–
			238	0+	47.309	4.468×10^{9}y **99.2742%**	α , SF
			239	5/2+	50.574	23.45 m	β–

Element Z El	Atomic Weight u	Valance	A	J^{π}	Δ MeV	$t_{1/2,}$ Γ or Abundance	Decay Mode
93Np	Non stable isotopes	3 to 6	**236**	6–	43.38	154×10^{3} y	ε, β–, α
			237	5/2+	44.873	2.144×10^{6}y	α, SF
			238	2+	47.456	2.117 d	β–
			239	5/2+	49.312	2.356 d	β–
			240	5+	52.31	61.9 m	β–
94Pu	Non stable isotopes	3, to 6	**238**	0+	46.165	87.7 y	α , SF
			239	1/2+	48.590	24110 y	α , SF
			240	0+	50.127	6561 y	α , SF
			241	5/2+	52.957	14.290 y	β– , α
			242	0+	54.718	3.75×10^{5}y	α , SF
			243	7/2+	57.756	4.956 h	β–
			244	0+	59.806	8.00×10^{7} y	α , SF
95Am	Non stable isotopes	2 to 6	**241**	5/2–	52.936	432.2 y	α , SF
			242	1–	55.470	16.02 h	β–, ε
			243	5/2–	57.176	7370 y	α , SF
			244	6–	59.881	10.1 h	β–
			254	5/2+	61.900	2.05 h	β–
96Cm	Non stable isotopes	3,4	**244**	0+	58.454	18.1 y	α , SF
			245	7/2+	61.005	8500 y	α , SF
			246	0+	62.618	4760 y	α , SF
			247	9/2–	65.534	1.56×10^{7}y	α
			248	0+	67.392	3.48×10^{5}y	α , SF
			249	1/2+	70.750	64.15 m	β–
97Bk	Non stable isotopes	3,4	**247**	3/2–	65.491	1380 y	α
			248		68.08	>9 y	α
98Cf	Non stable isotopes	3	**250**	0+	71.172	13.08 y	α , SF
			251	1/2+	74.135	898 y	α , SF
			252	0+	76.034	2.645 y	α , SF
99 Es	Non stable isotopes	3	**252**	5–	77.29	471.7 d	α , SF
			253	7/2+	79.014	20.47 d	α , SF
100Fm	Non stable isotopes	3	**256**	0+	85.486	157.6 m	SF, α
			257	9/2+	88.590	100.5 d	α
101Md	Non stable isotopes	2,3	**258**		91.688	51.5 d	α, SF

References:

1. A. Bohr, B. R. Mottelson, Nuclear Structure, Vol. I, Single-Particle Motion, W. A. Benjamin, Inc., Reading, Massachusetts (1969)

2. A. Bohr and B. R. Mottelson, Nuclear Structure Vol. 11, Nuclear Deformations, W. A. Benjamin, Inc., Reading, Massachusetts (1975)

3. A. Das and T. Ferbel, Introduction to Nuclear and Particle Physics, Second Edition, World Scientific Publishing Co. Pte. Ltd. 5 Toh Tuck Link, Singapore 596224, USA, (2003)

4. A. M. Jacobs, , D. E. Klineand, F. J. Remick, Basic Principles of Nuclear Science and Reactors, Van Nostrand Company, Inc., (1960)

5. A. R. Edmonds, Angular Momentum in Quantum Mechanics, 3rd printing, Princeton University Press, Princeton, New Jersey (1974)

6. A. R. Foster and R. L. Wright, Basic Nuclear Engineering, 3rd Edition, Allyn and Bacon, Inc., (1977)

7. Academic Program for Nuclear Power Plant Personnel, Volume III, Columbia, MD, General Physics Corporation, Library of Congress Card #A 326517, (1982)

8. Academic Program for Nuclear Power Plant Personnel, Volume IV, General Physics Corporation, Library of Congress Card #A 397747, April (1982)

9. B. A. Brown, Proc. Int. Nucl. Phys. Conf., Harrogate, U. K., eds. J. L. Durell, et al., Inst. of Phys. Conf. Series No. 86, Bristol (1987)

10. B. Blattel, V. Koch, W. Cassing, and U. Mosel, Phys. Rev. C38,1767 (1988).

11. B. R. Martin, Nuclear and Particle Physics, John Wiley & Sons, Ltd. ISBN: 0-470-01999-9 (2006)

12. D. F. Jackson and D. J. Hawkes, X-ray attenuation coefficients of elements and mixtures. Phys. Reports 70 (1981)

13. E. M. Ameen, K. M-S. Abdullah, Evolution of Thermal Neutron Flux in IRT-2000 Fuel Cell Using Numerical Technique, 7^{th} Conference of Iraqi Society of Physics and Mathematics (1985)

14. F. Dyson, in Aspects of Quantum Theory edited by A. Salam and E.P. Wigner, Cambridge U. Press, Cambridge, (1972)

15. G. E. Brown, Unified Theory of Nuclear Models, North-Holland Publishing Company, Amsterdam (1964)

16. G. F. Knoll, Radiation Detection and Measurement, John Wiley and Sons, ISBN 0-471-49545-X, (1979)

17. General Electric Company, Nuclides and Isotopes: Chart of the Nuclides, 14th Edition, General Electric Company, (1989)

18. H. Al-Dujaily, K. M-S. Abdullah, Steady State Temperature Distribution Calculation in IRT-M Nuclear Fuel Assembly, Iraqi Journal of Mathematics and Physics, Vol.11, No.1 (1989)

19. H. Cember, Introduction to Health Physics, Pergamon Press Inc., Library of Congress Card #68-8528, (1985)

20. H. Feshbach, Theoretical Nuclear Physics Vol. II, Nuclear Reactions, John Wiley and Sons, Inc., New York (1991)

21. I. J. R. Aitchison and A. J. G. Hey, Gauge Theories in Particle Physics, 2nd edition, Adam Hilger, Bristol and Philadelphia (1989)

22. I. Kaplan, Nuclear Physics, 2nd Edition, Addison-Wesley Company, NY (1962)

23. ICRU Report 16, Linear Energy Transfer. Bethesda, MD, International Commission on Radiation Units and Measurements (1970)

24. ICRU Report 33, Radiation Quantities and Units. Bethesda, MD, International Commission on Radiation Units and Measurements (1980)

25. ICRU Report 37, Stopping Powers for Electrons and Positrons. Bethesda, MD, International Commission on Radiation, (1984)

26. ICRU Report 49, Stopping Powers and Ranges for Protons and Alpha Particles. Bethesda, MD, International Commission on Radiation Units and Measurements (1993)

27. J. D. Bjorken and S. D. Drell, Relativistic Quantum Mechanics, McGraw-Hill, New York (1964)

28. J. D. Walecka, Electron Scattering for Nuclear and Nucleon Stmcture, Cambridge University Press, Cambridge, U.K. (2001)

29. J. D. Walecka, Theoretical Nuclear and Subnuclear Physics, Oxford University Press, New York First Edition, (1995)

30. J. D. Walecka, Theoretical Nuclear and Subnuclear Physics, Imperial College Press and World Scientific Publishing Co., Second Edition, (2004)

31. J. E. Parks, Attenuation of Radiation, James Edgar Parks, (2001)

32. J. E. Turner, Atoms, Radiation, and Radiation Protection, WILEY-VCH Verlag GmbH & Co. KGaA, Weinheim ISBN: 978-3-527-40606-7, (2007)

33. J. J. Duderstadt and L. J. Hamilton, Nuclear Reactor Analysis, John Wiley and Sons, Inc., New York (1976)

34. J. K. TULI, Nuclear Wallet Cards, Brookhaven National Laboratory Upton, New York 11973–5000, USA, (Seventh edition) April (2005)

35. J. L. Basdevant, J. Rich, M. Spiro, Fundamentals in nuclear physics , Springer Science & Business Media, Inc. 233 Spring Street, New York, NY 10013, USA (2005)

36. J. M. Blatt, V. F. Weisskopf, Theoretical Nuclear Physics, John Wiley and Sons Inc., New York (1952)

37. J. R. Lamarsh, Introduction to Nuclear Engineering, Addison-Wesley Publishing Company, NY (1977)

38. J. R. Lamarsh, Introduction to Nuclear Reactor Theory, Addison-Wesley Publishing Company, NY (1972)

39. J. W. Negele, E. W. Vogt, Advances in Nuclear Physics, eBook ISBN: 0-306-47067-5, Kluwer Academic Publishers, (2002)

40. K. Arshak, O. Korostynska, Advanced Materials and Techniques for Radiation Dosimetry, Artech House, INC. 685 Canton Street Norwood, MA 02062 (2006)

41. K. Hagiwara et al, Review of Particle Physics, Phys. Rev. D66, 010001, (2002)

42. K. Heyde, Basic Ideas and Concepts in Nuclear Physics, an Introductory Approach, IOP Publishing Ltd, Second Edition (1999)

43. K. M-S. Abdullah, Development of a Computer Code to Simulate a PWR In-Core Fuel Management, J. Duhok Univ., Vol.7, No.2, pp.52-64 (2004)

44. K. M-S. Abdullah, F. A. Najim, Effect of Charged Beta Particles on Electrical Properties of Some Polymers, J. Duhok Univ., Vol.7, No.1, pp.59-64 (2004)

45. K. M-S. Abdullah, M. T. Ahmed, Environmental and Radiological Pollution in Creek Sediment and Water from Duhok-Iraq, The Nucleus 49, No. 1, NCLEAM, ISSN 0029-5698, pp 49-59 (2012)

46. K. M-S. Abdullah, R. A. Ramadhan, Determination of Gamma-emitting radionuclides in Duhok City-Iraq, The Nucleus 48, No. 4, NCLEAM, ISSN 0029-5698, pp 295-300 (2011)

47. K. M-S. Abdullah, S. K. Loyalka, Thermal Disadvantage Factor: An Efficient Calculation, Nuclear Science and Engineering NSE,Vol.104, No.1, January (1990)

48. K. M-S. Abdullah, Simulation of (PWR) Reactor by Personal Computer, J. Duhok Univ., Vol.7, No.1, pp.1-5 (2004)

49. L. David, the ARABS Journeys Beyond the Mirage, Random house. Inc., NY, First Edition, (1987)

50. P. J. Siemens and A. S. Jensen, Elements of Nuclei, Addison-Wesley Publishing Co. Inc., Redwood City, California (1987)

51. Q. R. Ahmad, et al. (The SNO Collaboration), Phys. Rev. Lett. 87, 071301, (2001)

52. Q. R. Ahmad, et al. (The SNO Collaboration), Phys. Rev. Lett. 89, 011301, (2002)

53. R. A. Knief, Nuclear Energy Technology: Theory and Practice of Commercial Nuclear Power, McGraw-Hill, (1981)

54. R. K. Hobbie, B. J. Roth, Intermediate Physics for Medicine and Biology, Fourth Edition, Springer Science+Business Media, LLC, 233 Spring Street, New York, NY 10013, USA, (2007)

55. R. Machleidt, The Meson Theory of Nuclear Forces and Nuclear Structure, in Adv. in Nucl. Phys. 19, eds. J. W. Negele and E. Vogt, Plenum Press, New York, (1989)

56. S. Glasstone and A. Sesonske, Nuclear Reactor Engineering, 3rd Edition, Van Nostrand Reinhold Company, NY (1981)

57. S. Glasstone, Source book on Atomic Energy, Robert F. Krieger Publishing Company, Inc., (1979)

58. S. N. Ahmed, Physics and Engineering of Radiation Detection, Academic Press Inc. Published by Elsevier (2007)

59. S. P. Ahlen, Theoretical and experimental aspects of the energy loss of relativistic heavily ionizing particles. Rev. Mod. Phys. 52, (1980)

60. S. S.M. Wong, Introductory Nuclear Physics, Prentice Hall, Englewood Cliffs (1990)

61. S. S.M. Wong, Introductory Nuclear Physics, second edition, Wiley-VCH Verlag GmbH & Co. KGaA (2004)

62. W. N. Cottingham, D. A. Greenwood, An Introduction to Nuclear Physics, Cambridge University Press 1986-2004, ISBN 0-5 11_03280_3 eBook, Second edition (2001)

63. Y-Kuo Lim, Problems and Solutions on Atomic, Nuclear and Particle Physics, World Scientific Publishing Co. Pte. Ltd. (2000)

Index: